Introduction - The Nature of an Advanced Propellant

Dr. Richard T. Holzmann

Aerojet-General Corporation
Von Karman Center
Azusa, California

The propellant chemist knows what is needed to make a truly advanced propellant - the energy of the cryogenics (fluorine/hydrogen); the density of solids and the ability to tailor properties to the mission at hand. The energetics are a direct consequence of the simplified specific impulse relationship:

$$I_s = \frac{F}{\dot{w}} = \frac{\text{thrust}}{\text{weight rate of flow}}$$

which is a major aspect of propellant performance expressed in units of pound per pound per second, or more commonly, just seconds. The over-all efficiency of the rocket system is, in turn, dependent on the combined efficiencies of the combustion chamber (where the propellants are burned) and the nozzle (where the thermal energy is to kinetic energy). As a rough approximation in screening potential propellant combinations, it is frequently considered that specific impulse is proportional to

$$\sqrt{\frac{\Delta H}{\bar{M}}}\ .$$

Thus, simply stated, a high heat release yielding low molecular weight products is most desirable.

The total figure of merit of propellant system performance is usually taken to be specific impulse multiplied by propellant bulk density to some exponent which may range from 0.05 to 1.0. The actual value of the exponent depends upon a complex relationship among the propellant, its properties, the mission, and design criteria. Thus, the high density of the propellant in a volume-limited application such as an air-launched missile is extremely important whereas for an upper-stage it is not nearly so critical.

The mission similarly influences the essential properties of the propellant ingredients. The military require rocket motors or engines which will withstand operational thermal cycling and handling. In addition, they must be safe under combat conditions in that they will not detonate in a fire or when struck by bullets for example. They must be capable of storage for years - ideally under hermetically sealed conditions. There are many who presume that a more energetic advanced propellant must necessarily be less safe due to the explosion hazard. This confuses the thermodynamic and kinetic parameters. On the other hand, rockets for space applications do not have the serious restrictions inherent in a military mission, and thus cryogenics find a notable use. Advanced propellant chemistry, as a consequence, is not generally concerned with cryogenics but rather with conferring the energetics of the cryogenics on earth-storable liquids and solids. With some levity then, one may strive to make hydrogen and fluorine, liquid or solid at room temperature! This leads directly to the context of this Symposium.

The first several papers concern themselves with a theoretical approach to extremely advanced oxidizers; the next group examine oxygen oxidizers primarily by the study of physical and combustion characteristics of importance in propellants. Following are two papers on binders which act as fuels as well as conferring desirable physical properties on solid propellants. It will be noticed at this point that there is no coverage of the light metal hydride fuels. This is a result of the vast synthetic efforts over the past ten years, which resulted in production capabilities for the boranes - diborane, pentaborane, decaborane and their derivatives. The tenacity with which the desirable hydrides of aluminum and beryllium hold on to their Lewis bases, ethers and amines, has prevented their isolation in a sufficient purity to make them useful as propellant fuels. The impure beryllium hydride prepared at Los Alamos ten years ago, just as the aluminum hydride prepared at Tufts shortly thereafter, offers little or no performance advantage over the use of the respective metals.

After the binder papers are five presentations which explore the physical, combustion and detonation properties of liquid systems. The balance of the Symposium is concerned primarily with the more energetic oxidizers based upon nitrogen-fluorine and oxygen-fluorine bonding. It is from this area that the most significant improvements will one day come. For with the oxidizer comprising 70 to 80 percent of the propellant combination, a relatively small improvement here is magnified as compared with the fuel. The use of metals, mentioned above, in both solid propellants and in liquid slurries, has been widely publicized and will not be discussed here. Their use, incidentally, originated in explosives technology and is commonplace at the present time.

It must be clearly indicated here, that as broad as the coverage of this Symposium appears, there is much propellant chemistry which has not been included. The experimental determination of thermodynamic properties such as heats of formation and equilibrium constants, as well as the calculations of theoretical performance have been presented at other symposia. The applied chemistry related to the modification of polymers, and hence mechanical and burning properties of solids, have other forums. The actual firing of solid motors and the determination of thrust and efficiency have been omitted, while the research into combustion instability and the transition from deflagration to detonation are only alluded to.

The Advanced Propellant

The ideal advanced propellant is then one which yields a high heat release in the chamber, converts this to translational kinetic energy in the nozzle while generating low molecular weight "perfect" gases. This latter requirement is rarely satisfied due to the presence of HF, CO, CO_2 and H_2O in the metal-free systems and to condensed metal oxides in the metal systems. This two-phase flow problem with a metallized propellant can easily result in a five percent efficiency loss. Therefore, although the metals have an extremely attractive heat release, a penalty of this five percent is imposed from the start even presuming perfect combustion efficiency. Everything considered, a performance of 92 percent of theoretical is close to maximum efficiency. The metal-free liquid bipropellant systems however are capable of achieving 97 to 98 percent of theoretical performance.

Low molecular weight "perfect" gases clearly point the way to hydrogen which accounts for the extreme performance of a nuclear propulsion unit. In this system, the reactor merely heats the light-weight gas. Although CH_4 and NH_3 have also been considered for nuclear applications, decomposed methane has a molecular weight of 5.4, ammonia of 7, while hydrogen has a molecular weight of 2. If too high temperatures are employed, the molecular hydrogen will dissociate into the atoms, and absorb additional

energy. In a chemical propulsion system the hydrogen will come, in the case of solids, from the binder and NH_4ClO_4 and, in liquids, from N_2H_4 and its derivatives or pentaborane or diborane - the latter being space-storable, but not earth-storable. Much of the simple theoretical comparisons of oxidizers are therefore based on combustion with N_2H_4 or B_5H_9 for liquids and on more complex systems for solids.

M. Barrère has published the following performance calculations.

Table I - Storables

Propellant		Composition	I_s	I_{sd}
SOLID	Present	Ammonium perchlorate Al + plastic	267	455
	Future	Ammonium perchlorate LiBe + plastic	290	377
LIQUID	Present	HNO_3–DMH	276	348
		HNO_3–N_2H_4	283	362
		N_2O_4–DMH	285	336
		N_2O_4–N_2H_4	292	356
		H_2O_2–DMH	278	345
		H_2O_2–N_2H_4	282	355
	Future	ClO_3F–N_2O_4	295	360
		N_2O_4–B_5H_9	306	337
		H_2O_2–B_5H_9	312	311
		ClF_3–N_2H_4	294	444
HYBRID	Present	H_2O_2–Al + plastic	289	435
		HNO_3–Al + plastic	273	414
		NO_2ClO_4–N_2H_4	295	428
	Future	ClF_3–LiH	293	445
		ClF_3–Li	318	369
		N_2O_4–BeH_2	351	530
		H_2O_2–BeH_2	375	566

Table II - Cryogenics

Propellant	Composition	I_s	I_{sd}
LIQUID	O_2–H_2	391	109
	O_2–N_2H_4	335	365
	F_2–H_2	410	185
	F_2–N_2H_4	363	476
	O_2-F_2–DMH	345	398
HYBRID	F_2–LiH	363	476
	F_2-O_2–plastic	343	412
	F_2–BeH_2	395	604
	O_2–BeH_2	371	486
	F_2–AlH_3	353	551

It can be seen that future storable liquid propellant systems are in the 300 to 315 sec. range, while future solid systems are around 290 secs. By the use of an "idealized" hybrid composed of H_2O_2/BeH_2, 375 secs. is possible in a storable propellant. Not only is the pure hydride unavailable, but hybrid technology leaves much to be desired.

Barrère's analysis did not mention N_2F_4 or OF_2 since these are "soft" cryogenics in that their boiling points are low. Their performance is excellent, however.

Table III

	b.p. °C	I_{sp} N_2H_4	I_{sp} B_5H_9
N_2F_4	-74	333	333
OF_2	-145	345	359

The performance of F_2, OF_2 and NF_3 or N_2F_4 gives the insight into where the synthesis potential of rocket oxidizers is.

An attempt has been made here to determine the relative value of an oxidizing group as a propellant with a model fuel, N_2H_4. Hydrazine was chosen for simplicity and availability of calculations. The ΔH_f has been chosen in most cases by analogy. For example, to obtain one point for an –O, one may use one-third of +30 kcal/mole, the ΔH_f of O_3. For another point, one-half of -3.48 kcal/mole, the ΔH_f of $O_{2(l)}$. In this manner a series of curves were generated (Figure I). Inherent then in any calculation of this type is the nature of the group to which the oxidizing group of interest is bonded.

Figure I

OXIDIZER GROUP CONTRIBUTIONS

(N_2H_4 1000 psia $\xrightarrow{\text{shifting}}$ 14.7 psia)

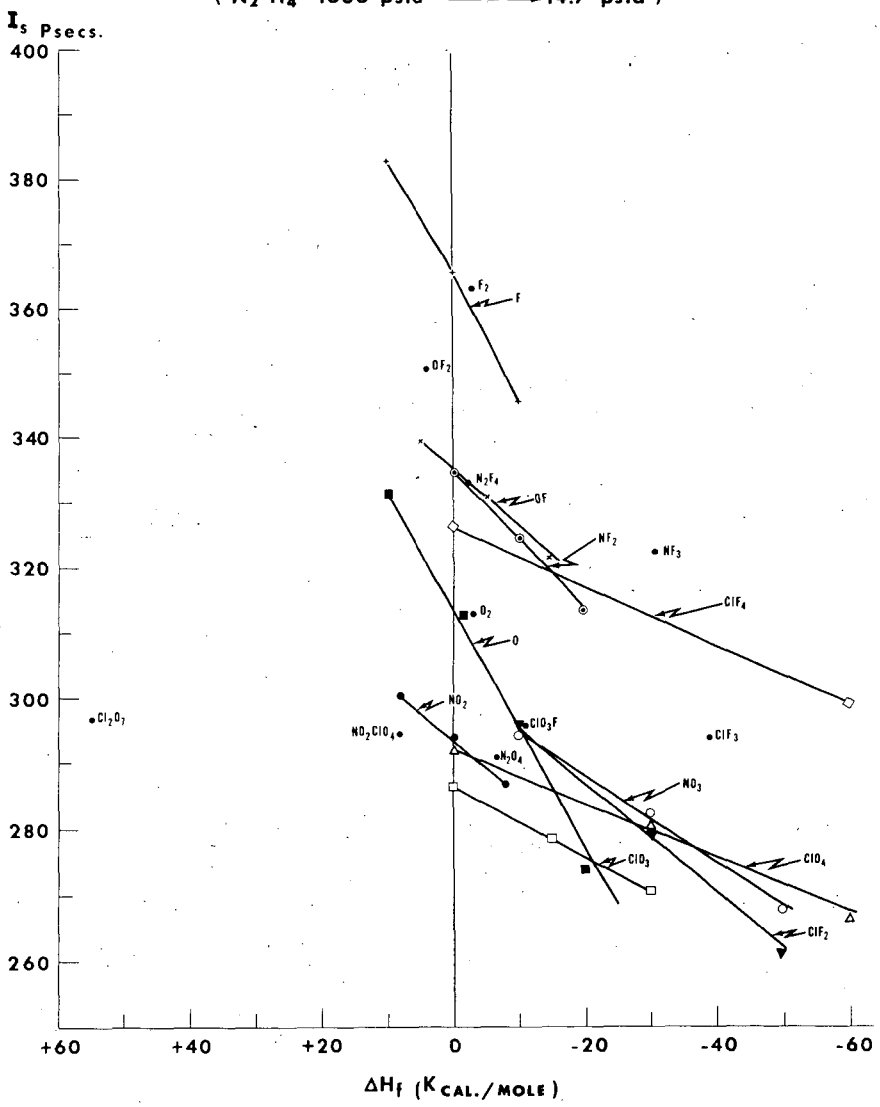

Several conclusions which can be drawn from such a curve would have been approximated "intuitively" by the synthesis chemist by reason of his background knowledge.

If one chooses a constant ΔH_f an index of oxidizing power may be obtained. For a ΔH_f = -10 kcal/mole the order in Table IV is observed.

Table IV - Relative Order of Oxidizing Power

-F	$-ClF_2$
-OF	$-NO_3$
$-NF_2$	$-ClO_4$
$-ClF_4$	$-NO_2$
-O	$-ClO_3$

If one chooses a target I_{sp} there appear to be certain groups which, if embodied in an oxidizer, would have difficulty in attaining the objective. Consider, if 310 secs. is chosen as the target, the groups in Table V would not be expected to reach the objective unless combined with the highly energetic groups above them in Table IV.

Table V - Oxidizer Groups Not Expected to Yield 310 Secs

$-ClF_2$
$-NO_3$
$-ClO_4$
$-NO_2$
$-ClO_3$

The steepest slopes observed are those for -F and -O indicating the dramatic contribution to impulse by a slight increase in ΔH_f. In general, then, -N compounds have a more positive slope than -Cl compounds, demonstrating the relatively better performance of N as a carrier atom over Cl.

A test of the value of such a curve (see Table VI) may be made by locating the known oxidizers relative to the group contribution curves.

Table VI - Correlation of Known Oxidizers with Group Contributions

Oxidizer	Location	Correlation
F_2	on F	excellent
OF_2	midway between OF and F	excellent
N_2F_4	on NF_2	excellent
O_2	on O	excellent
NF_3	---	poor
ClF_3	midway between ClF_4 and ClF_2	good
ClO_3F	above ClF_2, much above ClO_3	poor
N_2O_4	close to NO_2	good
NO_2ClO_4	between NO_2 and extrapolated ClO_4	good
Cl_2O_7	far removed from extrapolated ClO_4 and ClO_3	poor

Hypothetical oxidizers may be tested in the same way. However, the question arises as to what ΔH_f to choose, and here lies the primary limitation. Having the curve, would one have chosen ΔH_f Cl_2O_7 = +55 kcal/mole or ΔH_f NF_3 = -29 kcal/mole?

In conclusion then, it appears that the most desirable oxidizer is one which packs in the maximum of fluorine bonded to itself (F_2), bonded to oxygen (OF_2, O_2F_2, O_3F_2, O_4F_2), or bonded to nitrogen (NF_3, N_2F_4, N_2F_2) in decreasing order of energy. The fuel must pack in the working fluid hydrogen while both should have high heats of formation and yield products with low heats of formation. With the covalent liquids and gases, our ability to predict heats of formation is quite good - with ionic solids, the unknown contributions from lattice energy preclude this.

The Feasibility of Predicting Properties of Oxidizers by Quantum Chemical Calculations

Joyce J. Kaufman, Louis A. Burnelle and Jon R. Hamann

Research Institute for Advanced Studies
(Martin Company)
7212 Bellona Avenue
Baltimore, Maryland

ABSTRACT

The objective of this research is to gain insight into the fundamental bonding and behavior of energetic N, O, F compounds. Such questions as relative stabilities of N, O, F compounds, possible existence or non-existence of new species, ionization potentials, electron affinities, π-bonding, and charge distribution of these species have been investigated by performing LCAO-MO calculations using a gamut of theoretical techniques (both semi-empirical and rigorous) and analyzing the resulting calculated wave functions, energy levels, charges and bond orders for their pertinence to the above topics.

From these calculations it has already been possible to: 1) predict correctly the greater stability of cis-N_2F_2 relative to trans-N_2F_2; 2) predict the correct order of the differing N-F bond lengths in such diverse species as NF_2, NF_3, trans-N_2F_2 and cis-N_2F_2 and of the differing N-N bond lengths in cis- and trans-N_2F_2 (prior to knowledge of the experimental electron diffraction measurements of N_2F_2 bond lengths); 3) predict the correct order of the symmetric N-F stretch frequencies in NF_2, NF_3, trans-N_2F_2, N_2F_4 and cis-N_2F_2; 4) reproduce by calculations the experimental ionization potential of NF_2; 5) verify the supposition of π-bonding in NF_2 and NF leading to a greater N-F bond dissociation energy in these species than in NF_3.

INTRODUCTION

The objective of our research is to investigate the theoretical and quantum chemistry of energetic N, O, F compounds with the aim of providing insight into the fundamental bonding and behavior of these species so necessary for the guidance and planning of the overall experimental research project in the oxidizer field.

The first question we asked ourselves at the inception of this research was -- what are really the most important fundamental problems to be faced in the program in high-energy oxidizers. To us it seems that one of the most over-riding problems is the question of energetics -- will or will not a particular molecule be stable or perhaps so unstable it can never be isolated; and further -- what can be predicted about dissociation paths and dissociation energies of molecules. In order to tackle the problem of molecular energy calculations by what we feel is the only realistically valid approach, we have undertaken rigorous non-empirical LCAO-MO-SCF calculations of N, O, F compounds in which we shall incorporate correlation and relativistic energy corrections. I shall discuss these more fully in a moment.

However, for these compounds there are many other properties of interest for which solutions using approximate wave functions may yield results of sufficient accuracy to permit interpretation of the desired phenomena. For this reason we have also undertaken research in semi-rigorous calculations with the goal of deriving methods correctly based on the many-electron Hamiltonian but with simpli-

fying approximations for the core and integrals which will make the calculations tractable at least for medium-sized polyatomic molecules. We have also modified the semi-empirical "extended Hückel method" to include a more justifiable physical interpretation of the matrix elements as well as iterative processes which introduce a measure of self-consistency. I shall discuss this latter method in detail later, present some results of the calculations and show their good agreement with experiment.

Rigorous Calculations

The calculational technique used for the rigorous calculations is based on Roothaan's SCF method for closed- and open-shell systems.[1] Molecular orbitals are constructed as linear combinations of atomic orbitals

$$\Phi_i = \sum_\mu c_{i_\mu} \chi_\mu$$

and a configurational wave function Φ_n is represented by an antisymmetrized product wave function. There are two choices for the form of the basis atomic orbitals which are most in current usage

$$\text{Slater orbitals} \quad \chi = (2\zeta)^{n-1}(2n!)^{-1/2}\, r^{n-1}\, e^{-\alpha r}\, \Theta_{\ell,m}(\theta)\Phi_m(\varphi)$$

$$\text{Gaussian orbitals} \quad X = r^{2k} x^{\ell} y^{m} z^{n}\, e^{(-\alpha r^2)}\, \Theta_{\ell,m}(\theta)\Phi_m(\varphi)$$

Slater orbitals are better approximations to the form of actual atomic orbitals and atomic wave functions composed of sums of Slater orbitals for each atomic orbital (rather than minimal basis sets which represent each atomic orbital by a single Slater function) have been shown to be good approximations to the true atomic wave functions and to reproduce quite accurately the atomic Hartree-Fock energies. Even atomic orbitals where each atomic orbital is represented by only two Slater orbitals (the double ζ technique) combine to give fairly good approximations to the atomic wave functions[2] (although for molecular wave functions where one wishes to calculate dissociation energies one must use better than a double ζ treatment and must include some higher orbitals to allow for atomic distortion upon molecular formation[3]. All improvements to the "best-atom" wave functions increase the binding energy since they represent increased flexibility in the orbital basis set for the molecule.) The great problem in using Slater orbitals for polyatomic molecular calculations is the lack of general computational expressions for most of the three- and four-center integrals involved.

The other alternative is to use Gaussians[4] as the basis functions for the atomic orbitals. A paper by Boys in 1956[4] pointed out that a set of Gaussian functions of the form shown is complete and that the required integrals involving these Gaussians (including three- and four-center ones) can be expressed as explicit formulas. Recent calculations by Moscowitz[5] and Harrison[6] and Krauss[7] have shown that molecular wave functions based on Gaussians (GF's) can be made comparable to those based on Slater orbitals (STO's), but for similar energy values about twice as many GF's as STO's are necessary. Since our main interest is in polyatomic systems for which, as yet, three and four-center Slater integral routines are not available, we are concentrating at present on performing our rigorous molecular calculations using basis Gaussian orbitals. We have been very fortunate, through the cooperation of Dr. Moscowitz, of New York University, (formerly of MIT) in

having the MIT POLYATOM program (rigorous SCF calculations based on Gaussian orbitals) made available for our research here at RIAS and additional supplementary routines for POLYATOM have been written at RIAS. As far as orbital energies go, calculations at MIT indicated that the Gaussian bases seem to give excellent results. Therefore, we have proceeded to explore SCF Gaussian calculations for NF compounds.

Before I mention our preliminary results to date on the Gaussian SCF calculations of NF compounds, I should just like to indicate how correlation and relativistic energy corrections will enter into the estimation of dissociation energies of NF compounds.

Correlation and Relativistic Effects

$$E_{exact} = E_{HF} + E_C + E_R$$

which holds for any state of any atomic or molecular system. E_{exact} is the actual energy of the state, E_{HF} is the computed Hartree-Fock energy for the state (accounting for 99 or more of E_{exact}), E_C is the correlation energy in the state (a correction term accounting for the deficiency in the Hartree-Fock model - the antisymmetrized product form of the wave function and the Pauli exclusion principle take into account most of the correlation between electrons of like spin - but none between electrons of opposite spin) and E_R is the relativistic energy in the state (which in this definition includes spin-orbit coupling effects in addition to true relativistic effects). In calculations by Clementi[8], McLean[9] and Yoshimine[10] on such diatomic molecules as HF, LiF, BeO, it was found that the net contribution of correlation energy to the molecular binding energy (molecule minus separated neutral atoms) was very nearly equal to the correlation energy difference between the atoms separated so as to maintain the structure of electron pairs in the molecule (for example HF giving F^- and H^+ at infinite separation) and the neutral atoms in their ground states. Alternatively the correlation energy was quite close to the difference between that of a united atom corresponding to the diatomic and the neutral atoms in their ground states. Professor Sinanoglu[11] has shown that pair correlations are nearly additive and he has calculated some of these correlations non-empirically for first row atoms. Thanks especially to the work of Clementi[12] there is now a great deal of empirical knowledge of correlation energies of first and second row atoms. The lament current some few years ago (that molecular orbital wave functions would never be good enough to calculate reliably dissociation energies) is now being replaced by the more optimistic statement that the results of Hartree-Fock molecular calculations combined with empirical knowledge of correlation energies can lead to accurate predictions of dissociation energies of molecules. Considering that the entire molecular extra correlation energy (of the order of 1.7 ev per bond) contributes directly to the dissociation energy and bond dissociation energies are only about 2 to 4 ev one sees why 1) correlation energy must be taken into account and 2) why we must strive for accurate wave functions.

N-F Results

The closed-shell POLYATOM program is operational and can handle up to 50 basis orbitals. We have already run a test of NF_3 with a minimal basis set for N and F of 3s and one each p_x, p_y, p_z orbitals to check it out. The ordering of the energy levels was as anticipated, first the four inner shell orbitals, then above them levels which may be associated with the three bonds and the lone pairs on fluorine; the highest occupied orbital finally corresponds

closely to the lone pair on nitrogen. Of course, due to the fact that the basis used was minimal the calculated energy was too high. In order to improve the accuracy of the wave function, the orbitals characterizing the gaussians had to be varied and the basis expanded. We then ran calculations on NF itself with larger basis sets in order to optimize the parameters for N and F in molecular combination.

At present we are performing these calculations on NF_2 and NF_3 and in the immediate future we shall calculate cis- and trans-N_2F_2 and N_2F_4.

We shall continue our research on these rigorous calculations of NF compounds until we have satisfactorily been able to reproduce the dissociation energy of an NF compound -- probably NF_3 since this is the simplest NF molecule whose heat of formation and first bond dissociation energy have been measured directly. It was actually the apparently anomolous pattern in bond dissociation energies of NF which led originally to our theoretical interest in NF compounds. In 1961 at an American Chemical Society Symposium on Chemical Bonding in Inorganic Systems, Dr. Colburn of Rohm and Haas at Huntsville made mention of the fact that while the N-H dissociation energies in NH_3 were $D(H_2N\text{-}H) > D(HN\text{-}H) > D(N\text{-}H)$ in NF_3 the order was $D(F_2N\text{-}F) < D(FN\text{-}F)$. We postulated at that time that the reason must in large part be due to the fact that although there is virtually no π-bonding in NF_3, there must be a considerable amount of $F \rightarrow N$ π-bonding in NF_2 which is planar.[13] (Our subsequent calculations have confirmed this $F \rightarrow N$ π-bonding in NF_2). π-bonding in NF_2 would increase the N-F bond strength over that in NF_3. The closeness of ionization potentials of NF_2 and NH_2 were also both predicted to be due to $F \rightarrow N$ π-bonding in NF_2 and NF_2^+. (Incidentally, there must also be $F \rightarrow N$ π-bonding in N-F).

Semi-empirical Calculations

Good rigorous SCF calculations on polyatomic molecules are long, difficult and tedious to program, and inevitably expensive in computer time. What was needed was a simple semi-empirical approximate method for three-dimensional molecular orbital calculations.

In recent years increasing use is being made of an extended Hückel type LCAO-MO-SCF method for calculation of wave functions and energies of three-dimensional molecules (as opposed to molecules having separable π-systems). This extended Hückel-type method is based on a technique apparently originally introduced by Wolfsberg and Helmholz[14] and used over the years by Longuet-Higgins[15], extensively by Lipscomb and co-workers[16] especially Hoffman, as well by Ballhausen and Gray[17]. From a molecular orbital Φ_i built up as a linear combination of atomic orbitals χ_μ

$$\Phi_i = \sum_\mu c_{i_\mu} \chi_\mu$$

and applying the variation principle for the variation of energy the following set of equations for the expansion coefficients is obtained

$$(\alpha_\mu + ES_{\mu\mu})c_\mu + \sum_{\mu \neq \nu} (\beta_{\mu\nu} - ES_{\mu\nu})c_\nu = 0 \qquad \nu = 1,2,\text{--}M \text{ where M is the number of atomic orbitals}$$

E = energy

$S_{\mu\nu} = \int \chi_\mu^* \chi_\nu \, dv$ = overlap integral

$H_{\mu\mu} = \alpha_\mu = \int \chi_\mu^* H \chi_\mu \, dv$ = Coulomb integral

$H_{\mu\nu} = \beta_{\mu\nu} = \int \chi_\mu^* H \chi_\nu \, dv$ = Resonance integral $\mu \neq \nu$

H is an effective one electron Hamiltonian representing the kinetic energy, the field of the nuclei and the smoothed-out distribution of the other electrons.

The diagonal elements are set equal to the effective valence state ionization potentials of the orbitals in question. The off-diagonal elements, $H_{\mu\nu}$, can be evaluated in several ways:

1) In the early work on the boron hydrides the relationship

$H_{\mu\nu} = K'S_{\mu\nu}$ with $K' = -21$ ev was used. However one was forced to use inordinately high values of K' due to the requirement that K' be smaller than any diagonal matrix element. (L-H+R [15])

2) A better-approximation was to set

$H_{\mu\nu} = 0.5K (H_{\mu\mu} + H_{\nu\nu})S_{\mu\nu}$ and to use $K = (1.75 - 2.00)$ (W-H [14])

3) A similar expression

$H_{\mu\nu} = K'' (H_{\mu\mu} \cdot H_{\nu\nu})^{1/2} S_{\mu\nu}$ which differs only in second order and has certain computational advantages has also been used. (B-G [17])

4) Cusachs reported at the Sanibel Quantum Chemistry Conference last winter[18] that the repulsive terms in the W-H model which assume electron repulsion and nuclear repulsion to cancel nuclear-electron attraction, consist of one-electron anti-bonding terms only. Cusachs noted that Ruedenberg observed that the two-center kinetic energy integral is proportional to the square of the overlap integral rather than the first power. We shall comment further on this point later - since we think there may be a slightly different interpretation. However, Cusachs used to develop the approximation

$$H_{\mu\nu} = \frac{(H_{\mu\mu} + H_{\nu\nu})}{2} S_{\mu\nu} (2 - S_{\mu\nu})$$

which contains no undetermined parameters and avoids collapse.

5) At Istanbul Professor Fukui[19] also reported a new scheme

$$H_{\mu\nu} = \left\{ \frac{1}{2} \left(H_{\mu\mu} + H_{\nu\nu} \right) + K \right\} S_{\mu\nu}$$

for approximating the off-diagonal elements.

Since the valence state ionization potentials are known to be functions of the electron population at that atom we have introduced iterative schemes for the calculation of $H_{\mu\mu}$ such as:

a) $$\alpha_{\mu_a}^{R} = H_{\mu_a\mu_a}^{R} = H_{\mu_a\mu_a}^{R-1} - \left(m_{\mu_a} - q_{\mu_a}^{R-1} \right) W$$

where R is the iteration cycle number, μ_a refers to orbital a on atom μ, m_{μ_a} is the occupation number for that orbital in the ground state and q_{μ_a} is the electron population on that atom in the molecule.

b) $$\alpha_{\mu_a}^{R} = H_{\mu_a\mu_a}^{R} = H_{\mu_a\mu_a}^{R-1} + A_{\mu_a} q_{\mu_a}^{R-1} + B_{\mu_a} \left(q_{\mu_a}^{R-1} \right)^2$$

which follows a Glockler-type equation and where $\alpha_{\mu_a}^{0}$ is equal to the valence state ionization potential. The iterative cycles are continued until

$$\left| q_{\mu_a}^{R-1} - q_{\mu_a}^{R} \right| < \text{constant}$$

The off-diagonal elements can be constructed in accordance with any of the schemes indicated earlier.

Preliminary calculations of the extended Hückel-type on NF and OF compounds have led to a number of interesting and fruitful observations.

Compound	N-F Distance (Å)	N-F Symmetric Stretch cm^{-1}	Calculated N-F Overlap Population
NF_2	1.365	1074	0.45
NF_3	1.371	1031	0.41
N_2F_2-trans	1.398	1010	0.37
N_2F_2-cis	1.409 (Bauer) 1.384 (Other research)	896	0.34

Quite striking is this table comparing our calculated N-F overlap populations with experimentally measured N-F bond lengths, N-F symmetric stretch frequencies and N-F bond dissociation energies. In this table are shown our original calculations which were performed using Sanborn's estimate for the geometry of N_2F_2 in which N-F and N-N bond distances were considered to be the same for both the cis- and trans-isomers. Our calculational results based on overlap population indicate quite clearly that the N-F distance in trans-N_2F_2 should be shorter than that in

cis-N_2F_2 -- and this point was experimentally verified by Professor Simon Bauer at Cornell. Professor Bauer sent us his student's unpublished results on electron diffraction measurements of NF compounds, and asked for our theoretical interpretation of the differing N-F bond lengths. The fact that our calculated N-F overlap populations, even when using the original Sanborn estimate of identical N-F bond lengths for cis- and trans-N_2F_2, are capable of predicting correctly the order of the experimentally measured bond distances PRIOR to our knowledge of Professor Bauer's results is very encouraging. The situation seems to be similar to that explored years ago in Hückel calculations of aromatic hydrocarbons. In condensed ring systems it is possible to do an original Hückel LCAO-MO π-electron calculation assuming all bond lengths equal. From the resulting differences in calculated bond orders it is possible to predict that certain of the bonds in the rings differ in length from the others. Refined calculations can then be made using differing values of β in order to predict more closely other properties of the molecules. The correlation of overlap population with bond length even seems capable of enabling one to evaluate the validity of experimental measurements. For example, the calculated N-F overlap population in cis-N_2F_2 of 0.34 compared to 0.37 for trans-N_2F_2 would indicate that the N-F distance of 1.409 A for cis-N_2F_2 as measured by Bauer is more reasonable compared to 1.398 A for trans-N_2F_2 than is the value of 1.384 A measured by another investigator. Also the order of N-F dissociation energies is entirely compatible with the order of their calculated overlap populations. Bauer also observed differences in the N-N distances in cis- and trans-N_2F_2 and these differences are also reproduced by our original calculations.

	N=N Distance A	Calculated N-N Overlap Population
cis-N_2F_2	1.209	1.29
trans-N_2F_2	1.224	1.19

Professor Bauer noted that the shorter N=N distance in cis-N_2F_2 is entirely compatible with the greater thermochemical stability of the cis-N_2F_2. Also, our calculated total energies for

cis-N_2F_2	-535.83 ev
trans-N_2F_2	-534.80 ev

confirm the experimental order of thermal stabilities

$$\text{cis-}N_2F_2 > \text{trans-}N_2F_2$$

A further discussion of some of the salient results of these particular species is elucidating. For NF_2 we had also performed a Pariser-Parr-Pople-type SCF open-shell[21,22] (including electron repulsion) calculation for the π-orbitals only of NF_2 assuming that the unpaired electron and a pair of electrons on each fluorine were in a π-orbital with a node in the plane of the molecule. We reasoned that if we were fortunate enough to make reasonable approximations for the core, the appropriate valence state ionization potentials and the electron repulsion integrals, we might arrive at a nearly correct value for the calculated ionization potential of NF_2 which we could check with the experimentally measured value. Applying the usual correction factor necessary for π-electron ionization potentials calculated by the Pople-SCF method, we calculated the ionization

potential of NF_2 to be 11.83 ev, in excellent agreement with the experimentally measured value of 11.8 ev. When one is dealing with open-shell species, the ionization potential is no longer equal to the negative of the orbital energy of the highest occupied molecular orbital but instead must be calculated from the differences in the total energies of the species and its positive ion. (The same holds true in calculating electron affinities.) This is because, due to the coupling terms between open- and closed shells in the species, one solves two pseudo-eigenvalue equations. Without applying any correction factors, we calculated the the electron affinity of NF_2 as 1.64 - this quantity is as yet unmeasured.

The results of the three-dimensional Hückel calculation also indicated that the highest occupied molecular orbital (HOMO) (which was singly filled) was indeed a π-type orbital in the NF_2 radical. This would lend support to the validity of computing the ionization potential from the Pople-SCF π-electron energies.

N_2F_2

Three-dimensional Hückel calculations led to the interesting correlation with stretching frequencies shown earlier, trans-N_2F_2 having both a greater stretching frequency and bond order than cis-N_2F_2. Whereas the N-F π-bond orders for these two isomers are nearly identical the total overlap populations are significantly different.

We had also performed Pariser-Parr-Pople-SCF π-electron only calculations on the two N_2F_2 isomers. The coefficients of the atomic orbitals in the four π-type molecular orbitals of the three-dimensional treatment are extremely close to the coefficients obtained in both the Hückel-π and Pople-SCF π-electron only calculations on both isomers. The calculations also indicate that the HOMO is not a π-type orbital; however lying immediately above and below the HOMO are two π-type orbitals.

NF_3

From the three-dimensional Hückel calculations the order found for the orbital energies agrees with that expected: above the four inner-shell levels which may be associated with the three bonds and the lone pairs on fluorine; the highest occupied level, finally, corresponds to the lone pair on nitrogen. This is exactly the same order found in our rigorous SCF calculation using gaussian basis orbitals.

Thus, for general descriptions of bonding in N-F compounds a three-dimensional Hückel treatment leads to results consistent with the properties and behavior of known NF compounds and thus gives promise of being applicable to the prediction of the properties of new compounds.

Acknowledgement

Research reported in this publication was supported in part by the Advanced Research Projects Agency through the U. S. Army Research Office - Durham.

This research was also supported in part by the Air Force Office of Scientific Research of the Office of Aerospace Research, under Contract No. AF49(638)-1220, to whom special thanks are due for support which enabled us to develop the general techniques and the three-dimensional Hückel program.

The authors should like to thank Professor R. Daudel, Director, Centre de Mecanique Ondulatoire Appliquee and Dr. O. Chalvet and Dr. G. Bessis of the Centre for the use of their Pople-SCF program.

The authors are also indebted to Mr. Sol James, Chief of Automatic Computations, Martin Company Computing Center for arranging to have some of the computations run there and to Mr. Joe Rachuba and Mrs. Jane Flinn of the Martin Company Computing Center for their assistance in writing the programs.

References

1. a) C. C. J. Roothaan, Rev. Mod. Phys., 23, 61 (1951).
   b) C. C. J. Roothaan, Rev. Mod. Phys., 32, 179 (1960).

2. E. Clementi, J. Chem. Phys., 40, 1944 (1964).

3. R. K. Nesbet, J. Chem. Phys., 40, 3619 (1964).

4. F. Boys, Proc. Roy. Soc. (London), A200, 542 (1950).

5. J. Moscowitz, private communication.

6. a) M. C. Harrison, J. Chem. Phys., 41, 495 (1964).
   b) M. C. Harrison, J. Chem. Phys., 41, 499 (1964).

7. M. Krauss, J. Chem. Phys., 38, 564 (1963).

8. E. Clementi, J. Chem. Phys., 36, 33 (1962).

9. A. D. McLean, J. Chem. Phys., 39, 2653 (1963).

10. M. Yoshimine, J. Chem. Phys., 40, 2970 (1964).

11. O. Sinanoglu, NATO International Conference in Quantum Chemistry, Istanbul, Turkey, August 1964.

12. a) E. Clementi, J. Chem. Phys., 38, 2248 (1963).
    b) E. Clementi, J. Chem. Phys., 39, 175 (1963).

13. Joyce J. Kaufman, J. Chem. Phys., 37, 759 (1962).

14. M. Wolfsberg and L. Helmholz, J. Chem. Phys., 20, 837 (1952).

15. H. C. Longuet-Higgins and M. de V. Roberts, Proc. Roy. Soc. (London), A224, 336 (1964).

16. a) L. L. Lohr, Jr., W. N. Lipscomb, J. Chem. Phys., 38, 1607 (1963).
    b) L. L. Lohr, Jr., W. N. Lipscomb, J. Am. Chem. Soc., 85, 240 (1963).
    c) T. Jordan, W. H. Smith, L. L. Lohr, Jr., and W. N. Lipscomb, J. Am. Chem. Soc., 85, 846 (1963).
    d) R. Hoffman and W. N. Lipscomb, J. Chem. Phys., 36, 2179 (1962).
    e) ibid., 37, 2872 (1963).
    f) R. Hoffman, J. Chem. Phys., 39, 1397 (1963).
    g) ibid., 40, 2745 (1964).

17. C. J. Ballhausen and H. B. Gray, Inorg. Chem., 1, 111 (1962).

18. L. C. Cusachs, Sanibel Conference in Quantum Chemistry, January 1964.

19. K. Fukui, NATO International Conference in Quantum Chemistry, Istanbul, Turkey, August 1964.

20. R. H. Sanborn, J. Chem. Phys., 33, 1855 (1960).

21. J. A. Pople, Trans. Faraday Soc., 49, 1375 (1953).

22. a) R. Pariser and R. G. Parr, J. Chem. Phys., 21, 466 (1953).
    b) R. Pariser and R. G. Parr, J. Chem. Phys., 21, 767 (1953).

The Lattice Energy of Nitrogen Pentoxide

R. M. Curtis and J. N. Wilson

Shell Development Company
Emeryville, California

Introduction

As an ionic crystal N_2O_5 is unusual in several respects. It possesses a layer structure in which each ion is surrounded by only three neighbors of opposite charge rather than the more usual coordinations sphere of six or eight neighbors. The heat of formation is quite small, the vapor pressure is high (50mm at 0°C) and the gaseous molecule is covalent rather than ionic. These factors plus the possible effects of charge distribution within both cation and anion indicate N_2O_5 to be a particularly interesting example for application of the ionic model of lattice energy.

The Heat of Formation of NO_3^-

In applying the Born-Haber cycle to N_2O_5 to determine the lattice energy it is found that the heat of formation of the nitrate ion is the only quantity for which an experimental value is not available. This quantity is obtained from calculated lattice energies of the alkali metal nitrates. Values ranging from -78[1] to -86[2] have been reported of which the average of -84 kcal/mole due to Ladd and Lee[2] is probably the most reliable. In all these evaluations of the nitrate ion heat of formation, a simplified crystal structure is implied in which the nitrate group is treated as a point charge ion. Although Topping and Chapman[3] considered NO_3^- as $N^{+5}O_3^{-2}$ in $NaNO_3$ we have felt it desirable to consider a variable charge distribution in at least one case, $CsNO_3$, where more recent data are available.

Since the nitrate ion is not spherically symmetric, the value calculated for the heat of formation of nitrate ion from a lattice energy will depend in general on the charge distribution assigned within the ion. If the charge distribution on the ion in the crystal differs from that in the free ion, then the calculated heat of formation is likely also to be different in some degree from the true heat of formation of the free ion. Nevertheless, if the charge distribution does not change appreciably from one nitrate crystal to another, a lattice energy calculated for N_2O_5 or some other nitrate from the Born-Haber cycle should still be meaningful.

Cesium nitrate crystallizes at room temperature in a hexagonal[4] lattice but the structure has not been determined. Above 160°C it exists in a cubic modification containing eight molecules per unit cell. The structure of this form is known[5] and is the basis for calculation with later correction to 25°C. The electrostatic energy of $CsNO_3$ was computed[6] for several assumed nitrate ion charge distributions and after correcting for the electrostatic self energy of the ion the results were fitted with a second degree equation in x, the nitrogen atom charge, giving the Coulomb energy

$$E_c = -150.40 + 0.534X - 0.979X^2 \text{ K cal/mole.} \quad (1)$$

This method of calculating the Madelung energy appears to be much simpler and faster than that of deriving an analytical function of point charges and multipole terms especially with more complex structures.

Equation (1) is relatively flat between the limits x = +1 and x = 0 which correspond, respectively, to a simple resonance hybrid for the nitrate ion and to placing the unit negative charge on the oxygen atoms with a neutral nitrogen atom. The exact value assumed for the charge distribution is thus unimportant. We shall assume x = 0.17 based on a molecular orbital treatment[7] which leads to E_c = -150.3 Kcal/mole. This is almost exactly the value E_c = -150.5 obtained by assuming a simple monomolecular unit all of the $CsCl$ type with interatomic distance r = 3.89A.

The non-electrostatic terms include the van der Waals, polarization, zero point, and repulsive energies. For the van der Waals terms Ladd and Lee[2] obtained 6.8 and 0.8 Kcal/mole corresponding to the dipole-dipole and dipole-quadrupole energies based on the simple $CsCl$ pseudocell. A more elaborate calculation of these terms is possible but does not seem justified. We have choosen to neglect the polarization energy. A preliminary calculation in the case of N_2O_5 revealed the contribution from this term to be quite small and a similar result is expected for $CsNO_3$. For the zero point energy a value of 1 Kcal/mole is assumed.

For the compressibility, β, Ladd and Lee report a value of 4.6×10^{-12} cm^2/dyne, apparently for the cubic modification, based on data from Bridgman.[8] Our own extrapolation of Bridgman's results leads to $\beta = 5.0 \pm 0.2 \times 10^{-12} cm^2/dyne$ for the room temperature (hexagonal) form and we are aware of no direct measurements on the high temperature form. However, the structural difference between the two forms of $CsNO_3$ is apparently not great [4] and there is no recourse but to apply the room temperature value of β to the cubic form. In order to correct this value of β to 167°C appropriate to the lattice parameters determination we assume a temperature coefficient $\frac{1}{\beta}\frac{d\beta}{dT} = 6 \times 10^{-4}\ deg^{-1}$ similar to that for the alkali halides. Accordingly, at 167°C, $\beta = 5.4 \times 10^{-12}$ cm/dyne and the repulsive energy, following the Ladd and Lee treatment[9] is 9.3 Kcal/mole. Thus at 167°C the total energy is -150.3 - 6.8 - 0.8 + 9.3 + 1.0 + E_{th} = -147.6+E_{th} Kcal where E_{th} is the thermal (vibrational) energy. Integration of the heat capacity equation given by Kelley[10] between 25 and 167°C gives the difference in heat content of 4.5 Kcal. The Debye temperature for $CsNO_3$ is probably quite small compared to 167°C so that $E_{th} \sim 6RT$ = 5.7 Kcal/mole. Using 5RT as the heat content of the gas ions at 298°C and combining terms the standard heat reaction is:

$Cs^+(g) + NO_3^-(g) = CsNO_3(c)$; ΔH_{298} = -147.6 - 4.5 + 5.7 - 3.0 = Kcal/mole.

From the Born-Haber cycle using as standard heats of formation $\Delta H_f(Cs^+)$ = 110.1 Kcal[11], $\Delta H_f(CsNO_3)$ = -121.5 Kcal[11,12] and the above heat of reaction, one finds $\Delta H_f(NO_3^-)$ = -82.2 Kcal/mole with an estimated uncertainty of ± 1 Kcal.

If the heats of formation of $RbNO_3$ and $CsNO_3$ are revised[12] by -0.5 and -3.4 Kcal respectively, Ladd and Lee's determinations of $\Delta H_f(NO_3^-)$ become -86.5 and 85.4 Kcal/mole.

The Lattice Energy of N_2O_5

Applying the Born-Haber cycle to N_2O_5 with $\Delta H_f(NO_2^+)$ = 233.5 ±0.6[13] $\Delta H_f(N_2O_5)c$ = -10.0±.3,[13] and $\Delta H_f(NO_3^-)$ = -82.2 ±1 from above gives as the heat of formation from the gas ions at room temperature a value ΔH = -161.3 ± 1.2. This value may be taken as the lattice energy at 0°K with an added error not exceeding 0.5Kcal.

Based on the known structure[14] the Coulomb energy for N_2O_5 was calculated, as with $CsNO_3$, by assuming specific charge distributions in the ions NO_2^+ and NO_3^-, correcting for the self energy and fitting the results with a quadratic equation in X, the nitrate N atom charge and Y, the nitronium N atom charge. Thus:

$$E_c = -150.65 - 5.20X - 10.63Y + 2.278X^2 + 1.694XY - 1.520Y^2. \quad (2)$$

There is evident in equation (2) a far greater dependence on charge distribution than exists in equation (1). Examples of the Coulomb energy for several conceivable charge distributions are given in Table 1.

Table 1. COULOMB ENERGY OF N_2O_5

Configuration	N Atom Charge in NO_3^- (X)	N Atom Charge in NO_2^+ (Y)	Coulomb Energy E_c
Minimum value of E_c	2.02	-2.37	-143.3
Point charges	-1	1	-157.0
Neutral nitrogen	0	0	-150.7
Resonance bond	1	1.67	-172.7
Molecular Orbital[7]	0.17	0.58	-158.0

The minimum value of E_c, while having no apparent physical significance, indicates the least energy that can be associated with this particular hexagonal structure. The most reliable result is probably that from quantum mechanics, the last entry in Table 1. This energy is surprisingly close to that for the point charge configuration.

In the derivation of equation (2) it was assumed that the self energy of each ion and hence the charged distribution and interatomic distance are the same in the free state and in the crystal. It is quite possible that a real difference exists for the ions in these two states. There is evidence,[15] for example, of a charge shift in the nitrate ions of molten alkali metal

nitrates depending on the cation polarizability and an even greater shift is expected in going to the isolated ion. Unfortunately no quantitive estimate of this effect is available but it should be noted that the results leading to equation (2) indicate that a difference of only .01 units in charge between gas and crystal ions can lead to 10 Kcal difference in E_c.

Errors arrising from such effects are probably small for the nitrate ion, since its heat of formation was obtained from a lattice energy. The heat of formation of NO_2^+, however, is obtained from the ionzation potential and heat of formation of $NO_2(g)$; in this case no cancellation of error occurs. The agreement between calculated and observed heats of formation suggests that the error from this effect is probably small for both ions.

The complexity of N_2O_5 and the absence of compressibility or elastic constant data precludes any reliable calculation of the non-electrostatic terms in the lattice energy. It would be desirable to sum the repulsive energy over near pairs of atoms but repulsive parameters for N and O atoms are not well established and doubtless depend on the charge density at each atom. Estimates of the van der Waals energy face similar difficulties. In consequence only an approximation is possible. In the simple Born-Mayer expression[16] for lattice energy the total non-Coulomb contribution is given by $\rho E_c/R$ in which ρ is the exponential repulsive parameter and R is the interionic distance. The paremeter ρ is often taken as 0.345 A, but is known[17] to range from at least 0.27 to 0.47. The minimum interionic distance in N_2O_5 between nitrogen atoms of the two ions is 3.12A for R. This is doubtless too small and a more effective value for R is the sum of the ion radii following Kapustinskii[18] Taking $r(NO_2^+) = 1.3$A from Grison et al[14] and $r(NO_3^-) = 1.9$A from Waddington[16] gives $.345E_c/R = 17$ Kcal. This estimate is still likely to be too large in that it tends to estimate the repulsive energy rather than the total non-Coulomb energy. In the case of $CsIO_3$ a similar estimate exceeds the sum of the repulsive and van der Waals energies by a factor nine. An examination of the alkali halides reveals a gradual cancellation of the repulsive and van der Waals terms as the ion sizes increase until with CsI the sum of these two terms is nearly zero. Since the ions in N_2O_5 approximate in size to the heavier alkali and halide ions it would appear that here too there is likely a near cancellation of non-electrostatic terms. The principal evidence that the non-electrostatic energy is small in N_2O_5, however, is the close agreement between the experimental lattice energy of -161 Kcal and the Coulomb energy valves in Table 1.

It was remarked earlier that an approximate calculation had been made of the polarization energy in N_2O_5. This estimate is well under 1 Kcal/mole and thus polarization may be neglected. The sum of the repulsion and dispersion energies, based on the preceeding comments, is not likely to exceed 10 Kcal and may be much smaller. As an estimate we take 5 ± 5 Kcal. Equating the lattice energy to the thermal value indicates a required Coulomb energy of $E_c = -166 \pm 5$ Kcal/mole. In terms of equation (2) this value for E_c cannot be used to establish a unique charge distribution but leads to rather broad limits such as $X = 0$, $Y = 1.2 \pm 0.4$ or $X = 1$, $Y = 1.1 \pm 0.4$. The most reliable assignment of charge is that from quantum mechanics and the value of E_c from this charge assignment, -158 Kcal/mole in Table 1, is close to the required range of -166 ± 5 Kcal/mole.

In view of the possibility of a significant energy difference associated with the free and lattice bound ions this agreement is quite satisfactory.

Acknowledgment

Research in this paper was supported by the advanced Research Projects Agency under contract No. DA-31-124-ARO(D)-54, monitored by the U.S. Army Research Office, Durham, North Carolina.

References

1. D. F. C. Morris, J. Inorg. Mec. Chem. 6, 295 (1958).
2. M. F. C. Ladd and W. H. Lee, J. Inorg. Nuc. Chem. 13, 218 (1960).
3. J. Topping and S. Chapman, Proc. Roy. Soc. A113, 658 (1927).
4. L. Waldbauer and C. C McCann, J. Chem Phys. 2, 615 (1934)
5. R. W. G. Wyckoff,'Crystal Structures' V2, 2nd ed., 1964; John Wiley and Sons, Inc.
6. The I. B. M. 7090 Madelung constant program was kindly provided by Dr. Q. Johnson of Laurence Radiation Labs., Livermore, California. It was adopted for 7040 operation by Dr. J. H. Schachtschneider.
7. F. S. Mortimer, pvt. communication.
8. P. W. Bridgman, Proc. Am. Acad. Arts Sci. 76, 1,9 (1945).
9. M. F. C. Ladd and W. H. Lee, Trans. Far. Soc. 54, 34 (1958).
10. K. K. Kelley, U. S. Bur. Mines Bull. 584 (1960).
11. F. D. Rossini, Nat. Bureau Standards Circ. 500 (1950)
12. Revised by - 3.4 Kcal according to G. N. Lewis, M. Randall, K. S. Pitzer, L. Brewer, 'Thermodynamics', 2nd Ed., 1961, McGraw Hill, page 678.
13. D. D. Wagman, Nat. Bureau Standards, Rept. No. 7437 (1962).
14. E. Grison, K. Eriks, V. L. de Vries, Acta. Cryst. 3 290 (1950).
15. G. J. Janz and D. W. James, J. Chem. Phys. 35, 739 (1961).
16. Waddington, T. C.'Lattice Energies' in Adv. Inog. Chem. and Radiochem. 1 (1959).
17. E. C. Baughan, Trans. Far. Soc. 55, 736 (1959).
18. A. F. Kapudtinskii, Quart. Rev. 10,283 (1956).

Estimated Stability of Perfluoroammonium Ion and its Salts

J. N. Wilson

Shell Development Company
Emeryville, California

Introduction

The hypothetical salt NF_4ClO_4 would clearly be an excellent oxidizing agent if it could be made. The object of the present paper is to present some estimates concerning the stability of the ion NF_4^+ and of its salts. Our first concern is to estimate the heat of formation of the perfluoroammonium ion in the gas phase.

A rough estimate can be made on the assumption that the dissociation energy of a fluorine atom from NF_4^+ is about the same as the average bond energy in NF_3^+. From the known heat of formation and ionization potential[a] of NF_3 we obtain

(a) See thermochemical data assembled in appendix.

$$NF_3^+ = N^+ + 3F \qquad \Delta H = 119 \pm 6 = 3 \times (40 \pm 2) \text{ kcal/mole}$$

$$NF_4^+ = NF_3^+ + F \qquad \Delta H \simeq 40 \text{ kcal/mole}$$

whence the heat of formation of NF_4^+ is about 255 kcal/mole.

An alternative estimate can be made by examining trends in the dissociation energy of a fluorine atom from the series of molecules CF_2, CF_3, CF_4, and the iso-electronic series NF_2^+, NF_3^+, (NF_4^+). The somewhat uncertain data (see appendix) are shown in the following table.

Dissociation Energy of Fluorine Atom from Various Species
kcal/mole

CF_2	CF_3	CF_4
133 ± 10	95 ± 7	122 ± 2
NF_2^+	NF_3^+	NF_4^+
74 ± 9	26 ± 6	?

The assumption of a parallel behavior in the two series leads to an estimate of for the dissociation energy of fluorine atom from NF_4^+ between perhaps 40 and 85 kcal/mole and a heat of formation for the ion of 208-253 kcal/mole.

A search has been made for the NF_4^+ ion as a possible product of the ion-molecule reaction

$$NF_3^+ + NF_3 = NF_4^+ + NF_2$$

in a mass spectrometer (Consolidated Model 21-103A). Observations were made at the partial pressure of 200 microns Hg of NF_3 in the sample reservoir, with the ionization chamber operating at 260°C and with 70 volt ionizing electrons.(a)

(a) These experiments were carried out by D. O. Schissler and P. A. Wadsworth of these laboratories, whose assistance is gratefully acknowledged.

No formation of NF_4^+ was observed though in an experiment with CD_4 under similar conditions the ion CD_5^+ was clearly detected. In a similar experiment with CD_4 and NF_3 each at 200 microns partial pressure, CD_5^+ and NF_3D^+ were clearly observed but no trace of NF_4^+ was found. If failure to find NF_4^+ is due to endothermicity of the reaction written above, then $\Delta H_f(NF_4^+)$ is not much less than 230 kcal/mole. Observation of the ion NF_3D^+ implies, on the other hand, $\Delta H_f(NF_3H^+) < 225$ kcal/mole. This corresponds to a dissociation energy $D(NF_3^+\text{-}H) > 100$ kcal/mole; the dissociation energy of H from the ions NH^+ to NH_4^+ is known to fall in the range 120-135 kcal/mole.

It seems then reasonable to conclude that the heat of formation of NF_4^+ is greater than 225 kcal/mole, and probably less than 260 kcal/mole. This implies that dissociation of NF_4^+ into NF_3^+ and F should be endothermic by 35 to 65 kcal/mole, and dissociation to $NF_2^+ + F_2$ endothermic by 15 to 60 kcal/mole. The increase of entropy in the latter dissociation is estimated about 45 e.u.; this will contribute -13.5 kcal/mole to the standard free energy of dissociation at 300°K and -24 kcal/mole at 260°C. Decomposition of $NF_4^+(g)$ into $NF_2^+(g) + F_2(g)$ thus appears unlikely at 300°K but may be possible at moderately elevated temperatures and low pressures.

Let us turn now to the question of the lattice energy of salts of NF_4^+. For tetrahedral ions such as this one, the simplest approach, though an approximate one, is that proposed many years ago by Kaputinskii.(1) He assumed

(1) Kaputinskii, A., Z. Physik. Chem. B22, 257 (1933) and subsequent papers reviewed by him in Quart. Revs. 10, 284 (1956).

that for salts made up of combinations of spherical or tetrahedral ions the lattice energy could be well approximated by assigning to the crystal structure (usually unknown) a Madelung constant equal to that of sodium chloride and estimating the repulsive contribution to the lattice energy by a Born-Mayer expression similar to that which holds approximately for the alkali halides. These assumptions lead to the following expressions for the lattice energy U:

$$U = Ne^2 \mu \frac{n}{2} \frac{\nu_+\nu_-}{R_+ + R_-} \left(1 - \frac{\rho}{R_+ + R_-}\right)$$

$$= 290.2\ n \frac{\nu_+\nu_-}{R_+ + R_-} \left(1 - \frac{0.345}{R_+ + R_-}\right) \text{ kcal/formula wt.} \qquad (1)$$

μ = Madelung constant = 1.7475 for NaCl
n = Number of ions per formula
ν = Ionic charge in units of electronic charge
R = Effective ionic radius
ρ = Born-Mayer repulsion parameter (exponential repulsive potential).

This expression has turned out to be remarkably useful for correlating the heats of formation of the salts of tetrahedral ions, provided suitable values are assumed for the "ionic radii" R_+ and R_-. It was recognized by Kapustinskii and his co-workers that these quantities are not necessarily equal to the packing radii of the ions in the actual structure of the crystal; as a consequence they have come to be known as thermochemical radii. The thermochemical radius and heat of formation for a tetrahedral ion are normally determined from equation (1) and the known heats of formation of two of its salts.

In order to apply (1) to the hypothetical salts of NF_4^+ it is necessary to estimate a thermochemical radius for that ion. We have found that a fairly good correlation exists for a number of symmetrical tetrahedral ions BX_4 between the thermochemical radius R_K and the sum of (a) the internuclear distance R(B-X) between the central atom of the ion and one of its ligands and (b) the van der Waals radius, $R_W(X)$ of the ligand. This correlation, shown in Figure 1, is described approximately by

$$R_K(BX_4^{-n}) = (0.75 \pm 0.07)\text{Å} + (0.55 \mp 0.024)(R(BX) + R_W(X)) \qquad (2)$$

with van der Waals radii 1.35 and 1.41 Å assigned to F and O respectively. The form of this correlation testifies to the artificial character of the thermochemical radii R_K.

The N-F distance in NF_3 is reported to be 1.37 Å[2]; the N-C distance in the approximately tetrahedral complex $(CH_3)_3N{:}BF_3$ is reported as 1.50 Å, about 0.03 Å larger than in trimethylamine[2]. A recent x-ray crystallographic study of $(CH_3)_4N^+Br^-$ gave 1.50 ± 0.02 Å also as the N-C distance in the tetramethylammonium ion.[3] We therefore take the N-F distance in NF_4^+ as 1.40 Å.

(2) Interatomic Distances, L. E. Sutton, ed., The Chemical Society, London (1958)

(3) Johnson, Q. C., USAEC, University of California Radiation Laboratory Report No. 9350 (1960).

From this and (2) we obtain a thermochemical radius of 2.26 Å for the perfluoroammonium ion.

Stability of Perfluoroammonium Salts

$NF_4^+F^-$: The lattice energy in this approximation is 147 kcal/mole (the Goldschmidt radius of 1.33 Å for fluoride ion was used in this computation since these radii were used by Kaputinskii). The recent photodetachment value for the electron affinity of fluorine[4] yields -60.7 kcal/mole for the heat of formation of $F^-(g)$. The calculated heat of formation of the hypothetical $NF_4^+F^-(c)$ is then 17 to 52 kcal/mole. This estimate is lowered only by

(4) Berry, R. S. and Reimann, C. W., J. Chem. Phys. 38, 1540 (1963).

5 kcal/mole if the heat of formation of $F^-(g)$ is estimated from the heat of formation of KF(c) and the Kaputinskii formula. On the other hand, the standard heat of formation of $NF_3(g) + F_2(g)$ is -29.7 ± 1.8 kcal/mole; decomposition of the crystal should be exothermic by 50 to 80 kcal/mole.

$NF_4^+ClO_4^-$: The estimated lattice energy is 116 kcal/mole; a value of -88 kcal/mole is obtained for the heat of formation of ClO_4^- from the heat of formation of $KClO_4(c)$. The estimated heat of formation of $NF_4ClO_4(c)$ is then 21 to 56 kcal/mole. This is to be compared with about -30 kcal/mole for the heat of formation of $NF_3(g) + FClO_4(g)$.

$(NF_4)_2^+SO_4^=$: The Kaputinskii heat of formation of $SO_4^=$ estimated from the heat of formation of K_2SO_4 is -151 kcal/mole; the calculated lattice energy of $(NF_4)_2SO_4$ is 352 kcal/mole and its heat of formation thus -53 to +17 kcal/mole. For comparison the heat of formation of the possible decomposition products $2NF_3 + F_2O + SO_3$ is -146 kcal/mole. The heat of formation of $F_2SO_4(g)$, if it exists, is not known.

$NF_4^+BF_4^-$: The Kaputinskii heat of formation of $BF_4^-(g)$ estimated from the heat of formation of $KBF_4(c)$ (-454 kcal/mole) is -426 kcal/mole. The calculated lattice energy of $NF_4^+BF_4^-$ is 118 kcal/mole whence its heat of formation is -319 to -284 kcal/mole. This estimate is raised to -299 to -264 kcal/mole if the heat of formation of $BF_4^-(g)$ is taken to be -406 kcal/mole as estimated from a calculation of the Madelung energy of KBF_4.(5) It seems more appropriate, however, to use heats of formation estimated by the Kaputinskii approximation for use with that approximation.

(5) Waddington, T.C., "Lattice Energies", Advance in Inorganic Chemistry and Radiochemistry, Vol. 1, pp. 158-221, Academic Press, New York, 1959.

The standard heat of formation of the possible dissociation products $NF_3 + F_2 + BF_3$ is 301 kcal/mole. The entropy of dissociation of the hypothetical crystal into these products is estimated to be about 120 e.u.. Thus, even if the heat of formation of $NF_4^+(g)$ is close to the estimated lower limit of 225 kcal/mole, crystalline NF_4BF_4 should be unstable relative to its decomposition products at temperatures about 150°K. It is possible, however, that the heat of formation of NF_4^+ is above 245 kcal/mole, in which case NF_4BF_4 may not be stable at any temperature.

Conclusion: Despite the uncertainties inherent in the Kaputinskii approximation and in the estimated heat of formation of $NF_4^+(g)$, it seems safe to conclude that the hypothetical salts NF_4F, NF_4ClO_4 and $(NF_4)_2SO_4$ are unstable relative to their possible decomposition products. The compound NF_4BF_4 may possibly be capable of existence at low temperatures; its estimated stability is marginal.

Acknowledgment: The work reported here was supported by the Advanced Research Projects Agency, Department of Defense, under Contract No. DA-31-124-ARO(D)-54, monitored by the Chemistry Division, U. S. Army Research Office, Durham, North Carolina.

APPENDIX

Thermochemical Data

Table 1.

Bond Dissociation Energies D, kcal/mole

Bond	D	Refs. and Notes
NF_2-F	56 ± 3.5	1, 2
NF-F N-F	Av. 70.4 ± 1	1, 2
NF-F	69 ± 16	3
NF_2^+-F	26 ± 6	4
	23 ± 11	5
NF^+-F	74 ± 9	6
CF_3-F	122 ± 2	7
CF_3-H	102 ± 2	7
CF_2-F	~ 110	8
	95 ± 7	9
CF-F	~ 120	8
	133 ± 2	9
CF_2-CF_2	< 112	10

Table 2.

Enthalpies of Formation (300°K), kcal/mole

Substance	$\Delta H°f(a)$	Reference
NF_3	-29.7 ± 1.8	11
NF_2	8.9 ± 1.7	2
CF_4	-218 ± 1	12-15
CF_3	-116 ± 5	7
C_2F_4	-151.8 ± 1	12,16
CF_2^+	247 ± 2	17
	249	18
CF_2	-30 ± 10	19,20
	-26 ± ?	21
	< -20	22
	> -39 ± 2	17
	-39	23
CF	74.7	20
BF_3	-271.2 ± 0.5	24
	-270.1 ± 0.5	25

Table 3.

Ionization Potentials, e. v.

Substance	I_z	Ref.
NF_3	13.20 ± 0.2	4
NF_2	11.8 ± 0.1	1,6
CF_2	≤ 12.4	17

References to Tables

1) Johnson, F. A. and Colburn, C. B., J. Am. Chem. Soc. 83, 3043 (1961).
2) Kennedy, A. and Colburn, C. B., J. Chem. Phys. 35, 1892 (1961).
3) Assuming ionization potential of NF is 12.0 ± 0.2 e.v. similar to isoelectronic O_2 as suggested by Reese and Dibeler (4).
4) From difference between appearance potentials $A(NF_3^+)$ and $A(NF_2^+)$ in mass spectrum of NF_3 by Reese, R. M. and Dibeler, V. H., J. Chem. Phys. 24, 1175 (1956).
5) From heats of formation and ionization potentials of NF_3, NF_2 and F.
6) From difference between $A(NF_2^+)$ and $A(NF^+)$ in mass spectrum of N_2F_4 by Loughran, E. D. and Mader, C., J. Chem. Phys. 32, 1578 (1960) assuming that the species reacting with electrons in their experiments was NF_2 as suggested in (1).
7) Patrick, C. R., Advances in Fluorine Chemistry 2, pp. 16-18, Editors Stacey, M. Tatlow, J. C. and Sharpe, A.G., Butterworths, Washington, 1961.
8) Thrush, B. A. and Zwolenick, J. J., Trans. Faraday Soc. 59, 582 (1963).
9) From heats of formation and ionization potentials listed in Tables 2, 3.
10) Atkinson, B., J. Chem. Soc. 1952, 2684.
11) Armstrong, G. T. Marantz, S. and Coyle, F., J. Am. Chem. Soc. 81, 3798 (1959).
12) Neugebauer, C. A. and Margrave, J. L., J. Phys. Chem. 60, 1318 (1956) (-217.1 ± 1.2).
13) Scott, P., Good, W. and Waddington, G., J. Phys. Chem. 60, 1080 (1956) (-218.3).
14) Vorob'ev, A. F. and Skuratov, S. M., Russ. J. Inorg. Chem. 679 (1960) (-219.2 ± 2.3).
15) Kirkbride, E. and Davidson, F., Nature 174, 79 (1954) (-218).
16) Kolesov, V. P., Zenkov, I. D. and Skuratov, S.M., Russ. J. Phys. Chem. 36, 45 (1962).
17) Steele, W. C., J. Phys. Chem. 68, 2359 (1964).
18) Various authors have obtained values from electron impact data clustering around 249. See Hobrock, D. L. and Kiser, R. W., J. Phys. Chem. 68, 575 (1964) and references cited therein.
19) Margrave, J. L. and Wieland, K. , J. Chem. Phys. 21, 1552 (1953).
20) Value selected by McBride, B. J., Heimel, S., Ehlers, J. G. and Gordon, S., "Thermodynamic Properties to 6000°K for 210 substances involving the First 18 Elements", NASA Publication SP-3001, Office of Technical Services, Washington, D. C., 1963.
21) From $\Delta H_f(CF)$ and $D(CF-F)$ of Ref. (8).
22) From $D(CF_2-CF_2)$ of Ref. (10).
23) Edwards, J. W. and Small, P. A., Nature 202, 1329 (1964). Value accepted here.
24) P. Gross, C. Hayman, D. L. Levi, M. C. Stuart, Fullmer Research Institute Report R146/4/23 (Nov. 1960).
25) S. S. Wise, J. L. Margrave, H. M. Feder and W. N. Hubbard, J. Phys. Chem. 65, 2157 (1961).
26) Foner, S. N. and Hudson, R. L., "Free Radicals in Inorganic Chemistry" p. 34, Am. Chem. Soc. Advances in Chemistry Series No. 36, 1962.
27) Watanabe, K., J. Chem. Phys. 26, 542 (1957).

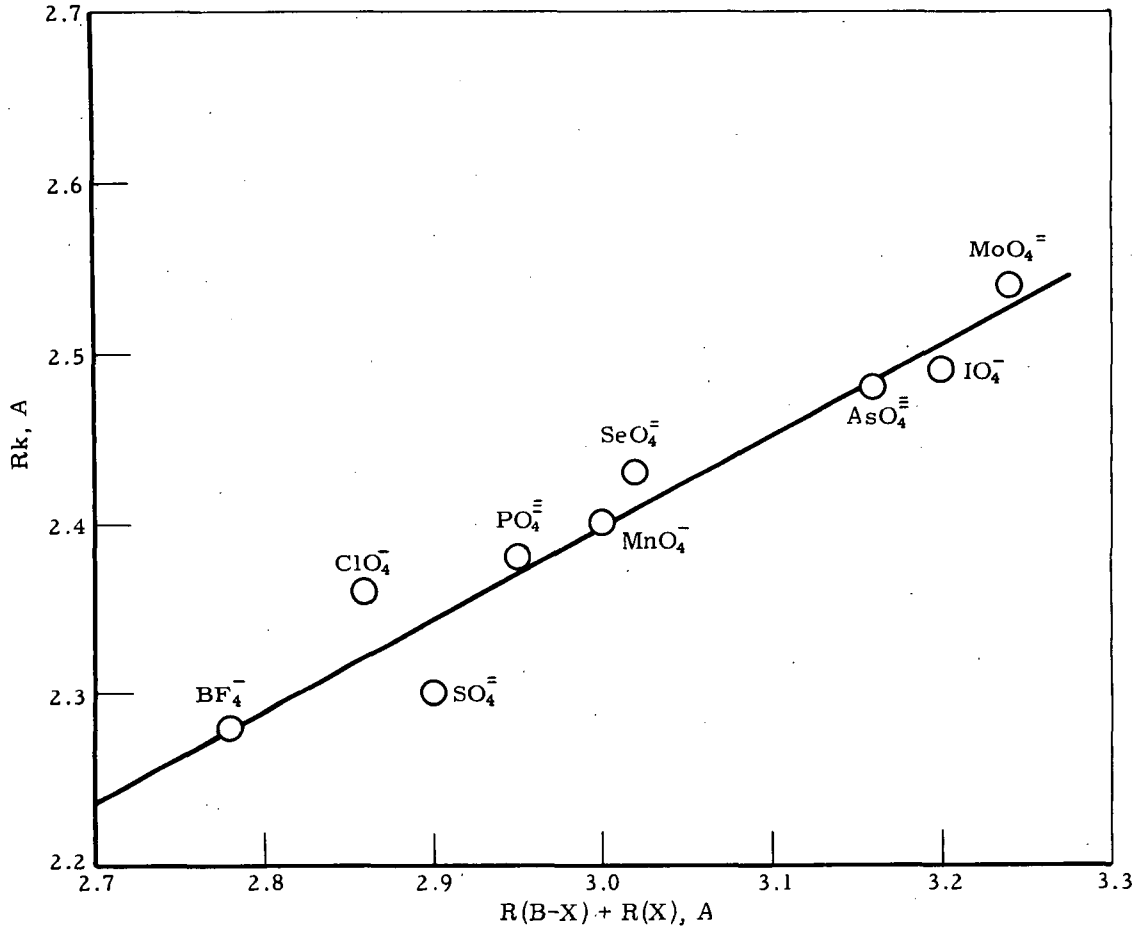

Figure 1. CORRELATION OF THERMOCHEMICAL RADIUS Rk WITH SUM OF BOND DISTANCE R(B-X) AND VAN DER WAALS RADIUS R(X) IN TETRAHEDRAL IONS

ENERGIES OF ATOMIZATION FROM POPULATION ANALYSES ON HÜCKEL WAVE FUNCTIONS

F. S. Mortimer

Shell Development Company, Emeryville, California

Abstract

Three-dimensional Hückel molecular orbital (MO) calculations have been performed on a series of molecules made from the atoms H, C, N, O, F, and Cl. Mulliken population analyses on the ground-state wave functions for the valence electrons have been related empirically to the observed energies of atomization. This is most successful when the compounds are first divided into two classes, those containing carbon and those without carbon. The population analysis is cast in the form of a charge density-bond order matrix, ρ, for all the valence electrons and for the π-electrons separately, in the case of planar molecules. The energy of atomization, E_{atom}, is then approximated as:

$$E_{atom} = A \cdot \sum_{\mu<\nu} \rho_{\mu\nu} + B \sum_{\mu<\nu} \rho^{\pi}_{\mu\nu} + C \sum_{\mu<\nu} \Delta X^2_{\mu\nu}$$

where $\rho_{\mu\nu}$ are interatomic overlap populations and $\rho^{\pi}_{\mu\nu}$ are the corresponding π-overlap populations. The $\Delta X_{\mu\nu}$ are electronegativity differences for bonded atoms. The second summation is over net positive values only. For 40 compounds not containing carbon the observed E_{atom} are fit with a mean deviation of 11.1 kcal/mole. Only constants A and C are needed. For the 22 compounds of carbon that were studied all three constants are needed, B being negative. The best fit requires a weighted function of $\Delta X^2_{\mu\nu}$ and even then the mean deviation is nearly twice that found for the compounds not containing carbon.

Introduction

The present study was initiated to see to what extent empirical molecular orbital (MO) theories of the Hückel type can provide information on the thermodynamic stability of a hypothetical unknown compound. The test, of course, has to be made on known compounds. Our interests have centered on compounds involving atoms such as N, O, F, and Cl but compounds with C and H have also been included. The results thus far have been encouraging.

It was from the papers of Lipscomb, Lohr, Hoffmann, et al[1-6] that we first learned of their work on an "extended" Hückel theory for polyatomic molecules. We also benefited from a visit to Harvard to discuss this work before their computer program became generally available. Our computer program is based on what we learned from them at that time and on our experience since then in applying it to our particular types of molecules.

The other major influence in the work has come from the papers of Mulliken and his co-workers, in particular the 1955 series[7] on population analysis of LCAO-MO wave functions and its relation to energies of atomization. As was suggested by Mulliken,[8] we have attempted to relate the calculated overlap populations to the energy of atomization for the molecule, with corrections for the polarity of the bonds.

Three-Dimensional Hückel Theory

The theory[1-6] will be outlined for molecules having n atoms with a total of P valence-shell electrons. We seek a set of molecular orbitals (LCAO-MO's), ψ, that are linear combinations of atomic orbitals centered on the atoms in the molecule. Since we shall not ignore overlap, the geometry of the molecule must be known or one must guess it. The molecule is placed in an arbitrary cartesian coordinate system and the coordinates of each atom are determined. s and p Slater-type orbitals (STO's) make up the basis and as indicated above we restrict ourselves to the valence-shell electrons for each of the atoms in the molecule. The STO's have the following form for the radial part of the function:[9][10]

$$R(r) = N\, r^m \exp(-\zeta r/a_H) \qquad (1)$$

where N is a normalization factor
m = 0 for 1 s electrons, 1 for 2 s or 2 p electrons and 2 for 3 s or 3 p electrons
ζ = orbital exponent
a_H = Bohr radius = 0.529175 A.

The mathematical representation of the basis is needed only for the calculation of the overlap matrix, which it is assumed gives a good representation of the tendency to form a bond.

If $\underline{\Phi}$ is a row vector of the atomic orbitals that make up the basis: $\varphi_1, \varphi_2 \text{ ---} \varphi_N$, then the molecular orbitals are given by an NxN matrix, $\underline{\Psi}$,

$$\underline{\Psi} = \underline{\Phi C} \,. \qquad (2)$$

$\underline{C}$ is a transformation matrix that satisfies the equations:

$$\underline{HC} = \underline{SC\epsilon} \qquad (3)$$

and

$$\underline{C'SC} = \underline{1} \qquad (C'_{ij} = C_{ji}) \qquad (4)$$

$\underline{\epsilon}$ is a diagonal matrix of the orbital energies and $\underline{S}$ is the overlap matrix of the atomic orbitals,[10]

$$S_{ij} = \int \varphi_i \varphi_j d\tau. \qquad (5)$$

It reflects the known or assumed geometry of the molecule.

The Hamiltonian matrix, $\underline{H}$, is approximated in the following way. The diagonal elements are effective valence-state ionization potentials for the s and p electrons of the atom in question. The off-diagonal elements are calculated according to one of the following options:[12]

$$1.\quad H_{ij} = -K_1 (H_{ii} H_{jj})^{\frac{1}{2}} S_{ij} \qquad (6)$$

$$2.\quad H_{ij} = K_2 \frac{(H_{ii}+H_{jj})}{2} S_{ij} \qquad (7)$$

K_1 and K_2 are adjustable parameters having an empirical value of ca 2.0.

A population analysis[7] is performed and a "charge density-bond order" matrix is calculated. The latter is an nxn matrix whose diagonal elements are "gross atomic populations" (its trace is P). The off-diagonal elements are "overlap populations". It is convenient to define a matrix, $\underline{R}$, of dimensions NxN whose elements are

$$R_{ij} = \sum_k n(k)\, C_{ik}\, C'_{kj} .$$

n(k) is the occupation number of the k^{th} MO, i.e., 2, 1 or 0. The elements of the charge density-bond order matrix, $\underline{\rho}$, can then be written:[7]

$$\rho_{\mu\mu} = \Sigma^{\mu} (\underline{SR})_{ii} \qquad (8)$$

$$\rho_{\mu\nu} = 2 \sum_{j>i}^{\mu\nu} S_{ij} R_{ij} \qquad (9)$$

The Σ^{μ} means that the sum goes over the atomic orbitals associated with the μ^{th} atom. Similarly, $\Sigma^{\mu\nu}$ means that the sum includes all terms where orbital i is on the μ^{th} atom and orbital j is on the ν^{th} atom. As indicated above, it can be shown that: trace $(\underline{SR})$ = P.

The individual diagonal elements of $\underline{\rho}$ can be associated with the atomic charges, q_μ:

$$q_\mu = p_\mu - \rho_{\mu\mu} \qquad (10)$$

where p_μ is the number of valence-shell electrons contributed by the μ^{th} atom.

If the molecule has a π-system that is completely separated by symmetry from the σ-system a separate π-electron ρ-matrix is also calculated from the π-MO's.

The H_{ii}'s are actually a function of the appropriate q_μ and when these are different from zero it is possible to make $\underline{H}(q)$ consistent with the calculated q_μ's by an iterative procedure. The $\underline{S}$ matrix is also a function of q through the dependence of the orbital exponents on q and these are also altered periodically during the course of the perturbation.

Parameters for the Calculations

The values for the valence-state ionization potentials, I_V, and their dependence on charge were obtained from the work of Hinze and Jaffé.[13][14] The values that have given the best overall results are those for ionization from s^2 or p^2 configurations. From the original tables of Hinze, Whitehead and Jaffé,[14] values of I_V were calculated for the neutral atom, A, and for A^+ and A^-. These values never quite lie on a straight line so a simple parabola was used to interpolate for any intermediate value of the charge. Table 1 gives the values used for the atoms of interest and the equations as a function of charge.

Orbital exponents for calculations (Table 1) have been taken from the paper of Clementi and Raimondi.[11] Their dependence on charge has been assumed to be that given by Slater's formulas for orbital exponents.[9] Various

values of K and the option of the arithmetic or geometric mean (equations 6 and 7) have been tried and the results cited here are all for the geometric mean (6) and for $K_1 = 2.0$.

Results

Sixty-two molecules made up of H, C, N, O, F and Cl have been used to test various relationships between calculated quantities and the observed energies of atomization, E_{atom}. Of these, 40 contained no carbon atoms and 22 contained carbon. Multiple regression techniques were used to test the significance of various relationships of the form:

$$E_{atom} = A \cdot \sum_{\mu<\nu} \rho_{\mu\nu} + B \cdot \sum^{+}_{\mu<\nu} \rho^{\pi}_{\mu\nu} + C \cdot f(\Delta X_{\mu\nu}). \qquad (11)$$

The sums of off-diagonal elements from the calculated charge density-bond order matrix, ρ, were considered both as net positive and net negative elements separately and combined. No significant advantage to separating them was found. All π-electron overlap populations are included in the first term, but the net positive ones only are considered separately as a second term. The last term introduces some function of the polarity of the molecule, $f(\Delta X_{\mu\nu})$. Approximate Coulomb energies were calculated for each molecule from the gross atomic charges, q_μ. These were tried as a third term but they were only moderately successful as a polarity function. Much more successful was one of the Pauling[15] type:

$$f^P(\Delta X_{\mu\nu}) = \sum_{\text{bonds}} \Delta X^2_{\mu\nu} \qquad (12)$$

where $\Delta X_{\mu\nu}$ is the difference between the electronegativities of the bonded atoms, μ and ν. A scale of electronegativities similar to Pauling's was determined so as to give a best fit to the data. This scale is given in Table 2; Pauling's values[15] are also given for comparison. The optimum value of C (in equation 11), however, was always less than half the value of 30 kcal/mole that was used by Pauling in deriving his electronegativity scale.[15]

A second closely-related polarity function has some advantages for the compounds of carbon:

$$f^C = f^P \left(1/b \sum^{+}_{\mu<\nu} \rho_{\mu\nu}\right); \qquad (13)$$

b is the number of bonds in the molecule and the sum is over net positive values of overlap population. f^C, then, is the Pauling function, f^P, weighted by the average bond overlap population. This was found to be important for strong covalent bonds such as occur in CO_2 but its use for weakly covalent bonds such as those in ClF_3 leads to an underestimation of their stability. An advantage to an altered set of electronegativities was also found. This set of electronegativities is also given in Table 2.

Table 3 gives a summary of the results of using equation 11 as a representation of the energies of atomization for the sixty-two test molecules. Results are quoted for both polarity functions, f^P and f^C. When the entire set of molecules is tested, f^C seems to be the preferred function; however, f^P is definitely superior for the compounds without carbon and f^C and the

alternate electronegativities are superior for the C compounds. For extrapolations to other molecules it would seem desirable to use f^P for compounds without carbon and f^C and the alternate electronegativities for those with carbon. It is interesting that the A-value is considerably larger for carbon compounds than for others. This, plus the need for a relatively large negative value for B, must reflect the particular stability of the tetrahedral hybrid orbitals used by carbon. Tables 4 and 5 give the results for the sixty-two compounds each calculated according to the preferred formula.

Only a few calculations have thus far been performed on unknown compounds, or on compounds whose energy of formation has not been reported. Our estimates for these are given in Table 6. For NCl_3, which is known to be unstable we estimate a positive energy of formation of +34 kcal while NF_3 which is stable is known to have a negative value of -31.9. CH_3NCl_2 and $(CH_3)_2NCl$ both of which are relatively stable have calculated energies of formation of -2 kcal/mole and -6 kcal/mole respectively. The recently-reported[16] molecule ClF_5, assumed to have a square pyramidal structure analogous to BrF_5, is predicted to have an energy of formation of -48 kcal/mole and the hypothetical molecule N_6, assumed to be an analogue of benzene, is predicted to have a positive energy of formation of +109 kcal/mole. It would thus be quite unstable relative to 3 moles of N_2, which probably explains why the compound has not been made. It would appear that were it not for repulsions between the lone pairs, the molecule might be stable.

Acknowledgement

The author wishes to acknowledge Dr. J. H. Schachtschneider for his contributions to this work. He wrote the first version of the computer program and has provided valuable guidance at many points during the writing of the program now being used. He also wrote the program for determining the cartesian coordinates of the atoms in a molecule from the known or assumed geometry.

The work reported here was supported by the Advanced Research Projects Agency, Department of Defense, under Contract No. DA-31-124-ARO(D)-54, monitored by the U. S. Army Research Office, Durham, N.C.

Bibliography

1. L. L. Lohr, Jr. and W. N. Lipscomb, J. Am. Chem. Soc., 85, 240 (1963).

2. J. Jordon, H. W. Smith, L. L. Lohr, Jr., and W. N. Lipscomb, J. Am. Chem. Soc. 85, 846 (1963).

3. R. Hoffmann and W. N. Lipscomb, J. Chem. Phys. 36, 2179 (1962).

4. R. Hoffmann and W. N. Lipscomb, J. Chem. Phys. 36, 2872 (1962).

5. L. L. Lohr, Jr. and W. N. Lipscomb, J. Chem. Phys. 38, 1607 (1963).

6. R. Hoffmann, J. Chem. Phys. 39, 1397 (1963).

7. R. S. Mulliken, I: J. Chem. Phys. 23, 1833 (1955), II: p 1841, III: p 2338, and IV: p 2343.

8. Papers II and IV, ref. 7.

9. J. C. Slater, Phys. Rev. 36, 57 (1930). See also summary by C. A. Coulson in "Valence", University Press, Oxford, 1953, pp 40-41.

10. R. S. Mulliken, C. A. Rieke, D. Orloff, and H. Orloff, J. Chem. Phys. 17, 1248 (1949).

11. E. Clementi and D. L. Raimondi, J. Chem. Phys. 38, 2686 (1963).

12. R. S. Mulliken, J. Phys. Chem. 56, 295 (1952).

13. J. Hinze and H. H. Jaffé, J. Am. Chem. Soc. 84, 540 (1962); J. Hinze, M. A. Whitehead, H. H. Jaffé, ibid. 85, 148 (1963); J. Hinze and H. H. Jaffé, Can. J. Chem. 41, 1315 (1963).

14. J. Hinze, M. A. Whitehead, and H. H. Jaffé. Air Force report referred to in ref. 39 of the first paper listed here in ref. 13.

15. L. Pauling, "The Nature of the Chemical Bond", 3rd edition, Cornell University Press, 1960, pp 88-95.

16. D. F. Smith, Science 141, 1039 (1963).

Table 1. ORBITAL EXPONENTS, ζ, AND EQUATIONS FOR H_{ii}

$$H_{ii} = -I_V - Aq_i - Bq_i^2$$

Atom	Orbital	ζ	I_V	A	B
H	1s	1.20[a]	13.20[a]	12.85	-
C	2s	1.6083	19.52	11.75	1.15
	2p	1.5679	9.75	10.86	1.55
N	2s	1.9237	25.58	13.31	1.78
	2p	1.9170	12.38	13.09	1.54
O	2s	2.2458	32.30	15.35	1.49
	2p	2.2266	14.61	14.77	2.17
F	2s	2.5638	39.42	17.27	2.21
	2p	2.5500	18.31	16.62	1.85
Cl	3s	2.3561	25.23	11.48	0.70
	3p	2.0387	13.92	10.44	0.24

a) I_V is altered so that the ionization potential of H_2 is moderately well reproduced, and ζ to agree with values used in the best simple LCAO treatments of H_2.

Table 2. EFFECTIVE ATOMIC ELECTRONEGATIVITIES

Atom	Electronegativity (a)	(b)	Pauling Scale[15]
H	1.70	1.7	2.1
C	-	2.3	2.5
N	3.10	2.85	3.0
O	3.45	3.45	3.5
F	4.08	3.95	4.0
Cl	2.90	3.0	3.0

(a) Determined for compounds not containing carbon. They are indicated as being significant to $\pm$ 0.05 to 0.1 unit.
(b) For compounds of carbon. Significance is ca 0.1 unit.

Table 3. CONSTANTS IN EQUATIONS FOR E_{ATOM}
(SEE EQUATION 11) AND STANDARD DEVIATIONS IN KCAL/MOLE

Calculation I uses f^P; Calculation II uses f^C.
All but one use set (a) of electronegativities from Table 2.

Calculation Type	Number of Molecules	Standard Deviation	Maximum Deviation	A	B	C
I	62	25.2	69.2	132.7 ± 1.9	-48.5 ± 6.3	10.35 ± 0.95
II		22.7	51.8	132.6 ± 1.6	-56.9 ± 5.5	15.2 ± 1.2
I*	40[a]	11.1	22.3	116.0 ± 1.1	--	11.63 ± .94
II		13.7	40.4	116.4 ± 1.4	--	17.3 ± 1.9
I	22[b]	24.4	63.8	138.2 ± 2.0	-57.8 ± 6.5	9.8 ± 1.0
II		20.0	49.2	137.6 ± 1.7	-65.2 ± 5.2	14.2 ± 1.2
II*	(c)	17.3	38.8	136.6 ± 1.5	-61.5 ± 4.5	16.8 ± 1.2

* Preferred formula for extrapolation.
a) All molecules without carbon.
b) Compounds of carbon; in each case maximum deviation is for CO_2.
c) Using alternate set (b) of electronegativities from Table 2.

TABLE 4. CALCULATED AND OBSERVED ENERGIES OF ATOMIZATION (ENAT) FOR COMPOUNDS WITHOUT CARBON. MEAN DEVIATION= 11.1 KCAL/MOLE. ELECTRONEGATIVITIES - H= 1.70, C= 2.30, N= 3.10, O= 3.45, F= 4.08, CL= 2.90

COMPOUND	SUM OVERLAP POPULATIONS ALL VALUES	+PI ONLY	SUM BOND (DELTA X)**2	ENAT(OBS) KCAL/MOLE	ENAT(CALC) KCAL/MOLE
H2	0.794	0.	0.	110.5	92.1
N2	1.791	0.905	0.	229.3	207.7
O2	0.854	0.170	0.	121.4	99.1
F2	0.281	0.	0.	39.0	32.6
CL2	0.484	0.	0.	59.7	56.1
NH3	2.105	0.	5.880	300.8	312.6
OH	0.685	0.	3.062	107.4	115.1
H2O	1.303	0.	6.125	234.3	222.4
HF	0.612	0.	5.664	141.5	136.9
HCL	0.717	0.	1.440	107.3	99.9
NO	1.205	0.417	0.122	153.4	141.2
N2O	2.482	0.918	0.122	272.6	289.3
NO2	1.951	0.420	0.245	229.0	229.1
N2O3	3.303	0.750	0.367	394.5	387.4
N2O4	4.110	0.765	0.490	472.0	482.4
N2O5	4.634	0.728	0.735	536.2	546.0
FNO	1.528	0.376	1.083	211.6	189.8
CLNO	1.505	0.373	0.162	192.8	176.5
FNO2	2.277	0.330	1.205	278.1	278.1
CLNO2	2.268	0.375	0.285	262.9	266.4
FONO2	2.681	0.344	0.764	316.6	319.9
NF	0.543	0.077	0.960	71.0	74.2
NF2	1.046	0.074	1.921	144.0	143.7
T-N2F2	2.060	0.402	1.921	251.4	261.3
C-N2F2	2.054	0.403	1.921	254.8	260.6
T-N2F4	2.438	0.	3.842	316.5	327.5
G-N2F4	2.438	0.	3.842	316.5	327.5
NF3	1.489	0.	2.881	206.0	206.2
O3	1.336	0.249	0.	149.7	155.0
OF	0.392	0.	0.397	53.0	50.1
F2O	0.739	0.	0.794	95.0	94.9
F2O2	1.227	0.	0.794	156.5	151.6
F2O3	1.680	0.	0.794	219.0	204.1
OCL	0.573	0.	0.302	65.0	70.0
CL2O	0.812	0.	0.605	103.0	101.2
CLO2	1.140	0.	0.605	126.6	139.3
CLO3	1.527	0.	0.907	177.0	187.7
CL2O7	3.347	0.	2.420	437.0	416.4
CLF	0.368	0.	1.392	62.3	58.9
CLF3	0.622	0.	4.177	128.8	120.7

TABLE 5. CALCULATED AND OBSERVED ENERGIES OF ATOMIZATION (ENAT) FOR COMPOUNDS OF CARBON. MEAN DEVIATION= 17.3 KCAL/MOLE. ELECTRONEGATIVITIES - H= 1.70, C= 2.30, N= 2.85, O= 3.45, F= 3.95, CL= 3.00

COMPOUND	SUM OVERLAP POPULATIONS ALL VALUES	SUM OVERLAP POPULATIONS *PI ONLY	SUM WT BOND (DELTA X)**2	ENAT(OBS) KCAL/MOLE	ENAT(CALC) KCAL/MOLE
C2	1.738	0.934	0.	145.0	180.0
CH4	2.991	0.	1.164	420.0	428.1
C2H6	5.025	0.	1.740	710.7	715.5
C3H8	7.056	0.	2.319	1005.3	1002.7
C4H10	9.087	0.	2.899	1300.7	1289.8
C3	2.978	1.272	0.	329.5	328.6
CN	1.741	0.916	0.527	178.0	190.3
(CN)2	4.451	1.970	0.926	504.0	502.4
C4N2	7.197	3.132	0.913	801.7	805.8
FCN	2.434	0.997	3.737	310.5	333.9
CLCN	2.495	1.022	1.015	285.3	295.0
CO	1.554	0.790	2.055	206.0	198.2
CO2	2.619	1.053	3.527	391.0	352.2
C3O2	5.149	2.087	3.560	654.0	634.7
F2CO	2.489	0.459	5.885	429.4	410.5
CL2CO	2.485	0.470	2.067	346.8	345.2
CF	0.729	0.201	1.985	117.0	120.5
CF4	2.550	0.	7.397	476.1	472.3
C2F4	3.605	0.500	8.398	582.0	602.5
C2F6	4.325	0.	10.998	775.0	775.2
CCLF3	2.475	0.	5.805	424.0	435.4
CCL4	2.338	0.	1.336	318.5	341.8

Table 6. ESTIMATED ENERGIES OF ATOMIZATION AND ENERGIES OF FORMATION FOR SOME MOLECULES

Molecule	E_a (calc) kcal/mole	$\Delta E_{formation}$ kcal/mole	Known Stability
NCl_3	205	+34	unstable
CH_3NCl_2	513	-2	stable
$(CH_3)_2NCl$	824	-6	stable
NHF_2	227	-18	stable
ClF_5	175	-48	stable
N_3*	579	+109	unknown

* Assumed to be the aromatic analog of benzene with bond lengths equal to 1.29A.

Synthetic Applications of Nitronium Tetrafluoroborate

By R. E. Olsen, D. W. Fish and E. E. Hamel
Aerojet-General Corporation
Sacramento, California

Nitronium tetrafluoroborate has been shown to be a versatile nitrating agent for nitrogen compounds, giving the corresponding N-nitro derivative when reacted with secondary aliphatic amines, an acyl aliphatic amine, a carbamate ester, a diacyl amine and primary amides. Reaction of secondary aliphatic nitronate salts with nitronium tetrafluoroborate gave mixtures of the gem-dinitro alkane and psuedonitrole, while treatment of secondary aliphatic nitronate salts with nitrosonium tetrafluoroborate yielded only the corresponding psuedonitrole.

Interest in the chemistry of stable nitronium salts, such as NO_2BF_4, NO_2AsF_6, NO_2PtF_6 and $(NO_2)_2SiF_6$, has been aroused by recent publications of Olah and co-workers concerning the preparation and use of such salts as nitrating agents for alcohols[1] and aromatics.[2,3] During an investigation into the mechanism of aromatic nitration, the perchlorate, sulfate and fluorosulfate nitronium salts were prepared and their ionic nature established spectrophotometrically;[4] however, these materials were not sufficiently stable to allow their use as nitrating agents. There appear to be no reported synthetic applications of nitronium salts to other types of organic compounds; this paper reports on the use of nitronium tetrafluoroborate to nitrate several amines, amine derivatives and alkyl nitronate salts.

The ease of preparation and stability of nitronium tetrafluoroborate has made it the nitronium salt of choice during our investigations. No difference in yields has been observed as due to an effect of different anions in nitronium salts;[2] hence, results similar to those reported here would be expected through employment of other stable nitronium salts. The only special requirements for the use of nitronium salts are the exclusion of moisture (which hydrolyzes the salt to nitric acid) and the selection of a solvent which does not react with nitronium ion.

---

1. G. A. Olah and S. J. Kuhn, Ber., 89, 2374 (1956).
2. S. J. Kuhn and G. A. Olah, J. Am. Chem. Soc., 83, 4564 (1961).
3. G. A. Olah, S. J. Kuhn, and A. Mlinko, J. Chem. Soc., 1956, 4257.
4. C. K. Ingold and E. D. Hughes, et al., ibid., 1950, 2400, and subsequent papers.

RESULTS AND DISCUSSION

Nitration reactions were carried out by adding nitronium tetrafluoroborate to a well-stirred acetonitrile or methylene chloride solution of substrate. The syntheses were carried out at low temperatures (-40 to 0°C) with short reaction times (10 minutes to one hour). The products were isolated by quenching of the reaction mixtures in ice water followed by purification using conventional techniques. In most of the reactions investigated, attempts were not made to find optimum conditions; hence, the reported yields may not represent maximum values.

Nitration of Amines and Amine Derivatives. - At present there are four good methods for the preparation of secondary nitramines. They are: (1) the oxidation of nitrosamines by peroxytrifluoroacetic acid,[5] (2) the chloride-ion catalyzed direct nitration of amines,[6] (3) the nitrolysis of dialkylamides with nitric acid,[7] and (4) the alkaline nitration of amines with acetone cyanohydrin nitrate.[8] All of the above methods have their limitations and are retarded by steric or electronic factors. The less basic aliphatic and alicyclic carbamates can be nitrated smoothly and in excellent yields with nitric acid and acetic anhydride,[9] while diacylamines are only nitrated with difficulty and in fair yields with a nitric acid - acetic anhydride mixture.[10]

Several secondary aliphatic amines of the type R_1R_2NH were converted to their N-nitro derivatives in yields ranging from 50 to 70 percent by the reaction of nitronium tetrafluoroborate with two equivalents of the amine in methylene chloride solvent. A quantitative yield of the ammonium fluoroborate salt was also recorded.

---

5. W. D. Emmons, J. Am. Chem. Soc., 76, 3468 (1954).
6. W. J. Chute, K. G. Herring, L. E. Toombs and G. F. Wright, Can. J. Research., 26B, 89 (1948).
7. J. H. Robson and J. Reinhart, J. Am. Chem. Soc., 77, 2453 (1955).
8. W. D. Emmons and J. P. Freeman, ibid., 77, 4387 (1955).
9. H. M. Curry and J. P. Mason, ibid., 73, 5043 (1951).
10. H. F. Kauffman and A. Burger, J. Org. Chem., 19, 1662 (1954).

The exact role of solvent is not clear, as the same reaction run in acetonitrile gave a quantitative yield of the ammonium fluoroborate, and little, if any, of the desired secondary aliphatic nitramine. Nitration of an acyl aliphatic amine, a urethane and a diacyl amine was accomplished in good yield by treatment of the amine derivative with one equivalent of nitronium tetrafluoroborate. Table I presents the amines and amine derivatives which were nitrated with nitronium tetrafluoroborate.

Reaction of a primary aliphatic amine, n-butylamine, with nitronium tetrafluoroborate in methylene chloride or acetonitrile did not give the desired primary nitramine, but rather gave n-butyl nitrate in 20 percent yield. However, treatment of an electronegatively substituted primary aromatic amine, picramide, with nitronium tetrafluoroborate did give the primary nitramine, N,2,4,6-tetranitroaniline, in 85 percent yield. Previously, Olah[11] had reported that aniline was vigorously oxidized by nitronium tetrafluoroborate.

---

11. G. A. Olah and S. J. Kuhn, Chem. & Ind., 1956, 98.

TABLE I

NITRATION OF AMINES AND AMINE DERIVATIVES WITH NITRONIUM TETRAFLUOROBORATE

$$R_1R_2NH + NO_2BF_4 \longrightarrow R_1R_2NNO_2 + HBF_4$$

Amine or Derivative	Yield of N-nitro derivative, %	b.p. (m.p.), °C	Ref.
Di-n-butylamine	54[a]	127-129 at 10 mm	12
Morpholine	72[a]	(51.0-52.0)	12
β,β'-Bis(cyanoethyl)amine	62[a]	(55.5-57.0)	13
Ethyl n-butylcarbamate	91	75-77 at 0.8 mm	7
n-Butylacetamide	40	45-47 at 0.5 mm	14
Succinimide	43	(92.0-93.0)	8
Picramide	85	(78.0[b] (def.))	15

[a] Methylene chloride solvent; all others used acetonitrile.

[b] Caution should be exercised during recrystallization, as N,2,4,6-tetranitroaniline has been found to deflagrate at temperatures near 50°C while in an impure state. An analytical sample was obtained by recrystallization from chloroform.

12. G. S. Myers and G. F. Wright, Can. J. Research, 26B, 257 (1948).

13. W. J. Chute, G. E. Dunn, J. C. MacKenzie, G. S. Meyers, G. N. R. Smart, J. W. Suggitt and G. F. Wright, ibid., 26B, 114 (1948).

14. E. H. White, J. Am. Chem. Soc., 77, 6008 (1955).

15. A. H. Blatt, "Data on Organic Explosives", OSRD-2014, February 28, 1944.

Nitration of Primary Amides. - Kauffman and Burger[8] have reported the preparation of materials tentatively identified as methyl N-nitrosuccinamidate and ethyl N-nitrophthalamidate by the alcoholysis of N-nitrosuccinimide and N-nitrophthalimide. The only other primary nitramide reported is N-nitroacetamide, which was described as "quite unstable in the free state".[14] In a review article on the chemistry of nitramines, Lamberton[15] has briefly commented on the rarity of primary nitramides and has speculated that this may be due to their decomposition under normal nitration conditions.

Utilizing nitronium tetrafluoroborate with acetonitrile or methylene chloride solvent in the presence of one equivalent of potassium acetate (to react with the hydrofluorobasic acid formed during the reaction), aliphatic and aromatic primary amides were converted to their N-nitro derivatives in fair yields. With the exception of N-nitroacetamide, the primary nitramides prepared thus far have proved to be relatively stable solids which decompose above their melting points. N-Nitroacetamide could be obtained only in low yields and decomposed during attempted purification. As expected, the primary nitramides were acidic in nature and could be converted to their alkali metal salts by stirring the nitramide with an acetate salt in a nonaqueous solvent. Infrared spectra were consistent with the proposed structure as the following characteristic[16] absorption bands were observed; a sharp single NH band at 3374-3390 cm^{-1}, two strong N-nitro bands at 1620-1610 cm^{-1} and 1307-1302 cm^{-1}, and a carbonyl band shifted down to 1751-1739 cm^{-1}. Table II shows the primary nitramides which were prepared, along with their yields and melting points.

---

14. V. Hinsberg, Ber., 25, 1092 (1892).

15. A. H. Lamberton, Quart. Revs., 5, 75 (1951).

16. K. Nakanishi, "Infrared Absorption Spectroscopy, Practical", Holden-Day, Inc., San Francisco, 1962.

TABLE II

NITRATION OF PRIMARY AMIDES WITH NITRONIUM TETRAFLUOROBORATE

$$RCONH_2 + NO_2BF_4 \longrightarrow RCON(NO_2)H + HBF_4$$

Primary Amide	Yield of N-nitro derivative, %	m.p., °C	Analysis					
			Calcd: C	H	N	Found: C	H	N
Acetamide	12.5[a]	65-72[a]						
2-Chloroacetamide	54.5	80-82	17.4	1.4	20.2	17.4	2.2	20.1
2,2,2-Trichloroacetamide	61.7	72-73	11.6	0.5	13.5	11.9	1.0	13.1
Benzamide	52.5	91-93	50.6	3.7	16.9	50.6	3.7	16.9
p-Chlorobenzamide	50.0	152-154	41.8	2.5	14.0	41.6	2.7	14.0
p-Nitrobenzamide	52.5	178-180	38.0	2.3	19.0	40.8	2.9	18.3

[a] Data obtained from crude reaction product which was identified as N-nitroacetamide by infrared analysis. Product decomposed during attempted purification.

Nitration of Alkyl Nitronates. - The oxidative nitration reaction of Kaplan and Shechter[17] appears to be the only general method for the preparation of secondary gem-dinitro compounds. We have found that secondary alkyl nitronates (i.e., the potassium, sodium and lithium salts of 2-nitropropane and nitrocyclohexane), when treated with nitronium tetrafluoroborate in acetonitrile give secondary gem-dinitro alkanes, although the yields were lower than those obtainable by the oxidative nitration technique and the reactions were characterized by the formation of considerable amounts of psuedonitrole byproduct. The cation appears to have a considerable influence on the reaction, as the potassium salts of 2-nitropropane and nitrocyclohexane, when treated with nitronium tetrafluoroborate, gave no gem-dinitro materials and only a 5 percent yield of the corresponding psuedonitrole. Under the same conditions, the sodium salt of 2-nitropropane gave a 50 percent yield of a one-to-one mixture of 2,2-dinitropropane and the psuedonitrole, 2-nitroso-nitropropane. With lithium isopropyl nitronate, a 35 percent yield of 2,2-dinitro-propane and a 25 percent yield of the psuedonitrole were obtained. The sodium and lithium salts of nitrocyclohexane gave similar yields of gem-dinitro and psuedo-nitrole derivatives when reacted with nitronium tetrafluoroborate. The reactions of alkyl nitronate salts with nitronium tetrafluoroborate are summarized in Table III.

$$R_1R_2C{=}NO_2M + NO_2BF_4 \longrightarrow R_1R_2C(NO_2)_2 + R_1R_2C(NO)NO_2 + MBF_4$$

M = Ka, Na, and Li

Dinitro products were separated from psuedonitroles by extraction of the reaction mixture with hexane followed by evaporation of the hexane to yield relatively pure 2,2-dinitropropane or 1,1-dinitrocyclohexane. The hexane-insoluble psuedonitroles were identified by elemental and infrared analysis and by their characteristic blue solutions in benzene.[18]

17. R. B. Kaplan and H. Shechter, J. Am. Chem. Soc., 83, 3535 (1961).

18. H. Shechter and R. B. Kaplan, ibid., 75, 3980 (1955).

Treatment of a primary alkyl nitronate (i.e., the potassium, sodium or lithium salt of 1-nitropropane) with nitronium tetrafluoroborate gave a low yield of the corresponding unstable nitrolic acid derivative which was identified by infrared analysis and neutralization with caustic to give a brilliant red solution.[19]

$$RCH{=}NO_2M + NO_2BF_4 \longrightarrow RC(NO_2){=}NOH + MBF_4$$

M = K, Na, and Li

The formation of psuedonitroles and nitrolic acid derivatives during the reactions of nitronium tetrafluoroborate led us to investigate similar reactions with nitrosonium tetrafluoroborate ($NOBF_4$). Again, the reaction of salts of secondary alkyl nitronates with nitrosonium tetrafluoroborate appeared to be influenced by the cation, as the potassium, sodium and lithium salts of 2-nitropropane when treated with nitrosonium tetrafluoroborate gave 60, 80 and 95 percent yields, respectively, of the psuedonitrole. Similar yields of psuedonitrole were obtained when salts of nitrocyclohexane were reacted with nitrosonium tetrafluoroborate. Table IV presents the experimental data obtained from the reaction of alkyl nitronate salts with nitrosonium tetrafluoroborate.

---

19. C. R. Noller, "Textbook of Organic Chemistry", W. B. Saunders and Co., London, 1958, p. 200.

TABLE III

NITRATION OF ALKYL NITRONATE SALTS WITH NITRONIUM TETRAFLUOROBORATE

$$R_1R_2C{=}NO_2M + NO_2BF_4 \longrightarrow R_1R_2C(NO_2)_2 + R_1R_2C(NO)NO_2 + MBF_4$$

Cation	Alkyl Nitronate	% Yield Dinitro	% Yield Psuedonitrole	Alkyl Nitronate	% Yield Dinitro	% Yield Psuedonitrole
Li	isopropyl	35	25	cyclohexyl	35	25
Na	isopropyl	25	25	cyclohexyl	25	25
K	isopropyl	0	5	cyclohexyl	0	5
Na	propyl	0	5[a]			

[a] Yield data estimated from weight of crude reaction product which was shown to be propylnitrolic acid by infrared analysis and neutralization to give a red solution. Product decomposed before further characterization could be accomplished.

TABLE IV

NITROSATION OF ALKYL NITRONATE SALTS WITH NITROSONIUM TETRAFLUOROBORATE

$$R_1R_2C{=}NO_2M + NOBF_4 \longrightarrow R_1R_2C(NO)NO_2 + MBF_4$$

Cation	Alkyl Nitronate	% Yield, Psuedonitrole	Alkyl Nitronate	% Yield, Psuedonitrole
Li	isopropyl	95	cyclohexyl	95
Na	isopropyl	80	cyclohexyl	80
K	isopropyl	60	cyclohexyl	60
Na	propyl	85[a]		

[a] Yield data estimated from weight of crude reaction product, which decomposed before complete characterization could be accomplished. Product tentatively identified as propylnitrolic acid by infrared and neutralization to give a red solution.

EXPERIMENTAL

Melting and boiling points are uncorrected. Reactions involving nitronium tetrafluoroborate were carried out in a dry box under a nitrogen atmosphere. Elemental analyses were conducted at the Analytical Laboratories of Aerojet-General Corporation, Sacramento, California.

Nitronium Tetrafluoroborate. - The procedure of Olah and Kuhn[2] was followed, in which nitric acid, hydrogen fluoride and boron trifluoride were allowed to react in a suitable solvent. The previously reported solvent was nitromethane; however, in view of the reported mineral acid sensitization of nitromethane toward detonation, it was decided to employ 2-nitropropane as solvent. In this modified procedure it was necessary to wash the nitronium tetrafluoroborate with Freon 113 and dry the nitronium salt for four hours at 60°C under reduced pressure (1 mm) to ensure complete removal of solvent.

At this point, it should be mentioned that occassional batches of nitronium tetrafluoroborate have exhibited poor nitrating ability. The poor reactivity has usually been associated with the sample of nitronium tetrafluoroborate adsorbing moisture, even under dry box conditions.

Preparation of Secondary Aliphatic Nitramines. - The following procedure is typical of that used during the reaction of secondary aliphatic amines with nitronium tetrafluoroborate. A solution of β,β'-bis(cyanoethyl)amine (10.0 g, 0.08 mole) in 60 ml of methylene chloride was cooled to -30°C and 5.3 g (0.04 mole) of nitronium

tetrafluoroborate was added over a ten-minute period. The mixture was stirred for one hour at 0°C, then four hours at room temperature. The hydrofluoroboric acid salt of β,β'-bis(cyanoethyl)amine, (8.3 g, 99% yield, m.p. 159-160°C) was removed by filtration.

Anal.: Calcd. for $C_6H_{10}N_3BF_4$: C, 34.2; H, 4.8; N, 19.9. Found: C, 34.8; H, 4.9; N, 21.2.

The filtrate was concentrated under reduced pressure to leave crude β,β'-bis(cyanoethyl)-nitramine, which after one recrystallization from methanol gave a product (3.3 g, 62% yield) which melted at 55.5-57.0°C (lit. value[13] 55.5-56.8°C). The other secondary aliphatic nitramines prepared, along with their yields and melting or boiling points are presented in Table I.

Preparation of Acyl N-Nitroamine Compounds. - The following procedure is typical of that employed for the preparation of acyl N-nitro derivatives. Ethyl n-butylcarbamate (4.0 g, 0.03 mole) was dissolved in 50 ml of acetonitrile, cooled to -30°, and treated with 4.0 g (0.03 mole) of nitronium tetrafluoroborate. The solution was allowed to warm, with stirring, to 0°C and quenched into 200 ml of ice water. A yellow oil separated which was dissolved in methylene chloride and dried over anhydrous magnesium sulfate. After removal of solvent, 5.0 g (91% yield) of ethyl N-nitro-n-butylcarbamate (b.p. 75-77 at 0.8 mm, n_D^{24} 1.4476, lit. value[7] n_D^{21} 1.4488) was obtained by fractional distillation under reduced pressure. Other acyl N-nitroamine derivatives, with their yields and melting or boiling points are shown in Table I.

Preparation of Primary Nitramides. - The following is typical of the procedure used for the preparation of primary nitramides. To a stirred suspension of 9.0 g (0.10 mole) of 2-chloroacetamide and 10.5 g (0.11 mole) of potassium acetate in 50 ml of acetonitrile at -35° was slowly added 15.0 g (0.11 mole) nitronium tetrafluoroborate.

The temperature was maintained at -35 to -30° for 30 minutes. Methylene chloride (25 ml) was added and the mixture allowed to warm to 10° and this temperature maintained for 30 minutes. The suspended solids were removed by filtration and the filtrate evaporated to dryness under reduced pressure. The residue was dissolved in methylene chloride and passed through a silica gel column to yield 12.5 g of a light yellow solid, m.p. 76-77°. Recrystallization from butyl chloride gave 7.4 g (54.5% yield) of a white solid, m.p. 80-82°, identified as N-nitro-2-chloroacetamide by infrared and elemental analyses. The yields of primary nitramides, their melting points and analytical data are presented in Table II.

Preparation of gem-Dinitroalkanes. - A methanolic solution of alkali metal hydroxide (Li, Na, or K) was treated with 10% excess nitroalkane and allowed to stir for 30 minutes. The solution was then evaporated to dryness in vacuo and the alkali metal alkyl nitronate dried over phosphorous pentoxide under reduced pressure (0.1 mm) for 24 hours.

(Caution: Nitronate salts may be shock sensitive and have been known to explode after prolonged storage).

Shown below is a procedure typical of that used for the preparation of gem-dinitroalkanes. A slurry of 3.3 g (0.02 mole) of lithium cyclohexylnitronate in 50 ml of acetonitrile was cooled to -35°C and 2.7 g (0.02 mole) of nitronium tetrafluoroborate was slowly added. The reaction was not exothermic and the reaction mixture turned a brilliant blue color upon the first addition of nitronium tetrafluoroborate. The reaction mixture was stirred for two hours at -30 to -40°C, then filtered to give a quantitative yield of potassium tetrafluoroborate. The filtrate was quenched into 100 ml of ice water to yield an insoluble oil, which was dissolved in methylene

chloride and dried over anhydrous magnesium sulfate. Removal of solvent under reduced pressure left a semisolid which was extracted with hexane. The hexane-insoluble residue (0.8 g, 25% yield) was a white powder identified as 1-nitroso-1-nitrocyclohexane, m.p. 78.0-79.0 (blue melt).

Anal.: Calcd. for $C_6H_{10}N_2O_3$: C, 46.6; H, 6.4; N, 17.7. Found: C, 46.4; H, 6.4; N, 18.0.

Evaporation of the hexane extract under reduced pressure followed by fractional distillation gave 1.2 g (35% yield) of 1,1-dinitrocyclohexane (b.p. 62-63° at 0.5 mm, lit. value[17] b.p. 67° at 0.7 mm). The yields of gem-dinitro and psuedonitrole derivatives obtained from the reaction of other salts of alkyl nitronates are shown in the Table III.

Preparation of Psuedonitroles. - The procedure used during the preparation of psuedonitroles was identical to that described above for the preparation of gem-dinitro alkanes, except that nitrosonium tetrafluoroborate was used in place of nitronium tetrafluoroborate. The yields of psuedonitrole obtained from the various nitronate salts are presented in Table IV.

ACKNOWLEDGEMENT

A portion of this work was supported by the Advanced Research Projects Agency and monitored by the Air Force Flight Test Center, Edwards Air Force Base, California, Contract AF 04(611)-9891.

THE DEFLAGRATION OF HYDRAZINE PERCHLORATE (1)

by

J.B. Levy, G. von Elbe, R. Friedman, T. Wallin and S.J. Adams
Atlantic Research Corporation
Alexandria, Virginia

I. ABSTRACT

Hydrazine perchlorate, like ammonium perchlorate, is a molecule containing within itself the elements of a fuel and an oxidizer. It should, therefore, like ammonium perchlorate, be capable of self-deflagration. This paper describes studies of hydrazine perchlorate deflagration and of various properties of hydrazine perchlorate pertinent to the question of its self-deflagration.

It has been found that hydrazine perchlorate will deflagrate reproducibly if a few per cent of fuel is present. Deflagration rates have been measured photographically with cylindrical strands pressed to 95-98% crystal density for ambient pressures from 0.26 to 7.7 atmospheres. A liquid layer was observed at the surface in these experiments. Steady deflagration could not be attained outside these pressure limits. Deflagration experiments were also performed with hydrazine perchlorate-catalyst mixtures.

In addition to the above experiments, vaporization rate measurements, measurements of the temperature profile of a deflagration wave at one atmosphere by means of fine thermocouples, and spectroscopic measurements of the flame temperature above a deflagrating strand were also made.

The temperature profile measurements indicate temperatures as high as 450°C in the condensed phase and are consistent with little heat release in the condensed phase. The vaporization measurements are consistent with a dissociative vaporization of hydrazine perchlorate. The flame temperature found was 2275 ± 50°K in satisfactory agreement with the value of 2224°K calculated on the basis of thermodynamic equilibrium in the products.

The above results are discussed in terms of the mechanism of the deflagration process.

II. INTRODUCTION

We are engaged in a general program of research whose goal is the understanding of the factors that govern the nature of the deflagration of composite solid propellants. Our efforts have been devoted to studies of the oxidizer alone, ever since early observations that ammonium perchlorate deflagrated as a monopropellant at rates comparable to those found for propellant formulations containing it (2). Earlier work in this laboratory dealt with the self-deflagration of ammonium perchlorate (3). We report here on studies with the related, but more energetic, material--hydrazine perchlorate.

Hydrazine perchlorate is a white crystalline solid melting at 140-142°C. It forms a hemihydrate which can readily be dehydrated at 64.5°C under vacuum. It has been reported (4) that dry hydrazine perchlorate can be detonated by shock or friction and that it has a shock sensitivity comparable to that of initiating explosives. We have observed the usual precautions in handling this material and have experienced explosions with it only under extreme conditions, i.e., in certain deflagration experiments. However, it is a very energetic material and must be handled with great care.

The thermal decomposition of hydrazine perchlorate has been investigated and ammonium perchlorate found to be a major product (5).

We know of no studies of the self-deflagration of hydrazine perchlorate. The results reported here are concerned with studies of pure hydrazine perchlorate and hydrazine perchlorate containing small amounts of additives.

III. EXPERIMENTAL PART

A. Preparation of Hydrazine Perchlorate

Hydrazine perchlorate was prepared by titrating a solution of 85% hydrazine hydrate to a pH of 3.2 with 40% perchloric acid. This yielded a stock solution which could be stored indefinitely. Hydrazine perchlorate was precipitated by pouring a volume of this solution into five volumes of isopropanol at 0°C. The hydrazine perchlorate was filtered, washed with cold isopropanol and vacuum dried at 80°C.

The material was analyzed iodometrically (6). Purities > 99%, as indicated by the analysis, were obtained. The melting point was 142-143°C.

B. Processing of Hydrazine Perchlorate

The hydrazine perchlorate used for the deflagration measurements was prepared in the form of small spherical particles of fairly uniform size distribution by means of a melt-shot apparatus copied from one in the literature. In this apparatus, solid hydrazine perchlorate is fed into a spinning aluminum dish maintained at a temperature above the melting point of hydrazine perchlorate and fitted with a small lateral hole in the side which permitted the ejection of the molten spheres which cool as they fly through the air. It was found that 160°C was a satisfactory temperature for the dish. With the dish spinning at 2400 RPM the particle sizes of the spheres obtained, as determined by microscopic examination of a random selection, varied from 50-300μ. Analysis of material prepared in this way indicated that no decomposition occurred during the shotting process.

C. Strand Preparation

Strands were either tamped or pressed. Tamped strands were prepared by pouring small increments of material into a tube and tamping each increment gently with a Teflon rod. Pressed strands were prepared in a steel mold by means of a hydraulic press. Pressures of ~ 40,000 psi gave strands of 95-98% of crystal density which was considered adequate. Pressing operations were performed remotely.

The mixtures of hydrazine perchlorate and the fuels or catalysts were prepared by mixing the hydrazine perchlorate shot with the finely-ground other ingredients in an ordinary vee mixer for several hours. The uniform deflagration rates observed with the various mixtures attest to the homogeneity of strands prepared in this way.

D. Sublimation Experiments

The sublimation experiments were performed with a conventional cold-finger vacuum sublimation apparatus, with a removable cold finger. The apparatus was evacuated by an oil pump to about 5 microns, lowered into a thermostat and the timer started.

Two sublimation apparatuses were used. At first a fairly small one with a cross sectional area of 0.5 cm^2 was used to keep the amount of hydrazine perchlorate required down to about 0.5 g. Subsequently a larger apparatus having a cross-sectional area of 4.90 cm^2 was used with amounts of hydrazine perchlorate of the order of 1.5 - 2.0 g.

At the conclusion of the experiment the sublimate was carefully removed from the cold finger and weighed. The weight of the residue was found by weighing the outer tube, washing out the residue and re-weighing the tube. The analyses were performed by iodometry.

E. The Flame Temperature Measurements

A tungsten ribbon filament lamp that had been calibrated by the National Bureau of Standards for the temperature range 1100 - 2300°C was used for these measurements, which were performed in the conventional manner (7).

IV. RESULTS

The experiments performed in this program are grouped into (a) experiments in which vaporization rates of pure hydrazine perchlorate were measured; (b) deflagration rate measurements; (c) temperature profile measurements; and (d) flame temperature measurements.

A. Vaporization Rate Measurements

These experiments were performed in the glass sublimation apparatuses described in the Experimental Part. The surface area of the liquid was quite undisturbed by bubbles during these experiments and its magnitude was constant during an experiment. The temperature of the liquid was assumed to be that of the bath in which the apparatus was immersed. The results are given in Table I.

TABLE I

Vaporization Rates of Hydrazine Perchlorate

Temp. (°K)	Area (cm^2)	Duration (sec)	Weights in Grams			% recov.	% Hydrazine Perchlorate in		10^6 × Rate of Vaporization (g/cm^2-sec)
			Charged	Sublimed	Residue		Sublimate	Residue	
453	4.90	18,900	1.56	0.22	1.32	99	99.8	99.4	2.38
463	0.50	21,240	0.244	0.073	0.163	97			6.85
473	4.90	18,900	1.70	0.54	1.14	99	95.0	99.0	5.84
492	0.50	2,220	0.239	0.036	0.200	99			32.4
508	4.90	2,400	1.65	0.83	0.79	98	99.0	100.0	70.5

The relation between vaporization rate and vapor pressure is given by $g = \alpha P \sqrt{\frac{M}{2\pi RT}}$ (8).

g = vaporization rate in g cm^{-2} sec^{-1}

α = evaporization coefficient

P = vapor pressure in dynes cm^{-2}

M = molecular weight of vaporizing species

T = absolute temperature

R = gas constant in ergs $mole^{-1}$ deg^{-1}

This expression can be written,

$$g\sqrt{T} = \alpha\sqrt{\frac{M}{2\pi R}}\ P$$

For many liquids α has been found to be unity. However a very low value for this quantity has been calculated (9) for ammonium chloride and, since very few species that are chemically similar to hydrazine perchlorate have been investigated, we do not feel justified in assigning a value of unity for α in the present case.

It is of interest to see how the parameter $g\sqrt{T}$ varies with T. Since it is proportional to P, we would expect a Clausius-Clapeyron relationship to hold, if α were constant, and in Fig. 1 we plot $\log\left(g\sqrt{T}\right)$ vs 1/T. The data are fairly linear and the line in Fig. 1, which was drawn visually, corresponds to the equation:

$$\log_{10}\left(g\sqrt{T}\right) = 10.0 - \frac{6475}{T}$$

The slope of the line is a measure of the heat of vaporization ΔH_v and leads to a value of 29.6 kcal/mole for this quantity. The corresponding value for ammonium perchlorate is 29 kcal/mole (10). It is of interest to compare the above value for ΔH_v to that calculated for the vaporization process. If we consider that hydrazine perchlorate vaporizes with dissociation, as is believed to be true for ammonium perchlorate, the equilibrium is

$$N_2H_5ClO_4(l) \rightleftharpoons N_2H_4(g) + HClO_4(g)$$

The enthalpy change for this process would be $2\Delta H_v$ or 59.2 kcal/mole. The heat of formation of crystalline hydrazine perchlorate is -42.5 kcal/mole (11) and a value of 3.84 kcal/mole has been reported for the heat of fusion (12). The heat of formation for the liquid is thus -38.7 kcal/mole. The values for gaseous perchloric acid and gaseous hydrazine are -1.1 (13) and 22.75 kcal/mole (14) respectively. These values yield 60.4 kcal/mole as the enthalpy change in the above equilibrium. The agreement with the experimental value supports our belief that the vaporization rates are proportional to the vapor pressure and that the vaporization process is dissociative.

B. Deflagration Rate Measurements

Deflagration rates were measured from motion picture records of the deflagration experiments. The lengths of strands used were in the range of 1.5 - 2.0 cm. In all cases the linear deflagration rate was determined from the slope of the curve of length deflagrated vs. time. These curves were all linear, i.e., the deflagration rates were constant over the length of the strand. In all the deflagration experiments a molten layer could be seen at the surface of the deflagrating strand. Gas evolution within the layer was so vigorous that the liquid layer never appeared transparent but rather like a foam. The liquid-solid interface was distinct however and the rate measurements were made by measuring the regression rate of this interface.

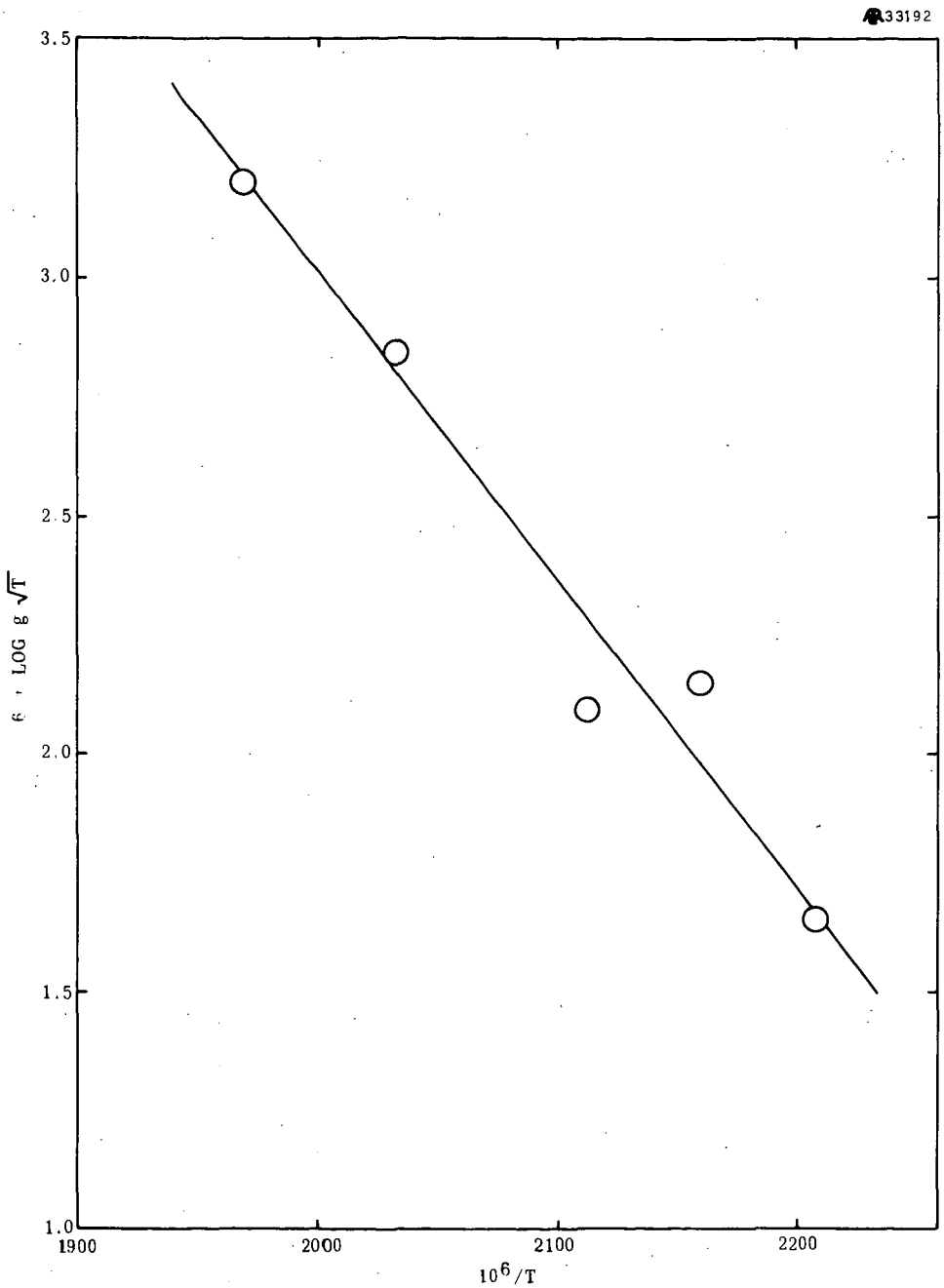

Figure 1. The Rate of Vaporization of Hydrazine Perchlorate.

1. The Deflagration of Pure Hydrazine Perchlorate

The behavior of pure hydrazine perchlorate, i.e., material containing no additives, was unreproducible. Smooth deflagration of tamped (ρ = 1.1 - 1.3 g/cc) and pressed(ρ = 1.8 - 1.9)g/cc strands of hydrazine perchlorate was attained for pressures from 0.25 to 4.3 atmospheres but at a subsequent time strands prepared and ignited in the same way did not propagate deflagration. When this was observed, experiments were performed with strands preheated to 50°C. Smooth deflagration was attained at two, four and six atmospheres but these results too were not reproducible at a later date.

2. The Deflagration of Hydrazine Perchlorate-Additive Mixtures

a. Fuel Additives

In the case of ammonium perchlorate, it has been found (15) that at pressures below that at which pure ammonium perchlorate will sustain deflagration, ammonium perchlorate-fuel mixtures containing of the order of 5% fuel do deflagrate smoothly. Paraformaldehyde was the most effective of the fuel additives in promoting deflagration and for that reason experiments were performed with mixtures of hydrazine perchlorate and various formaldehyde polymers.

Experiments with paraformaldehyde were unsuccessful because it was found that when these additives were mixed with hydrazine perchlorate the mixture became yellow and the consistency changed from that of the original powders to that of a dough. S-trioxane, a more stable formaldehyde polymer than paraformaldehyde, gave a less reactive mixture than paraformaldehyde, but the results were still unsatisfactory. Del-rin*, a stabilized formaldehyde polymer, proved even less reactive than S-trioxane. Magnesium oxide was added to hydrazine perchlorate-Del-rin mixtures on the theory that acidity in the hydrazine perchlorate might be responsible for the reaction occurring. It was found that mixtures of 94.5% hydrazine perchlorate - 0.5% MgO - 5% Del-rin were stable and a series of experiments was performed with this mixture.

Other fuel-type additives were effective in promoting the deflagration of hydrazine perchlorate. Experiments have been performed with thiourea and naphthalene. The results of the deflagration experiments for preheated pure hydrazine perchlorate and for the hydrazine perchlorate-fuel mixtures are summarized in Table II and Fig. 2. The strands used were all pressed to about 95% of the crystal density, i.e., to a density of about 1.85 g/cc.

* DuPont trade name

TABLE II

Deflagration Rates for Hydrazine Perchlorate

No.	Composition	ρ (g/cc)	P (atm)	$\dot{r}$ (cm/sec)	$\dot{m}$ (g/cm^2-sec)
1	5% Del-Rin 0.5% MgO	1.87	0.26	0.01-0.02	0.02-0.04
2	5% Del-Rin 0.5% MgO	1.85	0.52	0.11	0.21
3	pure HP preheated to 69°C	1.87	1.0	0.24	0.45
4	5% Del-Rin 0.5% MgO	1.85	1.0	0.22	0.41
5	5% Del-Rin 0.5% MgO	1.85	1.0	0.22	0.41
6	2% Thiourea	1.86	1.0	0.17	0.32
7	5% Naphthalene	1.83	1.0	0.21	0.38
8	20% Thiourea	1.79	1.0	0.18	0.32
9	preheated to 50°C	1.91	2.0	0.52	0.98
10	5% Del-Rin 0.5% MgO	1.85	3.0	0.56	1.0
11	5% Del-Rin 0.5% MgO	1.85	4.3	0.90	1.67
12	preheated to 50°C	1.91	6.0	1.29	2.48
13	5% Del-Rin 0.5% MgO	1.85	7.0	1.39	2.5
14	5% Thiourea	1.82	7.7	1.73	3.18
15	10% Thiourea	1.81	7.7	1.21	3.1

Deflagration rates are given for pressures ranging from 0.26 atmospheres to 7.7 atmospheres. The experiment at 0.26 atmospheres yielded a curve of length-deflagrated vs. time that was somewhat concave upward. The rate cited is thus a rather crude value but is of interest because of the low pressure. All the other rates were constant. Attempts to measure rates at higher pressures than 7.7 atmospheres resulted either in a complete lack of ignition or in a deflagration that proceeded down the sides of the strands leaving a central unburned core.

Fig. 2 shows that all the data fall fairly well around a single line, $\dot{r} = 0.22\ P$, where $\dot{r}$ is in cm/sec and P is in atmospheres.

b. The Effects of Catalysts

It has been found that copper chromite, potassium dichromate, and magnesium oxide promote the deflagration of hydrazine perchlorate. Since none of these additives has any fuel content, they must be considered to be catalysts. The results of experiments with these additive species are shown in Table III. Experiments were performed both with pressed ($\rho \approx 1.9$ g/cc) and tamped ($\rho \approx 1.1$ g/cc) strands.

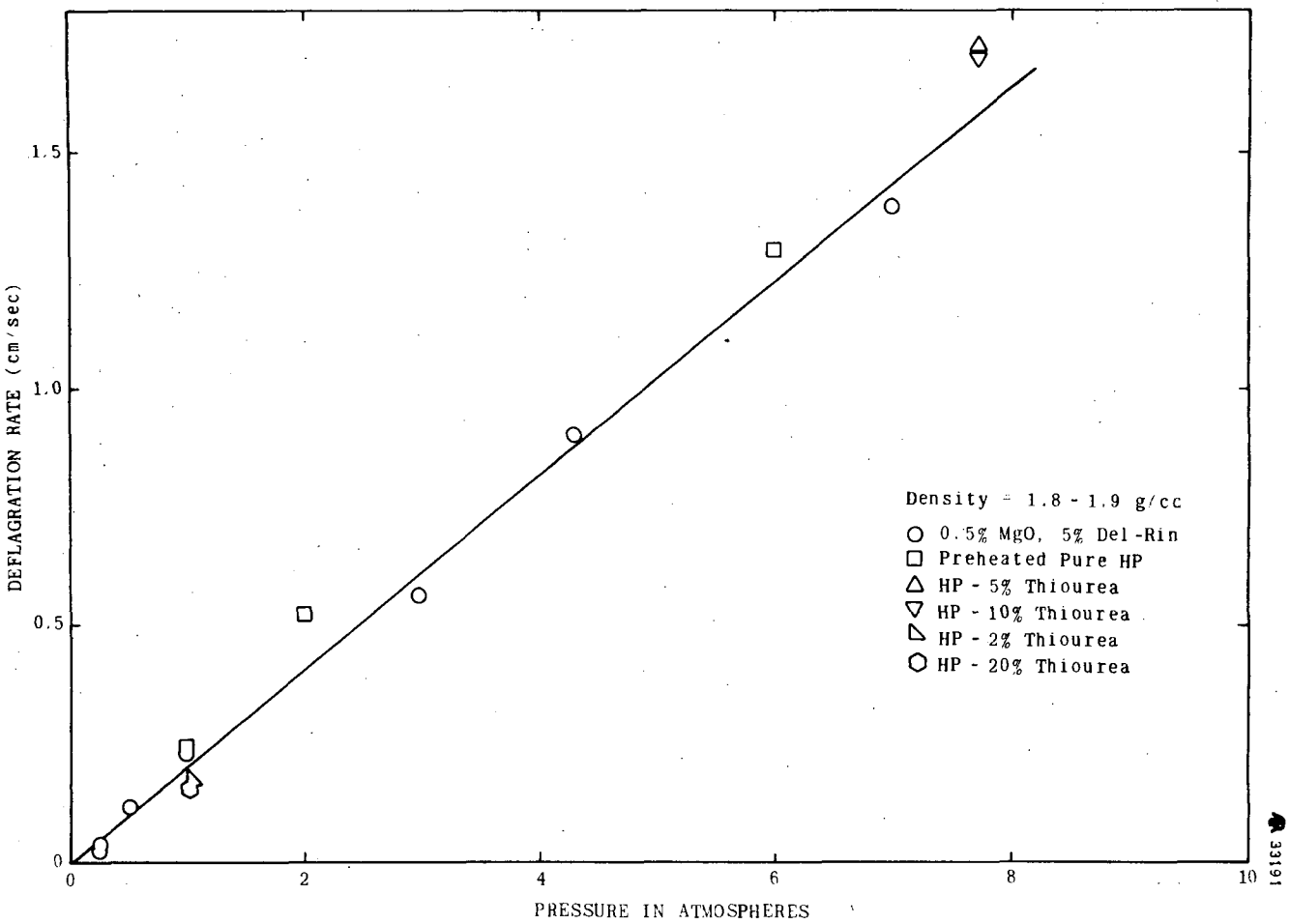

Figure 2. The Rate of Deflagration of Hydrazine Perchlorate With Small Amount of Fuel.

TABLE III

The Effect of Catalysts on the Deflagration of Hydrazine Perchlorate

No.	Composition (% of additives)	ρ (g/cc)	P (atm)	$\dot{r}$ (cm/sec)	$\dot{m}$ (g/cm^2/sec)
1	2.5% $CuCrO_2$	1.13	1	did not deflagrate	
2	5% $CuCrO_2$	1.10	1	1.20	1.32
3	5% $CuCrO_2$	1.93	1	0.71	1.37
4	5% $CuCrO_2$	1.95	0.52	0.36	0.69
4a	5% $CuCrO_2$	1.93	2	exploded	
5	2.5% $K_2Cr_2O_7$	1.17	1	did not deflagrate	
6	5% $K_2Cr_2O_7$	1.19	1	0.75	0.89
7	2% MgO	1.90	1	0.26	0.50
8	5% MgO	1.91	1	0.21	0.59
9	10% MgO	1.89	1	0.35	0.66
10	20% MgO	1.86	1	partial deflagration	
11	2% CaO	1.31	1	0.12	0.16

It may be noted that for copper chromite and potassium dichromate a minimum of around 5% catalyst was necessary in order to attain steady deflagration; however when deflagration did occur the rate was high compared to the case for fuel-promoted deflagration. It may be noted too, table entries 2 and 3, that for strands containing 5% copper chromite but having different densities, the mass deflagration rates agree well while the linear rates do not. It thus seems satisfactory to compare mass rates for strands of different densities. A comparison of this type shows that potassium dichromate is a powerful catalyst but not as powerful as copper chromite.

Magnesium oxide exerts quite a different effect than do the above catalysts. Thus less of it, 2%, is required to promote steady deflagration, but it is not capable of producing as spectacular a rate as copper chromite or potassium dichromate, even in amounts as great as 10%.

The effect of calcium oxide was briefly examined since it is chemically similar to magnesium oxide. A tamped strand deflagrated at 1 atmosphere to give a somewhat lower rate, i.e., as compared to the curve of Fig. 2. Calcium oxide is quite deliquescent and there were indications in this experiment of some moisture absorption.

In a side experiment to see if there was any generality to the effect of magnesium oxide, a tamped strand of hydrazine nitrate containing 2% magnesium oxide was found to deflagrate steadily at 0.04 cm/sec (ρ = 0.93 g/cc, $\dot{m}$ = 0.037 g/cc sec) while pure hydrazine nitrate would not propagate deflagration.

3. The Temperature Profile Measurements

Temperature profiles of the deflagration wave have been made using thermocouples of 0.0005-inch Pt - Pt, 10% Rh wires joined in a fused bead of approximately 0.001-inch diameter. The voltage changes were recorded by a Visicorder which registers voltage changes by the deflection of a light point on a moving film. The deflagration rates were measured simultaneously so that it was possible to convert temperature-time records to temperature-distance records. The turbulence of the liquid layer as observed in the deflagration rate measurements indicated that one could not expect a smooth temperature-time record. Figures 3 and 4 illustrate the type of record obtained. There are some irregularities in the curves, but the data are not too erratic for analysis.

Fig. 3 shows tracings of the records obtained at 0.5 atmospheres with a pressed strand of 94.5% hydrazine perchlorate, 5% Del-Rin, 0.5% Magnesium Oxide, ρ = 1.85 g/cc and Fig. 4 shows the tracing of the record obtained for a tamped strand of the same composition, ρ = 1.24 g/cc, at one atmosphere. In Fig. 5 and 6 are shown the experimental data converted to a temperature-distance function by means of the measured deflagration rates.

The solid curves in Figs. 5 and 6 are the theoretical curves obtained for indicated values of thermal diffusivity of the solid. The following treatment has been applied. The temperature gradient within the zone bounded by the deflagrating surface on the one hand and ambient temperature on the other can be written

$$k \frac{d^2T}{dx^2} - c\rho r \frac{dT}{dx} + q_c = 0$$

where

k = coefficient of heat conduction

c = specific heat

ρ = density

q_c = heat produced within the zone

T = temperature at point x

r = deflagration rate

If $q_c = 0$, the above on integration yields

$$\ln \frac{T_2 - T_u}{T_1 - T_u} = \frac{r}{K} (x_2 - x_1)$$

where $K = \frac{k}{cp}$ = thermal diffusivity, T_2 and T_1 are the temperatures at point x_2 and x_1, and T_u is the ambient temperature.

It is possible to evaluate K for the particular experimental data and to fit a T - x curve to the points. As Figs. 5 and 6 show, the values for K that give the best fits are 0.0012 cm^2/sec for the pressed (ρ = 1.85 g/cc) strand and 0.0018 cm^2/sec for the tamped (ρ = 1.24 g/cc) strand. These values can be compared to the value of 0.00285 cm^2/sec which can be calculated for ammonium perchlorate of crystal density, from reported values (16) of heat capacity and thermal conductivity. The values found here thus appear to be of the right order of magnitude.

The curves of Figs. 5 and 6 fit the data fairly well. Thus Fig. 5 gives no indication of heat release in the condensed phase below 450° C. Fig. 6 shows the same result at least to 400° C. It may be further noted that at 0.5 atm, for the pressed strand, Fig. 5, the condensed phase reaction zone was about 0.5 mm thick while at one atmosphere, for the tamped strand, it was about 0.3 mm thick.

4. Temperature Profiles for Catalyzed Strands

Fig. 7 shows the temperature-time records of a hydrazine perchlorate-2% MgO strand at one atmosphere. The distinctive feature is the thickness of the reaction zone ~1.6 mm. This may be compared to Fig. 4 for the hydrazine perchlorate-5% Del-Rin-0.5% MgO strand where ambient pressure was also one atmosphere but the zone thickness was about 0.3 mm.

5. Flame Temperature Measurements

Thermodynamic calculations of the nature of the products of hydrazine perchlorate self-deflagration at a series of processes were performed by an IBM-7090 computer program. The results are shown in Table IV. The calculations were made assuming constant-pressure adiabatic combustion to give equilibrium products. As Table IV shows the flame temperature at 1 atmosphere is 2245.5° K; this is about 800° higher than that for ammonium perchlorate (2b).

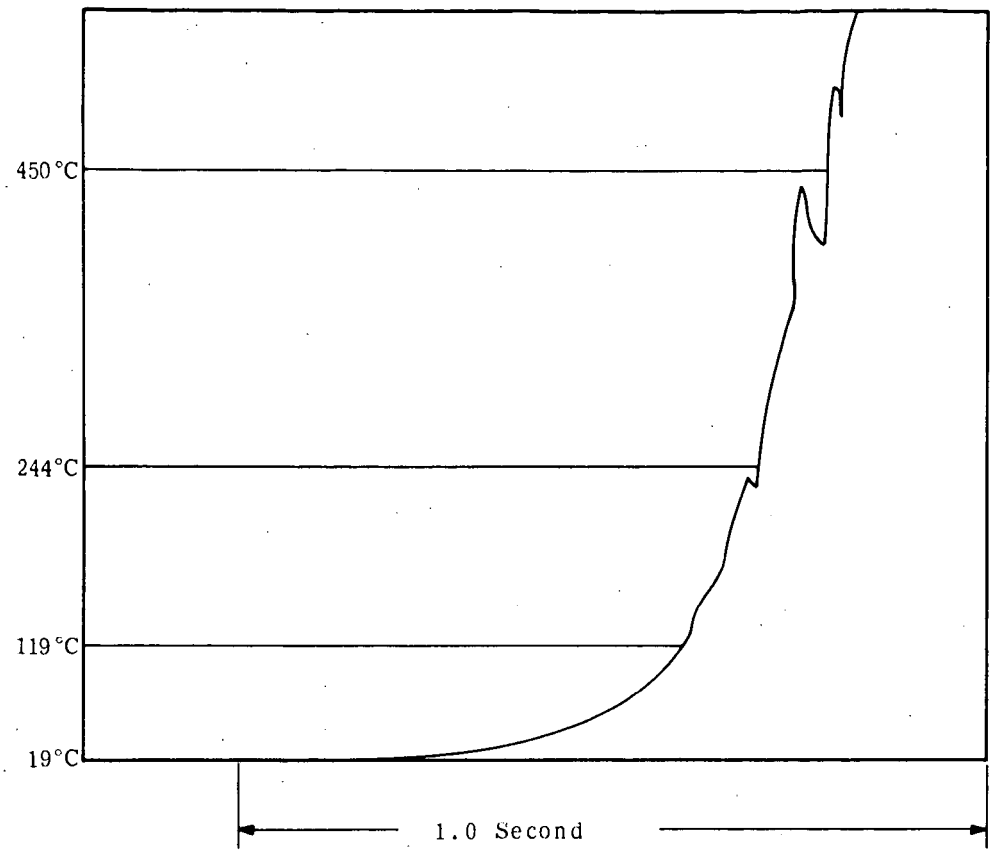

Strand Composition: 94.5% Hydrazine Perchlorate
5% Del-Rin, 0.5% Magnesium Oxide
Density = 1.85 g/cc
Pressure = 0.5 Atmosphere
Deflagration Rate = 0.09 cm/sec

Figure 3. Tracing of Thermocouple Record of Hydrazine Perchlorate Deflagration Wave.

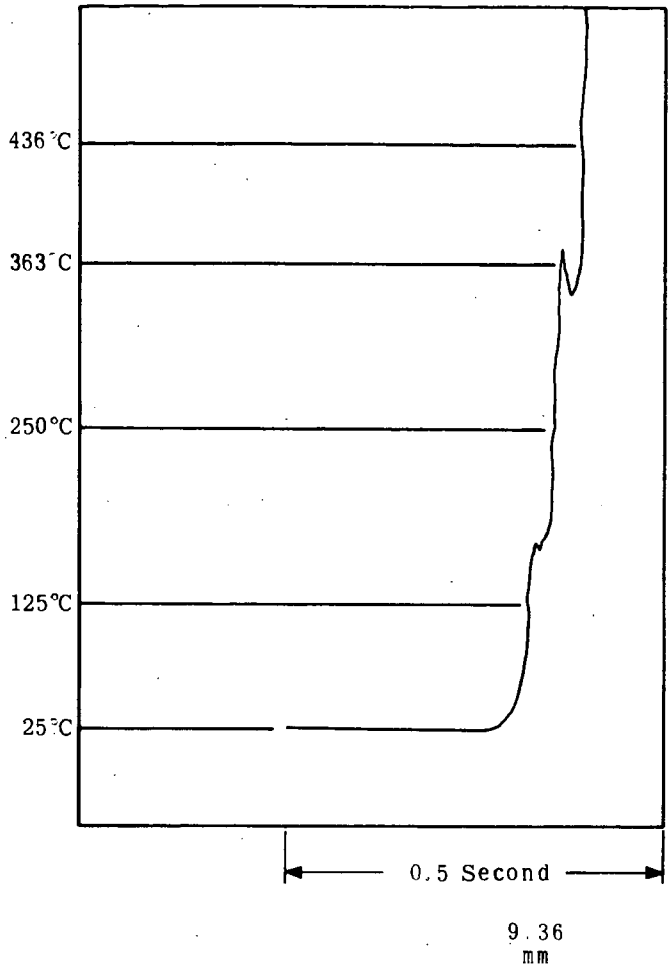

Strand Composition: 94.5% Hydrazine Perchlorate
5% Del-Rin, 0.5% Magnesium Oxide
Density = 1.24 g/cc
Pressure = 1 Atmosphere
Deflagration Rate = 0.30 cm/sec

Figure 4. Tracing of Thermocouple Record of Hydrazine Perchlorate Deflagration Wave.

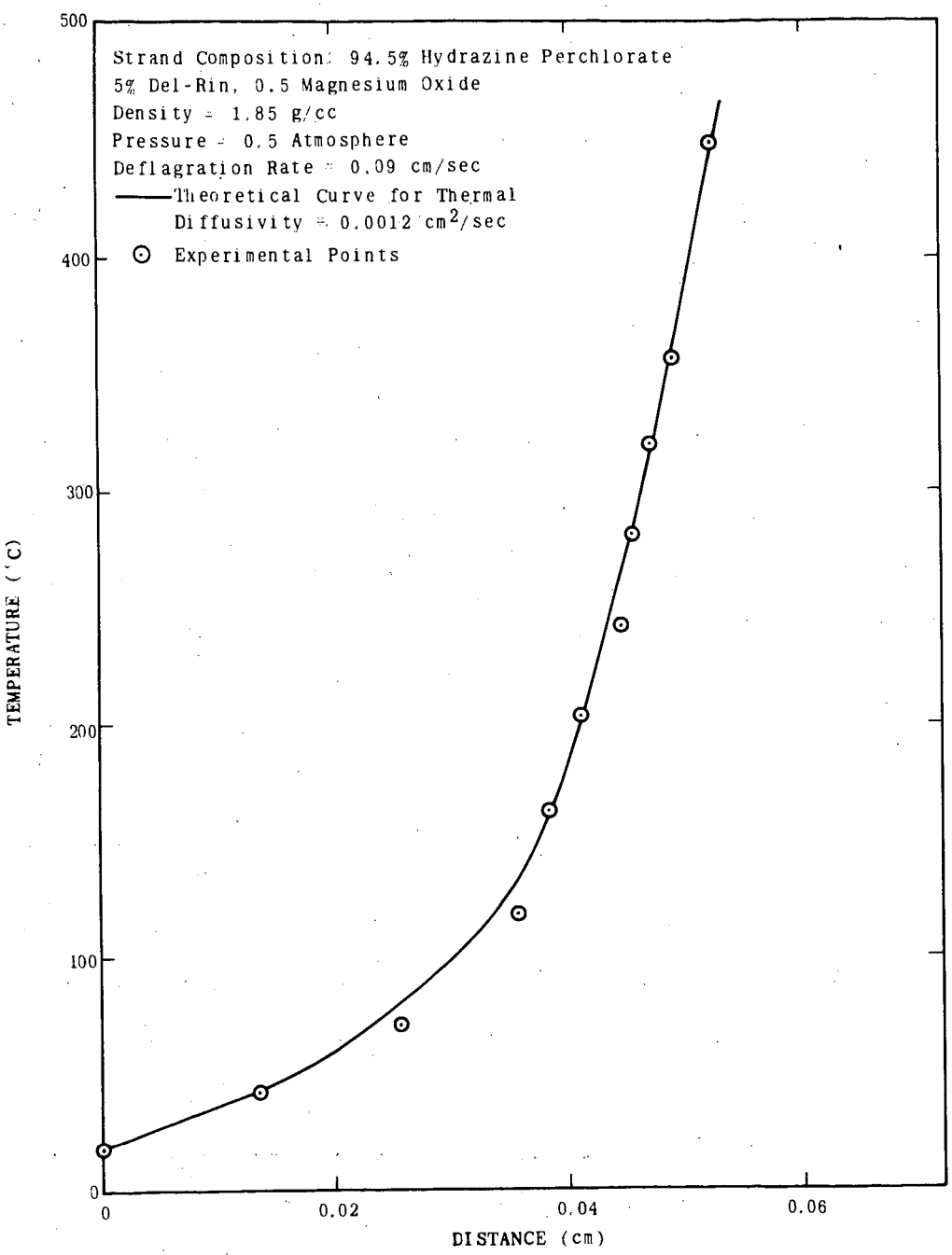

Figure 5. Temperature Profile of a Hydrazine Perchlorate Deflagration Wave.

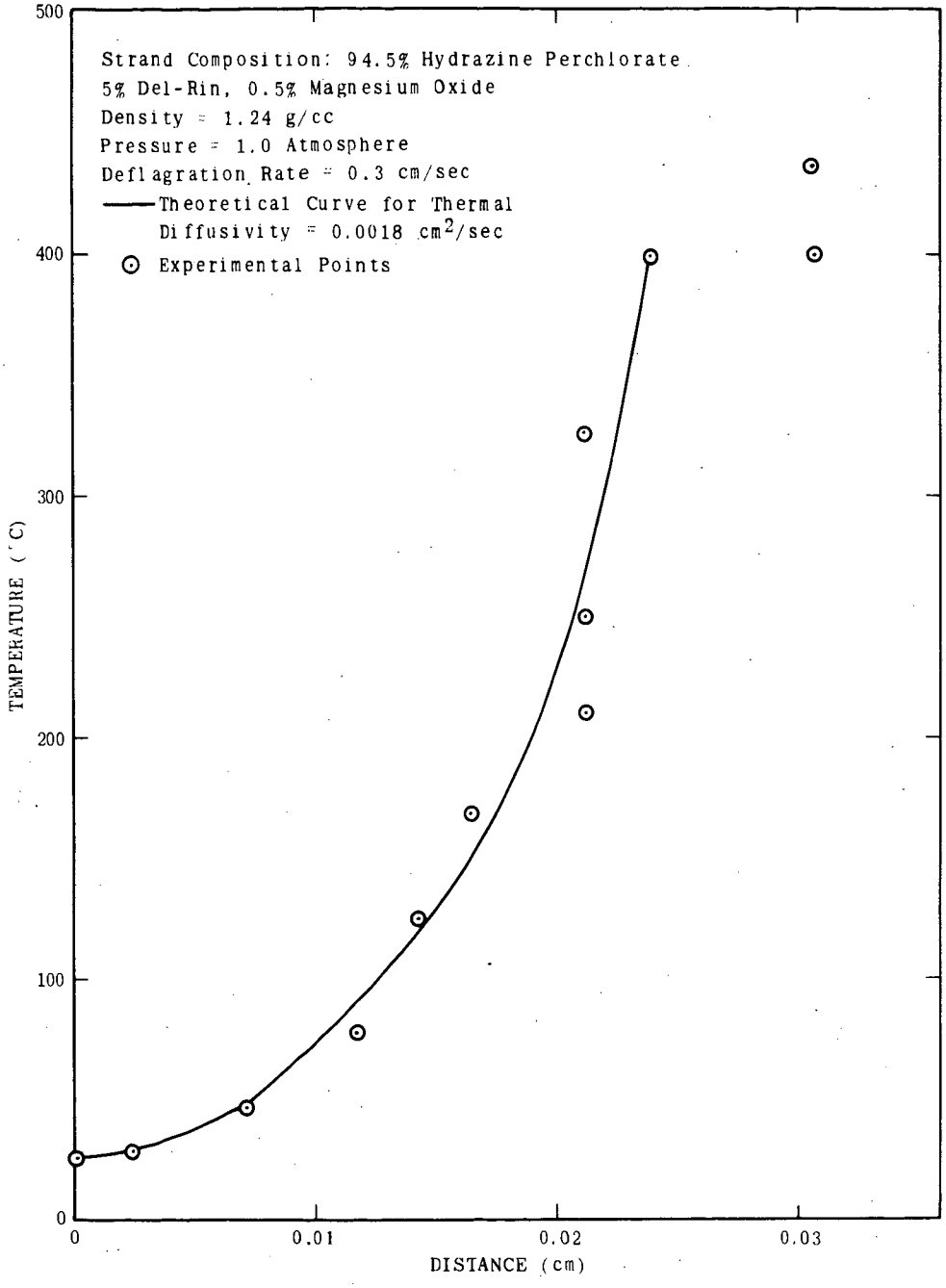

Figure 6. Temperature Profile of a Hydrazine Perchlorate Deflagration Wave.

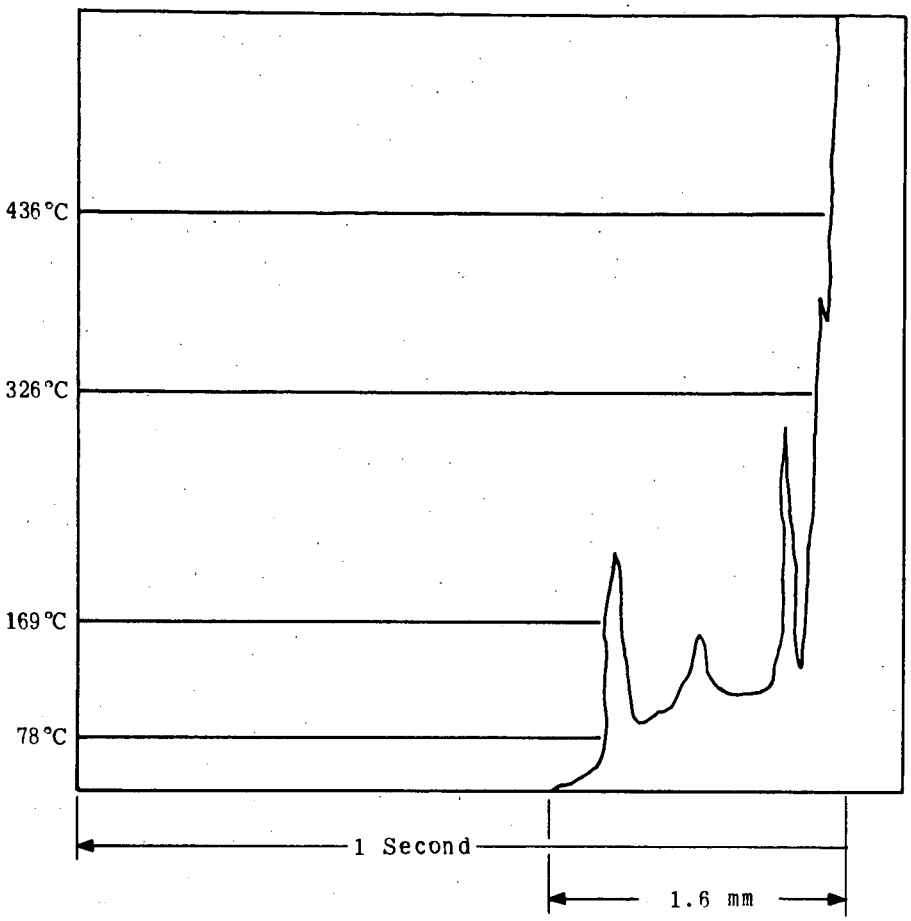

Strand Composition: 98% Hydrazine Perchlorate
2% Magnesium Oxide
Density = 1.05 g/cc
Pressure = 1 Atmosphere
Deflagration Rate = 0.46 cm/sec

Figure 7. Tracing of Thermocouple Record of Hydrazine Perchlorate Deflagration Wave.

TABLE IV.

HYDRAZINE PERCHLORATE

Constant-pressure adiabatic combustion. Initial temperature 25° C

(ΔH_f = -42.5 kcal/mole)

P (atm) →	1	10	68.05	100
T (°K)	2245.5	2291.6	2318.7	2323.2
Total moles per 100 gm	3.815	3.798	3.787	3.784
Species (Moles/100 gm) ↓				
H	1.008×10^{-3}	2.606×10^{-4}	0.766×10^{-4}	5.949×10^{-5}
O	5.871×10^{-3}	2.456×10^{-3}	1.103×10^{-3}	9.341×10^{-4}
N	0	0	0	0
Cl	0.940×10^{-1}	6.146×10^{-2}	4.112×10^{-2}	3.774×10^{-2}
H_2	5.369×10^{-3}	2.204×10^{-3}	0.982×10^{-3}	8.313×10^{-4}
H_2O	1.526	1.523	1.524	1.525
HCl	0.659	0.688	0.699	0.700
O_2	0.705	0.715	0.719	0.720
OH	4.872×10^{-2}	3.262×10^{-2}	2.231×10^{-2}	2.060×10^{-2}
N_2	0.741	0.740	0.739	0.739
NO	2.606×10^{-2}	2.889×10^{-2}	3.062×10^{-2}	3.090×10^{-2}
NO_2	2.698×10^{-5}	0.898×10^{-4}	2.410×10^{-4}	2.933×10^{-4}
N_2O	0	2.354×10^{-6}	6.512×10^{-6}	0.796×10^{-5}
Cl_2	7.932×10^{-4}	2.588×10^{-3}	6.764×10^{-3}	0.816×10^{-2}

The stoichiometry corresponds closely to

$$N_2H_5ClO_4 \rightarrow N_2 + HCl + 2H_2O + O_2$$

Since it has been found that the self-deflagration of ammonium perchlorate does not lead to the products calculated on the basis of thermodynamic equilibrium, we felt it desirable to measure the flame temperature for hydrazine perchlorate. A flame temperature appreciably different from that calculated would indicate a non-equilibrium distribution of products which would require investigation.

Preliminary experiments were performed in which lengths of one mil platinum wire were stretched through the center of tamped strands of hydrazine perchlorate. Examination of the wire after deflagration showed that the passage of the flame had melted it. The melting point of platinum is 2042° K and the heat loss by radiation was estimated at about 40° K. This placed the flame temperature at somewhere above 2082° K.

Flame temperature measurements by the sodium line reversal method were made with hydrazine perchlorate strands containing 2% thiourea and 2% sodium chloride. It was found that this amount of sodium chloride was necessary to achieve a sufficient intensity of emission of the sodium D line for these experiments. It may be pointed out that in oxygen-rich, chlorine-containing flames, as this one is, the concentration of sodium atoms is decreased because the equilibrium

$$H + NaCl \rightleftharpoons HCl + Na$$

is shifted to the left because the hydrogen atom concentration is so low.

Thermodynamic calculations for the composition containing 2% thiourea and 2% sodium chloride were made and the theoretical flame temperature was found to be 2224° K. A series of measurements by the sodium line reversal method gave a figure of 2275 ± 50° K for the flame temperature. This is close enough agreement so that we feel that thermodynamic equilibrium is achieved in the flame and the reaction products are as written above. This differs markedly from the results with ammonium perchlorate where a substantial fraction of the nitrogen was present as oxides of nitrogen even at elevated pressures (3).

V. DISCUSSION

A. A General Description of the Hydrazine Perchlorate Deflagration Process

Let us first assemble a description of the deflagration process for hydrazine perchlorate from the above results. It is a process characterized by the formation of a molten zone which is quite turbulent and foamy; it is a very erratic process, particularly for the pure material and it is subject to very potent catalysis by copper chromite and potassium dichromate and to moderate catalysis by magnesium oxide. The process is comparatively reproducible in the presence of small amounts of fuel, and the rate obtained is apparently not dependent on the nature of the fuel but only on the ambient pressure. It is expressible by $\dot{r} = 0.22P$ where $\dot{r}$ is in cm/sec and P in atmospheres. This corresponds to a rate, at one atmosphere, some 15 times that calculated by extrapolation for ammonium perchlorate (3). However the process is unstable at pressures above about 7 atmospheres and steady deflagration cannot be attained above this pressure.

The temperature profile in uncatalyzed strands is such as to indicate little heat production in the condensed phase, and a liquid layer thickness of 0.3 mm at one atmosphere and 0.56 mm at half an atmosphere. This layer is much thicker for magnesium oxide-catalyzed strands.

Finally, from the measured flame temperature, we conclude that thermodynamic equilibrium is attained in the deflagration products.

B. The Mechanism of Deflagration Hydrazine Perchlorate

One approach to the consideration of the mechanism of hydrazine perchlorate deflagration is to consider whether it fits the classification of a vaporization type process like ammonium perchlorate, i.e., where the material vaporizes without decomposition and exothermic gas-phase reactions occur with resultant heat transfer to the condensed phase. The alternative to a process of this type is one wherein heat production occurs in the molten zone as a result of condensed phase reactions.

Here it is of interest to consider the vaporization rate measurements. The data obtained corresponded to the expression

$$\log_{10}(g\sqrt{T}) = 10.0 - \frac{6475}{T}$$

In the temperature profiles of the deflagration experiments both at one atmosphere, Fig. 6, and one-half atmosphere, Fig. 5, temperatures of the order of 450°C were attained. Insertion of this temperature in the above expression yields a vaporization rate of 0.4 gm/cm^2 -sec. The deflagration rate found at one atmosphere was 0.36 gm/cm^2 -sec while that at half an atmosphere was 0.18 gm/cm^2-sec. The vaporization rate measurements are thus not inconsistent with a vaporization-type mechanism for hydrazine perchlorate deflagration.

If this is considered as one point in favor of a vaporization-type mechanism, a second point in favor of it is the observation that the shape of the temperature profile in the condensed phase was that expected for the case where there is no heat release in the condensed phase. A third point consistent with this picture is the increase of deflagration rate with pressure, a relation that can be explained on the basis that, as the pressure is increased, the exothermic gas-phase reactions occur ever closer to the condensed phase resulting in a higher rate of heat transfer.

The main features of our results which are inconsistent with the above picture are the very erratic nature of the deflagration of pure hydrazine perchlorate and the turbulent behavior of the molten zone. It is difficult to see how, for example, small amount of impurities could affect the vaporization process from the turbulent molten layer. In other words if the deflagration were dependent on vaporization it appears that it should be more reproducible. Contrariwise, if condensed phase reactions are important, then the presence of small amounts of impurities which could catalyze these reactions could easily be important in deciding whether deflagration occurred or not. The turbulent, foaming appearance of the molten zone also suggests that gas evolution, i.e., reaction, is occurring within the body of the molten liquid.

The most plausible description of the process is one in which the mechanism is predominantly a vaporization process but where there is a small (because the temperature profile does not show it) but necessary contribution from condensed-phase reaction.

We feel that the erratic deflagration behavior of pure hydrazine perchlorate is attributable to the presence or absence of small amount of impurities that catalyzed the condensed-phase process, which implies that

when the condensed phase process did not occur, deflagration would not propagate. The function of the fuels then would be to allow exothermic oxidation-reduction reactions to occur in the condensed-phase that would likewise promote deflagration. The fact that the deflagration rates observed depended only on ambient pressure, irrespective of whether the strand was pure hydrazine perchlorate, whether it was preheated, or what the nature of the fuel was, suggests that although a condensed-phase reaction is a sine qua non for stable deflagration, the actual rate is determined by the ambient pressure.

We attribute the effects of copper chromite, potassium dichromate and magnesium oxide to catalysis of condensed-phase reactions, of the catalysis of the pyrolysis reaction by species of this type (12).

Finally we consider the apparent upper pressure limit of deflagration occurring at about seven atmospheres. A similar phenomenon was observed for ammonium perchlorate at pressures near 2000 psi. This was found to be due to convective cooling and was eliminated by alteration of the strand geometry or by wrapping the strand with asbestos. It does not appear that convective cooling is occurring here, since cessation of deflagration occurs even when the material is contained within a glass tube, which should minimize convective effects. At present we can only conclude that at pressures of the order of seven atmospheres, the liquid layer becomes too thin to support the contribution of condensed-phase reaction necessary for stable deflagration and it is for this reason that the upper limit is observed.

VI. REFERENCES

1. This research was supported by the Advanced Research Projects Agency through the Propulsion Research Division of the Air Force Office of Scientific Research under Contract No. AF 49(638)-1169, ARPA Order No. 332-62.
2. (a) Adams, G.K., B. H. Newman and A. B. Robins, "Selected Combustion Problems: Fundamentals and Aeronautical Applications," Butterworths, London, 1954, P. 387; (b) Friedman, R., R. G. Nugent, K. E. Rumbel and A. C. Scurlock, "Deflagration of Ammonium Perchlorate," Sixth Symposium (International) on Combustion, Reinhold, New York, 1958, pp. 612-618.
3. Levy, J. B. and R. Friedman, "Further Studies of Pure Ammonium Perchlorate Deflagration," Eighth Symposium (International) on Combustion, Williams and Wilkins Co., Baltimore, Md., 1962, pp. 663-671.
4. Barlot, J. and S. Marsaule, Compt. rend., 228, 1497 (1949).
5. Private Communication, P. W. M. Jacobs.
6. Audrieth, L. F. and B. A. Ogg, "The Chemistry of Hydrazine", John Wiley and Sons, Inc., New York, 1951.
7. Lewis, B. and G. von Elbe, "Combustion, Flames and Explosives in Gases," Second Edition, Academic Press, New York, New York, 1961, pp. 620-628.
8. Dushman, S. and J. M. Lafferty, "Scientific Foundations of Vacuum Technique", Second Edition, John Wiley and Sons, Inc., New York, New York, 1962, p. 14.
9. Schultz, R. D. and A. O. Dekker, J. Phys. Chem., 60, 1095 (1956).
10. Inami, S. H., W. A. Rosser and H. Wise, J. Phys. Chem., 67, 1077 (1963).
11. Estimated from the heats of formation of the ions in solution, the heat of hydration of anhydrous hydrazine perchlorate to the hemihydrate and the heat of solution of the hemihydrate.
12. Private Communication, G. B. Rathmann, Minnesota Mining and Mfg. Company.
13. McD. Cummings, G. A. and G. S. Pearson, "Perchloric Acid: A Review of its Thermal Decomposition and Thermochemistry," R.P.E. Tech. Note No. 244, Rocket Propulsion Establishment, Ministry of Aviation, London, Oct. 1963.
14. Scott, D. W., et al, J. Am. Chem. Soc., 71, 2293 (1949).
15. Arden, E. A., J. Powling and W. A. W. Smith, Combustion and Flame, 6, 21 (1962).
16. Baer, A. D., N. W. Ryan and D. L. Salt, "Ignition of Composite Propellants," AFOSR-TN-59-516, University of Utah, March, 1959.

THE THERMAL REACTIONS OF SOME ADVANCED SOLID OXIDIZERS

C. J. Grelecki and W. Cruice

Thiokol Chemical Corporation
Reaction Motors Division
Denville, New Jersey

INTRODUCTION

The perchlorates of hydrazine, namely, hydrazinium monoperchlorate ($N_2H_5ClO_4$) and hydrazinium diperchlorate ($N_2H_5(ClO_4)_2$) are receiving increasing attention as high energy solid propellant ingredients. While both of these compounds have been known for some time, very little has appeared concerning their thermal reactions.

The monoperchlorate was first reported by Salvadori in 1907 (Ref 1). He reported decomposition after prolonged heating at 131-132°, a rapid increase in rate with increased temperature, and explosion at 240°. Barlot and Marsule (Ref 2) reported decomposition beginning at 145°. The most recent information was reported by Shidlovskii, Semishin and Shmagin (Ref 3) who studied weight loss at temperatures from 160° to 250°. The dihydrate of hydrazinium diperchlorate was reported by Turrentine in 1915 (Ref 4), however, there is no information reported on the properties of the anhydrous material.

In our program to elucidate the chemistry of these important compounds, we have examined their thermal reactions as a first step.

EXPERIMENTAL

A. Materials

Hydrazinium Diperchlorate (HP-2)

The HP-2 used in this study consisted of uniform small crystals (0.3 to 0.8 mm). Its purity was determined by a potentiometric titration with a standard base. The major impurities were hydrazine (mono-) perchlorate or free perchloric acid. Their presence depended on the extent of drying and the precise balance was difficult to maintain. Examples of the purity of various batches used are shown in Table I.

TABLE I

ANALYSIS OF VARIOUS HP-2 SAMPLES

Batch No.	% HP-2	% Impurity
1	99.86	0.42 - HP
2	99.89	0.26 - HP
3	99.79	0.15 - $HClO_4$
4	99.37	0.15 - HP
5	99.58	0.04 - $HClO_4$

Hydrazinium Monoperchlorate (HP)

High purity HP was prepared by neutralizing 60% $HClO_4$ with 75% N_2H_4 at temperatures from 0°-25°. The salt precipitated from water at 0° and was filtered cold in scintered glass funnels. The fine white crystals were gently removed from the filter with a Teflon spatula and placed in a drying tube at 70° for two hours at a constant vacuum of 0.05 mm Hg to break down the hemihydrate. Samples were titrated either potentiometrically or with phenolphthalien indicator by 0.1000 N. NaOH. Characteristic purity factors range from 99.83% to 99.94%.

B. Apparatus and Procedure

The decompositions were followed manometrically by monitoring pressure rise at constant temperature in a constant volume reactor. The apparatus was fabricated completely of glass and contained a thin glass membrane which was used for sensing pressure. A diagram of the apparatus is shown in Figure 1. A glass pointer was fused to the diaphragm and the apparatus was used as a null device by adjusting the pressure in the external volume until the pointer came to rest at the reference mark. The sensitivity of the gauge varied from one diaphragm to another, however, all gave perceptible deflections of the pointer for pressure differentials of 1 mm.

At the completion of the reaction, gas samples were collected through the break-off seal and analyzed on the mass spectrometer. Condensed phase residues were analyzed by conventional wet analytical techniques.

RESULTS AND DISCUSSION

A. General Nature of the Reaction

In a sealed system the reaction of HP-2 is characterized by an induction period, during which time a gradual pressure rise is observed. At the end of the induction period the reaction accelerates very sharply and complete decomposition results. A typical pressure vs time curve is shown in Figure 2. The initial phase of the HP reaction is also acceleratory, however, there is no sign of the acceleration of the type characteristic of HP-2. A typical pressure vs time curve for HP is shown in Figure 3.

B. Stoichiometry

Analysis of the vapor and condensed products of the overall HP-2 reaction indicate the following stoichiometry.

$$12N_2H_6(ClO_4)_2 \longrightarrow 4NH_4ClO_4 + 12HClO_4 + 22H_2O + 10N_2 + 5O_2 + 4Cl_2$$

The overall stoichiometry of the HP reaction is:

$$8N_2H_5ClO_4 \longrightarrow 7NH_4ClO_4 + NH_4Cl + 4N_2 + 4H_2O$$

C. Rate Measurements

Hydrazinium Diperchlorate

For the case of HP_2 there is a very sharp transition at the initiation of the accelerated phase. The assumption was made that when the reaction goes into the accelerated phase the concentrations of all reacting species are equal.

Thus the expression for the rate of disappearance of HP-2 may be written as follows:

$$\frac{-d[HP\text{-}2]}{dt} = kf(C) \qquad (1)$$

where k is the specific rate constant and f(C) is some function of the concentration of reactants.

Integration of (1) gives

$$kt_i = f'(C_i) \qquad (2)$$

the subscript $_i$ represents the initiation of the accelerated phase of decomposition.

The assumption is made that at t_i, the concentrations of all reactants are equal and $f'(C_i)$ is constant. Thus the time to acceleration is inversely proportional to the specific rate constant.

$$1/t_i = k_o k \qquad (3)$$

where $1/k_o$ is $f'(C_i)$.

In any series of experiments the rates of reaction were compared on the basis of $k_o k$ or $1/t_i$.

Hydrazinium Monoperchlorate

The reaction of HP is not characterized by the same type of rapid acceleration as is found for HP-2. Rather the first 10% of reaction is acceleratory following the expression

$$\alpha/No = At^2$$

where η = number of moles of gaseous products
No = number of moles of HP originally present
t = time in minutes

The rate of reaction remains constant from approximately 10% to 70% decomposition and is given by the following expression:

$$\eta/No = C(t-D)$$

For comparison of rates at various temperatures the linear portion of the curve was used.

D. Effect of Temperature

The time to acceleration (t_i) for HP-2 is shown as a function of temperature in Table II.

TABLE II

TIME TO ACCELERATION AS A FUNCTION OF TEMPERATURE

Temperature (°C)	Induction Period (hrs)
120	77
130	32
140	22
150	9

The dependence of reaction rate on temperature is given by the Arrhenius relationship

$$k = Ae^{-E/RT} \qquad (4)$$

Substituting for the specific rate constant from (3) gives:

$$1/t_i = k_o Ae^{-E/RT} \qquad (5)$$

or $$\ln(1/t_i) = \ln(k_o A) - E/RT \qquad (6)$$

For HP-2 between 100 and 150°C the relationship between 1/ti and temperature is:

$$\log 1/t_i = 11.203 - \frac{5,143}{T(^\circ K)}$$

and the activation energy, E, is 23.5 kcal/mole.

The effect of temperature on the decomposition rate of HP is shown in Table III. The table gives the values of A, C and D which are the parameters of the power expression:

$$\eta/No = At^2 \qquad 0 > \eta/No > 0.1$$

and the linear expression:

$$\eta/No = C(t-D) \qquad 0.1 > \eta/No > 0.7$$

Values of t_i (time of transition from the power law to the linear law) and values of η/No at t_i are also given.

TABLE III

TEMPERATURE EFFECT OF HP DECOMPOSITION

T °C	A X 10^8	C X 10^4	D	t_i*	η/No at t_i*
140	6.25	1.31	552	1200	0.090
150	22.9	3.25	320	480	0.080
158	107	6.9	166	300	0.090
170	260	10.9	104	170	0.070
181	1070	21.0	53	95	0.090
200	18,000	86.0	10	27	0.140

*Approximate values-time in minutes.

A plot of values of log C versus $1/T^oK$ gives an activation energy for the linear portion of the curve of 23.8 kcal/mole from 140°C to 200°C.

E. Effect of Reaction Products

The reaction of HP-2 is self accelerating and suggests autocatalysis by reaction products. The effect of two of the reaction products are given below.

1. Perchloric Acid Dihydrate

The addition of perchloric acid dihydrate has the effect of accelerating the decomposition of HP-2. The exact effect in terms of the time to acceleration ($1/t_i$) is given by the following expression.

$$1/t_i = k_o k_1 + k_o k_2 [HClO_4 \cdot 2H_2O]$$

at 140°, $k_o k_1 = 0.04\ hr^{-1}$ which is the rate of the reaction in the absence of additive and $k_o k_2 = 0.04\ hr^{-1}\ (wt\ \%)^{-1}$.

Thus the rate of the reaction is doubled when one percent of the acid dihydrate is added.

2. Anhydrous Perchloric Acid

The addition of anhydrous perchloric acid accelerates the reaction of HP-2 to such an extent that it exceeds the capacity of the experimental technique at 140°. Using the above convention, however, it was possible to determine a lower limit on the value of the rate constant k_0k_2. At 140° the value of k_0k_2 is greater than 2.5 hr^{-1} $(wt\ \%)^{-1}$. Thus the rate of HP-2 decomposition is increased by a factor of at least 60 when one percent of anhydrous $HClO_4$ is present.

F. Reaction Mechanism

The initial step in the decomposition of HP-2 is the dissociation to HP and perchloric acid:

$$N_2H_5ClO_4 \cdot HClO_4 \rightleftharpoons N_2H_5ClO_4 + HClO_4$$

This step was verified by isolation of anhydrous $HClO_4$ as the only vapor phase specie during the early phases of the reaction. The equilibrium constants in terms of the pressure of $HClO_4$ were determined as a function of temperature and are given by the following expression.

$$\log P_{(mm)} = 22.86 - \frac{8{,}650}{T\ (^\circ K)} \qquad 100^\circ \text{ to } 140^\circ C$$

and the heat of dissociation is 37 kcal/mole.

The initial step of the HP decomposition is a proton transfer to produce free hydrazine and anhydrous perchloric acid:

$$N_2H_5ClO_4 \rightleftharpoons N_2H_4 + HClO_4$$

The dissociation pressures for this reaction could not be measured directly in the Sickle gauge apparatus. No dissociation pressure could be detected to 150°. At higher temperatures the decomposition was too rapid to attain equilibrium.

The initial dissociation in both cases is followed by decomposition of $HClO_4$ since it is considerably less stable than HP-2 or HP.

The reaction of anhydrous $HClO_4$ has been studied by Levy (Ref 5). At high temperatures (above 300°) the vapor phase reaction is a homogeneous one. Below approximately 300°C the reaction is a heterogeneous one, the rate of which depends on the nature of the surface with which it is in contact. Zinov'ev and Tsentsiper (Ref 6) report an activation energy of 22.2 kcal/mole for the low temperature reaction. The similarity of the temperature coefficient of the HP, HP-2 and $HClO_4$ reactions suggest that the decomposition of $HClO_4$ may be the controlling step in each case.

Since the decomposition of $HClO_4$ is mainly a heterogeneous one in the temperature range of interest, tests were performed to determine the effect of

surface on the HP-2 reaction. The Pyrex surface was increased by the addition of known quantities of Pyrex micro spheres. These were intimately mixed with the reactant. The presence of the glass surface increased the rate. The overall rate of the heterogeneous reaction is given by the following expression:

$$1/t_i = k_o k_1 + \Sigma k_o k_j [S_j]$$

where $k_o k_1$ is the rate in the absence of added surface; kj is the specific rate constant on surface j and Sj is the surface area of the jth surface.

At 140° on Pyrex glass the value of $k_o k_{Pyrex}$ is 0.005 hr^{-1} $(cm^2)^{-1}$. Thus the heterogeneous nature of the reaction is important and this further suggests that the decomposition of $HClO_4$ is a controlling step in the reaction.

At 140° the perchloric acid decomposes on a surface as follows:

$$HClO_4 \longrightarrow HO\cdot + \cdot ClO_3$$

Only the two products formed by the initial dissociation of $HClO_4$ are shown. Many other active oxidizing species such as ClO_2, ClO_4, Cl_2O_3, are undoubtedly also formed. The oxidizing species formed can oxidize the hydrazine moiety of HP-2 to ammonia thereby releasing a mole of perchloric acid. The reaction is illustrated below for the HO· and ClO_3· radicals. The same overall results are obtained with other oxidizing intermediates.

$$HO\cdot + N_2H_5ClO_4\cdot HClO_4 \longrightarrow H_2O + 1/2N_2 + NH_4ClO_4 + HClO_4$$

$$ClO_3\cdot + 6N_2H_5ClO_4\cdot HClO_4 \longrightarrow 3H_2O + 3N_2 + 6NH_4ClO_4 + 1/2Cl_2 + 6HClO_4$$

Each mole of perchloric acid has the capacity to oxidize seven moles of hydrazine which in turn releases seven additional moles of perchloric acid. Such a rapid chain-branching step can account for the rapid transition from the slow preacceleration phase of the reaction to the rapid acceleration.

The suggested reactions are also consistent with the fact that HP does not accelerate rapidly. Oxidizing intermediates formed by the decomposition of $HClO_4$ react with HP as follows.

$$N_2H_5ClO_4 + \cdot OH \longrightarrow H_2O + NH_4ClO_4 + 1/2N_2$$

$$7N_2H_5ClO_4 + \cdot ClO_3 \longrightarrow 3H_2O + 6NH_4ClO_4 + 3\ 1/2N_2 + NH_4Cl$$

An approximate kinetic expression based on the above consideration in which all oxidizing species are included, reduces to:

$$\frac{dn}{dt} = [HP]\,(k_1[OH] + k_2[ClO_3] + \ldots\ldots k_1[O_i])$$

This expression shows that the rate of gas evolution should increase until steady state concentrations of all oxidizing species are reached. After this time (t_i) the concentrations of oxidizing intermediates remain constant and are dependent on the equilibrium dissociation pressure of HP at the experimental temperature. The rate then remains constant until the HP becomes depleted.

SUMMARY AND CONCLUSIONS

The initial step in the thermal decomposition of HP-2 and HP is the dissociation of the acid-base complex to give free perchloric acid. The subsequent decomposition of perchloric acid controls the rate of the overall reaction.

In the case of HP-2 the reaction is self-accelerating due to autocatalysis by reaction products. The general form of the reaction sequence is as follows:

$$A \xrightarrow{k_1} B + \text{Products}$$

$$7A + B \xrightarrow{k_2} 7B + \text{Products}$$

The large branching coefficient (7) and the fact that $k_2 > k_1$ leads to a very sharp transition from a slow preacceleration reaction to a rapid accelerated phase.

The HP reaction differs from that of HP-2 in that no autocatalysis is involved. The initial rate of the HP reaction does increase as active oxidizing intermediates are built up, but after a steady state concentration is reached the rate remains constant until the concentration of HP becomes depleted.

ACKNOWLEDGEMENT

This report is based on work performed under Air Force Contract No. AF04(694)334 and Navy Contract No. NOnr 4364(00) under the sponsorship of the Advanced Research Projects Agency.

REFERENCES

1. Salvadori, R., J. Soc. Chem. Ind., 26, 1066 (1908) (abstracted from Gazz. chim. ital., 37, II, 32 (1907)).

2. Barlot, J. and Marsaule, S. Compt. Rend. Acad. des Sciences, 228, 1497 (May 1949).

3. Shidlovskii, A. A., Semishin, V. I., and Shmagin, L. F. Zhur. Priklad. Khim. 35, No. 4, 756 (1962).

4. Turrentine, J. W. and Gill, A. C. JACS, 37, 1122 (1915).

5. Levy, J. B. J. Phys. Chem., 66, 1092 (June 1962).

6. Zinov'ev, A. A., and Tsentsiper, A. B. Zhur. Neorg. Khim., 4, 724 (1959).

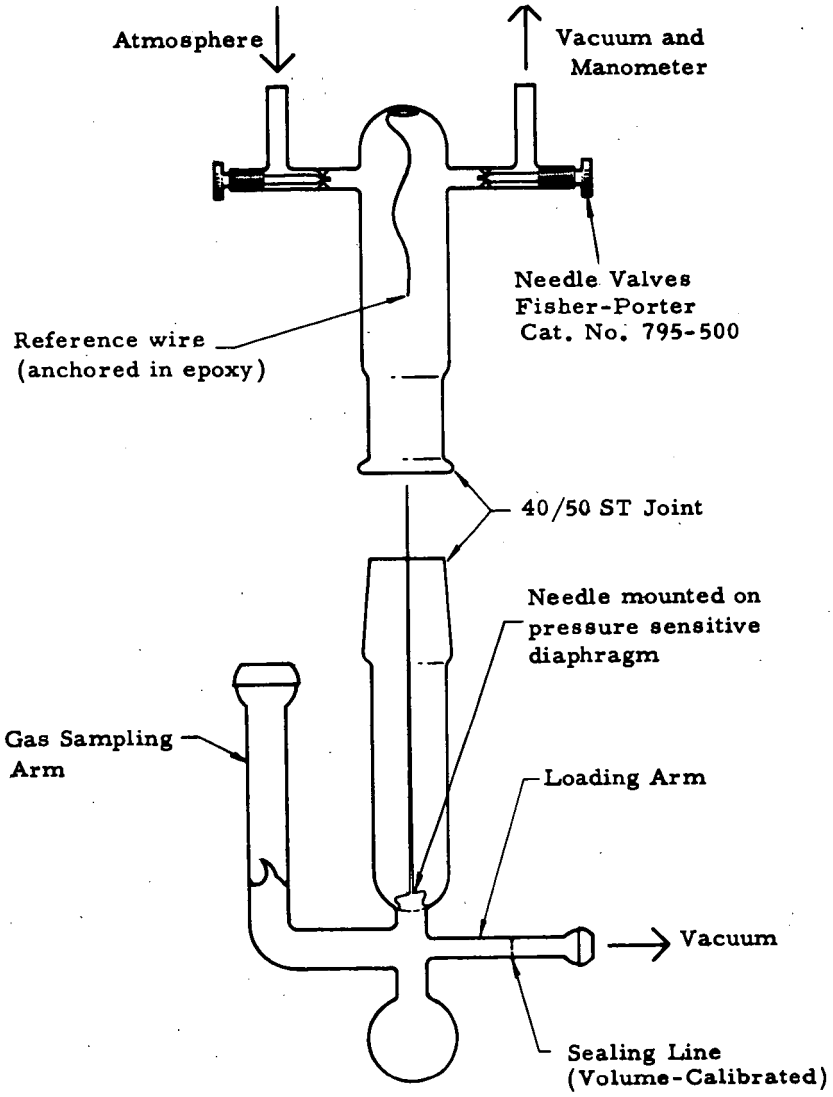

Figure 1. Sickle Gauge Apparatus

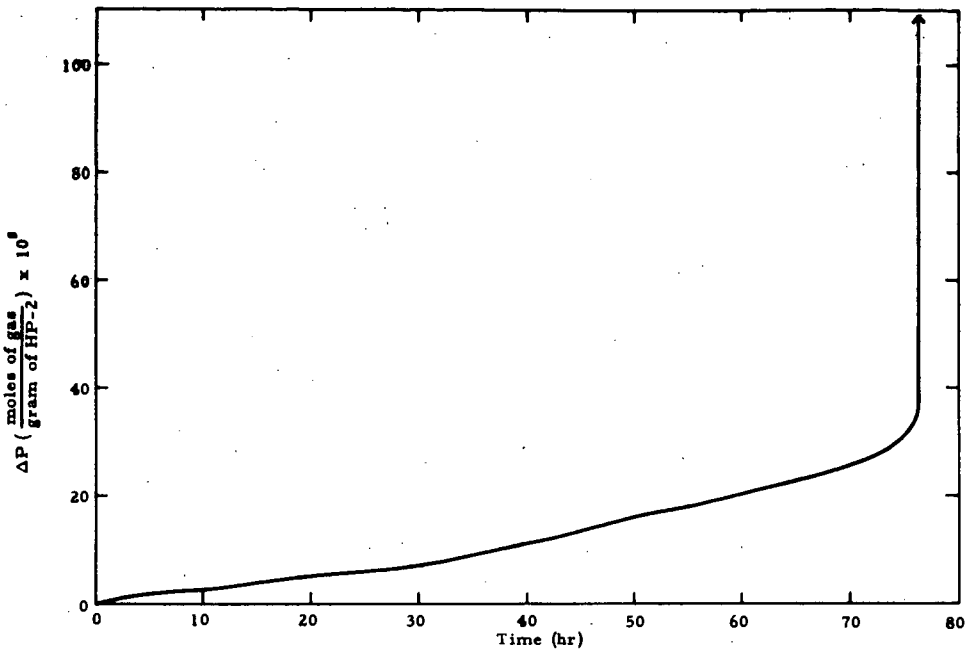

Figure 2. Pressure vs Time Curve for Hydrazinium Diperchlorate at 140°C

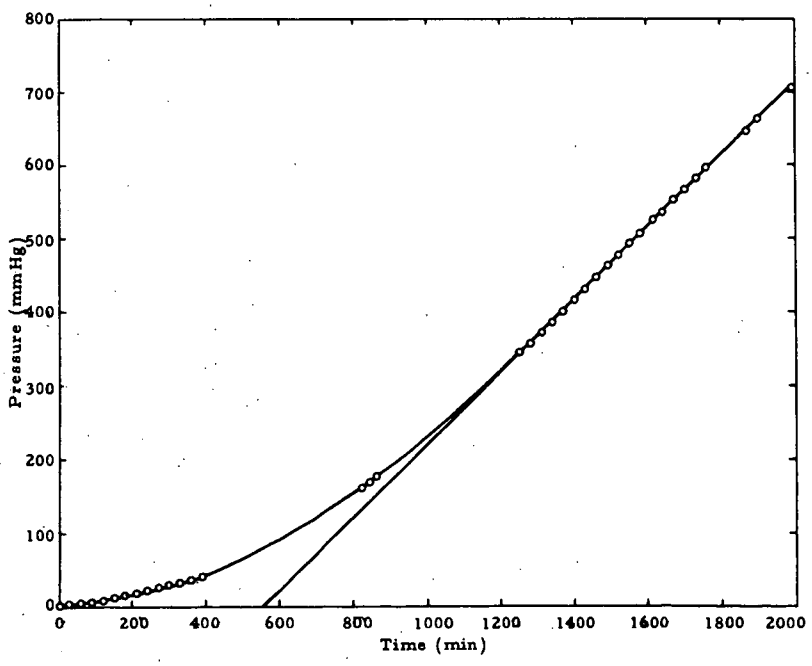

Figure 3. Pressure vs Time Curve for Hydrazinium Perchlorate at 140°C

DECOMPOSITION OF NITRONIUM PERCHLORATE*

M. D. Marshall and L. L. Lewis

Callery Chemical Company, Callery, Pennsylvania

Abstract

The decomposition reaction for nitronium perchlorate is believed to be the formation of nitrosonium perchlorate and oxygen. The other products (NO_2, Cl_2, ClO_2) observed during the decomposition appear to be the result of the subsequent decomposition of nitrosonium perchlorate. This mechanism is clearly demonstrated *in vacuo* by a preponderance of oxygen in the volatiles during the early stages of the decomposition of nitronium perchlorate and by the products of the latter stages which describe the decomposition of nitrosonium perchlorate.

In sealed tubes, the reaction of dinitrogen tetroxide with nitronium perchlorate ultimately predominates, giving nitrosonium perchlorate and oxygen as products. This reaction has been shown to be catalyzed by dinitrogen tetroxide.

Introduction

Nitronium perchlorate begins to decompose slowly at approximately 50°C resulting in the production of gaseous products. There is some evidence that the purity of the sample is related to the decomposition. On the other hand, despite efforts by several investigators to obtain high-purity samples, decomposition is significant by 60°C.

Our interest in this problem was one of establishing the mechanism for the decomposition. By doing so we hoped to obtain information that would allow us to prevent or suppress the decomposition.

The decomposition of nitronium perchlorate between 70 and 112°C has been reported by Cordes[1] as proceeding to the gaseous products: NO_2, Cl_2, ClO_2, NO_3Cl and O_2. As a result of some screening experiments at Callery we were aware that, at 65°C in sealed tubes, nitrosonium perchlorate was a major decomposition product. We were also aware that dinitrogen tetroxide, at least in the liquid phase, would quantitatively convert nitronium perchlorate to nitrosonium perchlorate. Thus, a mechanism involving only gaseous products appeared unlikely.

To avoid any such back reaction of dinitrogen tetroxide with nitronium perchlorate we decided to carry out our study under vacuum, with continuous removal of products. The temperature of 65°C was chosen so as to give a significant decomposition rate, but one at which the gaseous products could be handled by the pumping system.

Experimental

The decompositions were carried out in glass reactors connected through a short coupling to a small vacuum system. Nitronium perchlorate is extremely hygroscopic, and even with utmost care, the presence of hydrolysis products cannot be avoided. Therefore, after completing the sample transfer to the decomposition

---

* This research was supported by the Advanced Research Projects Agency under the U. S. Army Research Office, Durham, North Carolina [Cont. No. DA-31-124-ARO(D)-12].

(1) Cordes, H. F., J. Phys. Chem. 67, 1693 (1963).

reactor, the removal of hydrolysis products (HNO_3 and $HClO_4$) were effected by pumping at 10^{-5} mm of mercury at room temperature until a constant weight was obtained.*

The decomposition was monitored at 65°C while continuously pumping on the sample. A pressure of at least 10^{-4} mm of mercury was maintained in the system. The volatile decomposition products were passed through a -196°C trap, where condensables were removed and periodically analyzed. Non-condensables, consisting entirely of oxygen, were Toeplerized either continuously, or periodically to check their rate of removal. The weight-loss of the sample was checked against volatiles recovered or measured and appropriate analyses carried out on the residue. Sublimed nitronium perchlorate was weighed with the residue. On most runs, the sublimed solids were measured and analyzed.

Results and Discussion

The decomposition experiments were characterized by: (1) An immediate deposition of sublimed materials on the cooled reactor walls within one minute after placing the sample in the 65°C bath; (2) An induction period of 24-40 hours during which no visible evidence of volatiles was observed; (3) An initially slow, but rapidly accelerating production of oxygen which maximized at approximately 100 hours with concurrent appearance of yellow condensable in the -196°C trap; and finally (4) A noticeable decrease in the rate of oxygen evolution which diminished slowly throughout the remainder of the run.

Oxygen Evolution

A plot of the total oxygen evolved versus time gave the typical sigmoid curve characteristic of solid decomposition (Figure 1). The induction and acceleration periods are clearly evident, along with the subsequent lower rate of total oxygen evolution during the decay stage.

A plot of the rate of oxygen evolution for one experiment is shown in Figure 1. The peak rate of oxygen release occurred at approximately 100 hours, at about a 10% weight loss, and with more than 80% of the nitronium perchlorate still intact in the sample (80% figure obtained from a similar run stopped at this point and the solids analyzed.).

The ratio of oxygen released per gram of weight-loss incurred also varied throughout the run. Table I summarizes this data for two experiments.

---

* The effectiveness of this procedure was demonstrated by adding a measured amount of water to a sample of nitronium perchlorate and, after pumping according to the procedure described, the weight-loss was measured for the sample and the nitric and perchloric acids titrated in the recovered volatiles. All values were theoretical within limits of the analyses.

TABLE I

RATIO OF OXYGEN EVOLVED PER GRAM WEIGHT-LOSS

Total Time (hrs.)	Wt. Loss (g)	O_2 (mmoles)	mmoles O_2 / g. wt. loss
Run No. 1			
29	-----	0.02	----
73	0.160	2.46	15.5
92	0.140	2.01	14.3
112	0.161	2.13	13.3
132	0.154	1.93	12.6
154	0.163	1.80	11.1
174	0.150	1.47	9.8
Run No. 2			
198	0.341	3.98	11.7
298	0.177	1.32	7.3
397	0.129	0.88	6.8
492	0.103	0.66	6.5

The change from 15.5 to 6.5 for the mmoles of O_2 per gram wt.-loss is significant in that it denotes a mechanism change, or the increasing importance of a secondary reaction. The 15.5 and 6.5 values are also significant since they cannot be obtained from nitronium perchlorate decomposition reactions giving only gaseous products, but they must arise from a combination of reactions in which the production and decomposition of $NOClO_4$ is involved. The highest and lowest possible values obtainable from NO_2ClO_4 for this ratio are shown by the equations

	(mmoles O_2/g. wt. loss)
$NO_2ClO_4 \longrightarrow NO_2 + 1/2\ Cl_2 + 2\ O_2$	13.8
$NO_2ClO_4 \longrightarrow NO_2 + ClO_2 + 1/2\ O_2$	6.9

On the other hand, values of 31.3 and 3.9 are possible from the production and decomposition, respectively, of nitrosonium perchlorate.

	(mmoles O_2/g. wt. loss)
$NO_2ClO_4 \longrightarrow NOClO_4 + 1/2\ O_2$	31.3
$NOClO_4 \longrightarrow NO_2 + ClO_2 + 1/2\ O_2$	3.9

Volatiles Condensable at -196°C

The condensed materials were identified as NO_2, Cl_2 and ClO_2 by means of infrared and mass spec. analyses. The sample was hydrolyzed and analyzed for chlorine and nitrogen content. The combined equivalents of chlorine (Cl_2 + ClO_2) invariably equaled the equivalents of nitrogen found, within limits of the analyses.

The nitrogen dioxide produced (measured as nitrogen in the hydrolysate) per gram of weight-loss of sample slowly increased as the decomposition progressed. The values for two runs are shown in Table II.

TABLE II

NO_2 PRODUCED PER GRAM OF WEIGHT-LOSS

Total Time (hrs.)	Wt. Loss (g)	NO_2 Produced (mats)	mmoles NO_2 / g. wt. loss
Run No. 1			
73	0.160	0.90	5.6
92	0.140	0.77	5.5
112	0.161	0.93	5.8
132	0.154	0.99	6.4
154	0.163	1.07	6.6
174	0.150	1.02	6.8
Run No. 2			
397	0.647	4.32	6.7
492	0.103	0.78	7.6

It is again significant that the value of 7.6 mmoles of NO_2 per gram of weight-loss of sample obtained over the last period from 397 to 492 hours of decomposition for Run No. 2 cannot be obtained from any decomposition reaction one may write for NO_2ClO_4. It is, however, nearly theoretical for the decomposition of $NOClO_4$ to volatiles.*

	mmoles NO_2 / g. wt. loss
$NOClO_4 \longrightarrow NO_2 + ClO_2 (Cl_2 + 1/2\ O_2$	7.7

Analysis of Solids

In our original hypothesis, we believed the formation of $NOClO_4$ in the residue would be avoided by carrying out the decomposition under vacuum. By doing so, we hoped to prevent the back reaction of the NO_2 produced in the decomposition with NO_2ClO_4. Nevertheless, $NOClO_4$ was observed in the residue in substantial quantities, possibly suggesting its formation by a different mechanism. Its presence was confirmed by x-ray, Raman and wet analysis techniques.

Figure 2 compares the $NOClO_4$ found in the residue with the NO_2ClO_4 decomposed as a function of time. With the limited data available, the peak production of $NOClO_4$ is observed to coincide with the peak rate of NO_2ClO_4 decomposition. The $NOClO_4$ also appears to decompose at a faster rate than the nitronium perchlorate as indicated by the slopes of the curves. This would most certainly be true if, as we suspect, nitrosonium perchlorate is also being continuously produced from the decomposition of nitronium perchlorate during this period.

A study of the decomposition of $NOClO_4$ under conditions identical to this study gave the following results: (1) Nitrosonium perchlorate decomposes with no noticeable induction period, giving only the gaseous products, NO_2, ClO_2, Cl_2 and O_2; nitronium perchlorate is reported as a major product of this decomposition at 99°C(2) but only trace quantities were observed in our study. (2) The decomposition

* A value of 7.6 mmoles of NO_2 per gram of weight loss was observed experimentally for the decomposition of $NOClO_4$ under similar conditions.

(2) Rosolovskii, V. Ya, and Rumyantsev, E. S., Russ. J. of Inorg. Chem., English Transl. 8, 689 (1963).

of $NOClO_4$ proceeds at a faster rate than that for NO_2ClO_4, at least after the acceleratory period of the latter compound. This observation is consistent with conclusions of Rosolovskii[2].

Several interesting facts concerning the sublimed solids should be noted: (1) Sublimation occurred immediately upon heating the sample to 65°C; (2) The sublimed solids analyzed to be NO_2ClO_4 both by x-ray and elemental analyses; (3) Analyses did not detect the presence of $NOClO_4$; (4) The rate of sublimation appeared to be comparatively constant over the decomposition period; sublimation usually occurred at about 1/2 to 1/3 the rate of decomposition. These facts are significant in that they indicate the sublimation to be entirely independent of the decomposition.

The Decomposition Mechanism

The vacuum decomposition of NO_2ClO_4 at 65°C proceeds by a mechanism which must take into account: (1) A decreasing ratio of oxygen evolution per weight-loss of sample; (2) An increasing ratio of NO_2 production per weight-loss of sample; (3) The production of $NOClO_4$ as a product and its subsequent decomposition, and (4) The decomposition of $NOClO_4$ as the predominant reaction in the latter stages. The observations are best explained by the following two-step mechanism:

(a) $NO_2ClO_4 \longrightarrow NOClO_4 + 1/2\ O_2$

(b) $NOClO_4 \longrightarrow NO_2 + ClO_2\ (Cl_2 + O_2) + 1/2\ O_2$

Assuming the mechanism as described, the ratios of O_2 and NO_2 per gram of weight-loss expected from equations (a) and (b) in various ratios can be calculated. These are tabulated in Table III.

TABLE III

CALCULATED QUANTITIES OF O_2 AND NO_2 PRODUCED PER WEIGHT LOSS OF NO_2ClO_4

Ratio Equations a:b	mmole produced/g. wt.-loss NO_2	O_2, Assuming all Cl as ClO_2	O_2, Assuming all Cl as Cl_2
10:0	none	31.2	31.2
10:1	3.5	19.0	22.5
10:2	4.8	14.4	19.1
10:3	5.5	11.8	17.3
10:4	5.8	10:3	16.2
10:6	6.4	8.5	14.9
10:8	6.7	7.5	14.2
10:10	6.9	6.9	13.8
8:10	7.0	6.3	13.4
6:10	7.2	5.8	12.9
4:10	7.4	5.2	12.5
2:10	7.5	4.5	12.1
0:10	7.7	3.9	11.6

The NO_2 and O_2 values thus lie between the extremes of none and 31.2 for the initial stage which describes the production of $NOClO_4$; and 7.7 and 3.9 to 11.6 for the latter stage which describes the decomposition of $NOClO_4$.

The experimental values for these same ratios for the two experiments previously cited are shown in Table IV.

TABLE IV

EXPERIMENTAL O_2 AND NO_2 WEIGHT-LOSS RATIOS

Total Time (hrs.)	mmoles O_2/g wt. loss	mmoles NO_2/g wt. loss
Run No. 1		
73	15.5	5.6
92	14.3	5.5
112	13.3	5.8
132	12.6	6.4
154	11.1	6.6
174	9.8	6.8
Run No. 2		
198	11.7	
298	7.3	6.7
397	6.8	
492	6.5	7.6

The general trends for the mmoles of O_2 and NO_2 produced per weight-loss are observed to follow those expected for the proposed mechanism. That reaction (a) predominates in the early stages is supported by the initially high experimental values obtained for the ratio of O_2 evolution per weight-loss of sample. A theoretical value of 31.3 would be expected if only (a) occurred, since oxygen is the only volatile. This would be true only momentarily, since $NOClO_4$ decomposes rapidly at 65°C without any induction period by equation (b) which would immediately become operative. Any contribution by (b) would lower the oxygen to weight-loss ratio, since at its highest possible rate of oxygen production, (giving NO_2, Cl_2 and O_2 as decomposition products), a theoretical 11.6 value for the ratio of mmoles of oxygen to weight-loss would be observed. The initial value of 15.5 observed after 73 hours is therefore a "net" figure for reactions (a) and (b) during this initial interval, and represents a substantial contribution from reaction (a).

A quantitative correlation of equations (a) and (b) with the oxygen ratio is not possible because of the uncertainty in the quantity of ClO_2 decomposed to Cl_2 and O_2. On the other hand, the ratio of NO_2 produced per weight-loss can be directly correlated. The initial ratio of 5.6 for NO_2, for example, indicates that, during the first 73 hours, the ratio of equation a:b averaged 10:3, or stated otherwise, approximately 30% of the $NOClO_4$ that was produced during this period by equation (a) subsequently decomposed.

At the finish of Run No. 1, during the interval of 154 to 174 hours, reactions (a) and (b) were operating at an approximate 10:9 ratio. Thus, $NOClO_4$ decomposed at nearly the same rate as its production from NO_2ClO_4.

The 7.6 value for the NO_2 ratio, obtained over the period of 397 to 492 hours of Run No. 2 indicates that the decomposition of $NOClO_4$ (equation b) was occurring ten times faster than it was being produced from equation (a), thus rapidly diminishing the excess produced during the accelerated period of the NO_2ClO_4 decomposition.

The 7.6 value for NO_2 production and the 6.5 value for the oxygen evolution obtained in the latter stages of the decomposition of NO_2ClO_4 are almost

identical to similar values obtained from the decomposition of $NOClO_4$ under similar conditions. The respective values for $NOClO_4$ were 7.6 and 6.9 mmoles per gram of weight-loss, indicating the predominance of this reaction in the latter stages of the NO_2ClO_4 decomposition.

As a further check on this mechanism, the decomposition of NO_2ClO_4 was monitored, using a Raman cell as a decomposition reactor. The changes in the Raman spectrum were measured periodically and compared with the production of oxygen throughout the course of the decomposition at 65°C. The rapid drop in the NO_2^+ absorption by NO_2ClO_4 coincides with the appearance and increase in the NO^+ absorption for $NOClO_4$ (Figure 3), as would be expected from the proposed mechanism. Only the NO_2^+ (1400 cm^{-1}) and NO^+ (2300 cm^{-1}) curves were plotted since the respective perchlorate absorptions closely parallel the cation absorption curves. The oxygen curves are similar to those previously observed (Figure 4). As before, the peak rate of oxygen evolution occurred at approximately 100 hours.

It is significant to note that the Raman data also indicates a break at about 100 hours in the absorption curves for NO_2^+, which was decreasing, and NO^+, which was increasing. Since a Raman spectrum of solids is predominantly a surface phenomenon, this agreement suggests an initially rapid surface reaction converting the surface NO_2ClO_4 to $NOClO_4$ which then controls continued decomposition.

A mechanism for the decomposition of NO_2ClO_4 in the presence of its decomposition products would have the dinitrogen tetroxide-catalyzed conversion of NO_2ClO_4 to $NOClO_4$ in addition to the reactions (a) and (b).

$$NO_2ClO_4 + N_2O_4 \longrightarrow NOClO_4 + N_2O_5$$

$$N_2O_5 \longrightarrow N_2O_4 + 1/2\ O_2$$

When a critical concentration of NO_2 has been reached from the decomposition of nitrosonium perchlorate, this catalytic conversion rapidly becomes the predominating reaction in the mechanism. Previous work at Callery had shown this reaction to be quantitative in the presence of liquid N_2O_4.(3) In the course of this investigation, gaseous N_2O_4 at ambient temperature, in less than equimolar quantities, was also demonstrated to effect the quantitative conversion presumably by the above mechanism.(3)

Discussion of Thermal Stability

The foregoing discussion does not explain the reasons for the instability of NO_2ClO_4, but with this information a reasonable picture as to the decomposition process can be presented.

Borrowing from the classical concept of solid decompositions, decomposition probably initiates at defect sites on the crystal surface where circumstances offer a lowered energy of activation.(4) It appears most probable that the decomposition initiates with $NOClO_4$ formation. Therefore, ion interactions are involved.

It can be stated that the instability of NO_2ClO_4 is not inherent in the nitronium ion. More stable nitronium species are known; NO_2BF_4 is reportedly

(3) A. D. McElroy and M. D. Marshall; to be published.
(4) Garner, "Chemistry of the Solid State" Butterworth Scientific Publications, London, (1955), Ch. 7.

stable at 170°C[5], and $(NO_2)_3Al(ClO_4)_6$ and $NO_2Zn(ClO_4)_3$ are quantitatively prepared at 125°C[6], a temperature at which NO_2ClO_4 rapidly decomposes. We are also well aware of stable perchlorate salts. Obviously, then the instability of NO_2ClO_4 is peculiar to the NO_2^+ and ClO_4^- ion combination.

The following mechanism is suggested as occurring at the crystal surface.

$$NO_2^+ + ClO_4^- \rightleftharpoons [NO_2ClO_4] \begin{cases} \rightarrow NO_2ClO_4(\text{sublimed}) \\ \rightarrow NOClO_4 + 1/2\ O_2 \end{cases}$$

Nitronium perchlorate, as an ion-complex may exist as a transitory intermediate which may either revert to ions, sublime or decompose. A similar mechanism has been proposed for the decomposition of ammonium perchlorate[7].

Evidence for interaction between the NO_2^+ and ClO_4^- ions has been observed in the NO_2ClO_4 crystal lattice. Distortions from linearity in the NO_2^+ ion, and from the tetrahedral angle for the Cl-O bonds of the ClO_4^- have been interpreted by Truter et al., as due to interaction between cation and anion[8]. In addition, both Raman and infrared spectra of nitronium perchlorate obtained here at Callery have shown the splitting of the perchlorate Cl-O bands which, according to Hathaway[9], is characteristic of bidentate coordination for the perchlorate group. Thus, something less than a truly ionic crystal lattice is present in NO_2ClO_4 and decomposition may therefore be facilitated by this interaction.

In complex perchlorates [e.g. $(NO_2)_3Al(ClO_4)_6$, $(NO_2)Zn(ClO_4)_3$], the ClO_4^- ion is coordinated by the aluminum or zinc ions and therefore has little tendency to interact with the NO_2^+ ion. In NO_2BF_4, the BF_4^- ion presumably exerts very little distorting influence. Thus, in these compounds, the ionic distortion of the NO_2^+ is minimized and an increased thermal stability results.

---

(5) Kuhn and Olah, JACS 83, 4565-71 (1961).
(6) McElroy, A. D., Guibert, C. R., Bellissimo, J. S., and Hashman, J. S., J. Inorg. Chem., to be published; presented Gordon Research Conference, August, 1963.
(7) Galwey, A. K. and Jacobs, P. W. M., Proc. of Royal Chem. Soc., Series A, 254, 455 (1960).
(8) Truter, M. R., Cruikshank, D. W. J., and Jeffrey, G. A., Acta Cryst. 13 855 (1960).
(9) Hathaway, B. M., and Underhill, A. E., J. Chem. Soc., 3091 (1961).

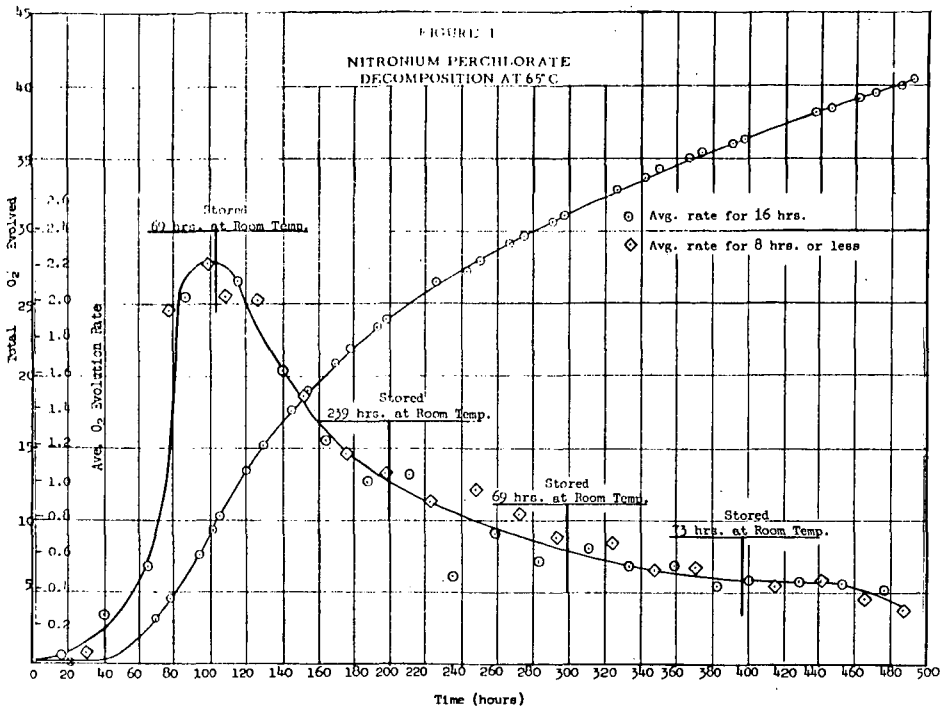

FIGURE 2

DECOMPOSITION OF NO_2ClO_4 AT 65°C

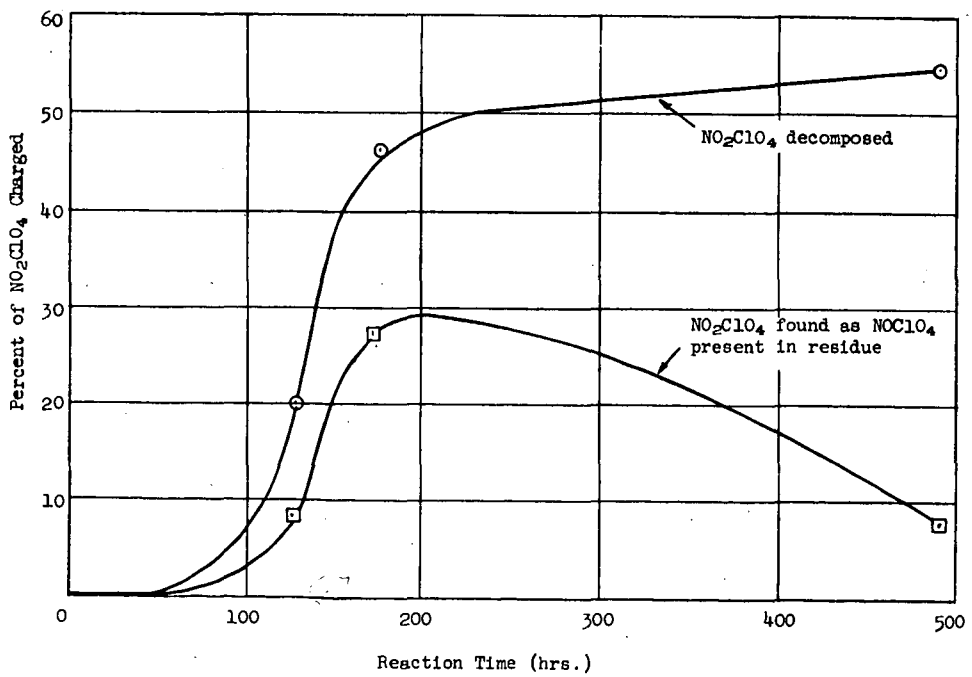

FIGURE 3

RAMAN ANALYSIS OF DECOMPOSITION OF NO_2ClO_4 at 65°C

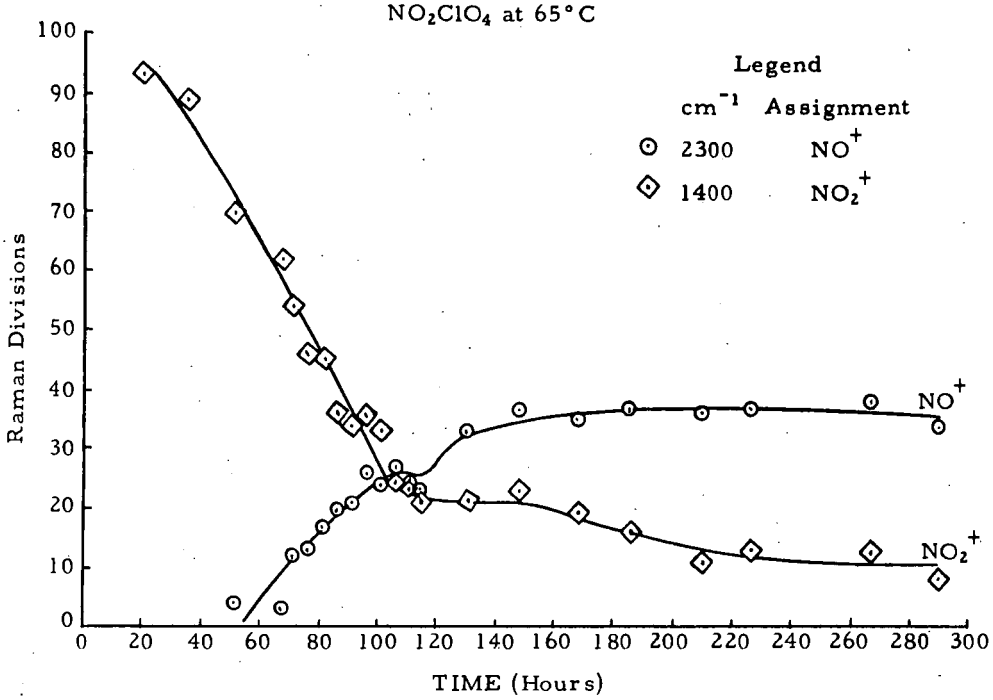

FIGURE 4

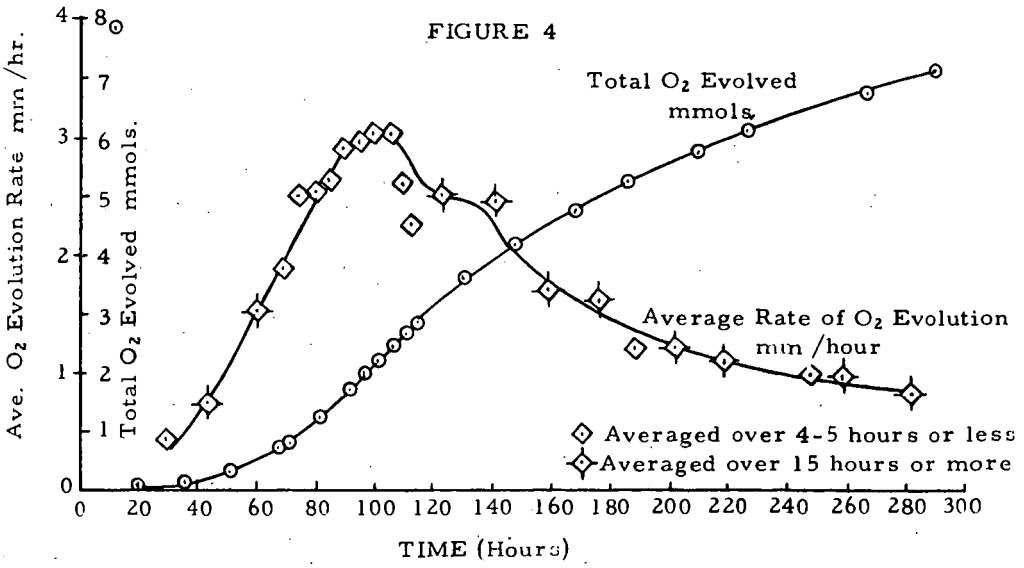

ADVANCED BINDERS FOR SOLID PROPELLANTS - A REVIEW

by Murray S. Cohen

Thiokol Chemical Corporation, Reaction Motors Division,
Denville, New Jersey

The earliest known use of solid propellants dates from reports of Chinese military rockets in the 13th Century. From that period up until relatively recent times the composition of solid propellants remained essentially constant, that is, a mixture of loose powder containing sulfur, nitrate salts and carbon (charcoal). A composition of this type could never be developed for a major role in propulsion because by its very nature it could not give reliable ballistic properties nor could it be used in large diameter (high thrust) motors. With the advent of World War II, smokeless powder or double base gunpowder was adapted to propelling rockets. Here again loose powder mixtures were first used with many of the previously mentioned limitations. Consolidation of the loose powders into homogeneous forms or grains was a major development in double base technology. The colloidal solution of the polymer, nitrocellulose, in the plasticizer, nitroglycerin, gave a solid mass or grain which could be molded to conform to a wide range of motor geometries and be used to deliver long duration thrust in a programmed manner. Early efforts at the development of castable composite systems were pioneered by the Jet Propulsion Laboratories and further developed by the Aerojet, Thiokol and Atlantic Research Companies. The earliest of the composites were asphalt-perchlorate, followed by polystyrene-perchlorate, then polysulfide-perchlorate. Polyvinyl chloride-plasticizer-perchlorate systems were then developed which made use of the plastisol technique. Compression molded propellants of another variety were the next development resulting from the fact that rubber could be mixed with an oxidant and the mass formed under heat and pressure into a strong, well-consolidated grain. These molding techniques, however, limited the size of the charge which could be formed because the total force exerted over the grain surface was limited to the size of the mold and the force capacity of the compression molding apparatus. Large diameter solid grains suitable for first stage ballistic missiles or space boosters could, however, be fabricated with the cast-composite manufacturing methods which called for a liquid fuel to be mixed with a solid oxidizer. When the solids were thoroughly dispersed, the semi-solid, pourable "batter" could then be cast into a rocket motor cavity. By cooling, or by controlled chemical reactions within the fuel the mixture would set up or cure to a solid. The liquid fuel thus became a binder, that is, a component which performed two functions; first, imparted good mechanical properties to the propellant and second, burned as a fuel. In practice, the mechanical properties of a solid propellant improves as the ratio of binder to oxidizer increases. However, in most systems, peak energetics occurs at the 9-11 percent by weight binder level whereas minimum acceptable physical properties are first achieved at the 14 to 16 percent level. The importance of reliable mechanical properties can be illustrated by showing that most operational systems accept the sacrifice in energy and operate at the 14 to 16 percent binder level. The effect of binder level on energetics is shown in Figure 1, a plot of energy (as specific impulse) vs binder level.

A major advance in propellant technology occurred when it was discovered that metallic fuels could be incorporated into the binder-oxidizer mixture to give higher energy as well as higher density propellants without affecting the mechanical properties of the system (i.e. without lowering the allowable binder level). This paradoxical situation can be understood if it is realized that a hydrocarbon-oxidizer system is balanced to give carbon monoxide, carbon dioxide and steam as combustion products. The metallic

additive is oxidized by the steam and therefore does not require additional oxidant. In the case where aluminum is added to a hydrocarbon-ammonium perchlorate system, the combustion proceeds in the following manner:

$$NH_4ClO_4 + (CH_2)_n + 2Al \longrightarrow 1/2\ N_2 + CO + 5/2\ H_2 + Al_2O_3 + HCl$$

The formation of hydrogen gas as a combustion product is very desirable because performance of a system is proportional to the factor

$$\sqrt{\frac{\Delta H}{\overline{M}}}$$

where ΔH is the heat released in combustion and $\overline{M}$ is the mean molecular weight of the combustion products. Figure 2 illustrates the performance improvement found in these metallized systems and shows, as well, the fact that the binder level for optimum performance stays the same as it would be in a metal-free system. The example shown is for a typical hydrocarbon-aluminum-ammonium perchlorate system.

With the foregoing background it is now possible to proceed with a discussion of the directions that research has taken in the development of new and improved binder systems. Two major efforts can be categorized in this review. The first was motivated by attempts to improve the physical properties of propellants while maintaining their energetics. The second effort is a straightforward attempt to increase energetics while maintaining acceptable mechanical properties.

For a treatment of binder developments leading to the improvement of physical properties one must recognize that all hydrocarbon binders are equal in energetics. Nevertheless the binding capability of a hydrocarbon polymer will vary with small changes in its geometrical structure. Although there was enough scientific information available early in the development of solid propellants to aid in the selection of the best polymeric structures, the actual developments followed a typical evolutionary route.

The earliest cast, composite binder to be used was molten asphalt. This material was heated until it formed a fluid melt, was mixed with oxidant and the heated mixture cast into a motor cavity and allowed to cool. This system was a poor one because of the limited temperature range, the low solids content which could be formulated, and the poor mechanical properties of highly loaded asphalt. A chemically cured system was then introduced when acrylate monomers were mixed with oxidizer and curative. The mixture could be cast, heated to cure temperature and the acrylate polymerized to give a well consolidated grain. The basic deficiencies encountered in this type of system were the exotherm, at times uncontrollable, during cure and the shrinkage of the solid due to the fact that the polymer had an appreciably higher density than the monomer. Furthermore, the acrylates used were not particularly rubbery so that their mechanical properties were only suitable for small grains. The addition of a polyfunctional unsaturate, such as divinyl benzene, to the acrylate acted as a cross-linking agent in this system.

The next advance in solid propellant binders came from the use of partially polymerized liquids which retained functionality for subsequent curing. The best example of such a system is the controlled molecular weight polymers obtained from butadiene and acrylic acid. This system is still a liquid of 200 to 300 poise viscosity at 25°C at 2000 to 3000 molecular weight. It is sufficiently fluid at processing temperatures (50 to 60°C) to allow formulation with 80 to 85 percent by weight of solids and still give a castable mix. Curatives of the epoxy or imine type are added to the mix and the system is

allowed to cure over a period of 3 to 24 hours to a resilient solid. The system can be represented in the following manner:

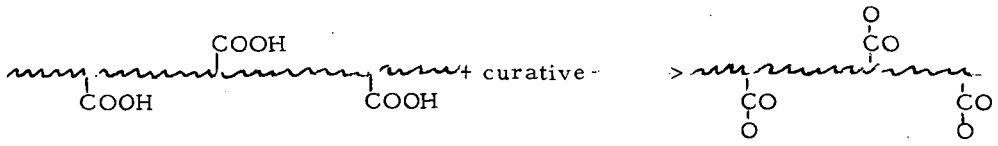

From a theoretical point of view the mechanical properties of a polymeric system can be optimized if the cross-links are introduced in a regular manner and not in a random fashion as shown in the previous equation. It was therefore considered a desirable development when controlled molecular weight systems were made available which had their functional groups only at the ends of chains. These systems were cured with tri and polyfunctional curing agents of the trisimine type. The following equation illustrates the curing reaction of a carboxy terminated hydrocarbon polymer.

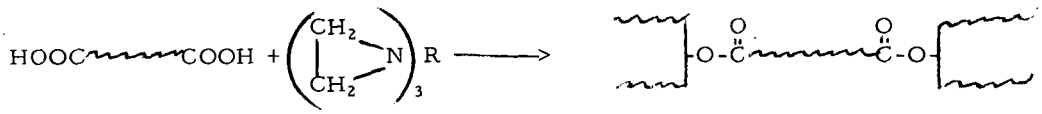

Various attempts have been made to reduce the solids loading of binders by incorporating oxygen into the polymeric structure. In order to maintain the oxidizing potential of the binder oxygen, groups such as the nitrato and nitro were first used. Actually the earliest solid propellant binder was cellulose nitrate plasticized with the nitrate ester nitroglycerin. This system however, was not castable in the conventional sense in that unwarranted extensive development work would be required. Other nitrate ester systems were studied such as that derived from glycidyl nitrate and petrin acrylate.

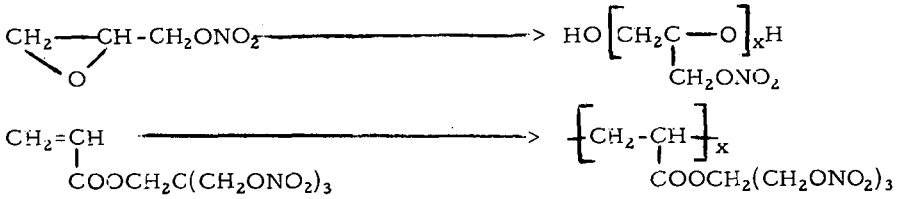

These nitrate systems were found to suffer from the same thermal instability characteristics encountered in the double base systems so that incorporation of oxygen as the more stable nitro groups appeared attractive. Both addition and condensation nitro polymers were prepared as illustrated in the following equations:

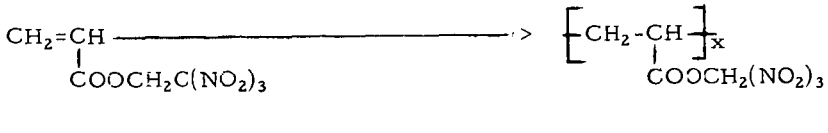

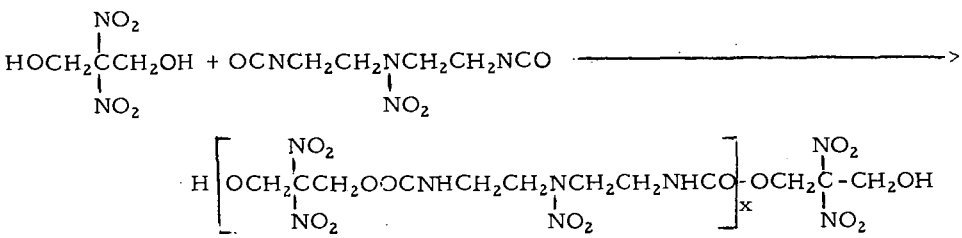

Another energetic oxygen rich binder was prepared which incorporates the perchlorate group as an amine salt.

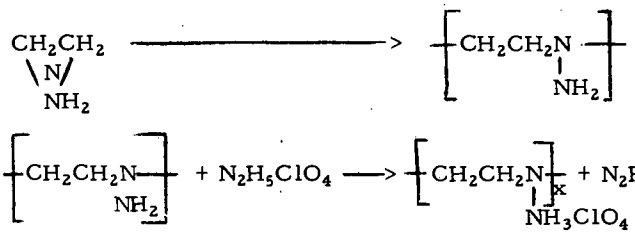

Recently, the discovery of organic compounds which possess the difluoramino group (RNF_2) has prompted study of polymers which have high concentrations of NF_2.

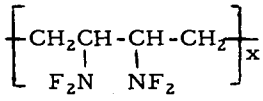

In addition, fluorocarbon polymers, which can be considered as low energy oxidizing binders have been investigated because they are compatible with reactive oxidants and are of high density. Examples of such systems are the fluoroalkyl acrylates and fluoropolyesters.

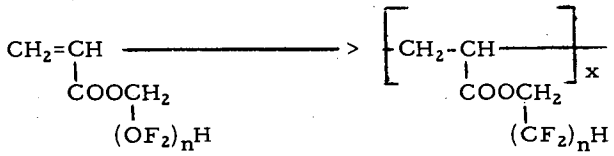

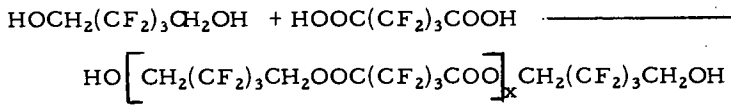

Paralleling the oxidizer binder developments has been work on energetic fuel binders. In this way the binder can be looked upon not only for its mechanical properties but also for its truly energetic contributions to the solid propellant. One example of such an approach was work carried out to incorporate the high heat of formation acetylenic group into the polymer structure. A castable system was prepared based upon the readily available acetylenic monomer butynediol and its reaction with formaldehyde.

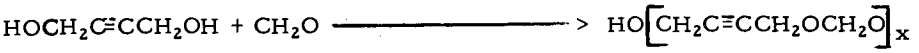

Also, polymers were prepared by the oxidative coupling of dipropargyl ether

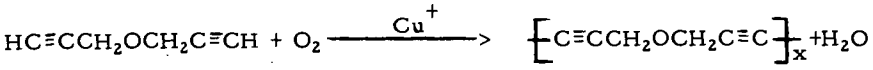

and the vinyl polymerization of isopropenylacetylene.

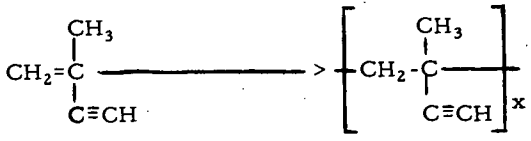

A successful effort was made in incorporating boron hydrides into polymer systems. The early studies made use of decaborane and its simple alkyl derivatives. The difunctionality of decaborane towards Lewis bases allowed the formation of coordination polymers of the following type:

$$NC(CH_2)_4CN + B_{10}H_{14} \longrightarrow H_2 + \left[NC(CH_2)_4CNB_{10}H_{12}\right]_x NC(CH_2)_4CN$$

These polymers tended to be resinous and were also still strong reducing agents. Therefore they could not be safely formulated with oxidants. A major development took place when the dicarbaclovododecaborane (carboranes) compounds were discovered because these materials were extremely stable and were organophilic in character. The basic reaction for carborane formation is described in the following equation.

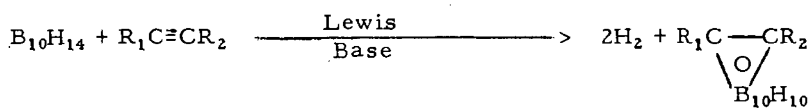

A wide range of monomers and polymers were synthesized; of these the polyester system, shown in the following equations, was most intensively developed.

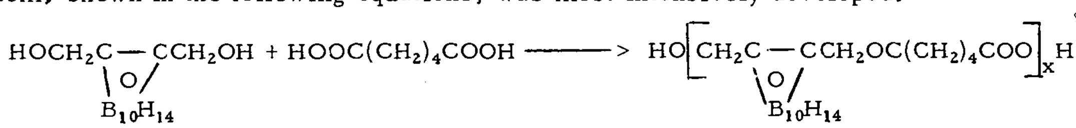

By adjusting the ratios of monomers it was possible to prepare OH, COOH and mixed terminal groups. The polymers were chain extended and cross-linked with isocyanates to give resilient rubbery producrs.

Other carborane systems which were studied included the copolymer of isopropenyl carborane with butadiene and a carboranyl acrylate, both of which are shown in the following equations.

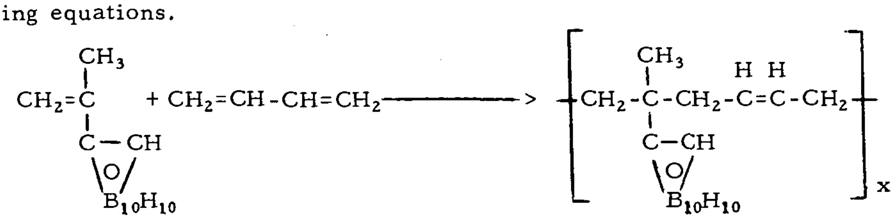

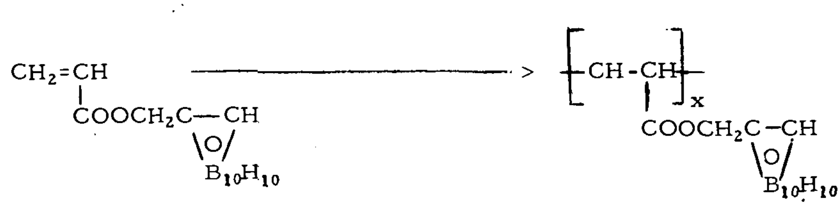

It can be seen from a review of the pertinent synthetic chemistry used for binder research that significant scientific contributions fell out of this work. Most of the advanced systems developed, however, have found very limited application to solid propulsion due to such factors as thermal and shock sensitivity, lower energy than originally calculated, high cost and lack of availability of chemicals, the physical properties of the polymers prepared.

I_{sp} vs. % Binder for a $-(CH_2)_{\overline{x}}$/AP Propellant

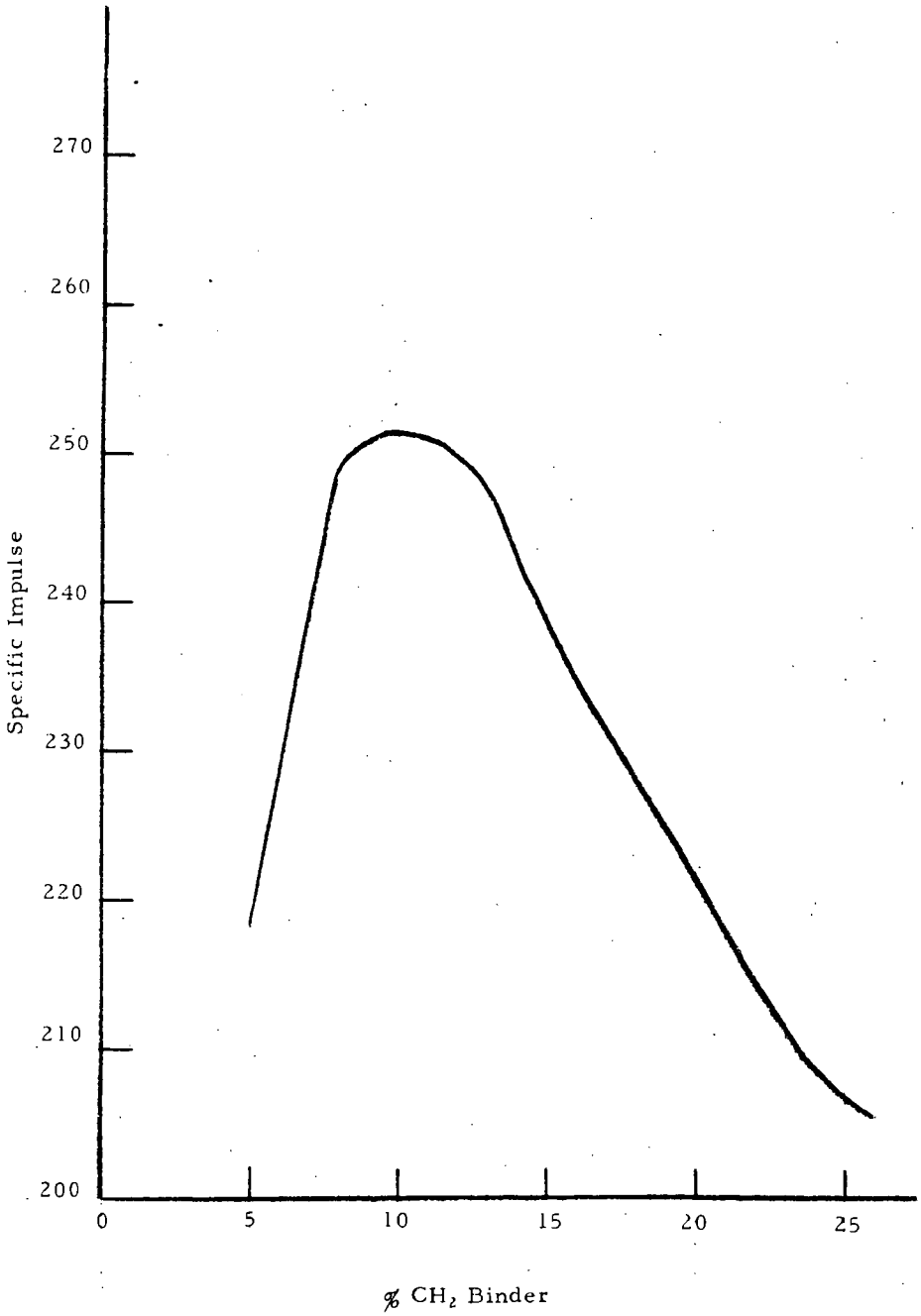

Figure 1

I_{sp} vs. % Binder at 3 Al Levels for a $-(CH_2)_x-$ -Al-AP Propellant

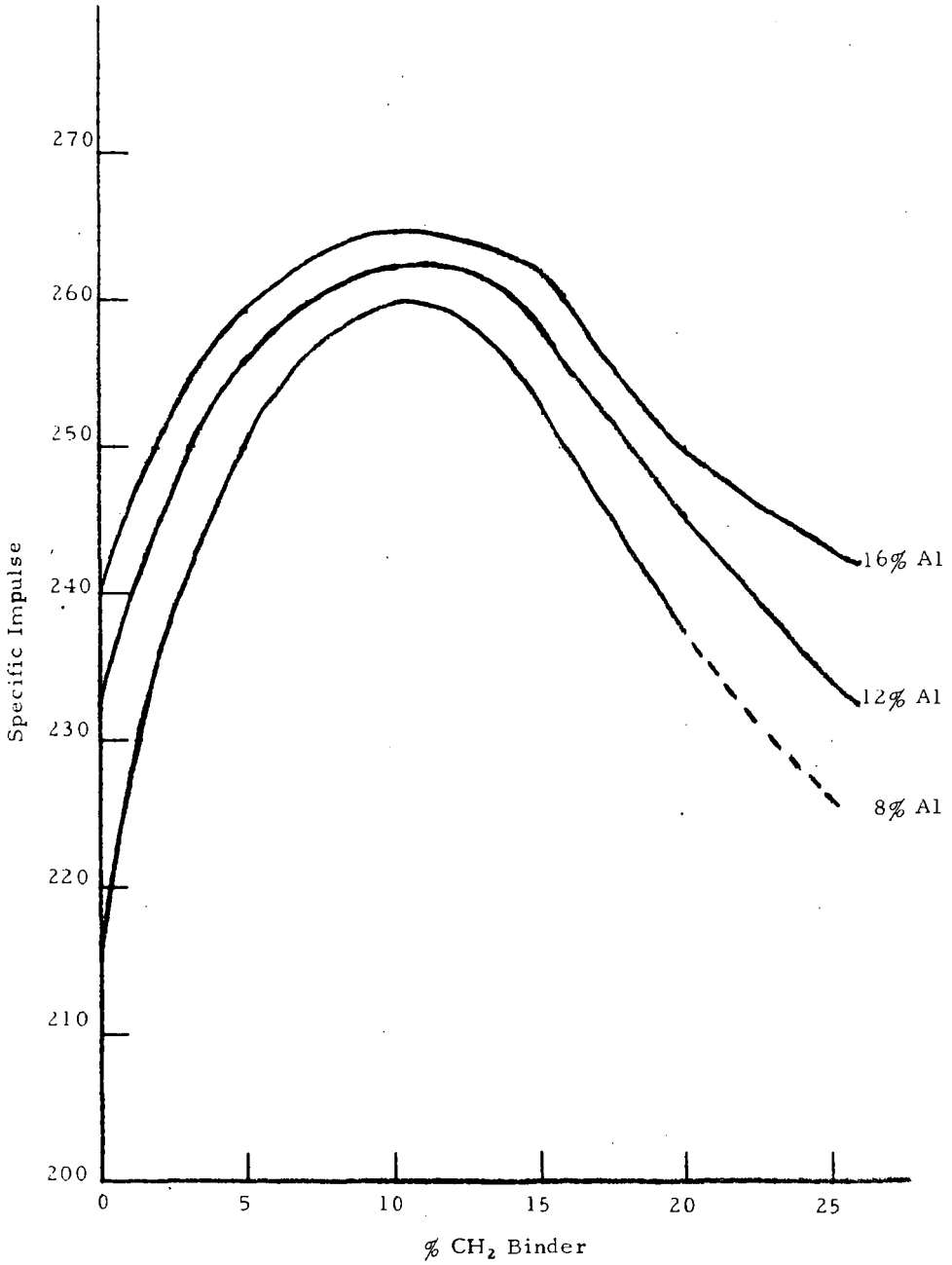

Figure 2

Synthesis and Thermochemistry of Tricyanomethyl and Other Polycyano Compounds

by

Milton B. Frankel, Adolph B. Amster, Edgar R. Wilson,
Mary McCormick, D. Marvin McEachern, Jr.

Stanford Research Institute, Menlo Park, California

ABSTRACT

A series of tricyanomethyl compounds were prepared in refluxing acetonitrile by the alkylation of potassium tricyanomethanide with alkyl iodides, allyl, propargyl, and benzyl bromides. Yields of 20-57% were obtained for mono and difunctional halides with a reflux time of 72 hours.

The heats of combustion of these tricyanomethyl compounds as well as of two polycyano compounds were measured using a Dickenson type calorimeter and heats of formation were calculated with a precision of approximately ±1.0%. From Pitzer's values for C-C and C-H bond energies, that of the tricyanomethyl moiety is calculated to be about 810 kcal/mole. Also the tricyanomethyl group is less stable than expected from comparison with ΔH_f^0 of propylcyanide.

As a result of the synthesis of tetracyanoethylene,[1] a large class of organic molecules heavily substituted with cyano groups has become available. Many of these have interesting physical and chemical properties. The only known tricyanomethyl compounds are the salts of tricyanomethane,[2-8] bromotricyanomethane,[9] 1,1,1-tricyanoethane,[3] 2,2,2-tricyanoethylbenzene,[3] and hexacyanoethane.[10] Tricyanomethane, itself, is an unstable compound and has not been isolated in the free state, although aquoethereal solutions of tricyanomethane have been used for synthetic reactions.[7] This paper describes the synthesis and thermochemistry of a new series of tricyanomethyl compounds.

I SYNTHESIS

A. Discussion

Hantzsch and Oswald[3] prepared 1,1,1-tricyanoethane and 2,2,2-tricyanoethylbenzene in very low yields from a heterogeneous mixture of silver tricyanomethanide with methyl and benzyl iodides, respectively. It was apparent that the silver salt of tricyanomethane was unsuitable for alkylation reactions because of its virtual insolubility in organic solvents. A search was made to find a salt of tricyanomethane which was partially

soluble in organic solvents. Since a ready preparation of potassium tricyanomethanide was now available,[8] attention was turned to studying the solubility characteristics of this salt. It was found that potassium tricyanomethanide was soluble to the extent of 19% in refluxing acetonitrile and that the salt could be alkylated in this medium with alkyl iodides, allyl, propargyl, and benzyl bromides. Optimum yields of 20-57% were obtained for mono and difunctional halides with a reflux time of 72 hours. The importance of the reactivity of the organic halide was demonstrated by the fact that 1,4-dibromobutyne-2 was converted to 1,1,1,6,6,6-hexacyanobutyne-3 in 43% yield while diiodomethane gave only a 2% yield of the monoalkylated product, 1,1,1-tricyanoethyl iodide, and none of the dialkylated product.

As an alternative method of introducing the tricyanomethyl group into organic compounds, the Michael reaction of cyanoform and α,β-unsaturated compounds was studied. Cyanoform was generated in situ by the addition of a stoichiometric amount of 100% sulfuric acid to an acetonitrile solution of potassium tricyanomethanide and the α,β-unsaturated compound. Under these conditions, addition of cyanoform to acrylonitrile, acrylic acid, methyl acrylate, acrylamide, and acrolein did not occur, for only the red polymer of cyanoform was isolated. However, methyl vinyl ketone did react in the expected manner to give 1,1,1-tricyano-4-pentanone.

The tricyanomethyl compounds are a stable class of organic compounds. The solid products can be purified by sublimation. Their exceptional thermal stability is evidenced by the fact that 1,1,1,6,6,6-hexacyanobutyne-3 was sublimed at $170^{\circ}/0.05$ mm. The infrared spectra of these compounds show a weak absorption for cyano at 4.4μ. The properties of the compounds are summarized in Table I.

In addition to the above tricyanomethyl compounds, 1,4-dicyanobutyne-2[11] and 1,1,2,2-tetracyanocyclopropane[12] were also prepared for the thermochemical studies.

B. Experimental

All analyses were made by Stanford University, Stanford, California. Melting points are uncorrected.

Alkylation of Organic Halides with Potassium Tricyanomethanide

The preparation of 1,1,1-tricyanobutene-3 is given as a typical example of the experimental procedures that were used in the reaction of organic halides with potassium tricyanomethanide.

A mixture of 29.0 g (0.225 mole) of potassium tricyanomethanide,[8] 26.6 g (0.32 mole) of allyl bromide, and 500 ml of acetonitrile was refluxed with stirring for 72 hours. The mixture was cooled and filtered

Table I

PROPERTIES OF TRICYANOMETHYL COMPOUNDS

Compound	m.p. °C	Recryst. Solvent	Yield %	Formula	Analyses					
					Calculated			Found		
					C	H	N	C	H	N
$(NC)_3CCH_3$	94-95	(a)	53.0	$C_5H_3N_3$	57.14	2.88	39.99	57.10	2.88	39.60
$(NC)_3CCH_2I$	102-103	(b)	2.2	$C_5H_2N_3I$	26.00	0.87	18.20	26.25	0.85	18.73
$(NC)_3CCH_2CH_2\overset{O}{\overset{\|}{C}}CH_3$	50-51	Ethanol	64.5	$C_8H_7N_3O$	59.62	4.38	26.07	59.58	4.50	26.23
$(NC)_3CCH_2C_6H_5$	140-141	(c)	55.3	$C_{11}H_7N_3$	72.91	3.89	23.19	72.89	3.99	23.40
$(NC)_3CCH_2CH=CH_2$	30(d)	(e)	57.8	$C_7H_5N_3$	64.11	3.84	32.04	64.00	3.85	32.30
$(NC)_3CCH_2CH=CHCO_2C_2H_5$	60-61	Isopropyl Alcohol	56.4	$C_{10}H_9N_3O_2$	59.11	4.47	20.68	59.35	4.82	20.86
$(NC)_3CCH_2C\equiv CH$	61-62	Isopropyl Alcohol	47.3	$C_7H_3N_3$	65.11	2.34	32.55	64.87	2.51	32.74
$(NC)_3CCH_2CH=CHCH_2C(CN)_3$	258-259	Acetonitrile	22.4	$C_{12}H_6N_6$	61.52	2.58	35.88	61.40	2.83	36.11
$(NC)_3CCH_2C\equiv CCH_2C(CN)_3$	219-220	(f)	43.4	$C_{12}H_4N_6$	62.07	1.74	36.20	62.11	1.83	36.30
$(NC)_3CCH_2C\equiv C-C\equiv CCH_2C(CN)_3$	177-178	Chloroform	27.2	$C_{14}H_4N_6$	65.62	1.57	32.80	64.95	1.47	32.22

(a) Sublimed at 40°/0.10 mm, (Lit[2], m.p. 93.5°)

(b) Sublimed at 70°/0.2 mm

(c) Sublimed at 100°/0.05 mm, (Lit[2], m.p. 138°)

(d) b.p. 95°/26 mm, $n^{20}D$ 1.4419

(e) Sublimed at 50°/1 mm

(f) Sublimed at 170°/0.05 mm

to give 21.8 g (83.5%) of precipitated potassium bromide. The filtrate was concentrated and diluted with ether to precipitate the residual potassium salts. After filtering, the filtrate was concentrated and distilled to give 16.7 (57.8%) of colorless liquid, b.p. 95°/26 mm, $n^{20}D$ 1.4419.

1,1,1-Tricyano-4-pentanone

To a stirred solution of 200 ml of acetonitrile containing 14.4 g (0.11 mole) of potassium tricyanomethanide was added 7.74 g (0.11 mole) of methyl vinyl ketone. Then 5.84 g (0.055 mole) of sulfuric acid was added dropwise at ambient temperature. There was an immediate precipitation of potassium sulfate. The reaction mixture was stirred for two hours and filtered to remove 8.86 g (92.6%) of potassium sulfate. The filtrate was concentrated to give 15.3 g of semi-solid product. This slurry was treated with isopropanol to give 11.4 g (64.5%) of white crystals, m.p. 49-50°. Recrystallization from ethanol raised the melting point to 50-51°.

1,4-Dicyanobutyne-2[11]

A mixture of 55.0 g (0.615 mole) of dry cuprous cyanide, 55.0 g (0.26 mole) of 1,4-dibromobutyne-2, and 175 ml of acetonitrile was heated under reflux with good mechanical stirring. After two hours a clear brown solution was attained. The solution was refluxed for an additional 1.5 hours, cooled, and treated with 500 ml of ether. The precipitated cuprous bromide was separated and the filtrate was treated four times with charcoal. The light yellow ether solution was then concentrated to give 12.4 g of yellow crystals. The product was recrystallized from 36 ml of benzene-hexane (80/20) to give 3.6 g (13.3%) of colorless needles, m.p. 91-92°.

Anal. Calc'd. for $C_6H_4N_2$: C, 69.2; H, 3.9; N, 26.9.

Found: C, 68.96; H, 3.73; N, 26.68.

The infrared spectrum showed a strong absorption for C≡N at 2280 cm^{-1}.

II THERMOCHEMISTRY

A. Experimental

A Parr Model 1221 oxygen bomb calorimeter was modified for isothermal operation and to ensure solution of nitrogen oxides.[13] The space between the water jacket and the case was filled with Vermiculite (exploded mica) to improve insulation. A flexible 1000 watt heater (Cenco No. 16565-3) was bent in the form of a circle to fit just within the jacket about 1 cm above the bottom. Heater ends were soldered through the orifices left by removing

the hot and cold water valves. A copper-constantan thermocouple and a precision platinum resistance thermometer (Minco Products Model S37-2) were calibrated by comparison with an NBS-calibrated Leeds & Northrup Model 8164 platinum resistance thermometer. The thermometer was used to sense the temperature within the calorimeter bucket; the thermocouple sensed the jacket temperature. A mercury-in-glass thermo-regulator (Philadelphia Scientific Glass Model CE-712) was used to control the jacket temperature.

Jacket temperature was controlled by connecting the thermoregulator and the heater to an American Instrument Co. Relay Model No. 4-5300. Power to the heater was supplied by a 60 cycle variable transformer normally operated at about 10 volts. Jacket temperature was recorded by feeding the thermocouple output through a Leeds & Northrup D.C. amplifier (Cat. No. 9835-B) to a Speedomax H Azar strip chart recorder.

Calorimeter temperature was measured with a Leeds & Northrup G-1 Mueller Bridge used in conjunction with a D.C. Null Detector (Cat. No. 9834) or with a moving coil galvanometer (Cat. No. 2284-D) and lamp and scale.

Time was measured with a 60 cycle synchronous motor clock. Sample weight was determined using an analytical balance and a set of Class S stainless steel weights.

B. Procedure

General

The samples were burned in the Parr bomb (360 ml capacity), containing, initially, 3 ml of water in the cup over the combustion crucible and 99.99% pure oxygen at 450 psi and about 23°C. The air was flushed out by filling several times with oxygen to 450 psi. The weight of the water for the calorimeter, 2000 g, was measured to 0.1 g on a high-capacity balance.

Sample pellets were weighed in the combustion crucible to 0.05 mg after overnight storage, in a desiccator, over anhydrous calcium sulfate. We do not know any of the compounds to be hydroscopic. The sample was ignited using the usual iron wire supplied by Parr.

For all samples except one the jacket temperature, during a run, was maintained constant to ±0.01°C at about 29°C and the calorimeter temperature at the start of a run was generally of the order of 25°C. 1,1,1-tricyanobutene-3 was treated specially because of its melting point ~30°C. (See below)

The temperature of the calorimeter was obtained by using the detector as a null instrument or the galvanometer in more conventional fashion. During the fore and after periods resistance was measured each minute. During the heating period the time was noted at which several predetermined values of resistance were attained. Resistance could be measured to within 3×10^{-4} ohms or about 0.0015°C.

The nitric acid produced in the combustion was determined by titration with standardized alkali using a methyl orange indicator. The thermal correction was calculated on the basis 14.0 kcal/mole evolved for each mole of aqueous acid formed. A correction was made for the average firing energy, 12.2 cal.

Calibration

The calorimeter was calibrated by burning standardized benzoic acid obtained from the Parr Instrument Co. (ΔH_c = 197.72 kcal/mole). Measurements were made under conditions paralleling as closely as possible those used during a run. For reasons explained below it was also necessary to determine the heat of combustion of Nujol brand mineral oil. For this purpose the contents of two one-pint bottles of Nujol were mixed thoroughly and stored in a one-liter bottle. Runs were made on aliquots withdrawn from this new mixture. Table II includes the results obtained both for the benzoic acid and the Nujol and gives an indication of the precision of the experiment.

Sample Preparation

Samples were purified by recrystallization; we believe each substance to be of better than 99% purity.

The 1,1,1-tricyanobutene-3 formed a glassy solid below 29°C with an unsharp transition. It was run as a liquid with the calorimeter jacket maintained at about 35°C. A small weighed pellet of benzoic acid was heated to above 30°C and the pellet wet with the liquid by dropwise addition. The weight of liquid added was determined by difference. The wet pellet was maintained above 29°C until ignition. Thus uncertainty as to the physical state of the liquid was avoided. No attempt was made to correct results for the heat of wetting.

All other samples were prepared by pressing solid pellets which were then wet with the calibrated Nujol.

C. Results

All computations were made according to the method described by Jessup.[14] The unit of energy used is the defined calorie = 4.183 int. joules. The unit of mass is the gram true mass derived from the weight in air against stainless steel weights and buoyancy corrections were made. Molecular weights were calculated using 1959 values of the Commission on Atomic Weights. Heats of formation were calculated from heats of combustion. The results of individual combustions and corrected values of the heats of formation are presented in Table II.

D. Discussion

It is now possible to compare the measured heats of formation with those predicted on the basis of bond or group additivity. We use the same method

Table II

Energies of Combustion[a]

Compound	State	Mass of Addend, g	Ms g	Es cal/g	E cal/°C	Cz Cal	Q_v 25°C cal/g	Q_p 25°C cal/g	ΔH°_f @25°C kcal/mole, in vacuo	ΔH°_f average @25°C, in vacuo
Benzoic Acid	solid		1.0494	2434.1	2434.5	1.8				
			0.9843	2435.7	2436.1	1.7				
			1.0006	2434.0	2434.4	1.8				
			1.0426	2434.1	2434.6	1.9				
			0.9934	2438.3	2438.7	1.8				
Nujol	liquid		0.9379	2439.8	2440.4	3.3	10976.8			
			0.9541	2439.8	2440.4	3.2	10962.1			
			0.9647	2439.8	2440.4	3.2	10982.0			
1,4-Dicyanobutyne-2	solid	1.1348	0.3300	2434.9	2435.7	17.1	7590.2	7590.2	88.7	
		1.1315	0.3325	2434.9	2435.7	17.1	7558.0	7558.0	85.3	87.0 ± 1.7
Tetracyanoethylene	solid	0.5902	0.9302	2438.4	2439.1	33.4	5585.0	5594.3	151.8	
		0.0964	1.0929	2438.4	2438.9	32.4	5577.9	5587.2	150.9	151.4 ± 0.5
1,1,2,2 -Tetracyanocyclopropane	solid	0.6351	0.6678	2434.9	2435.5	26.6	6131.9[b]	6138.2	145.0	
		0.7467	0.7313	2434.9	2435.6	28.2	6096.6	6102.9	140.0	142.5 ± 2.5
1,1,1-Tricyanoethane	solid	0.7063	0.7560	2435.5	2436.2	30.3	6263.4	6267.7	85.6	
		0.6812	0.6957	2435.5	2436.2	27.6	6240.7	6245.0	83.2	84.4 ± 1.2
1,1,1-Tricyanobutene-3[c]	liquid	1.0932	0.3191	2445.5	2446.1	14.5	7148.5	7149.6	108.0	
		1.0902	0.3222	2445.5	2446.1	14.0	7187.0	7188.1	112.9	110.3 ± 2.5
1,1,1-Tricyanobutyne-3	solid	1.0402	0.4275	2434.9	2435.7	21.7	7002.9	7006.4	143.3	
		1.0373	0.4230	2434.9	2435.7	21.3	7030.9	7034.4	146.9	145.1 ± 1.8
1,1,1,6,6,6-Hexacyanohexene-3	solid	1.0315	0.4490	2434.9	2435.7	22.0	6578.2	6582.0	207.1	
		0.9573	0.4983	2434.9	2435.7	23.2	6525.3	6529.1	194.5	200.8 ± 6.3
1,1,1,6,6,6 Hexacyanohexyne	solid	0.7415	0.7839	2435.5	2436.2	28.9	6494.5	6499.6	242.8	
		1.1114	0.3212	2434.9	2435.7	19.2	6483.0	6488.1	240.5	241.7 ± 1.2
1,1,1,8,8,8-Hexacyanooctadiyne-3,5	solid	1.1165	0.3362	2434.9	2435.7	18.3	6825.0[d]	6829.7	295.0	
		1.1254	0.3309	2434.9	2435.7	17.6	6801.6	6806.3	289.0	292.0 ± 3.0

a. Notation is that of Jessup (loc. cit.)

b. Unburned carbon correction: 4.7 cal.

c. A separate calibration, not given, was performed with benzoic acid, because of the high temperature used. Benzoic acid was used as the addend.

d. Unburned carbon correction: 4.7 cal.

as that discussed by Boyd.[15] Assume ΔH for the following reaction is zero:

$$m\ R\text{-}CN + C_l H_{m+n} \longrightarrow mR\text{-}H + C_l\ (CN)_m H_n$$

R-CN is taken to be proplycyanide (gas) for which $\Delta H_f^o = 7.45$ kcal/mole.[16] The heats of formation used for the compounds $C_l H_{m+n}$ are given in Table III. The heats of sublimation of all the solids were estimated to be 20.0 kcal/mole; for the one liquid we used an estimated value for the heat of vaporization of 5.0 kcal/mole.

Table III

Compound	ΔH_f^o (kcal/mole) (gas)	Reference
Ethane	-20.236	17
Propane	-24.826	18
Ethylene	12.496	17
Cyclopropane	12.74	20
Butyne-1	39.70	18
Hexyne-3	25.84	19
Hexyne-1	29.55	18
Hexane	-39.96	18
Butyne-2	35.37	18
Hexene-3 (cis)	-11.56	18
(trans)	-12.56	18
Average	12.06	
Butene-1	0.28	18
Octadiyne-3,5	93.8*	

*Calculated from ΔH_f^o octane = -49.82 kcal/mole (Ref. 17)
ΔH hydrogenation (octa - 1,7 diyne) = 139.7 (Ref. 21, p. 53)
and ΔH hydrogenation (dodeca - 1,7 diyne) minus
ΔH hydrogenation 3,9 isomer = -3.9 kcal/mole (Ref. 21, p. 54)

The results of the comparison are shown in Table IV where the last column, Δ, represents the excess of the measured heat of formation over that calculated. Accordingly, the positive values are evidence of the decreased stability of the polysubstituted cyanocarbons.

Table IV

Compound	ΔH_f^o (gas), (kcal/mole) Measured	Calculated	Δ
1,4-Dicyanobutyne-2	107.0	99.9	7.1
Tetracyanoethylene	171.4	141.6	29.8*
1,1,2,2-Tetracyanocyclopropane	162.5	141.8	20.7
1,1,1-Tricyanoethane	104.4	76.6	27.8
1,1,1-Tricyanobutene-3	115.3	97.1	18.2
1,1,1-Tricyanobutyne-3	165.1	136.5	28.6
1,1,1,6,6,6-Hexacyanohexene-3	220.8	181.6	39.2
1,1,1,6,6,6-Hexacyanohexyne-3	261.7	219.5	42.2
1,1,1,8,8,8-Hexacyanooctadiyne-3,5	312.0	287.4	24.6

*See R.H. Boyd[15] for comparison.

It is also possible to calculate the bond energy of the tricyanomethyl moiety in each of the molecules. To do this we calculate standard heats of formation at 0°K from the values given in Table III for 298°C. In the absence of reliable data we note the following reported[23] specific heats, c:

Acetonitrile: 0.54 cal/g
Propionitrile: 0.538 cal/g
Butynonitrile: 0.547 cal/g

Taking an average value for c = 0.54 cal/g, we can, for each compound, calculate $H^o_{298}-H^o_o$ = 298 Mc where M = molecular weight. The bond energy of the $-C(CN)_3$ group is then calculated using values for other bond energies as given by Pitzer[22] and values for the heats of formation of H, N, and C atoms as given in reference 13. The results of these calculations are listed in Table V.

Table V

Compound	$E(-C(CN)_3)$ kcal
1,1,1-Tricyanoethane	800
1,1,1-Tricyanobutene-3	816
1,1,1-Tricyanobutyne-3	819
1,1,1,6,6,6-Hexacyanohexene-3	814
1,1,1,6,6,6-Hexacyanohexyne-3	814
1,1,1,8,8,8-Hexacyanooctadiyne-3,5	822

The following are our conservative estimates, expressed in kcal, of the uncertainties in the calculated values of the stabilization energies:

Combustion process	1.0
Heat of vaporization	1.0
Heat of sublimation	4.0

The bond energy calculations are in error, in addition, because of the uncertainty in the enthalpy calculation. For, not only is c estimated at 25°C but the further assumption is made that c is temperature-independent. This may introduce an error as large as 2 or 3 kcal. Consequently neither the scatter in the stabilization energies nor the apparently increasing trend in the bond energy with increasing unsaturation is significant. Nevertheless, assigning a bond energy to the tricyanomethyl group is reasonable. To calculate the heat of formation of linear or cyclic hydrocarbons with the group substituted in one or more locations, an average value of 810 kcal for the $-C(CN)_3$ bond energy would appear to introduce an error of about 10 kcal. We are in the process of determining the latent heats and heat capacities necessary to improve the significance of the data.

ACKNOWLEDGEMENT

Research reported in this publication was supported by the Advanced Research Projects Agency through the U.S. Army Research Office-Durham. The authors wish to thank Dr. Harry S. Mosher for his interest and helpful suggestions throughout the course of this work.

REFERENCES

1. T.L. Cairns et al., J. Am. Chem. Soc., 80, 2775 (1958).
2. H. Schmidtmann, Ber., 29, 1172 (1896).
3. A. Hantzsch and G. Oswald, ibid, 32, 641 (1899).
4. L. Birckenbach and K. Hutner, ibid, 62B, 153 (1929).
5. E. Cox and A. Fontaine, Bull, Soc. Chim. France, 948 (1954).
6. W.J. Middleton and V.A. Engelhardt, J. Am. Chem. Soc., 80, 2788 (1958).
7. W.J. Middleton, E.L. Little, D.D. Coffman, and V.A. Engelhardt, ibid, 80, 2795 (1958).
8. S. Trofimenko, E.L. Little, Jr., and H.F. Mower, J. Org. Chem. 27, 433 (1962).
9. L. Birchenbach and K. Huttner, Ber., 62B, 2065 (1929).
10. S. Trofimenko and B.C. McKusich, J. Am. Chem. Soc., 84, 3677 (1962).
11. Private communication, Dr. J.A. Elvidge, University of London.
12. R.M. Scribner, G.N. Sausen, and W.W. Prichard, J. Org. Chem., 25, 1440 (1960).
13. G.T. Armstrong and S. Marantz, J. Phys. Chem. 64, 1776 (1960).
14. R.S. Jessup, "Precise Measurement of Heat of Combustion with a Bomb Calorimeter," NBS Monograph 7, dated February 26, 1964.
15. R.H. Boyd, J. Phys. Chem., 38, 2529 (1963).
16. F.W. Evans and H.A. Skinner, Trans. Faraday Soc. 55, 255 (1959).
17. F.D. Rossini, et al., Circular 500, National Bureau of Standards, Selected Values of Chemical Thermodynamic Properties.
18. F.D. Rossini, et al., Circular C461, National Bureau of Standards, Selected Values of Properties of Hydrocarbons.
19. API Project 44, Carnegie Press, Pittsburgh, Penn. (1955).
20. J.W. Knowlton and F.D. Rossini, Jr., J. Res. NBS, 43, 13 (1949).
21. C.T. Mortimer, "Reaction Rates and Bond Strengths," Pergamon Press, 1962.
22. K.S. Pitzer, J. Am. Chem. Soc., 70, 2140 (1948).
23. N.A. Lange, Handbook of Chemistry, 10th ed., McGraw-Hill, 1961.

Acetylenic Propellant Binders

Donald D. Perry, Gerald Golub, Rita D. Dwyer and Paul F. Schaeffer

Chemistry Department, Thiokol Chemical Corporation,
Reaction Motors Division, Denville, New Jersey

INTRODUCTION

One approach to improving the performance of composite solid propellants containing organic fuel binders is to introduce endothermic groups into the binder structure. Since the acetylenic bond is one of the most energetic organofunctional groups, a program was undertaken to synthesize polymers containing carbon-carbon triple bonds and to evaluate these polymers as binders in castable propellant systems. The studies reported here include the synthesis of prepolymers, curing of the prepoymers to elastomeric binders with diisocyanates, laboratory propellant evaluation, and small rocket motor tests.

PREPOLYMER PREPARATION

The formation of acetals by the reaction of aldehydes with alcohols (equation 1)

$$2ROH + R'CHO \overset{H^+}{\rightleftharpoons} (RO)_2CHR' + H_2O \qquad (1)$$

is a well-known and useful preparative method in organic chemistry.[1] As indicated in equation 1, it is an equilibrium reaction, which is catalyzed by strong acids and favored by the removal of water. A modification of this method is the acetal exchange reaction (equation 2). The success of this method depends on the ability to remove

$$2ROH + (RO)_2CHR' \overset{H^+}{\rightleftharpoons} (R\cdot O)_2CHR' + 2R''OH \qquad (2)$$

R''OH preferentially and thereby shift the equilibrium in equation 2 to the right. This is generally accomplished by distillation, and the conversion therefore requires that R''OH be significantly more volatile than ROH. The acetal exchange reaction has found application in the preparation of acetals where direct reaction of an alcohol and aldehyde is difficult or inconvenient, or where the acetal of a low-boiling alcohol is more readily available. Both reactions have been used frequently to protect carbonyl groups during other synthetic operations, since regeneration of the free aldehyde or ketone can usually be accomplished readily.

Hill and Carothers[2] investigated the acetal exchange reaction as a method of preparing polymers (equation 3). When n was 3 or 4, cyclic formals were the

$$HO(CH_2)_nOH + BuOCH_2OBu \xrightarrow[\text{acid cat.}]{150^0} \left[CH_2O(CH_2)_nO\right]_m + 2\,BuOH \qquad (3)$$

principal products. Pentamethylene glycol (n = 5) afforded a syrupy liquid polymer. The reaction with decamethylene glycol, where cyclic structures are not favored, was studied most extensively. Initially a waxy polymer (m.p. 56.5-57^0) of

molecular weight 2190, was formed. On heating this product in vacuo at 230-250°, polymers of 10-20,000 molecular weight, capable of being drawn into fibers, were obtained.

The present study had as its objective the preparation of low molecular weight hydroxy-terminated polymers containing acetylenic bonds and their evaluation as binders for castable solid propellant formulations. Since 2-butyne-1, 4-diol (II) was commercially available, the formation of polyacetals from this glycol seemed to be an attractive route to the desired polymers. It was believed that the rigid triple bond would inhibit the cyclic acetal formation observed by Hill and Carothers with the lower members of the saturated glycol series. Thus, in an acetal exchange reaction the linear polymer (I) should be favored over the cyclic acetal (III):

$$n\mathrm{HOCH_2C{\equiv}CCH_2OH} + n(\mathrm{RO})_2\mathrm{CH_2} \xrightarrow{H^+} 2n\mathrm{ROH} + n\mathrm{CH_2C{\equiv}CCH_2} \quad (3a)$$

II → III

$$\mathrm{H(OCH_2{\equiv}CCH_2OCH_2)_nOR} + (2n-1)\mathrm{ROH} \quad (3b)$$

I a R = n-propyl
I b R = n-butyl

Initial studies with butynediol (II) employed the reaction with di-n-butyl formal and di-n-propyl formal. The reaction of the former with II required relatively high temperatures (ca. 190°) in order to remove the by-product n-butyl alcohol (b.p. 117.7°), and this apparently caused some polymer degradation. As a result, only a semi-solid polymer (I b) of molecular weight 475 was obtained. The reaction with di-n-propyl formal, however, gave polymers with molecular weights of 680 and 1020 in two experiments. The higher molecular weight material was obtained by heating an equimolar mixture of the reactants at 130-180° for nine hours in the presence of polyphosphoric acid and continuously removing the n-propyl alcohol by distillation into a Dean-Stark trap. The product was a waxy material, m.p. 55°, which was shown by chemical and infrared analysis showed to have the structure I a where R = n-propyl.

Similar acetal exchange reactions were carried out between II and di-n-propyl acetal (IV) and II and diethyl propional (V), to give low molecular weight, liquid polyacetals (VI a and VI b):

$(\mathrm{CH_3CH_2CH_2O})_2\mathrm{CHCH_3}$ (IV) + $\mathrm{HOCH_2C{\equiv}CCH_2OH}$ + $(\mathrm{C_2H_5O})_2\mathrm{CHCH_2CH_3}$ (V) + $\mathrm{HOCH_2C{\equiv}CCH_2OH}$ (4)

$$\mathrm{HO\{CH_2C{\equiv}CCH_2OCHO\}_{\overset{|}{R}}R_1}$$

VI a R=CH_3-; R_1=C_3H_7-
VI b R=C_2H_5-; R_1=C_2H_5-

Despite the success achieved in preparing low molecular weight acetylenic ether polymers by the acetal exchange reaction, an improved method was desired, since it was difficult to obtain molecular weights above 1,000, and the reactions were slow. It was found at this point that direct reaction of II with paraformaldehyde (equation 5) proceeded rapidly in refluxing benzene or toluene to yield polymers

$$n\mathrm{HOCH_2C{\equiv}CCH_2OH} + n(\mathrm{CH_2O})_x \xrightarrow{H^+} \mathrm{HO\{CH_2C{\equiv}CCH_2OCH_2O\}_nH} + (n-1)\mathrm{H_2O} \quad (5)$$

II Ic

having molecular weights in the 1500-2500 range. These were hard, brownish-colored waxes, quite similar, except for their molecular weights, to the products obtained in the acetal exchange reactions. The reaction proceeded approximately twice as fast in toluene as in benzene due to the higher temperature attainable. The generality of the method was shown by the fact that it could also be successfully employed with 2,4-hexadiyne-1,6-diol and paraformaldehyde, and with II and 2-ethylbutyraldehyde, although in these cases only low molecular weight (600-800) products were obtained.

The polyacetals obtained in these reactions were characterized by wet chemical and infrared analyses, and by cryoscopic molecular weight determinations. For the latter, the preferred method was the freezing point depression of an ethylene bromide solution.

Infrared and functional group analyses showed the presence of two hydroxyl end-groups in the products obtained from formaldehyde (Ic). In addition, the results of chain extension and cross-linking reactions with diisocyanate (vide infra) confirmed the presence of two terminal hydroxyl groups.

CURING STUDIES

Curing of the acetylenic polyacetals to rubbery polyurethanes could be achieved with any of a number of commercially available diisocyanates, including 2,4-toluene-diisocyanate (TDI), hexamethylenediisocyanate (HDI), dianisidine diisocyanate (DADI), and 4,4'-diisocyanatodiphenylmethane (MDI). The first two diisocyanates were studied most extensively. The reactions were carried out in solution in benzene, toluene, or ethylene bromide, or in bulk. The bulk reaction in general gave products with superior properties and, of course, it is the only suitable method for use in a practical propellant process.

In addition to the diisocyanate, cross-linking agents, catalysts and plasticizers were used to accelerate the cure reaction and to improve the physical properties of the ultimate binder composition. The cross-linking agents consisted of trifunctional alcohols (castor oil and trimethylolpropane), aminoalcohols and aliphatic or aromatic diamines. Best results were obtained with castor oil and trimethylolpropane. Castor oil was preferred because of its lower rate of reaction with the isocyanate, which resulted in a longer pot life for the propellant mix. Catalysts for the polyurethane formation reaction included tertiary amines and ferric acetonylacetonate. A variety of typical ester-type plasticizers were investigated to give improved physical properties. The best of these was butyl cyclohexyl phthalate. Finally, a study of reaction stoichiometry vs. physical properties showed that a molar ratio of polyformal:diisocyanate:cross-linking agent of 1:1.5:0.2 gave

Table I

Physical Properties of Selected Acetylenic Polyurethane Binders

Sample No.	Prepolymer Mol. Wt.	Diiso-cyanate	Cross-linking Agent	Plastic-izer	(%)	Catalyst	Ult. Tensile Strength (psi)	Ult. Elongation (%)	Permament Deformation (%)	Shore A-2 Hardness
1	1915	TDI	TMP	-----	--	-----	913	73	31	97
2	1915	HDI	TMP	-----	--	-----	773	63	37	--
3	1180	HDI	TMP	-----	--	-----	681	64	28	96
4	1180	HDI	TMP	BCPH	14	FeAA, DPPD	257	412	184	64
5	1915	HDI	CO	BCPH	14	FeAA, DPPD	1300	506	215	--

Abbreviations:

TDI = 2,4-Tolylene diisocyanate
HDI = Hexamethylenediisocyanate
TMP = Trimethylolpropane
CO = Castor Oil
BCPH = Butyl cyclohexylphthalate
FeAA = Ferric acetonylacetonate
DPPD = Diphenyl-p-phenylenediamine

the best results. Cure was essentially complete in 20 hours at 80°C.

In Table I are listed the physical properties of some typical binder compositions, both with and without plasticizer. These all used the stoichiometry and cure conditions given above, except for sample 5 for which a 44 hour cure time was used.

LABORATORY PROPELLANT FORMULATION AND EVALUATION

Propellant compositions containing the acetylenic fuel binder and ammonium perchlorate oxidizer were prepared and cured and their physical and ballistic properties determined. Formulations containing up to 83% by weight of ammonium perchlorate oxidizer have been prepared. This represents the optimum level of oxidizer for this fuel binder. Processing characteristics and propellant physical properties were good. A description of the preparation of a typical propellant batch is given in the Experimental Section, and Table II summarizes the principal physical properties of a characteristic batch of cured propellant. The tensile properties were measured on dumbell specimens, 4 to 6 inches long with a 1-inch guage length 3/32 inch thick and ends of 1/4 inch thickness.

Table II

Physical Properties of Acetylenic Polyurethane Propellants

Formulation No.	Tensile Strength (psi)	Elongation (%)	Density ($lbs./in.^3$)	Impact Sensitivity (in.)	Autoignition Temp. (°F)
57	90	16	0.0625	9-10	670
66	108	14	0.061	8	660
73	110	25	0.061	9-10	685

Notes:

1. Formulations 57 and 73 used HDI; 66 used TDI.
2. All three formulations contained about 5% (by wt. of propellant) of BCPH and used castor oil as cross-linking agent.
3. Oxidizer loadings for formulations 66 and 73 were 75%, for 57, 77.8%.

Among the most interesting features of the acetylenic polyurethane propellants were their ballistic properties. Burning rates of propellant strands were determined in a Crawford bomb apparatus. The burning rates measured at 1,000 psia were normal for ammonium perchlorate type composite propellants, ranging from 0.5 to 1.25 in./sec. What was unusual was the occurrence of a plateau in the burning rate vs. pressure curves in the 700-2000 psia region. The exact position and extent of the plateau region varied somewhat from batch to batch, but it was a constant feature of all the compositions containing the acetylenic polyurethane binder. The value of such a region of relative lack of pressure dependence of burning rate in providing controlled burning despite pressure fluctuations is obvious. It was

possible through the use of a catalyst to increase the propellant burning rate up to 2.2 in./sec. Curves of burning rate vs. pressure for catalyzed and uncatalyzed propellant compositions are shown in Figure 1.

Safety tests were carried out in order to determine the handling characteristics of the propellant system. The impact sensitivity of the propellant was found to be approximately the same as that of pure ammonium perchlorate (9-12 inches) when tested with a 2 kg weight in the Picatinny Arsenal impact dropweight tester.[3] Detonation tests made with a number eight blasting cap and 20 grams of tetryl indicated that the propellant is not sensitive to detonation. The autoignition temperature of these propellants is in the range of 220 to 240°C as measured by the Picatinny Arsenal test method.[3] Propellant samples have been stored at 80°C (175°F) for periods up to 30 days without any signs of degradation or change in their physical properties.

SMALL MOTOR FIRINGS

Although the program was primarily concerned with the synthesis and laboratory evaluation of these new propellant compositions, some practical confirmation of their theoretical performance was also desired. Consequently, a limited number of small motor firings were carried out.

Theoretical performance calculations were first made on propellant compositions containing the acetylenic polyurethane binder and ammonium perchlorate as the oxidant. These calculations assumed a shifting equilibrium in the rocket exhaust. Specific impulse values of 251-252 lbf-sec./lbm. were calculated at 1000 psia chamber pressure for optimum oxidizer loadings. For the actual compositions tested, the theoretical values were somewhat lower. In all, 18 acetylenic polyurethane propellant grains were test fired in small motors. These ranged in weight from 0.40 to 6 lb. and included both 3-inch and 6-inch diameter end-burning grains. Two compositions were used, one containing 75% oxidizer, which had a theoretical Isp of 243 seconds at 1000 psia chamber pressure, and one containing 77.8% oxidizer, having a calculated Isp of 249 seconds. Experimental Isp values for these motors ranged from 214 to 222 seconds for the 75% oxidizer compositions, indicating efficiencies of 88.1 to 91.2%. For the 77.8% oxidizer grains, the experimental values were from 225 to 229 seconds, with the corresponding efficiencies being 90.4 to 92.0%. Chamber pressures in these tests ranged from 300 to 1000 psi and thrust levels were in the range of 25 to 100 lbs.

EXPERIMENTAL

Poly(2-butyne-1, 4-dioxymethylene)

A. From Di-n-propylformal (1) - A three-necked, round-bottom flask, fitted with a gas inlet tube, a mechanical stirrer and a graduated Dean-Stark moisture trap with a condenser attached, was charged with 66 g. of di-n-propyl formal, 45 g. of 2-butyne-1, 4-diol and 0.5 g. of p-toluenesulfonic acid. A slow stream of nitrogen was passed through the system via the gas inlet tube to aid in entrainment of the by-produced n-propanol, and the mixture was heated in an oil bath. When it became sufficiently fluid, the mixture was stirred mechanically and was heated for two to three hours at 125° to 150°. During this time 60-70 ml. of n-propanol was distilled into the Dean-Stark trap. The mixture then was heated for another three hours under reduced pressure (1 to 3 mm.). Traps cooled with Dry Ice-acetone were placed in the system to collect any additional alcohol formed in the reaction. An additional 5 to 15 ml. of n-propanol was isolated during this heating cycle. The reaction mixture then was allowed to cool. The product, a waxy solid, weighing 46 g., melted at 60°, and represented a 90% yield. Its molecular weight, based on the freezing-point depression in ethylene bromide, was 680.

Anal. Calcd. for $C_5H_6O_2$: C, 61.26; H, 6.75.

Found : C, 60.76; H, 6.75.

An experiment, in which the same reactants and substantially the same procedure were used as in A, except that polyphosphoric acid was the catalyst and a longer reaction time (9 hours) and higher temperature (130-180°) were employed, resulted in a quantitative yield of a polymer in the form of a dark brown, waxy solid, m.p. 55° with a molecular weight of 1020 (determined cryoscopically).

Anal. Found: C, 60.44; H, 6.58.

B. From Di-n-butyl Formal - When 2-butyne-1, 4-diol and di-n-butyl formal were allowed to react in a similar manner at temperatures up to 190° in the presence of a catalytic amount of p-toluenesulfonic acid, nearly two equivalents of n-butanol distilled off. The product was a mushy, light brown solid, of molecular weight 475, as determined cryoscopically in a benzene solution.

C. From Paraformaldehyde - A three-necked, 300 ml. flask was equipped with a thermometer, mechanical stirrer and Dean-Stark trap with a condenser attached. The flask was charged with 130 g. of toluene and 43 g. of 2-butyne-1, 4-diol. Paraformaldehyde (15 g.) and 0.5 g. of p-toluenesulfonic acid were added portionwise to the mixture, over a 3.5-hour period. After addition of the first portion of paraformaldehyde and catalyst the mixture was heated to reflux temperature (100°-110°). During the reaction nearly 9 ml. of water were collected in the Dean-Stark trap. The reaction mixture was allowed to cool, and the toluene was decanted from the solid polymer, which had separated from the solution. The polymer then was heated for 4 hours, under a vacuum of 1 to 2 mm., at 80°-115°. A yield of 46 g. (94%) of a hard, waxy polymer, of molecular weight 2300, was obtained.

Poly(2, 4-Hexadiyne-1, 6-dioxymethylene) - A three-necked flask, equipped as in Example A, was charged with 130 g. of benzene, 22 g. of 2, 4-hexadiyne-1, 6-diol, and 6.1 g. of paraformaldehyde. p-Toluenesulfonic acid (0.2 g.) was added, and the

mixture was heated at reflux temperature for 3 hours. Approximately 3.0 ml. of water was distilled into the Dean-Stark trap during this time. The mixture was allowed to cool, and the benzene was decanted from the solid polymer. The polymer then was heated for 3 hours at 90°-100° under a vacuum (2 to 3 mm). The product was a dark-colored, waxy solid, melting at 70°-75°, and having a molecular weight of 810.

Poly(2-butyne-1, 4-dioxyethylidene)- A 250 ml., three-necked flask equipped as in Example I, was charged with 43 g. of 2-butyne-1, 4-diol, 73 g. of di-n-propyl acetal, and 0.5 g. of p-toluenesulfonic acid. The mixture was heated at 125° to 150° for three hours at atmospheric pressure, under a slow stream of nitrogen to aid in the entrainment of the by-produced alcohol during which time 65 ml. of n-propanol were collected. The reaction mixture then was heated for an additional four hours at 1 to 3 mm. pressure; and an added 10 ml. of n-propanol were isolated. The product, obtained in quantitative yield, was a viscous, dark-brown liquid. Its molecular weight was 920 when determined cryoscopically in ethylene bromide.

Poly(2-butyne-1, 4-dioxy-2'-ethylbutylidene)- A 500 ml., three-necked, round bottom flask, equipped as in Example A above, was charged with 43.0 g. of crude 2-butyne-1, 4-diol, 0.5 g. of p-toluenesulfonic acid, and 250 ml. of benzene. The mixture was heated to 60°, and 50.1 g. of 2-ethylbutyraldehyde was added. The theoretical amount of water was collected by azeotropic distillation during an 8-hour heating period at 75°-82°. To remove the acid catalyst a mildly basic ion exchange resin, Amberlite IR-45 (10 g.), was added, and the mixture was stirred at room temperature for 2 to 3 hours. The resin and impurities then were filtered off, and benzene and volatiles were distilled from the remaining product during a 5-hour heating period at 80°-90°/2-15 mm. A dark, viscous liquid was obtained. Its molecular weight, measured by the cryoscopic method, was 620.

Polyurethanes from Poly(2-Butyne-1, 4-dioxymethylene)

A. Reaction with 2, 4-Toluene Diisocyanate - A sample of polyformal of molecular weight 1915 (95.7 g., 0.05 mole) was melted in a 500 ml. beaker, and 1.34 g. (0.01 mole) of trimethylolpropane (TMP) was added. The mixture was heated to 80°, agitated thoroughly, and then degassed at 80°/5mm. in a vacuum oven. After cooling to 50°, 13.05 g. (0.075 mole) of 2, 4-toluenediisocyanate (TDI) was added and the mixture was again heated to 80° and thoroughly mixed. It was then cast into a Teflon-coated mold, degassed at 80°/5mm again for one hour, and cured at 80° for 20 hours. The physical properties of the resulting polyurethane are given in Table I (Sample 1).

B. Reaction with Hexamethylene Diisocyanate - 1. The above procedure was repeated using 12.60 (0.075 mole) of hexamethylenediisocyanate (HDI) instead of TDI. The physical properties of the product are listed in Table I (Sample 2).

2. When the same procedure was repeated with 60 g. (0.05 mole) of polyformal prepolymer of molecular weight 1180, a polyurethane with similar physical properties was obtained (Sample 3, Table I).

C. Preparation of Plasticized Polyurethane Compositions - 1. The procedure given in B.2 was repeated, except that 10.5 g. butylcyclohexylphthalate

(BCPH) was added to the original mixture as a plasticizer, and 0.5 g. of di-p-phenylphenylenediamine and 0.05 g. of ferric acetonylacetonate were used as catalysts. The properties of the resulting cured polymer are given in Table I (Sample 4).

2. The above procedure was repeated using 95.7 (0.05 mole) of the 1915 molecular weight prepolymer and 9.18 g. (0.01 mole) of castor oil as the cross-linking agent. Physical properties are listed under Sample 5 in Table I.

D. Mixing, Casting and Curing of Propellants - The propellant was mixed in a sigma-blade mixer. The order of addition of ingredients had little effect on the properties of the final propellant. For safety reasons, however, the ammonium perchlorate was added to the fuel binder ingredients, except for the diisocyanate. The latter was added portion-wise to the remainder of the propellant mix. This procedure was employed to increase pot life. The most important factors in the propellant mixing were the mixing temperature and the mixing time. The mixing temperature was governed primarily by the temperature-viscosity relationships of the particular prepolymer batch. Propellants containing up to 77.8 percent oxidizer were cast through a "bayonet" with 1/16 in. to 1/8 in. wide slits into an evacuated, vibrated mold. Propellant containing 80% oxidizer was cast by applying 20 psig nitrogen pressure to the casting feed can. The propellant and casting equipment were maintained at 70-75°C during casting. The measured densities of the propellants were 0.063, 0.061, and 0.058 lb/in.^{3} at 80, 77.8, and 75 wt% ammonium perchlorate respectively. These densities represent 98.5, 97, and 95% of the theoretical densities. Grains were cured at 75 to 80°C for 16 to 44 hours; a satisfactory cure was generally obtained in 20 hours at 80°C.

REFERENCES

1. See, for example, L. F. and M. Fieser, "Organic Chemistry", D. C. Heath and Co. 3rd ed. (1956) p. 215.
2. J. W. Hill and W. H. Carothers, J. Am. Chem. Soc., 57, 925 (1935).
3. Picatinny Arsenal Technical Report No. 1401, Rev. 1.

Acknowledgement - This work was supported by the United States Navy under Contracts NOrd 16575 and 17851. The authors also wish to thank Dr. David J. Mann of these laboratories for his guidance and encouragement during the course of this work.

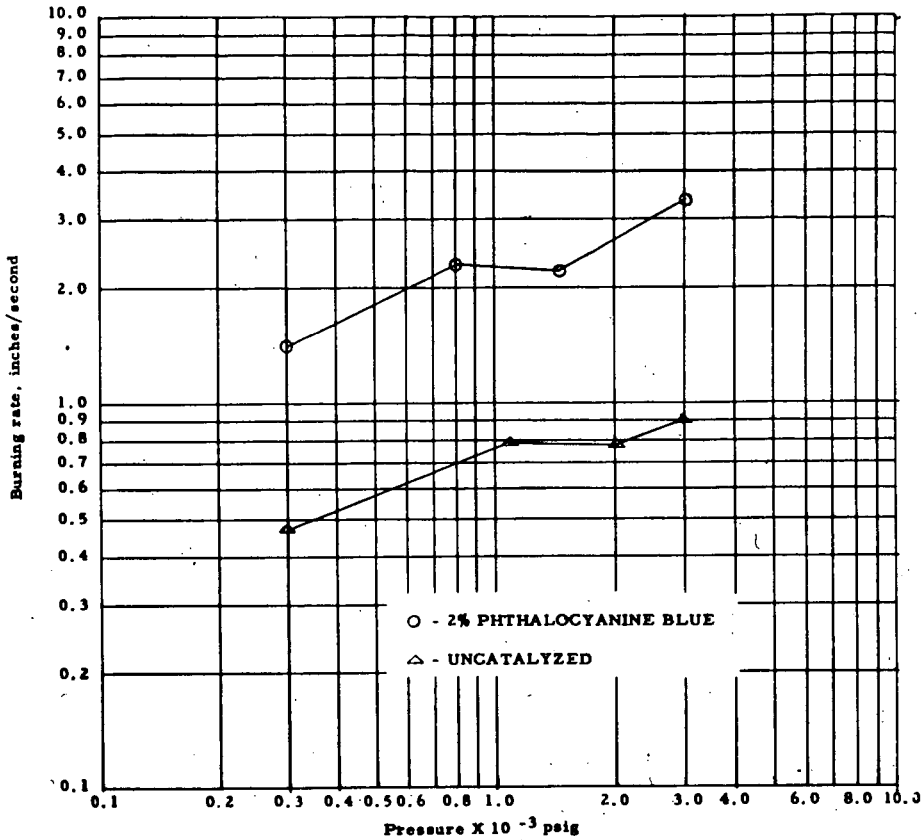

Fig. 1.-BURNING RATE OF CATALYZED AND UNCATALYZED ACETYLENIC POLYURETHANE PROPELLANT COMPOSITIONS CONTAINING 80 PERCENT AMMONIUM PERCHLORATE

PHYSICAL PROPERTIES OF THE LIQUID OZONE-FLUORINE SYSTEM*

Charles K. Hersh and A. J. Gaynor

IIT Research Institute
Chicago, Illinois

INTRODUCTION

The utilization of ozone and fluorine as liquid oxidizers has been an aim of rocket technologists for many years. It has been known for some time that liquid ozone and fluorine are miscible over the entire composition range, in contrast to the ozone-oxygen system, which has a consolute temperature of 93°K.

Investigators at NASA have computed the specific impulse of ozone-fluorine mixtures with JP-4 and have shown that a maximum occurs at about 30 wt % ozone.[1] The physical properties necessary for a more complete evaluation of this system have not been available. It was, therefore, the purpose of this study to measure the density, surface tension, viscosity, and vapor-liquid equilibria.

EXPERIMENTAL

Density

A borosilicate glass U-tube, 4 mm in I.D. and 10 cm long, was used for the density measurements.[2] A measured amount of liquid ozone was transferred to the U-tube, and the procedure was repeated with enough liquid fluorine to result in a solution of the desired concentration. The valves separating the legs of the U-tube were closed and the solution was mixed. The metal tubes containing the equilibrium vapor over each leg were then heated slightly. Since the vapor consisted almost entirely of fluorine, it is believed that heating did not change the composition, but caused the gas to bubble through the liquid, thus insuring thorough mixing. While a slight pressure was maintained on one leg of the U-tube, the liquid level of the ozone-fluorine mixture and the level of the reference fluorocarbon manometer were measured with a cathetometer. The densities obtained in this manner are shown in Table 1.

These data were then reduced to straight line functions on the Institute's Univac 1105 computer by the method of least squares. The computer program for this purpose was available from a previous study, hence the reduction was readily accomplished. Equations for determining the density of liquid ozone-fluorine mixtures at the two temperatures investigated are:

$$\rho_{-183°C} = 0.1009\ (\text{wt fraction } O_3) + 1.4704 \qquad (1)$$
$$(\text{deviation} = \pm 0.0013)$$

*This work was supported at IIT Research Institute by the National Aeronautics and Space Administration under Contract No. NASw-76.

$$\rho_{-195.8°C} = 0.0534 \text{ (wt fraction } O_3) + 1.5611 \quad (2)$$
$$\text{(deviation} = \pm 0.0024)$$

Table 1

DENSITY OF LIQUID OZONE-FLUORINE MIXTURES

Temperature, °C	Ozone Concentration, wt %	Density, g/cc Measured	Density, g/cc Calculated*
-183	0.0	1.472	1.470
	31.0	1.499	1.502
	84.6	1.557	1.556
	100.0	1.571	1.571
-195.8	0.0	1.561	1.561
	23.0	1.573	1.573
	61.8	1.595	1.594
	100.0	1.614	1.615

*From Eq (1) and (2).

Viscosity

The viscosity of ozone-fluorine mixtures was determined in a modified Ostwald viscometer,[2] which was used with a variable volume of liquid. The viscometer was made from precision-bore, glass tubing (4 mm in I.D.) with a capillary section 0.203 mm in diameter and 12 cm long.

To force the liquid to a convenient height above the capillary section, either helium pressure was used, or the metal tubes containing the equilibrium vapor over each leg were heated after the valves had been closed. Then the valve isolating the two arms of the viscometer was opened and the readings of the height, h, of liquid as it fell through the capillary were taken as a function of time. The driving pressure was proportional to the difference between the liquid and the equilibrium levels ($h - h_e$) and, in uniform bore tubing, the rate of flow was proportional to dh/dt. Hence, for liquids following Poiseuille's law, log ($h - h_e$) should be proportional to the time of flow. In every case a linear relation between log ($h - h_e$) and time was obtained, which shows that ozone-fluorine solutions are Newtonian fluids.

For convenience, the half time ($t_{1/2}$), which is the time required for the liquid to fall one half the distance from the initial level to the equilibrium level, was determined from graphs of the time-height functions. The viscosity was calculated from the equation:

$$\mu = Ct_{1/2}\rho \quad (3)$$

where

μ = viscosity
ρ = density of the fluid, g/cc
C = an apparatus constant determined with liquids of known viscosity (1.289×10^{-2} centipoise-cc/sec-gram).

The results shown in Table 2 represent at least two independent measurements for each viscosity reported.

Table 2

VISCOSITY OF OZONE-FLUORINE MIXTURES

Ozone Concentration, mole %	Viscosity, cp -183°C	Viscosity, cp -195.8°C
100.0	1.55 ± 0.01	4.15 ± 0.04
79.1	0.905 ± 0.01	
70.5		1.95 ± 0.01
30.5	0.343 ± 0.03	
26.8		0.682 ± 0.02
0.0	0.208 ± 0.01	0.344 ± 0.01

Surface Tension

The surface tension of various ozone-fluorine mixtures was determined by the capillary rise method in the apparatus used for the viscosity measurements.[2] The following equation was used:

$$T = \frac{rh\rho g}{2} \qquad (4)$$

where

T = surface tension
r = radius of capillary, cm
h = capillary rise, cm
ρ = density of solution, g/cc
g = gravitational constant, cm/sec^2

Results at -183 and -195.8°C are given in Table 3.

Table 3

SURFACE TENSION OF OZONE-FLUORINE MIXTURES

Ozone Concentration, mole %	Surface Tension, dynes/cm	
	-183°C	-195.8°C
100.0	39.9	43.5
79.1	30.2	
70.5		35.6
30.5	19.1	
26.8		22.4
0.0	12.3	15.5

Vapor Pressure

Two different techniques were used in determining the vapor pressure of various liquid ozone-fluorine mixtures, depending on the pressures to be measured. The first technique was developed for measurements at low pressures (to 1.5 atm). The liquid ozone, which was condensed at liquid oxygen temperature (-183°C) into a calibrated glass tube, was pumped on at reduced pressure to remove any residual oxygen, and then the total volume was measured with a cathetometer. The measured amount of ozone was then transferred quantitatively to a glass tube by distillation. The above procedure was repeated with liquid fluorine condensed at liquid nitrogen temperature (196°C), and the two liquids were allowed to come to equilibrium before a vapor pressure reading was taken. Readings were taken at bath temperatures of 75.7, 77.7, and 90.2°K. These temperatures were measured with an oxygen vapor pressure thermometer. After the initial values had been determined, additional known amounts of fluorine were admitted to the U-tube, and vapor pressure readings were again taken. The data obtained in this manner for a series of ozone-fluorine mixtures are given in Fig. 1.

Considerable time was required for the liquid mixtures to come to equilibrium in the original U-tube, and it was thought that a stirring bar would ensure a homogeneous solution of the two liquids in the modified apparatus. However, in each of the three attempts to use a Teflon-coated stirring bar on the 90 mole % ozone mistures, the apparatus was destroyed by an explosion. Apparently, the mixtures which have high ozone concentrations are as sensitive to the wiping action of the stirring bar along the glass surface of the reservoir as is 100% ozone (from previous experience).

The values at greater than 50 mole % ozone were obtained in a reservoir which has a large cross-sectional area, in the hope that this apparatus would facilitate mass transfer between the two liquid phases (fluorine on top of ozone).

In the second technique (to 20 atm), the apparatus was an all-metal system similar to that used for measurements on ozone-

oxygen mixtures.[3] The test chamber was constructed of stainless steel. It consisted of 1-inch bar stock (1-1/2 inches long), Swagelok fittings, a pressure gauge, and a copper-constantan thermocouple. The system had a volume of 20.1 cc.

The experimental procedure consisted of determining the liquid lines. The results are shown in Fig. 2. When the volume of vapor in a closed system is kept small relative to the volume of liquid, the amount of liquid that must be vaporized to give a 20-atm pressure is small. Thus, the composition of the liquid will be changed by only a negligible amount. For these determinations the composition of the charge was known accurately, and provision was made for agitation of the test bomb.

As determined by this method, the vapor pressure of pure fluorine was found to be in agreement with the value reported by Landau,[4] and the vapor pressure of oxygen was found to be in agreement with the value reported in NBS Circular No. 564.[5] This verified that fact that the pressure and temperature indicators were correct relative to each other.

RESULTS AND CONCLUSIONS

The density studies indicate that liquid ozone-fluorine mixtures are homogeneous and not subject to decomposition at the temperatures investigated. Some of the liquid mixtures detonated during this study, but only those of high (greater than 60 wt %) ozone concentration. This apparent hazard should not be disturbing, since calculations show that the theoretical specific impulse of systems containing JP-4 and ozone-fluorine mixtures is at a maximum when the oxidizer consists of 30 wt % ozone in fluorine. A mixture of this composition requires very few handling precautions over those observed with 100% liquid fluorine.

Liquid ozone is approximately ten times more viscous than fluorine at -183°C; but even liquid ozone supercooled at -195.8°C flows readily (4.15 cp). The viscosity of the solutions decreases rapidly as fluorine is added, and a semilog relation is approximated when viscosity is plotted as a function of composition at -183 and -195.8°C. The surface tension of ozone is approximately three times that of fluorine.

The vapor pressure studies were straightforward, and the results indicate nothing out of the ordinary when the vapor pressures of the individual components are compared with those observed for the mixtures. The importance of these tests, however, lies in the fact that they show the liquid ozone-fluorine mixtures to be homogeneous and not subject to decomposition at the temperatures investigated.

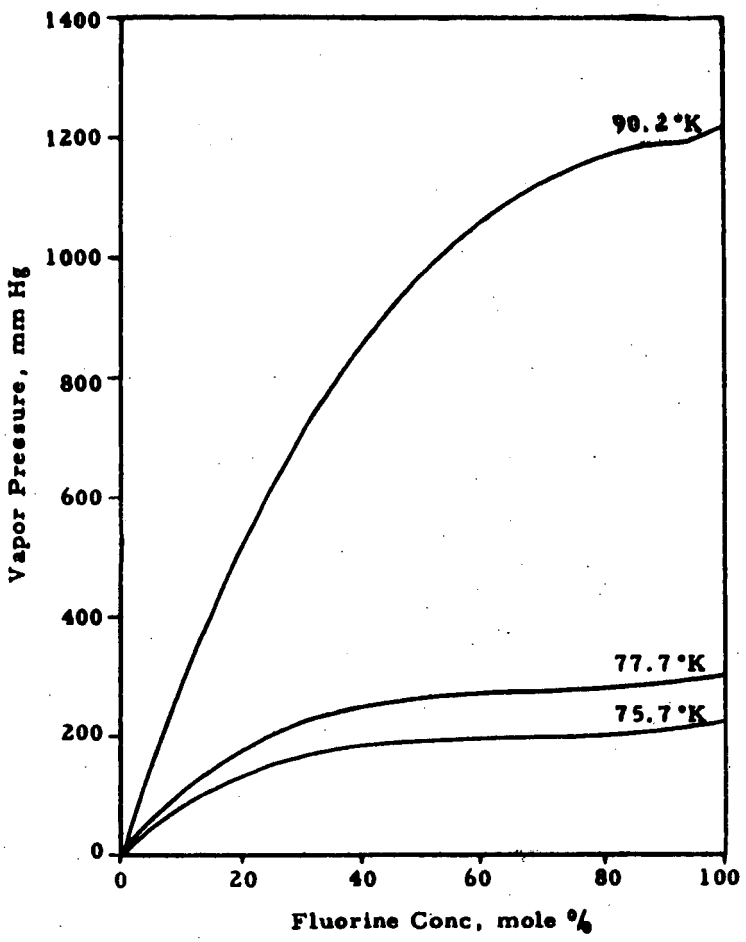

Figure 1

VAPOR PRESSURE OF LIQUID OZONE-FLUORINE MIXTURES

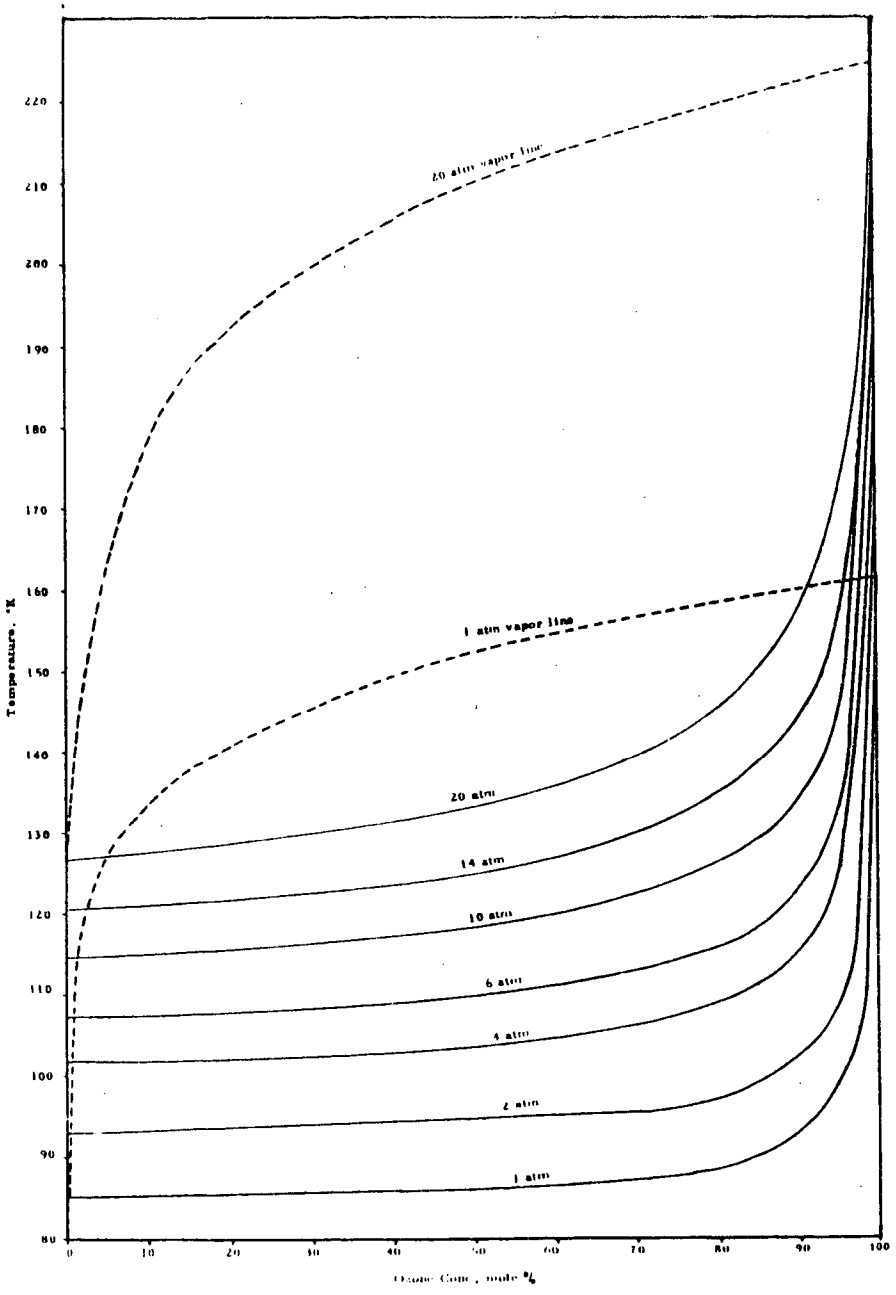

Figure 2

VAPOR-LIQUID EQUILIBRIUM DIAGRAM OF OZONE-FLUORINE SYSTEM

REFERENCES

1. V. N. Huff and S. Gordon, "Theoretical Rocket Performance of JP-4 Fuel with Mixtures of Liquid Ozone and Fluorine," NACA Research Memorandum E56K14.

2. C. K. Hersh, A. W. Berger, and C. Brown, "Liquid Ozone-Oxygen System: Density, Viscosity, and Surface Tension," in "Advances in Chemistry Series," Vol. 21, "Ozone Chemistry and Technology," American Chemical Society, Washington, D. C., p. 22, 1959.

3. C. K. Hersh, R. I. Brabets, G. M. Platz, R. J. Swehla, and D. P. Kirsh, "Vapor-Liquid Equilibria of Ozone-Oxygen Systems," ARS Journal, Vol. 30, p. 264, 1960.

4. R. Landau and R. Rosen, "Industrial Handling of Fluorine," Chapter 7 in "Preparation, Properties and Technology of Fluorine and Organo-Fluoro Compounds," C. Slesser (editor), McGraw-Hill Book Company, New York, 1951.

5. J. Hilsenrath, et al., "Tables of Thermal Properties of Gases," NBS Circular 564, 1955.

High Energy Oxidizers in Solution: The System $F_2/NF_3/HF$

W.E. Tolberg, R.S. Stringham, M.E. Hill

Stanford Research Institute, Menlo Park, California

Introduction

The system $F_2/NF_3/HF$ has been studied as an experimental system in which it was thought possible to observe interactions leading to the formation of highly energetic ionic species. The driving force for these interactions was expected to consist primarily of the highly exothermic formation of fluoride ion in liquid HF. The system has been studied experimentally through measurements of the solubilities of F_2, NF_3, and mixtures of the two in liquid HF, along with nmr and epr spectra of these components and their mixtures and some conductivity measurements on NF_3 in HF.

The interactions possible between liquid HF and NF_3 or F_2/NF_3 mixtures are (1) the formation of ions, (2) the formation of complexes of NF_3 and HF, (3) decomposition of NF_3, (4) fluorine exchange reactions among the three components, and (5) formation of unstable, solvated complexes of F_2 and NF_3, these being precursors to ion formation.

Knowledge of the solution chemistry, the nmr and epr spectra, and the conductivities were used to determine which of the interactions occur and to support further experimental work directed toward the synthesis of ionic compounds from these oxidizers.

Results and Discussion

The interactions which are possible are more probable under certain conditions of temperature and pressure than others. Complex formation between HF and NF_3 is more likely at temperatures not much above the freezing point of HF while decomposition of NF_3 in highly purified HF may be expected at 200°C. The formation of solvated $F_2 \cdot NF_3$ or $F_2 2NF_3$ complexes followed by formation of ions is more likely to occur, if at all, at ambient or higher temperatures and pressures. All of these interactions are germane to the strict interpretation of results from the solubility and other measurements.

Solubility Measurements. The solubilities of F_2 and of NF_3 in HF are shown in Fig. 1. In addition, the solubility behavior on addition of F_2 to a known mixture of NF_3 in HF is shown in Fig. 2. For pressures up to twelve atmospheres and at 20°C, the individual solubilities are given by $p_i = k_i n_i$ where $k(NF_3) = 1.02 \times 10^{-5}$ cm of Hg·moles HF/mole NF_3 and $k(F_2) = 1.84 \times 10^{-5}$ in the same units.

The lack of an intercept indicates no appreciable compound formation, no strong interaction with the solvent, nor reaction with the vessels. The slopes show that F_2 is about half as soluble as NF_3. This is the order to be expected from Hildebrand's ideal solubilities.

The solubility behavior in the ternary system shown in Fig. 2 shows that on addition of F_2 to NF_3 in HF, the F_2 is initially four times more soluble than when added to pure HF and about twice as soluble as NF_3 itself. Subsequently, further addition of F_2 to the ternary system proceeds according to the expected solubility of F_2 in HF alone.

There is, therefore, apparently an interaction between F_2 and NF_3 in HF. This conclusion is based on the solubility behavior as shown in Fig. 1 and on the lack of apparent interaction between F_2 and HF as well as NF_3 and HF. It has

further been shown that F_2 and NF_3 behave ideally in the gas phase and in liquid/vapor equilibrium at -196°C. The apparent interaction can be attributed to the formation of complexes of F_2 with one or two molecules of NF_3 and, possibly, subsequent formation of ion pairs such as NF_3^+/F^-.

Solubilities were also measured in Kel-F vessels to be used as nmr tubes. In these, F_2 was 15 times more soluble than in an all metal system. This was, of course, due to interaction of F_2 with the Kel-F. As will be shown later, no evidence for products of this interaction have been observed except when decomposition of the Kel-F occurs in spontaneous, incandescent reactions.

NMR and EPR Spectra. NMR spectra of the components and mixtures of the system NF_3-F_2-HF in Kel-F, were explored as a possible means of detecting new species. These spectra showed only the F^{19} resonances of the starting materials, but the HF/F^{19} resonance was broadened substantially on addition of NF_3 and further broadened by addition of F_2. This resonance also shifted with temperature. The line broadening was attributed to chemical exchange with the solvent but it could not be shown what the HF was exchanging with.

The line shift with temperature was shown via epr spectra to be due to the presence of paramagnetic species. These were from a reaction of F_2 with the Kel-F and from F_2 dissolved in HF. The latter resonance disappeared on adding as much NF_3 as F_2 and was present in F_2/HF mixtures and not in any of the components alone. It was therefore evidently not related to a paramagnetic entity involving NF_3.

Thus both nmr and epr studies gave no direct evidence for the presence of new NF species although it appeared that the NF_3 nmr line diminished appreciably on adding F_2 and, conversely, the F_2 line diminished on adding NF_3. At the concentrations attainable, the nmr is not sufficiently sensitive while the epr, though sensitive, is most effective at temperatures at which HF is solid. At the solid transition, the HF is out-gased, and it is probable that, if present, little F_2/NF_3 adduct would be trapped in the solid.

Conductivity Measurements. These were carried out only on the NF_3/HF system. The conductivity of the NF_3 in HF was not greater than that of the HF alone. This was 3×10^{-5}/ohn cm at 0°C. The upper limit for the ionization of NF_3 was estimated to be 10^{-7} and is probably much lower since this implies a degree of ionization of 10^{-3}. If this were true, ionic derivatives of NF_2^+ would be easily prepared.

Experimental

Apparatus. The vacuum systems used in this work were assembled from copper and/or monel tubing, vessels and bellows valves. Valve gaskets, conductivity cells, nmr and epr tubes were of Kel-F plastic. All permanent joints were silver soldered or heliarc welded. Demountable joints were $\frac{1}{8}$ inch pipe fittings sealed with Teflon tape. There were no leaks detectable by means of a helium leak detector. Pressures were measured with Wallace and Tiernan gauges equipped with resistant metal capsules. Thermocouple gauges were used to monitor low pressures in the vacuum system but were isolated from the system to prevent destruction of the gauge by F_2 and HF contamination of the system by reaction products. The systems were passivated with respect to F_2 and HF after any exposure to the atmosphere.

Materials. Anhydrous HF was prepared by distillation through an 80 plate plastic column. Its specific conductivity before exposure to metal parts of the vacuum system was 10^{-4}/ohm-cm or less.

Fluorine, which contains about 2% impurities composed mainly of air, HF, CO_2, and CF_4, was purified in two steps. The less volatile impurities were frozen out

at about -187°C in a metal trap charged with the desired quantity of the gas. Air was removed by extracting the supernatant gases above the liquid condensed in a cold finger at -196°C.

Nitrogen trifluoride was obtained in 99.9% purity from Air Products and Chemicals, Inc., and used without further purification for solubility studies but was passed through liquid HF at -80°C, condensed and pumped on at -196°C for use in conductivity studies.

Solubility Measurements. Solubilities were determined in the apparatus shown in Fig. 2. For the system NF_3/HF, 50 gm of HF were charged into the 450 ml monel pressure vessel, Vs, and, successively, quantities of NF_3 (PVm) were condensed quantitatively into the vessel cooled to -196°C. The resulting pressure in Vm was 0.0 mm and the valve on the monel vessel was closed. The vessel and its contents were allowed to equillibrate at 20°C in a water bath. The HF was stirred magnetically. The mixture of HF and NF_3 gases was admitted to Vm, and the system, Vs and Vm, was allowed to reach equilibrium at P_f.

For the F_2/HF system, the procedure was the same except that F_2 was transferred quantitatively at about 55°K with the aid of a solid nitrogen/liquid oxygen bath. Solid nitrogen was prepared by pumping on the dewar, filled with liquid nitrogen and cooling the 450 cc pressure vessel. Subsequently, the solid nitrogen sublimed away from the vessel and liquid oxygen was added to maintain efficient heat transfer from the vessel to the solid nitrogen.

For the F_2/NF_3/HF system, the behavior was observed two ways. Successive quantities of F_2 were added to the vessel containing a known quantity of NF_3 and HF. Secondly, successive quantities of NF_3 were added to a known F_2/HF system.

In addition, the composition of the mixture of gases above the liquid phase was determined. HF was separated from F_2 and NF_3 and its pressure was measured. F_2 and NF_3 were determined from their total pressure both at room temperature and at liquid nitrogen temperature where they behave as an ideal solution. Temperature control was achieved by means of a nitrogen thermometer.

NMR Spectra. NMR spectra of components and mixtures were obtained in Kel-F tubes of two types. Spinnable tubes were made by heat sealing both ends of a tube machined to resemble standard 200 ml glass tubes. Tubes to which components were added successively in order to observe changes in spectra were made from $\frac{1}{2}$ inch rod and equipped with a valve. A Varian A-60 Spectrometer was used.

EPR Spectra of components and mixtures were obtained in Kel-F capillaries drawn from $\frac{1}{4}$ inch tubing. Spectra were observed at temperatures down to -190°C.

Conductivity Studies were carried out in an all Kel-F vacuum system and conductivity cell with platinum electrodes. The cell constant was .03/cm determined by calibration with KCl solutions at ice temperature.

Conclusions

The existence of the interactions justified some speculation on its nature. There are three reactions of interest which could occur in this system:

1. $NF_3 \xrightarrow{HF} NF_2^+ F^-$
2. $NF_3 + \frac{1}{2}F_2 \xrightarrow{HF} NF_3^+ F^-$
3. $NF_3 + F_2 \xrightarrow{HF} NF_4^+ + F$

None of these violate valence rules but the extent of reaction (1) is small from its conductivity while (2) and (3) may very well proceed through the proposed unstable $F_2 \cdot NF_3$ and $F_2 \cdot 2NF_2$ complexes. It is planned to determine whether any ions of interest can be derived from this system by addition of SbF_5 in order to obtain a solid derivative.

Acknowledgment

Research reported in this paper was supported by the Advanced Research Project Agency through the Air Force Rocket Propulsion Laboratory, Edwards, California, Contract AF 04(611)-9370. The authors express their appreciations to Dr. Henry Taube, Stanford University for his assistance.

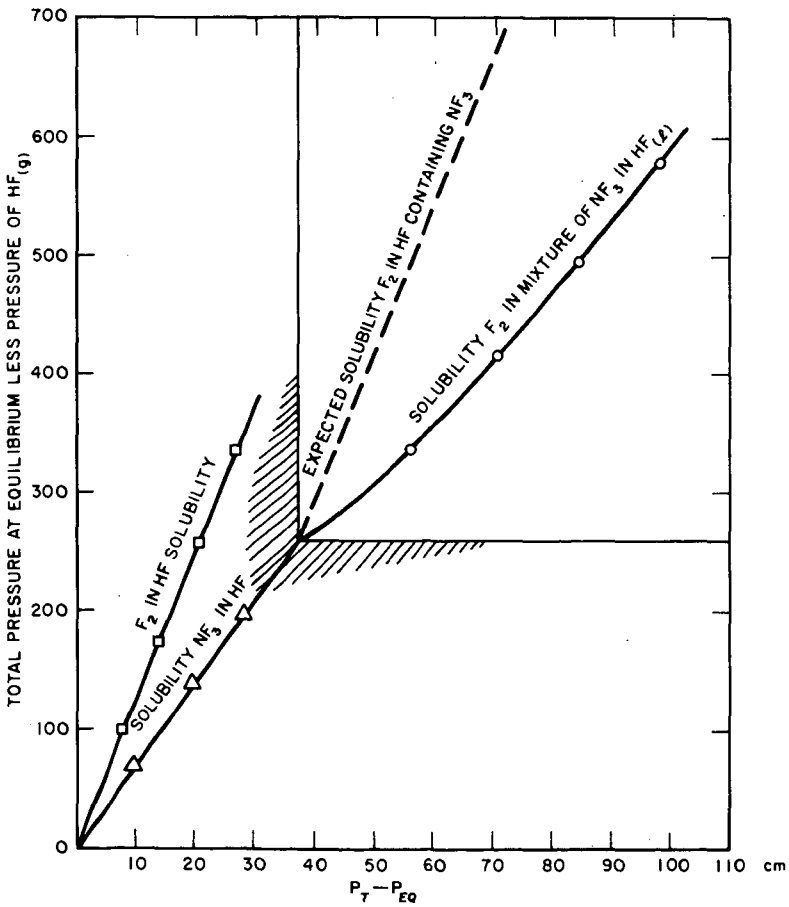

FIG 1 SOLUBILITY OF F_2 AND NF_3 IN HF

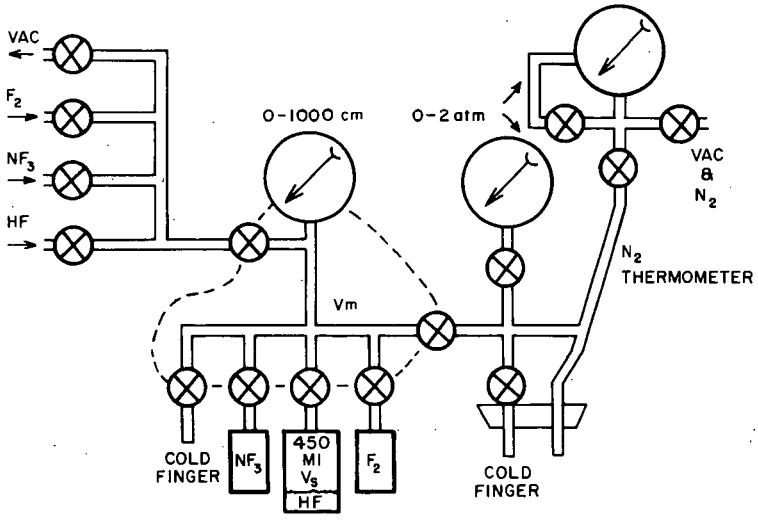

FIG 2 SOLUBILITY APPARATUS

COMBUSTION CHARACTERISTICS OF SELECTED LIQUID PROPELLANTS

S. D. Rosenberg, F. E. Miller, and J. M. Robinson

Aerojet-General Corp.
1100 W. Hollyvale
Azusa, California

ABSTRACT

The propellant development and combustion research reported herein have as their ultimate objective the development of liquid bipropellant systems which have a theoretical specific impulse greater than 315 sec (mobile equilibrium, P_c/P_e = 1000/14.7 psia).

The ignition characteristics of four bipropellant systems were determined with the Aerojet Ignition Delay Device.

The combustion characteristics of one NF-system were determined with the Aerojet Liquid-Liquid Combustor. The performance characteristics of this system was determined at the nominal 400-lb thrust level (P_c/P_e = 500/14.7 psia), and at the nominal 5000-lb thrust level (P_c/P_e = 400/14.7 psia).

CRUCIAL PRESSURE INDEX FOR NITROGLYCERINE SENSITIVITY

Ted A. Erikson

IIT Research Institute
Chicago 16, Illinois

INTRODUCTION

The vapor pressure of nitroglycerine can be varied by applying a relatively moderate hydrostatic pressure at a constant temperature. In an ideal and oversimplified approximation, the vapor pressure is shown to approach one value that is designated here as a crucial pressure. The existence of any such pressure implies an enhanced volatility. With increased volatility, vaporization steps that are affected can be so fast that even a high-velocity detonation can be supported in the vapor phase.

Although such results are only qualititative, the implication that vapor pressures are profoundly affected by hydrostatic pressures is verified by both theory and experiment (ref. 1,2). This role of hydrostatic pressures in the explosive decomposition of propellants and explosives has not been considered.

BACKGROUND DISCUSSION

The increased volatility of a condensed phase under hydrostatic pressure was noted as early as 1881 (ref. 1). This effect has been studied and confirmed by many investigators, and a survey of the subject is available (ref. 2). The effects of hydrostatic pressure are generally described as the sum of two independent factors, namely, enhancement of the vapor pressure of the condensed phase and effects of intermolecular forces between gas-vapor molecules. The phenomena are comparable to osmosis in which solution pressures greater than that of the pure solvent are generated and maintained in an equilibrium situation. An illustration of the scheme is given in Figure 1.

For the purpose of this paper, the effect of intermolecular forces can be ignored. The enhancement of the vapor pressure can then be evaluated directly by equating the chemical potential changes of the liquid and the vapor, respectively, which are influenced by the hydrostatic pressure, π. Thus, at constant temperature, T,

$$\Delta G_L = \int_P^{\pi} V_L \, dP = \Delta G_g = \int_{P^\circ}^{P} f(P) \, dP \qquad (1)$$

where G and V are molal free energies and volumes, respectively, P is the pressure, f(P) is an appropriate equation of state, the subscripts L and g refer to the liquid and vapor, respectively, and the superscript ° refers to the pure system.

The liquid is generally assumed to be impermeable to, and incompressible by, the pressurizing medium since these restructions allow the direct evaluation of the first integral. A fair approximation to the second integral is obtained by a virial equation for the vapor of the form RT/P + B, where B is the second virial coefficient (ref. 3). The results of both integrations are equated and rearranged in the following form:

$$P + P^\circ e^{\frac{V\pi}{RT} + \frac{B\,P}{RT} + \frac{P^\circ (V + B)}{RT}} \qquad (2)$$

This equation relates the vapor pressure of a condensed phase in a manner that is independent of intermolecular forces. It suggests as a first approximation the exponential dependency of the vapor pressure with the external pressure.

From the standpoint of chemical kinetics the rates of vaporization and condensation must be equal at equilibrium. Condensation rates are proportional to the pressure and a maximum rate is predicted from the kinetic theory (ref. 3) as

$$\dot{n} = 1/(2\,\pi\,M\,RT)^{-1/2}\,P \qquad (3)$$

where $\dot{n}$ is the collision frequency in moles per unit area per unit time. Hence, the maximum rate of vaporization is predicted by Equation 3, and, subject to some oversimplification, the enhanced vapor pressure of Equation 2 leads to an enhanced vaporization rate.

APPLICATION

The purpose of this paper is simply to call attention to the significance of the fact that the vapor pressure of a liquid can be affected by the application of a hydrostatic pressure at a constant temperature. Explosive sensitivity and initiation are usually interpreted on the basis of at least two mechanisms that may or may not be independent, namely, vaporization and reaction. In the case of a compound for which vaporization is a rate-controlling step (i.e., by a required supply of reactant to support the reaction in the vapor phase), it seems likely that a theoretical index to explosive sensitivity can be based on a defined ease of volatility.

Equation 2 predicts the manner in which the vapor pressure of a liquid can increase with the application of a hydrostatic pressure. Under the restrictions that

$$B = 0 \quad \text{and} \quad V\pi \gg P^\circ (V + B)$$

(i.e., an ideal gas) a condition is indicated in which the new vapor pressure of the liquid can in principle approach the value of the

applied hydrostatic pressure. Although it is obvious that such an interpretation of the state of affairs is limited, it is informative to calculate such variations in the vapor pressure up to the limiting pressure, which is designated here as a crucial pressure for a material such as nitroglycerine. These values of the vapor pressure are converted to maximum volatilities by the kinetic theory approximation of Equation 3.

DISCUSSION

Several simplifications that have been introduced make the results listed in Table 1 appear quite inapplicable to the real situation. However, the implications of such an analysis persist, namely, that an increased volatility of nitroglycerine at constant temperature can occur by the application of a hydrostatic pressure.

Table 1 shows that quite moderate pressure will increase the volatility to rates near detonation. The product of molecular density and low and high-velocity detonation rates (approximately 2000 and 8000 m/sec (ref. 4), respectively) give estimates of specific consumption rates of 1410 and 5640 moles/cm^2-sec, respectively. Pressures of less than 4 kilobars can generate such vaporization rates. For comparison, the pressures that exist in propagating shock fronts are in the range of 5 to 100 kilobars (ref. 5); the value of 40 kilobars has been quoted for nitroglycerine (ref. 6). With such pressures available it does seem desirable to introduce the concept of a crucial pressure, since the ease of volatility has been enhanced so much that it is unnecessary to consider vaporization as a rate-limiting step in the process. Thus, this effect can act in a cascade fashion -- where increased pressure causes faster reactant supply by vaporization, exothermic reaction causes more pressure (because of temperature rises and generally more product moles per reactant mole), ad infinitum.

The crucial pressure, when calculated with an appropriate approximation can be an index to the explosive sensitivity of a material when the initiation process is rate-controlled by vaporization.

Of course, it should be recognized that it is not the pressure alone that is crucial, since the causes of this effect are the intermolecular forces that are involved in solutions. For example, although recent results (ref. 7) report a hundredfold increase in the vapor pressure of napthalene in argon for a hydrostatic pressure of only 200 bars at 22°C, but a twofold decrease is reported for a comparable situation in helium.

ACKNOWLEGEMENTS

The support of both the Bureau of Naval Weapons Contract No. NOw-61-0603-c, and the Air Force Office of Scientific Research under Contract No. AF 49(638)-1121, is hereby acknowledged.

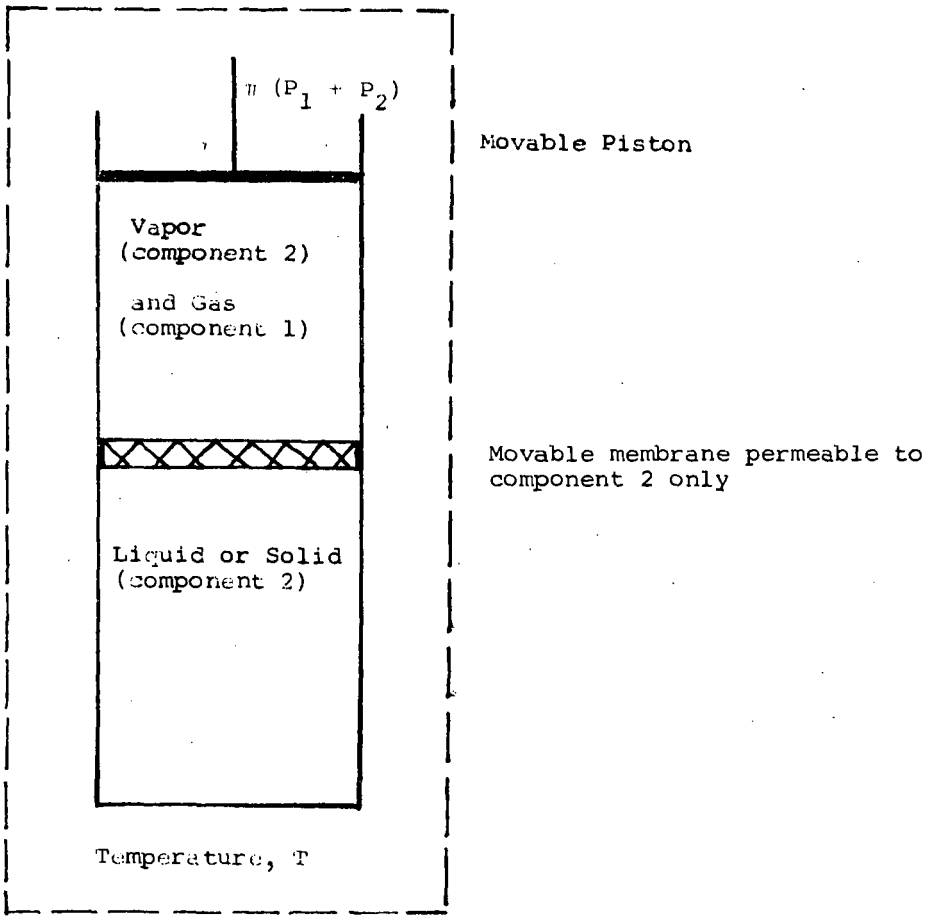

Figure 1

SCHEME OF THE HYDROSTATIC PRESSURE EFFECT

Table 1

HYDROSTATIC PRESSURE EFFECTS ON NITROGLYCERINE

Hydrostatic Pressure, π, bars	Vapor Pressure of Nitroglycerine, bars	Vaporization rate, moles/cm^2-sec
0	0.00000068	0.000000115
68	0.00000100	0.000000169
341	0.00000494	0.000000839
680	0.0000347	0.00000588
1020	0.000248	0.0000420
1360	0.00166	0.000282
1730	0.015	0.00254
3470	330	55.8
3610	806	1410*
3850	2980	5640*
3920	3920	---

*Vaporization rate required to maintain consumption rate of low- and high-velocity detonations, 2000 and 8000 m/sec, respectively (ref. 4) in nitroglycerine.

REFERENCES

1. Poynting, J. H., Phil, Mag. 12, 32 (1881)

2. Rowlinson, J. S. and Richardson, M. J., "The Solubility of Solids in Compressed Gases," Advances in Chemical Physics, Vol. II, Interscience Publishers, Inc., New York, 1959.

3. Glasstone, S., Textbook of Physical Chemistry, D. Van Nostrand Co., New York, 1948.

4. Ordnance Corps Pamphlet ORDP 20-177, Properties of Explosives of Military Interest, May 1960.

5. Jaffe, I., Beauregard, R., and Amster, A., ONR Symposium Report' ACR-52, Vol, II, Princeton University, September 26-28, 1960, pp. 584-605.

6. Winning, C. H., ibid, pp. 455-468.

7. King, A.D. Jr. and Robertson, W. W., J. Chem. Phys. 37, 1453-5 (1962).

Measurement of Impact Sensitivity of Liquid Explosives and Monopropellants

Donald Levine and Carl Boyars

U.S. Naval Ordnance Laboratory, White Oak, Silver Spring, Md.

INTRODUCTION

Because of the importance of knowing what mechanical shocks a liquid explosive will withstand, what the relative order of sensitivity is for different liquid explosives and monopropellants, and how effective are those additives considered desensitizers, much work has gone into the development of standard methods for determination of impact sensitivity. Starting with Bowden and Yoffe's adiabatic compression hypothesis (1), a method and apparatus, the Olin-Mathieson (O-M) Drop Weight Tester, were developed by a committee (2). In the course of investigating the effect of desensitizers on nitroglycerin (3), the authors introduced certain significant modifications in the O-M Tester. The published results of that investigation describe the instrumented drop weight apparatus in possibly insufficient detail. The modification does not affect the measured values of impact sensitivity of nitroglycerin solutions (comparing data obtained on the same apparatus prior to incorporation of instrumentation), and a fuller description of the apparatus may be useful to other workers. In addition, further work has revealed certain interesting phenomena relative to the measurement of impact sensitivity, which will be discussed here.

APPARATUS

The original O-M apparatus has been adequately described (2). The modifications which permit determination of pressurization rate, maximum pressure, and impulse due to impact have been briefly described (3). The piston type pressure gauge has now been calibrated over the range of 1 to 6800 atm. A photograph of the gauge is shown in Fig. 1. It is machined from a single piece of metal and consists of a piston, column, and a threaded base which serves to anchor the gauge firmly to the sample cup assembly. The sensing elements are Baldwin strain gages (BLH FAB 12-12) which are bonded to the surface of the column with an adhesive; they are protected with a cloth covering. The strain of the column is directly proportional to the applied pressure. Calibration with a Tinius Olsen dead weight tester showed the response of the pressure gauge to be linear over the entire range. Placing the two strain gauges on opposite faces of the pressure gauge compensates for any bending of the column.

A line filter removes any extraneous signals generated from other electrical equipment in the area. The 3-conductor, shielded cable from the gauge to the Wheatstone bridge (Fig. 2) is about 6 feet long. Type D Tektronix plug-ins are used in their differential mode with the oscilloscopes. The bridge is balanced by means of variable resistance R_2. This is done very accurately by means of a Leeds and Northrup potentiometer or a calibrated galvanometer. Alternatively, it can be done (less accurately) by changing the input setting from AC to DC at the oscilloscope until there is no deflection of the beam when switching from AC to DC.

The sample cup is then precompressed by means of a spanner wrench. The resistance change of the strain elements unbalances the bridge current, providing a deflection of the potentiometer, galvanometer, or oscilloscope beam. The same electrical equipment was used in calibrating the gauge. In this manner, an accurate measure of initial precompression and pressure versus time during impact and explosion is obtained. Temperature compensation is not a prime consideration in these tests. Heat conduction during the test cannot affect the gauge elements because of the short duration of the test.

The pressure developed in the initial pre-compression is measured with the more sensitive galvanometer or potentiometer; the higher pressures due to impact and explosion are read as a function of time on the oscillograph. The falling weight triggers the oscilloscope sweep when it contacts the ball and piston of the sample cup assembly. Fig. 4 is a block diagram of the apparatus.

An instrumented drop weight apparatus has also been described by Griffin (4). It contains the standard sample holder components. Pressure from the impacted sample cup is transmitted through a system of pistons with O-rings and hydraulic fluid to a transducer. Considerable frictional losses and binding occur in this system. Substantial energy losses were noted by Griffin, who found that much greater impact energies were required for initiation of explosives in his instrumented apparatus as compared to the uninstrumented apparatus. Such deficiencies do not exist in the apparatus described in this paper*.

RESULTS AND DISCUSSION

The earlier paper (3) reported results obtained by use of the instrumented drop weight apparatus. Impact pressure, rate of pressurization, ignition delay time, and pressure-time relationships during explosion were determined as a function of concentration of desensitizers in nitroglycerin. The data helped to explain the difficulty in getting reproducible test results on liquid explosives when the impacting weight is small; it was found that excessive pressure oscillation occurred during impact when a 1 kg weight was used. The oscillographic data also threw light on a number of phenomena associated with impact testing, e.g., the effect of impacting weight and of drop height on the efficiency of conversion of momentum to impulse delivered to the sample and also on the pressurization rate of the sample. It was concluded that, in order to eliminate differences in rate of impact pressurization, weights should be dropped from a constant height, as far as practicable, so that variation in the energy delivered is obtained by varying the weight only. The paper reported the increases in initiation delay time, in deflagration rate, in impulse delivered to the sample, and in impact weight required for 50% probability of initiation as a function of increasing desensitizer concentration. No difference was detected in effectiveness of the common desensitizers, triacetin, dibutylphthalate, and dimethylphthalate. A plot of impact weight at the 50% point versus desensitizer concentration showed a much lower slope for the region 0-16% desensitizer (by weight) than for 16-30%. A "memory effect" was found, i.e., repeating the drop test with the same weight and height on a sample which had previously failed to ignite at or near the 50% point resulted in a positive test every time.

---

* Credit is due Mr. H. Cleaver of this Laboratory for development of the instrumentation.

We have now found that a plot of peak impact pressure (rather than impacting weight) versus desensitizer concentration gives a continuous, nearly linear relationship. Fig. 4 is a plot of peak impact pressure versus impacting weight from a height of 1 cm. Fig. 5 is the plot of peak impact pressure versus desensitizer concentration. These data were obtained, using samples pre-compressed by the technique specified in the standard procedure (2), i.e., by tightening the sample assembly cap with a torque wrench to a reading of 7 inch-pounds. This procedure we have found to give an initial pressure (before impact) of 18.5 ± 2 atm.

In order to get better reproducibility of initial pressure, we have changed the pre-compression technique, using a spanner wrench and controlling pressurization by reading the galvanometer or potentiometer. This is of some importance in obtaining reproducible data, for it has been shown (5) that the percent of impacts which result in explosion is decreased when initial pressure is increased. We have also found that the ratio of peak impact pressure to initial (pre-compressed) pressure is a most significant factor in determining probability of explosion of nitroglycerin. This is consistent with quasi-adiabatic compression as a mechanism of initiation. Fig. 6 shows probability of explosion as a function of compression ratio for nitroglycerin impacted from a height of 1 cm with varying weights, using pre-compression to various initial pressures. The measurements of probability of explosion in Fig. 6 are rather crudely performed (from a statistician's viewpoint); for each point, ten nitroglycerin samples were prepared, the sample cups pre-compressed to identical initial pressures, the same weight dropped on each sample, and the number of positive tests recorded. Although the limit of precision of each impact pressure reading is estimated at ± 3 to ± 5%, a correlation between compression ratio and probability of explosion is apparent.

The "memory effect" we had noted in the earlier paper has been found to be due to the fact that pressurization within the sample cup is decreased following an impact which does not produce explosion. Twenty samples initially pressurized to 18.5 atm were found to average 12.0 atm after impact without explosion; the loss is presumably leakage from the sample cup. On subsequent impact of the same sample cup with the same weight, the pressure ratio is substantially higher and explosion results.

A significant conclusion from the data on the importance of compression ratio in initiating explosion of nitroglycerin is that the processing or handling of liquid explosives and monopropellants under reduced pressure introduces a hazard by sensitizing the liquid to weak impacts.

REFERENCES

(1) Bowden, F. P., and Yoffe, A. D., Initiation and Growth of Explosion in Liquids and Solids, Cambridge University Press, 1952.

(2) Liquid Propellant Test Methods, Test Number 4, Drop-Weight Test, Chemical Propulsion Information Agency, Johns Hopkins University Applied Physics Lab., Silver Spring, Md., 1964.

(3) Levine, D., and Boyars, C., The Sensitivity of Nitroglycerin to Impact, Combustion and Flame, in press.

(4) Griffin, D. N., The Initiation of Liquid Propellants and Explosives by Impact, Propellants, Combustion, and Liquid Rockets Conference, American Rocket Soc., Apr 26-28, 1961, Palm Beach, Fla., Paper No. 1706-61.

(5) Bowden, F. P., and Yoffe, A. D., op.cit., p. 34-35.

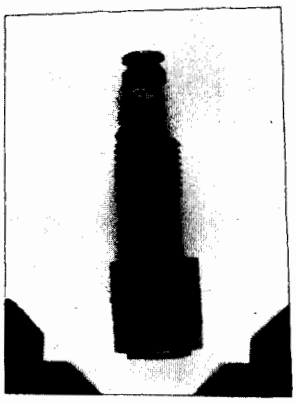

Fig. 1 - Pressure Gauge

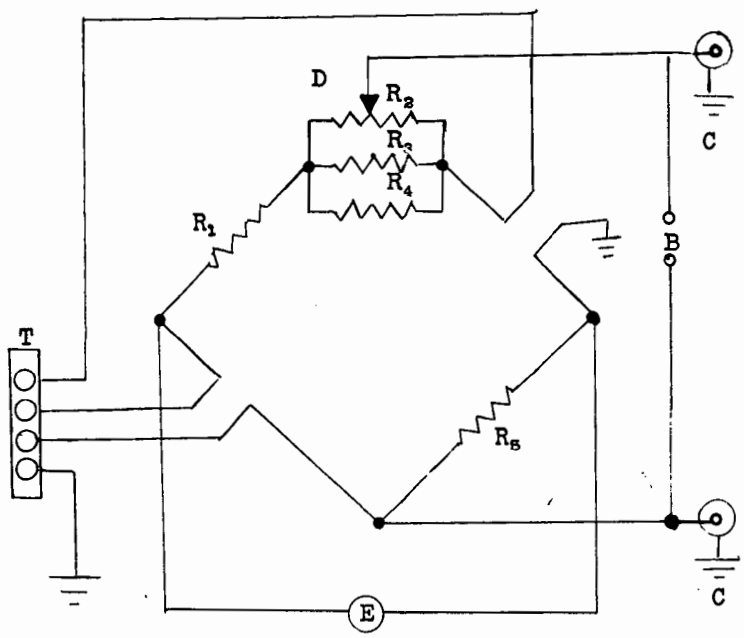

Fig. 2 - Bridge Circuit
R_1 =R_5 =120 Ohm Resistor; R_2 =100 Ohm 10 Turn Resistor;
R_3 =R_4 =10 Ohm Resistor; C=Signal Output to Oscilloscope
E= 6 Volt Power Supply; D=Balance Control; T=To NOL Gauge;
B= Zero Balance Checkpoint To Galvanometer/Potentiometer

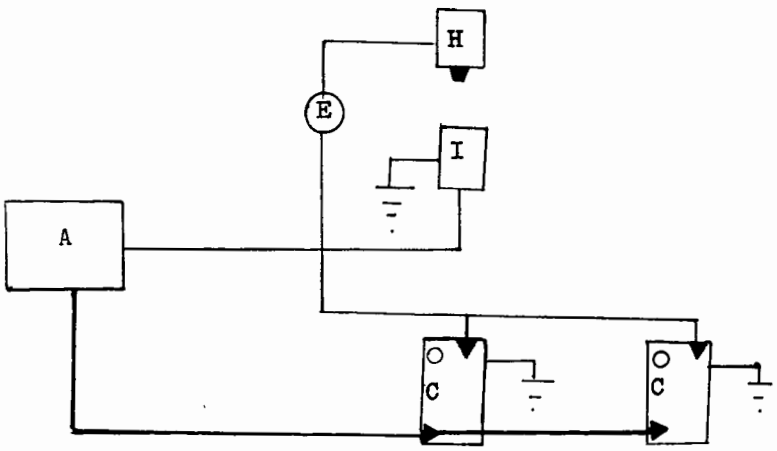

Fig. 3 - Instrumentation on Drop Weight Apparatus
A=Bridge; E=22 Volt Battery; H=Drop Weight Hammer;
I=Assembly Containing Sample Cup and NOL Gauge;
C=Oscilloscopes

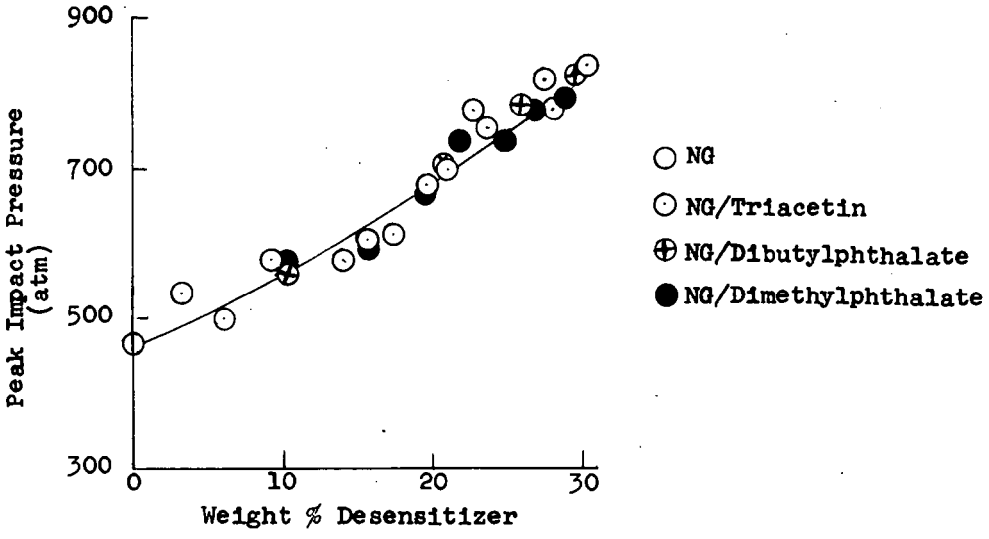

Fig. 5 - Impact pressure necessary to cause explosion (50% point) of NG solutions when impacted from a height of 1 cm with varying weights

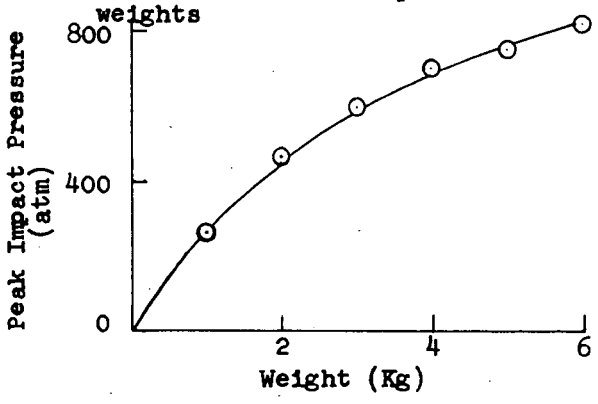

Fig. 4 - Peak pressure due to impacting weight from a height of 1 cm

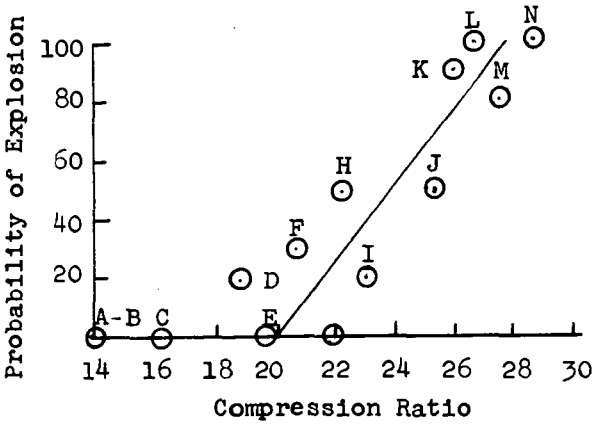

Fig. 6 - Probability of ignition vs. compression ratio for NG impacted from a height of 1 cm. with varying weights, using pre-compression to various initial pressures

	Weight (Kg)	Initial Pressure (atm)
A	4.8	51.2
B	2.3	37.6
C	2.8	36.9
D	4.8	38.4
E	1.5	18.5
F	2.3	25.6
G	1.7	18.5
H	6.0	38.4
I	1.8	18.5
J	2.0	18.5
K	4.8	27.8
L	6.0	32.0
M	2.2	18.5
N	2.3	18.5

ISOTOPIC EXCHANGE REACTIONS OF DIFLUORAMINE WITH DEUTERIUM OXIDE AND TRIFLUOROACETIC ACID

Warren E. Becker and Fred J. Impastato
Ethyl Corporation, Baton Rouge, La.

The isotopic exchange of hydrogen between HNF_2 and D_2O was followed by NMR using deuterated tetrahydrofuran-d8 as solvent. The growth of the H_2O peak was followed by NMR and the fraction of exchange F at time t was calculated by dividing the area of the H_2O peak at time t by the area at time t ∞. The half-life of exchange $t_{1/2}$ was obtained from the plot of log (1-F) vs. t which, of course, is linear. The rate of exchange R was then calculated from the equation

$$R = \frac{2[D_2O][HNF_2]}{2[D_2O] + [HNF_2]} \cdot \frac{0.693}{t_{1/2}} \qquad (1)$$

The exchange of hydrogen between HNF_2 and D_2O is first order with respect to HNF_2 and zero order with respect to water as shown in Table I. A reasonable mechanism is

$HNF_2 = H^+ + NF_2^-$	Slow
$H^+ + D_2O = D^+ + H_2O$	Fast
$D^+ + NF_2^- = DNF_2$	Fast

where the rate-determining step is the ionization of HNF_2.

The exchange was followed at several temperatures by using a temperature-controlled probe which regulated the temperature to $\pm$ 1°C. The activation energy of 4.5 kcal/mole was calculated from the Arrhenius equation. The plot of log K vs. 1/T is shown in Figure 1.

The fact that the exchange is acid catalyzed induced us to investigate the exchange of hydrogen between HNF_2 and

Table I

Summary of HNF_2-D_2O Exchange Runs

Conc. moles $l.^{-1}$					
$[D_2O]$	$[HNF_2]$	$t_{1/2}$ (min)	R (moles l^{-1} min^{-1})	K (min^{-1})	t°C
1.27	1.28	9.2	0.064	0.050	-20
1.40	0.69	11.3	0.034	0.049	-20
0.64	1.18	13.4	0.060	0.051	-20
1.91	1.16	9.8	0.063	0.054	-20
1.38	2.08	10.3	0.080	0.038	-20
1.31	1.87	10.3	0.073	0.039	-20
1.04	0.28	14.1	0.012	0.043	-20
			Avg.	0.046	
1.97	1.02	11.8	0.048	0.047	-10
1.97	2.02	6.2	0.150	0.075	-10
2.80	2.03	6.7	0.154	0.076	-10
			Avg.	0.066	
2.82	1.38	5.3	0.144	0.105	0
1.36	1.52	6.3	0.107	0.070	0
			Avg.	0.088	

Figure 1. Temperature Dependence of Rate Constants

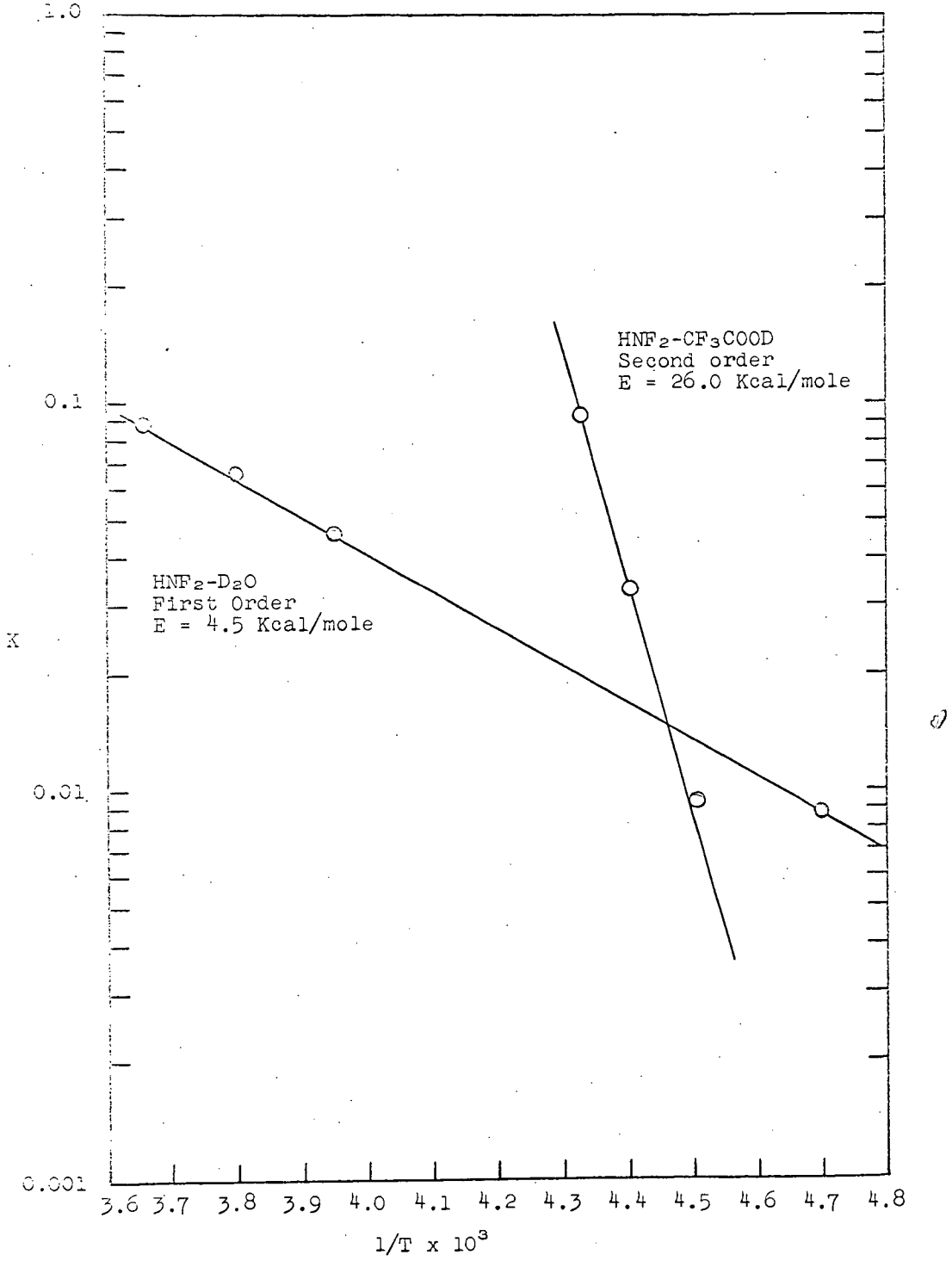

CF_3COOD. This exchange was also studied in deuterated tetrahydrofuran-d8 at several temperatures. The results are summarized in Table II.

The mechanism found for the exchange of hydrogen between HNF_2 and D_2O (the ionization of HNF_2) will also lead to exchange of hydrogen between HNF_2 and CF_3COOD. Therefore, we must subtract the contribution of this first order mechanism from the total rate of exchange. The rate of exchange R, then, is the sum of two rates.

$$R_{total} = K_1[HNF_2] + K_2[HNF_2][CF_3COOD]$$

At -60° only the first order path is observed and the first order rate constant falls on the same line in the Arrhenius plot as the points obtained for the HNF_2-D_2O exchange. This is shown in Figure 1.

At -51° both paths proceed at about the same rate while at higher temperatures the second order path proceeds faster. The activation energy for the second order path is 26.0 kcal/mole. The Arrhenius plot for this path is shown in Figure 1 which also shows that the plots for the two paths intercept at about -50°C.

There are two possible mechanisms for the second order path as shown below. The first is the protonation of HNF_2

$$HNF_2 + CF_3COOD = HDNF_2^+ + CF_3COO^- \quad \text{Slow}$$

$$HDNF_2^+ = DNF_2 + H^+ \quad \text{Fast}$$

$$H^+ + CF_3COO^- = CF_3COOH \quad \text{Fast}$$

Table II

Summary of HNF_2-CF_3COOD Exchange Runs

Conc. moles $l.^{-1}$								
$[HNF_2]$	$[CF_3COOD]$	$t_{1/2}$ (min)	R(moles l^{-1} min^{-1})	R from 1st Order Path	R from 2nd Order Path	2nd Order K (l mole^{-1} min^{-1})	1st Order K (min^{-1})	t°C
1.53	0.95	30.5	0.0133				0.0087	-60
1.56	1.98	46.0	0.0131				0.0084	-60
1.50	1.50	36.4	0.0143				0.0095	-60
1.47	0.75	30.1	0.0114				0.0078	-60
0.81	1.45	39.3	0.0092				0.0113	-60
0.72	1.52	74.4	0.0046				0.0063	-60
						Avg.	0.0087	
1.56	1.84	1.86	0.315	0.031	0.284	0.099		-42
0.78	1.76	2.75	0.136	0.015	0.121	0.088		-42
0.83	0.47	3.98	0.052	0.016	0.036	0.092		-42
						Avg. 0.093		
1.02	2.00	7.2	0.065	0.017	0.048	0.024		-46
0.96	0.98	8.5	0.040	0.016	0.024	0.026		-46
2.05	1.01	4.4	0.107	0.034	0.073	0.035		-46
0.96	1.98	4.3	0.104	0.016	0.088	0.046		-46
						Avg. 0.033		
1.43	0.75	18.1	0.0188	0.0190	-			-51
1.52	1.50	12.6	0.0415	0.0202	0.0213	0.0094		-51
0.83	0.75	27.3	0.0100	0.0110	-			-51

while the second involves a 1:1 complex

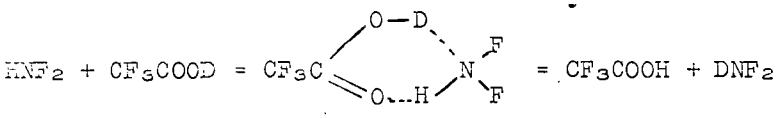

The relative merits of these mechanisms will be discussed.

REACTIONS OF DIFLUORAMINE WITH LEWIS ACIDS*

R. J. Douthart,** J. N. Keith, and W. K. Sumida

IIT Research Institute
Chicago 16, Illinois

INTRODUCTION

Craig[1] has recently reported the results of a study of the reactions of several nitrogen-fluorine compounds with Lewis acids. As was expected, he found that all of the compounds studied were extremely weak bases, difluoramine and its methyl derivative being among the strongest. We are prompted to report some of our data on the reactions of the latter compounds with certain other strong acids.

With the purpose of obtaining new nitrogen fluorine type oxidizers, we have been studying the possibility of preparing difluorammonium salts, $H_2NF_2^+X^-$, and of introducing difluoramino groups into compounds of light metals, such as $Al(NF_2)_3$. To this end, the reactions of difluoramine and methyl difluoramine with certain acids have been studied.

RESULTS AND DISCUSSION

Difluoramine, HNF_2, and methyl difluoramine, CH_3NF_2, have been shown to form isolable complexes with BF_3, BCl_3, and SO_2, and in some cases dissociation data could be obtained. It is evident from Craig's work that usable thermodynamic data will be available only with the strongest acids. The problem is further complicated by the tendency for irreversible decomposition to occur in most of these systems. The acids chosen for this study included the protic acids, hydrogen chloride and trifluoroacetic acid, the metal alkyls, trimethyl aluminum and trimethyl gallium, and sulfur trioxide, one of the strongest gaseous Lewis acids known. Pressure-composition studies were made of these systems in the usual manner, to detect adduct formation or other condensed phase interactions.

The pressure-composition diagrams of the difluoramine-protic acid systems did not indicate compound formation. With HCl, HNF_2 was miscible in all proportions, with large positive deviations from Raoult's Law, while with CF_3CO_2H, partial solubility was

*This research was supported by the Advanced Research Projects Agency under ARPA Order No. 350-62, Project Code No. 9100. Technical Direction was provided by the Director of Engineering Sciences, SREP, Air Force Office of Scientific Research.

**Present Address: Department of Chemistry, University of Illinois Urbana, Illinois.

[1] A.D. Craig, Inorg. Chem. 3, 1628 (1964).

observed, and the solution was ideal. The stronger base, methyldifluoramine, was also miscible with HCl in all proportions, with large negative deviations from Raoult's Law. At the lowest temperature, -127°C, a plateau was obtained, indicating the formation of a 1:1 adduct. This is to be expected, since the methyl derivative should be a significantly stronger base.

Both fluoramines from 1:1 adducts with SO_3, although the adducts probably do not have similar structures. The pressure-composition diagram of the HNF_2-SO_3 system has a minimum at a mole fraction of 0.4, and an inflection at about 0.5. Whether or not these observations indicate the formation of a 1:1 and a 1:2 compound is difficult to decide, due to the fact of slow decomposition of the product, and of the difficulty of obtaining true equilibrium in systems containing condensed SO_3. N.m.r. spectroscopy supports the structure, F_2NSO_2OH (difluorosulfamic acid). The CH_3NF_2-SO_3 system is more conventional. A good pressure plateau, and a sharp pressure rise past a mole fraction of 0.5 indicate the formation of a 1:1 compound.

Irreversible decomposition interferes with pressure-composition studies of these amines with trimethyl aluminum. Coordination compounds are probably intermediates, but no evidence was obtained for their existence. The reaction of trimethylaluminum with difluoramine produces methane, even at -80°C, and often results in explosions. The reaction appears to be the usual elimination which occurs with many hydrogen-containing bases:

$$(CH_3)_3Al + HNF_2 = (CH_3)_2AlNF_2 + CH_4$$

Although this reaction renders the system useless for the purpose of obtaining thermodynamic data on the basicity of difluoramine, it does suggest the possibility of a new oxidizer, $Al(NF_2)_3$. In an attempt to obtain this compound by the use of an excess of difluoramine, twofold substitution was obtained, presumably producing $CH_3Al(NF_2)_2$, although the compound has not been definitely identified.

The reaction of equilimolar amounts of methyl difluoramine with trimethylaluminum produces two moles of methane and a smaller amount of HCN. The reaction is evidently the decomposition of the amine:

$$CH_3NF_2 = HCN + 2\ HF$$

followed by reaction of the HF with trimethylaluminum, liberating methane.

The difluoramine-trimethylgallium system was studied briefly, in an attempt to isolate a coordination compound. No evidence was obtained for such a compound from the pressure-composition data, and the mixture obtained was easily resolved into its components by simple trap-to-trap distillation. At room temperature, however, the elimination of methane occurred, very slowly.

EXPERIMENTAL

A standard Stock-type high vacuum line was used, except for experiments with SO_3 or CH_3NF_2. In these cases stopcocks lubricated with Kel F-90 grease were used, and pressures were measured with a Bourdon gauge.

The commercially available materials, HCl, $(CH_3)_3Al$, and CF_3CO_2H, were purified by trap-to-trap distillation in the vacuum line. SO_3 was generated as needed by passing the vapors from a sample of "Sulfan B" over a P_2O_5 column. Trimethyl gallium was prepared by the reaction of gallium with dimethyl mercury at 130°C. Difluoramine was prepared by the thiophenol reduction of tetrafluorohydrazine.[2]

The HNF_2-HCl System

A pressure-composition study of the system HNF_2-HCl was performed by adding successive small samples of HCl to a sample of HNF_2 held at constant temperature by an appropriate "slush" bath. The data obtained at -112, -127, and -138°C indicated that the two compounds are miscible in all proportions. Deviations from Raoult's Law were positive, indicating no compound formation in the condensed phase.

The CH_3NF_2-HCl System

The pressure composition data were obtained in the same manner as above, except that the mercury-free system was used. In an early experiment with this system, the mercury manometer rapidly became fouled in contact with the mixture of gases. In later exploratory experiments, however, no apparent reaction occurred in several days between a mixture of these gases and mercury in a sealed tube. However, one of these tubes exploded when shaken gently. The previous fouling of the manometer may have been caused by some impurity in the difluoramine.

The pressure-composition diagrams show large negative deviations from Raoult's Law at -95, -112, and 127°C, and at the lower temperature, a plateau indicating the formation of a 1:1 compound.

The HNF_2 - CF_3CO_2H System

Because of the corrosive nature of sulfur trioxide and the tendency of the low-melting form to undergo transition to more highly polymerized forms, it is a rather difficult material to use in an equilibrium process. It was not possible to obtain reproducible saturation pressures for this system by adding HNF_2 to SO_3 at low temperatures. However, at 0°C, a liquid was obtained over the whole composition range studied (up to $x = 0.6$) and equilibrium could be obtained, although slowly. The pressure-

---

[2] J.P. Freeman, A. Kennedy and C.B. Colburn, J. Am. Chem. Soc. 82, 5304 (1960).

composition diagram shows a minimum at $X_{HNF_2} = 0.4$, and an inflection at about 0.5, with a sharp increase in pressure beyond that. Possibly, a 2:1, as well as a 1:1 compound is formed.

The proton and F^{19} n.m.r. spectra indicated only single frequencies for hydrogen and fluorine, neither of which was split, indicating that the hydrogen is no longer on the nitrogen atom. These observations are consistent with the structure F_2NSO_2OH, but not with the coordination compound, $HNF_2:SO_3$.

Slow decomposition of the product occurs at room temperature, the volatile products being N_2F_4 and SO_2. The reaction is probably the following:

$$2\ NF_2SO_2OH \longrightarrow N_2F_4 + SO_2 + H_2SO_4$$

The CH_3NF_2 - SO_3 Systems

The CH_3NF_2 - SO_3 system was examined in a similar manner. At -63.5°C, the pressure-composition diagram indicated only slight solubility of SO_3 in the difluoramine. At -45.2°C, however, the curve is typical of a system in which a 1:1 adduct is formed. The adduct is a white solid, melting at about -10°C, to a clear, colorless liquid. At about 0°C, an exothermic reaction occurs, the liquid becomes yellow, and HCN and SiF_4 are found in the volatile products.

The HNF_2-$(CH_3)_3Al$ System

When attempts were made to study the pressure composition curve of this system, it was soon discovered that explosions occurred whenever the HNF_2 is added in such a manner that the liquid can contact the condensed $(CH_3)_3Al$, even at low temperatures. When successive small amounts of gaseous HNF_2 are added to a reactor containing the alkyl at -80°C, methane is slowly evolved. In one such experiment, 9.5 cc of $(CH_3)_3Al$ was condensed in a small tube at -80°C, and small amounts of HNF_2 added, taking care to keep the total pressure below 25 mm. The methane, which was pumped out each time between additions, totaled 12.1 cc before an explosion occurred.

In an attempt to moderate the reaction, and to obtain more extensive substitution, 9.9 cc of $(CH_3)_3Al$ was dissolved in 5 ml dry isopentane, and 30.8 cc HNF_2 was allowed to distill into the solution at -80°C. The evolution of methane was very slow, even when the solution was brought to room temperature. A total of 19.4 cc CH_4 was obtained over a period of three days, very close to that required for a 2:1 reaction. No new volatile product was found. The yellow solid residue, presumably $CH_3Al(NF_2)_2$, liberated only a trace of iodine when dissolved in a KI solution.

CH_3NF_2-$(CH_3)_3Al$ System

In a single experiment, 9.8 cc CH_3NF_2 and 9.9 cc $(CH_3)_3Al$ were combined and allowed to thaw. Vigorous effervescence began as soon as an appreciable pressure was observed, and was soon

complete at room temperature. The only volatile products were 19.7 cc CH_4 and 3.5 cc HCN.

The HNF_2-$(CH_3)_3Ga$ System

HNF_2 and $(CH_3)_3Ga$ were combined in a small reactor and thawed. The reaction to form methane was very slow, about 2/3 mole being produced overnight at room temperature. No explosion occurs, even in the presence of large excess of HNF_2. A preliminary pressure-composition study did not reveal an adduct at -[illegible].5°C or -45.2°C. Distillation of the mixture through a -80° trap separated the components almost completely in one pass.

A Study of the Chemistry of Difluoramines

A. D. Craig, G. A. Ward, C. M. Wright, and J. C. W. Chien

Research Center, Hercules Powder Co., Wilmington, Delaware

INTRODUCTION

Compounds containing the NF_2 group are commonly referred to as difluoramines. The chemistry of these compounds has been studied more intensively during recent years than previously and has been the subject of three review articles (1,2,3). The aims of our work, part of which we describe here, are to get a picture of the relative electron distributions in $X\text{-}NF_2$ compounds, to gain an understanding of the nature of the N-F and N-X bonds, and to determine the existence and stabilities of N-F radicals and ions. We have concentrated on $X\text{-}NF_2$ compounds, where X = F, Cl, H, NF_2, CH_3, C_2H_5, and CF_3. The radical and ionic species which have held our attention are $\cdot NF$, $\cdot NF_2$, NF^+, NF^-, NF_2^+, NF_2^-, NF_3^+, and $H_2NF_2^+$. This paper emphasizes the chemistry of difluoramine, HNF_2, and the existence of NF_2-containing ions to illustrate our investigations in NF_2 chemistry.

RESULTS AND DISCUSSION

Theoretical Considerations

One of the approaches which we have taken is the calculation of molecular parameters of various N-F species by employing molecular orbital treatments (4,5). Of particular relevance to NF_2 chemistry are the π-bond orders and atomic charges calculated for NF_2 moieties (Table I).

TABLE I
CALCULATED CHARGES AND BOND ORDERS OF NF_2 SPECIES

	ATOMIC CHARGES		
	Q_N	Q_F	π-Bond Orders
NF_2^+	+1.706	-0.353	0.3
NF_2	+0.86	-0.43	0.35
NF_2^-	0	-0.5	0

Kaufman and coworkers have made similar calculations and have shown that, in covalent NF_2 compounds, there are no orbitals available on the nitrogen of energy low enough for significant π-bonding with the unshared electrons on the fluorine atoms (6,7). In a series of $X\text{-}NF_2$ compounds, the relative electron distributions are thus a function of the inductive effects of the X group. The various situations are envisioned as follows:

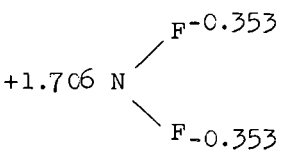

I

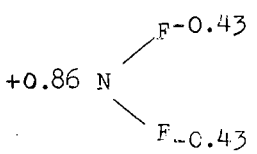

II

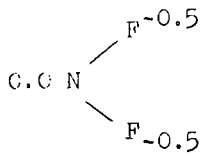

III

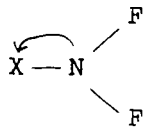

IV

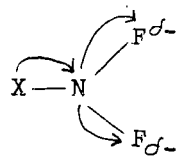

V

The relatively high negative charge on fluorines causes many NF_2 species to decompose readily by loss of a fluoride ion. This work indicates that the NF_2-containing ions which have the greatest probability of long term existence are the cations, because, of any of the NF_2 species, NF_2^+ has the lowest negative atomic charge on the fluorines. In all of the difluoramine derivatives studied, the non-bonding L-shell electrons of the nitrogen are more displaced toward the fluorines than strictly localized on the nitrogen. As a result, the nitrogen in many NF_2 species carries a relatively high positive charge. Any cationic NF_2 species would be expected to have a high electron affinity, probably higher than that of NO_2^+. Considerations in isolating an NF_2 cation are to stabilize it with a large anion of low charge density so that polarization can occur, or to select a hypothetical NF_2 salt in which the lattice stabilization energy is very high. Candidates for the latter are moderate-sized divalent anions. No NF_2-containing ions of any type have been observed, except for NF_2^+ which has been observed in the mass spectrometer (8).

Experimental Observations

The nearest we have come to demonstrating the existence of N-F ions is in the electrochemical oxidation-reduction reactions of HNF_2. The oxidation has been carried out in water and in various polar organic solvents under acid condition (9). The first step of this reaction has been shown to be formation of the $\cdot NF_2$ radical. The $\cdot NF_2$ radical undergoes combination processes on the surface of the electrode rather than diffusing into the body of the solution before being involved in further reactions. The combination process on the electrode surface has been used to prepare a variety of NF_2 compounds by simultaneously generating other radical species, e.g.,

$$HNF_2 \longrightarrow H^+ + e^- + \cdot NF_2$$
$$CH_3COOH \longrightarrow \cdot CH_3 + H^+ + CO_2 + e^-$$
$$\cdot NF_2 + \cdot CH_3 \longrightarrow CH_3NF_2$$

The oxidation of HNF_2 involves the removal of an electron from the nitrogen in a solvated HNF_2 species rather than from NF_2^-. All of our work on the solution chemistry of HNF_2 shows that under conditions favoring the formation of NF_2^- (proton removal), this species loses a fluoride ion to form difluorodiazine.

$$NF_2^- \longrightarrow 1/2\ N_2F_2 + F^-$$

The reduction of HNF_2 in aqueous media is a four-electron process in which HNF_2 is reduced to ammonia (10). In nonaqueous solvents, the reduction is dependent on the availability of protons in the system and the reduction potential is strongly influenced by the degree and type of solvation (Table II). Nitrogen trifluoride is electrolytically reduced in aqueous solution at ~-1.40 v. vs. S.C.E.

Six electrons per molecule of NF_3 are involved in the reduction.

$$HNF_2 + 4e^- + 2H^+ \longrightarrow NH_3 + 2F^-$$
$$NF_3 + 6e^- + 3H^+ \longrightarrow NH_3 + 3F^-$$

NF_3 could not be electrolytically oxidized in systems similar to those used for the reduction.

TABLE II
EFFECT OF SOLVENT ON THE POLAROGRAPHIC REDUCTION OF HNF_2

Solvent	$E^{1/2}$ HNF_2 (volts versus S.C.E.)
H_2O	1.22
C_2H_5OH	1.64
CH_3CN	1.42
Dimethyl Formamide	1.61
Dimethyl Sulfoxide	1.64

The solvation of HNF_2 in a variety of solvents was studied by conventional and low-temperature infrared techniques and by determining the dissociation pressure-temperature relationships of several HNF_2-solvent complexes (6,10). Total enthalpies of dissociation were determined where experimentally feasible. Shifts in the N-H and N-F stretching frequencies in the IR spectra of 1:1 complexes of HNF_2 with solvents and of one-molar solutions of HNF_2 were examined to determine the nature of the bonding in the solvated species (Table III). In general these data indicate the order $H_2O < CH_3OH < CH_3CN < HCONH_2 < HOCN(CH_3)_2 \sim (CH_3)_2SO$ for the strength of solvation of HNF_2. It was found that 1:2 complexes of HNF_2 with DMF and DMSO exert very little vapor pressure at room temperature. Equimolar complexes of HNF_2 with formamide, dimethyl formamide, and dimethyl sulfoxide exert relatively little vapor pressure at 0°. HNF_2 is by far least solvated by water.

In all of the solvents studied, the most important factor, determined from vibrational spectra, is the strength of the difluoramine hydrogen bond with the solvent. Thus, HNF_2 appears to be bonded to these solvents in structures of the type

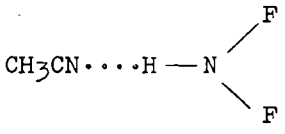

However, in some systems the infrared spectra indicate moderate bonding of the fluorines with the solvent, e.g.,

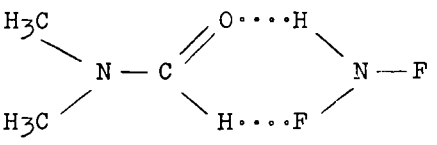

Attempts were made to protonate HNF_2 and CH_3NF_2 to determine if ammonium-type ions such as $H_2NF_2^+$ and $CH_3NF_2H^+$ could be formed. Three approaches were employed. First, 1 M amounts of H_2O and $HClO_4$

were added to 1 M solutions of HNF_2 in acetonitrile or dimethyl formamide. Conventional infrared spectroscopic techniques indicated that no interaction with the HNF_2 occurred. Second, the strengths of association of CH_3NF_2 and HNF_2 with anhydrous HCl, anhydrous HBr, and water were measured. The techniques employed were similar to those described earlier (11). No association of the difluoramines with any of the acids was observed. Third, infrared spectra of the solid equimolar mixtures HNF_2-H_2O, HNF_2-HCl, HNF_2-HBr, CH_3NF_2-H_2O, CH_3NF_2-HCl, and CH_3NF_2-HBr showed no evidence of protonation. Spectra were obtained at -160°. Both HNF_2 and CH_3NF_2 were observed to oxidize HBr to bromine. No reaction was observed with HCl or H_2O.

TABLE III
INFRARED ABSORPTION MAXIMA OF HNF_2 COMPLEXES

Material	N-H Stretch	N-H Asym. Bend	N-H Sym. Bend	N-F Sym. Stretch	N-F Asym. Stretch
$CH_3CN \cdot HNF_2$ (solid)(a)	2710	1424		960	860
1 M HNF_2 in CH_3OH (liquid)(b)	2725	*	1325*	955	855
$H_2O \cdot HNF_2$ (solid)(a)	2800 2975	1390	1320	973	875
$DMF \cdot HNF_2$ (solid)(a)	2725	*	*	952	850
1 M HNF_2 in DMSO (liquid)(b)	2740	*	*	*	855
HNF_2 (solid)(a)	3110	1450	1350	972	880

*Solvent interference
(a) At -160°
(b) At 25°

A measure of the relative distribution of electrons in a variety of NF_2 compounds was obtained by studying the interaction of the difluoramines with Lewis acids (11). The low-temperature infrared spectra of complexes of difluoramines showed that bonding occurs through donation of electrons on the nitrogen to the Lewis acid. In no cases was evidence found for fluorine bridging or complete charge transfer. The strength of the complexes formed was directly dependent on the electron-withdrawing or -donating power of the attached group. A strongly electron-withdrawing group such as CF_3 renders the X-NF_2 compound an essentially nonpolar species. An electron-donating group such as CH_3 increases the electron density on the nitrogen but also increases the apparent electron density on the fluorines so that compounds such as $CH_3CH_2NF_2$ or HNF_2 readily undergo fluoride abstraction reactions, e.g.,

$$CH_3CH_2NF_2 \longrightarrow CH_3CN + 2HF$$
$$HNF_2 \longrightarrow 1/2\ N_2F_2 + HF$$

Studies of the proton resonance of CH_3NF_2 and $C_2H_5NF_2$ showed that the effective electronegativity of the NF_2 group is about 3.3. Recently, the electronegativity was calculated to be between 3.6 and 3.7 (12). Thus, the NF_2 group is a strong electron-withdrawing moiety itself. The competition for nonbonded electrons may be pictured as in IV and V above. In V the N-F bond is weakened so that reactions of XNF_2 favor routes which involve loss of F^-. In IV the N-F bond is stronger so that XNF_2 reactions favor the

loss of $\cdot NF_2$. We examined the mass spectral cracking patterns of CH_3NF_2 and CF_3NF_2 at low ionization potentials (11 electron volts) and found that the most abundant ions (99%) were $CH_3NF_2^+$ and CF_3^+, respectively. These data indicate that the C-N bond in CF_3NF_2 is weaker than that of CH_3NF_2. This observation is also consistent with analysis of the ultraviolet spectra of these compounds (13). The N-F bond in CH_3NF_2, however, appears to be weaker than in CF_3NF_2. The thermal decompositions of these two difluoramines probably occur through different mechanisms. CF_3 will lose an NF_2 radical in the first step, whereas CH_3NF_2 will lose a fluorine:

$$CF_3NF_2 \longrightarrow \cdot CF_3 + \cdot NF_2$$
$$CH_3NF_2 \longrightarrow CH_3\dot{N}F + \cdot F$$

The $\cdot NF_2$ and $\cdot F$ will probably then undergo further reactions with the parent molecules:

$$\cdot NF_2 + CF_3NF_2 \longrightarrow NF_3 + CF_3\dot{N}F$$
$$\cdot F + CH_3NF_2 \longrightarrow HF + \cdot CH_2NF_2, \text{ etc.}$$

The CF_3NF_2 does not easily lose a fluoride ion to Lewis acids such as BF_3 (9).

Conclusion

These studies tend to substantiate the prediction of the theoretical calculations that if N-F anions are formed, the electron density on the fluorines will be so high that loss of a fluoride ion would be almost impossible to prevent. Further, the electron affinity of NF_2^+ appears to be extremely high, so that addition of an electron to form $\cdot NF_2$ or addition of an anion to form a covalent NF_2 compound is highly favored. In general, the reaction routes of NF_2 compounds appear to be favored where the reaction intermediate is an $\cdot NF_2$ radical. The $\cdot NF_2$ radical is a relatively stable species with a π-bond order of 0.35. The electron distribution in this species is much more symmetrical than those of the anion or cation. Reaction routes which involve an NF_2 anion intermediate are not very favorable because of the ease of fluoride loss. The NF_2 cation is equally as unfavorable since its oxidizing power will probably prevent it from existing in most systems.

REFERENCES

1. C. J. Hoffman and R. G. Neville, Chem. Rev., 62, 1 (1962).
2. C. B. Colburn in "Advances in Fluorine Chemistry", Vol. 3, M. Stacey, J. C. Tatlow, and A. G. Sharpe, Ed., Butterworths, Washington, D. C., 1963, p. 92ff.
3. A. V. Pankratov, Russ. Chem. Rev., 32, 157 (1963).
4. J. C. W. Chien, Hercules Powder Co., Annual Report, April 15, 1964, Contract No. DA-31-124-ARO(D)-62, ARPA Order No. 402.
5. Hercules Powder Co., Quarterly Report No. 6, September 21, 1964, Contract No. DA-31-124-ARO(D)-62, ARPA Order No. 402.
6. J. J. Kaufman, J. Chem. Phys., 37, 759 (1962).
7. J. J. Kaufman and J. R. Hamann, paper presented before the Division of Fluorine Chemistry at the 148th American Chemical Society National Meeting, September 1964.
8. J. T. Herron and V. H. Diebler, J. Chem. Phys., 33, 1595 (1960).

9. G. A. Ward and C. M. Wright, J. Amer. Chem. Soc., 86, 4333 (1964).
10. G. A. Ward, C. M. Wright, and A. D. Craig submitted to J. Amer. Chem. Soc.
11. A. D. Craig, Inorg. Chem., 3, 1628 (1964).
12. J. E. Huheey, J. Phys. Chem., 68, 3073 (1964).
13. J. C. W. Chien, to be published. Also in Ref. 5.

Contribution from the Chemistry Research Section,
ROCKETDYNE, A Division of North American Aviation, Inc.,
Canoga Park, California

DIFLUORAMINE : AN INFRARED STUDY OF THE COMPLEXES BETWEEN DIFLUORAMINE AND THE ALKALI METAL FLUORIDES

By H. E. Dubb, R. C. Greenough, and E. C. Curtis

(ABSTRACT)

Difluoramine, HNF_2, was condensed on alkali metal fluoride optical crystals and the infrared spectra of the resulting compounds were measured. Complex formation was observed with KF, RbF, and CsF. An analysis of the infrared spectra indicates that two compounds may be formed, one a simple hydrogen bonded complex, and the other a new species $MNF_2 \cdot HF$.

INTRODUCTION

Potassium, rubidium, and cesium fluorides form complexes with difluoramine (that dissociate reveraibly) when the latter is condensed onto these materials. When the potassium and rubidium complexes are allowed to warm to room temperature they react further to form the cis and trans difluorodiazine isomers and the alkali metal bifluorides. The cesium complex explodes before reaching room temperature.[1]

---

1. Lawton, E. A., D. Pilipovich, and R. D. Wilson, U. S. Patent 3,109,711 (Nov. 5, 1963).

It has been postulated that the explosive nature of the cesium complex as contrasted with the nonexplosive nature of the potassium and rubidium

complexes might be due to the formation of a highly unstable difluoramide ion, NF_2^-. The present infrared study of the structures of these complexes was undertaken with the purpose of determining whether such an ion does exist.

Infrared spectra of the complexes were obtained by condensing difluoramine onto optical blanks of the alkali metal fluorides at -95 C and scanning through the rock salt region with a Beckman IR-7 spectrometer. Examination of the spectra indicates that potassium and rubidium fluorides primarily form hydrogen bonded complexes of the structure $M^+F^-\cdot HNF_2$ with possibly small amounts of a difluoramide complex, $M^+\cdot FH\cdot NF_2^-$, also present. Cesium fluoride seems at first to form a complex with two (or more) moles of difluoramine. On pumping this is converted to a mixture of $Cs^+F^-\cdot HNF_2$ and $Cs^+\cdot FH\cdot NF_2^-$. The evidence for the existence of a difluoramide ion is strongest in the case of cesium.

EXPERIMENTAL

The difluoramine was prepared by the action of concentrated sulphuric acid on fluorinated urea. It was then purified by distillation under a vacuum at reduced temperatures.[2] The potassium and cesium fluoride crystals

---

2. Lawton, E. A., and J. Q. Weber, J. Am. Chem. Soc. 81, 4755 (1959), E. A. Lawton and D. F. Sheehan unpublished work.

---

were obtained from the Harshaw Chemical Co. and the rubidium fluoride from Semi-Elements, Inc.

The alkali fluoride single crystal was mounted on a copper block inside an infrared cell fitted with rock salt windows. Gaseous difluoramine was condensed onto a 1" x 1" optical blank of the appropriate alkali metal fluoride maintained at about -95 C by a slush bath of methylcyclohexane. The copper block was in contact with the slush coolant so that the alkali fluoride plates could be kept at the proper temperature, which was measured with a copper-constantan thermocouple. The apparatus will be described in detail elsewhere.[3]

---

3. Bell, R. E., R. C. Greenough, G. Brull, Jr., and H. E. Dubb, to be published.

There was considerable difficulty in handling the crystals since they are very hygroscopic. The crystals were polished on a felt cloth wet with a butanol solution saturated with the appropriate salt, and then were mounted on the copper block and sealed into the infrared cell. All these manipulations were done inside a very carefully constructed dry box with a 97% Ar - 3% H_2 atmosphere maintained at a positive pressure so that the alkali fluoride plate was not exposed to air at any time.

The difluoramine was admitted through a nozzle directly onto the plate. Actually, the vapor pressure of difluoramine is high enough so that a portion of the gas condensed on the copper block; however, most of it did condense on the window. The spectra of the resulting complexes were then scanned with a Beckman IR-7 spectrometer set at low resolution and high speed. The machine was not especially calibrated for this experiment, but it is felt that frequencies reported are good to $\pm$ 2 cm^{-1} at 1000 cm^{-1} and $\pm$ 20 cm^{-1} at 3000 cm^{-1}.

At the end of the experiment the potassium and rubidium fluoride plates were allowed to warm and the spectrum of the bifluoride salt was detected on the plates by comparison with the known KHF_2 spectrum[4]. The cesium fluoride blank was destroyed at the end of the experiment by condensing

4. J. A. A. Ketelaar and W. Vedder, J. Chem. Phys. 19, 654 (1951).

methanol onto the plate to avoid an explosion and subsequent harm to the apparatus when it was warmed to room temperature.

There was some difficulty with leaks with this apparatus; even a very small amount of water on the alkali fluoride plates gives a very intense band at 3290 cm^{-1}.

RESULTS

The spectra of HNF_2 on KF and HNF_2 on CsF are shown in Figure 1. The spectrum of HNF_2 on RbF was very similar to that on KF. An assignment of all spectra measures is given in Table I. A spectrum of liquid HNF_2 on NaCl was also measured. Bands appeared at approximately the same frequencies as the gas phase bands.

There was some air leakage into the cell during the KF and CsF experiments, raising some doubt about the HF frequency. It is felt that absorption around 3500 cm^{-1} was not due to water but was caused by a HF stretching mode. This assignment was more certain in the case of the CsF complex.

KF and RbF seem to form similar complexes. The N-H stretching frequency at 2600 cm^{-1} is shifted down 600 cm^{-1} from the gas phase frequency. The N-H stretching band in the complex is considerably more intense than the same band in the gas phase.[5] The other vibrational modes are at

5. J. J. Comeford, D. E. Mann, L. J. Schoen, and D. R. Lide, J. Chem. Phys. 38, 461 (1963).

about the same frequencies as in the gas phase spectrum. The probable structure of this complex is shown in Figure 2 as Form A, and seems to be that of a strongly hydrogen-bonded complex. It is possible that some $M^{+}\cdot FH\cdot NF_2^{-}$ complex exists also but if this is so, its concentration is smaller than in the CsF case.

The spectrum of the CsF complex is somewhat more complicated in agreement with the fact that evidence for two complexes has been reported.[6]

6. E. A. Lawton, D. Pilipovich, and R. D. Wilson ~~to be published~~. in press, J. Inorg. Chem.

The bands in the early spectrum (labeled complex plus gas) are shifted even further from the gas phase frequencies than in the KF and RbF cases. The increased complexity of the NH stretching frequencies supports the existence of at least two types of complexes, but hardly permits speculation on their exact structure. On pumping off the excess gaseous HNF_2 the spectrum is simplified and all bands shift to the blue indicating that the complex is now of a single type very probably one mole of CsF to one mole of HNF_2. A new band appears at 720 cm^{-1} and one at 3500 cm^{-1}.

These bands can be accounted for by an NF_2^- ion and HF. It would appear that here also two types of complexes are present, one a hydrogen bonded complex similar to the $KF \cdot HNF_2$ and the second complex containing the difluoramide ion, $Cs^+FH \cdot NF_2^-$ (Fig. 2, Form B).

An attempt was also made to find the bending mode of the NF_2^- ion which should be shifted well to the blue from the 500 cm^{-1} frequency in HNF_2. This would have proved the existence of an NF_2^- ion, but unfortunately the CsF plate was opaque in this region and an attempt to deposit CsF powder on a AgCl window was unsuccessful as there was too much light scattering from the powder.

Discussion

This data provides possibly the best indication to date that a NF_2^- ion exists. The evidence for the existence of the NF_2^- ion is more conclusive for $Cs^+ \cdot FH \cdot NF_2^-$ than for $K^+ \cdot FH \cdot NF_2^-$ or $Rb^+ \cdot FH \cdot NF_2^-$. The CsF 1:1 complex can be pictured as a mixture of two tautomeric forms where the hydrogen resides in one of two potential energy minima, one corresponding to $Cs^+F^- \cdot HNF_2$ and the other to $Cs^+ \cdot FH \cdot NF_2^-$ (Figure 3a). The KF and RbF complexes are of the same type as the CsF complex but with less favorable potential energy minima for their NF_2^- ion forms. In fact, it is not certain that they contain such minima (Figure 3b). The evidence seems only slightly to favor their existence. Since both forms of the CsF complex were observed in the spectrum, they must have an interconversion rate which is slow compared to the measuring infrared frequencies of about 10^{14} cps.

When there was excess gaseous HNF_2 in contact with CsF additional absorptions were observed in the N-H stretch region. This indicated that more then one HNF_2 may be complexed with each CsF entity. When the higher complex was present, no evidence of NF_2^- ion was found in the spectrum. Thus the NF_2^- ion may not exist except under exceptionally favorable conditions.

Even though the existence of NF_2^- ion is indicated by this work, this should in no way encourage a belief that it might be found in other systems; both the driving force of forming an HF bond and the positioning of the HNF_2 in the $M^+F^-\cdot HNF_2$ complex would seem to provide the best possible conditions for forming and stabilizing NF_2^- ion.

ACKNOWLEDGMENTS

We would like to thank Drs. E. A. Lawton and D. F. Pilipovich for suggesting this project and providing encouragement. Also we would like to thank Mr. R. D. Wilson for preparing the difluoramine and aiding in several of the experiments.

This work was supported by the Advanced Research Projects Agency under contract AF04(611)-9377, ARPA Order No. 24.

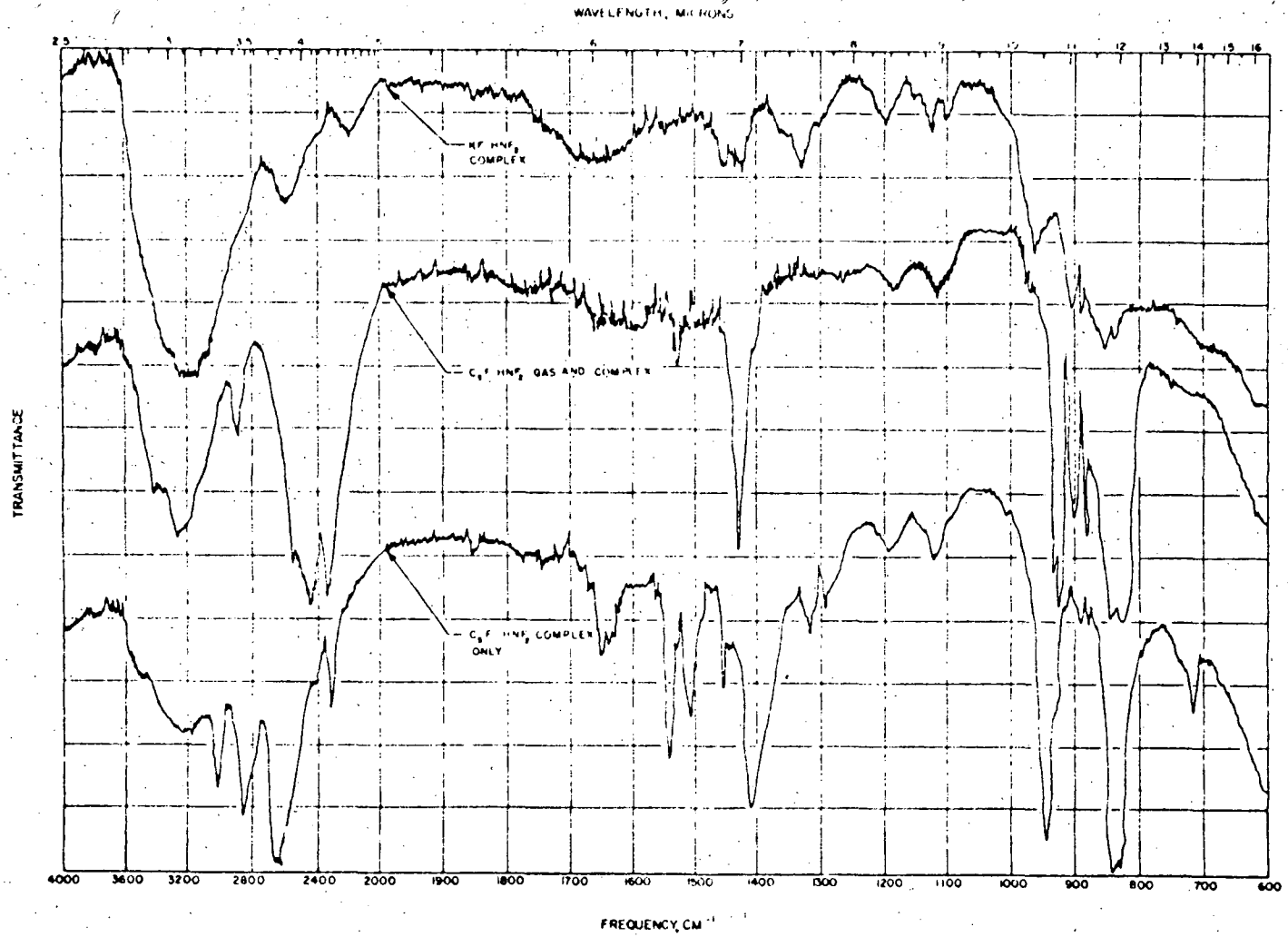

Fig. 1.-INFRARED SPECTRA OF THE DIFLUORAMINE/ALKALI-METAL FLUORIDE COMPLEXES

Table 1.-ASSIGNMENTS OF INFRARED SPECTRA

Assignment	Frequency, cm^{-1}				
	HNF_2 Gas and HF Cold Film	$KF + HNF_2$	$RbF + HNF_2$	$CsF + HNF_2$ Complex + Gas	$CsF + HNF_2$ Pumped On Complex
HF Stretch	3400 3100		3300b?		3500? 3200?
NH Stretch	3193vw	2900? 2850? 2600	2850? 2600 2450?	2850 2650 2300?	2900 2450 2350
NH Bend (asymmetric)	1424s	1410	1440	1510	1545
NH Bend (symmetric)	1307s	1320		1410	1460 1432
NF Stretch (symmetric)	972s	965	960	942	942 930
NF Stretch (asymmetric)	888vs	850 830	850	830	840 825
Liquid and Ionic	800	800	800		
NF Stretch	700	700	700	720	720

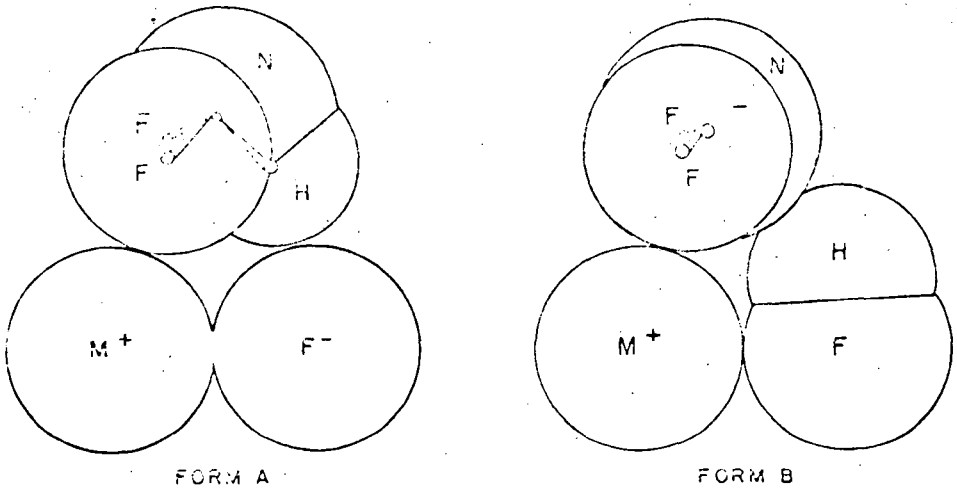

Fig. 2.-APPROXIMATE SCALE DRAWING OF THE HNF_2 COMPLEXES

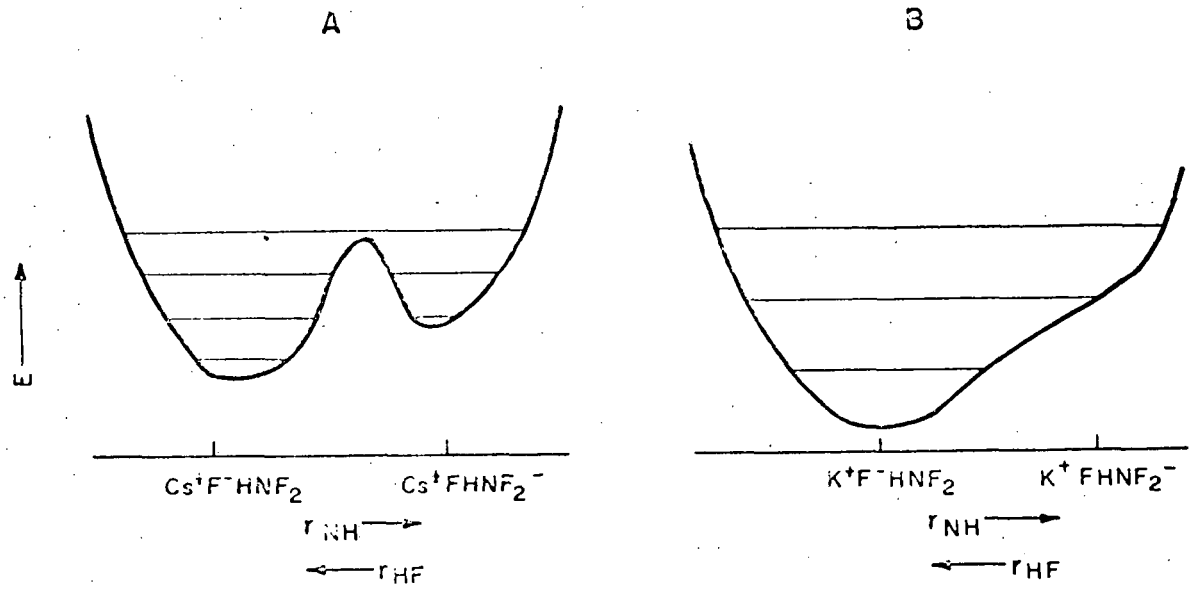

Fig. 3.-POTENTIAL ENERGY OF THE COMPLEX AS A FUNCTION OF THE POSITION OF THE HYDROGEN ATOM

Some Reactions of Alkyldifluoramines[1]

Harry F. Smith, Joseph A. Castellano, and Donald D. Perry

Contribution from the Chemistry Department,
Reaction Motors Division, Thiokol Chemical Corporation, Denville, New Jersey

The continuing search for more energetic rocket propellant compositions has focussed attention on several previously unexplored fields of chemistry. Compounds containing fluorine bound to nitrogen offer attractive prospects in such applications. Since effective utilization of any chemical system requires an understanding of the components involved, we have undertaken a study of the reactions of some simple model compounds of this class.

The first synthesis of an N, N-difluoroalkylamine (alkyldifluoramine) in 1936[2] introduced a new family of organic compounds. The perfluoroalkyldifluoramines obtained by fluorination of various carbon-nitrogen compounds[3] have more recently been supplemented by a limited number of analogous compounds containing non-fluorinated alkyl groups.[4] This paper constitutes the first in a series devoted to the study of the chemical properties of these interesting compounds.

Reactions with Organometallic Reagents

Triphenylmethyldifluoramine ("trityldifluoramine", I) has been found to react rapidly with n-butyllithium to yield n-octane and benzophenone anil (II). With equimolar quantities of the reactants the reaction was incomplete and some I was recovered. Only 40% of the fluorine was converted to fluoride ion under these conditions. Increasing the amount of organometallic reagent to two molar equivalents resulted in complete disappearance of the difluoramine; 77% of the total fluorine was recovered as fluoride ion and the yield of II was 70% of theory.

---

1. Research reported in this publication was supported by the Advanced Research Projects Agency and administered by the Department of the Navy, Office of Naval Research.

2. O. Ruff and M. Giese, Ber., 69B, 598 (1936).

3. a. G. E. Coates, J. Harris, and T. Sutcliffe, J. Chem. Soc., 1951, 2762.
   b. R. N. Haszeldine, Research, 4, 338 (1951).
   c. J. A. Attaway, R. H. Groth, and L. A. Bigelow, J. Am. Chem. Soc., 81, 3599 (1959).
   d. L. A. Bigelow, "Fundamental Research in Organic Fluorine Chemistry", Terminal Report, Office of Naval Research, AD No. 207549, 31 August 1958.
   e. R. K. Pearson and R. D. Dresdner, J. Am. Chem. Soc., 84, 4743 (1962).

4. a. J. W. Frazer, J. Inorg. Nucl. Chem., 16, 23 (1960).
   b. R. C. Petry and J. P. Freeman, J. Am. Chem. Soc., 83, 3912 (1961).
   c. W. H. Graham and C. O. Parker, J. Org. Chem., 28, 850 (1963).
   d. H. F. Smith and J. A. Castellano, "A Convenient Synthesis of t-Butyldifluoramine" in press.

t-Butyldifluoramine (III) reacted rapidly with either n-butyllithium or phenyllithium to produce n-octane and biphenyl, respectively. Recovery of fluoride ion was 20-27% in equimolar systems and increased to approximately 50% when more than one equivalent of n-butyllithium was used.

Two additional products, present in small quantity, were detected and identified by infrared and mass spectral analyses. These products were azoisobutane (IV) and 1,2-difluoro-1,2-di-t-butylhydrazine (V).

$(CH_3)_3CN{=}NC(CH_3)_3$ IV

$(CH_3)_3CNNC(CH_3)_3$ (F, F) V

The reaction of III with two or four equivalents of n-butyllithium resulted in the formation of a new product, N,N-di-n-butyl-t-butylamine (VI), in yields up to 16% of theory. This previously unknown tertiary amine, b.p. 80-82°/0.3 mm, was identified by infrared and mass spectrometric analyses. A comparison of the mass spectrum of VI with that of the known tri-n-butylamine (Table I) shows that the same major peaks appear, but in quite different relative intensities. The mass peaks due to rearrangements were generally more intense and two such peaks (m/e = 86, 114) which do not occur in tri-n-butylamine were observed.

Table I

Principal Mass Peaks of N,N-n-Butyl-t-Butylamine and Tri-n-Butylamine

m/e	Ionic Species		Relative Intensity $(n\text{-}Bu)_2N\text{-}t\text{-}Bu$	Relative Intensity $(n\text{-}Bu)_3N$[a]
41	$C_3H_5^+$		90	21.4
42	$C_3H_6^+$		34	16.0
43	$C_3H_7^+$		85	7.8
57	$C_4H_9^+$		100	13.4
58	C_4H_{10} or $C_3H_3NH_2$+	(Rearrangement)	75	5.0
72	C_4H_9NH+	(Rearrangement)	91	1.16
86	$C_4H_9NHCH_2$+	(Rearrangement)	92	4.26
99	$C_4H_9N(CH_2)_2$+	(Rearrangement)	12	-----
100	$C_4H_9NH(CH_2)_2$+	(Rearrangement)	8	26.3
113	C_4H_9-N-$(CH_2)_3$+		8	-----
114	C_9H_9-NH$(CH_2)_3$+	(Rearrangement)	4	0.25
128	$(C_4H_9)_2N$+		68	1.03
142	$(C_4H_9)_2NCH_2$+		63	100.0
170	$(C_4H_9)_2NC_3H_6$+		26	0.14
185	$(C_4H_9)_3N$+		8	5.22

a. Mass Spectral Data, A. P. I., Serial No. 1132

The results of this series of experiments are summarized in Table II.

Table II

Reactions of t-Alkyldifluoramines with Organolithium Reagents

Reactants			Products		
RNF_2	R'Li	Molar Ratio	%R'R'	$\%F^-$	Others
I	n-BuLi	1:1	------	40.1	I, II
I	n-BuLi	1:2	present	77.0	I, 42+% II
I	n-BuLi	1:2	------	----	72% II
III	ϕLi	1:1	present	21.1	III, IV, V
III	ϕLi	1:1	50.8	19.5	III
III	n-BuLi	1:1	88.0	25.6	III
III	n-BuLi	1:1	present	25.6	III
III	n-BuLi	1:2	present	48.8	VI
III	n-BuLi	1:4	------	52.0	16.2% VI

Proposed Mechanism of Organolithium Reactions

The various products obtained in the experiments described above can be explained on the assumption that the organometallic reagents reduced the tertiary alkyldifluoramines via a succession of one-electron transfer steps. A possible

$$R_3CNF_2 + R'Li \longrightarrow R_3CNF\cdot + R'\cdot + LiF \qquad (1)$$

I VII a, R = CH_3; b, R = ϕ

$$R_3CNF\cdot + R'Li \longrightarrow R_3CN\cdot + R'\cdot + LiF \qquad (2)$$

VII VIII a, R = CH_3; b, R = ϕ

alternative for the step shown in equation 2 would be interaction of the R' radical derived from the organometallic reagent with the fluoramino radical (VII). Such a process would also produce the nitrene (VIII), but would require different stoichio-

$$R_3CNF\cdot + R'\cdot \longrightarrow R_3CN\cdot + R'F \qquad (3)$$

VII VIII

metry. No trace of the fluorocarbon by-products which would be formed in this process has been detected.

The array of final products obtained in any one experiment was found, as expected, to depend upon the reactant ratio and the order and rate of addition. The reactive intermediate species are capable of interacting in various combinations and products arising from several of these possibilities have been detected.

In each case the hydrocarbon produced by the coupling of two of the radicals derived from the organometallic reagent was a prominent product. Diphenyl and n-octane were obtained from phenyllithium and n-butyllithium, respectively. When an equimolar quantity of phenyllithium was added slowly to t-butyldifluoramine (III), the homogeneous coupling product (V) of the amino radical (VII a) was detected among the products, along with the coupling product (IV) of the nitrene (VIII a). The diradical nature of nitrenes, which leads to dimerization and the production of azo

$$2(CH_3)_3\dot{C}NF \longrightarrow (CH_3)_3CN(F)-N(F)C(CH_3)_3 \quad (4)$$

VII a V

$$2(CH_3)_3C\dot{N}\cdot \longrightarrow (CH_3)_3N{=}N(CH_3)_3 \quad (5)$$

VIII a IV

compounds, is well known.[5] The cross-coupling of VIII a with the n-butyl radical has been observed when an excess of n-butyllithium was used.

$$(CH_3)_3C\dot{N}\cdot + 2CH_3(CH_2)_3\cdot \longrightarrow (CH_3)_3CN(CH_2CH_2CH_2CH_2)_2 \quad (6)$$

VIII a VI

In reactions involving trityldifluoramine (V) rearrangement of the nitrene (VIII b) appears to be favored energetically, since benzophenone anil (II) was the only product found. II has been reported as the principal product of thermal decom-

$$\phi_3C\dot{N}\cdot \longrightarrow \phi_2C{=}N\phi \quad (7)$$

VIII b II

position of tritylazide, N-tritylhydroxylamine, and a number of related compounds[6,7,8] presumably also via the nitrene intermediate. An analogous rearrangement of the t-butyl nitrene (VIII a), if it occurred, would yield the imine (IX) which would be subsequently hydrolyzed to acetone and methylamine. A careful search failed to reveal the presence of any volatile base.

$$(CH_3)_3C\dot{N}\cdot \longrightarrow (CH_3)_2C{=}NCH_3 \xrightarrow{H_2O} (CH_3)_2C{=}O + CH_3NH_2 \quad (8)$$

VIII a IX

5. L. Horner and A. Christmann, Angew. Chem. (Int. Ed.), 2, 599 (1963).
6. Steiglitz, et al., J. Am. Chem. Soc., 36, 272 (1914); ibid., 38, 2081, 2718, 2717 (1916); ibid., 44, 1270, 1293 (1922).
7. L. W. Jones and E. E. Fleck, ibid., 50, 2022 (1928).
8. W. H. Saunders and J. C. Ware, ibid., 80, 3328 (1958).

Reactions with Nitric Acid

Since concentrated nitric acid exhibits both oxidative and electrophilic properties, one can anticipate several possible modes of attack on a tertiary alkyldifluoramine. The difluoramine might be protonated and subsequently hydrolyzed, oxidation might produce an amine oxide analog, oxidative cleavage might occur at N-F, C-N, or C-C bonds, or a nitroalkane might be produced. It has been reported, for example, that trityldifluoramine is protonated in concentrated sulfuric acid and decomposes with the liberation of difluoramine.[9] We have confirmed this observation and found, furthermore, that a secondary alkyldifluoramine is similarly protonated but decomposes with the evolution of hydrogen fluoride.[10] Trityldifluoramine has been found to dissolve in glacial acetic acid and to be recovered unchanged upon dilution with water. It was not affected by contact with concentrated hydrochloric acid at room temperature.

The room temperature reactions of t-butyldifluoramine and trityldifluoramine with concentrated nitric acid, in both equimolar quantities and with a large excess of acid, have been studied. Table III presents a summary of the products obtained in each case, as determined chiefly by infrared spectral evidence.

Table III

Reactions of Alkyldifluoramines with 70% Nitric Acid

	t-Butyldifluoramine		Trityldifluoramine	
Product	Equimolar acid	Excess acid	Equimolar acid	Excess acid
NO_2	-------	Large	Present	Large
N_2O	Present	Present	-------	Present
CO_2	-------	Large	-------	-------
NO_3F	Trace	Trace	-------	Trace
NOCl or NO_2F	-------	-------	-------	Trace
SiF_4	Present	Present	-------	Present
Alkylnitrate	Present	Present	-------	Present
Alkylnitrate	-------	Present	-------	Present
Nitroalkane	-------	-------	-------	Present
Carbinol	-------	-------	-------	Major
Alkyldifluoramine	Present	-------	Major	-------

Several points are worth considering in some detail. The large amount of nitrogen dioxide obtained when excess acid was used is apparently the result of decomposition of nitric acid catalyzed by the difluoramine or one of the reaction products. This interpretation is supported by the fact that the quantities of gas obtained were greatly in excess of stoichiometric, based on the difluoramine, and by the observed exponential pressure rise following a protracted induction period.

9. W. H. Graham and C. O. Parker, J. Org. Chem., 28, 850 (1963).
10. Unpublished experiments, this laboratory.

The presence of carbon dioxide among the products of the reaction of t-butyldifluoramine with excess nitric acid is a clear indication that C-C bond cleavage occurred. The nitrate and nitrite esters produced in this experiment were mixtures of various alkyl derivatives, and not solely t-butyl derivatives as in the other cases where nitrate esters were detected. The relative stability of trityldifluoramine toward oxidative cleavage is fully in accord with known differences between aromatic and aliphatic systems.

The appearance of silicon tetrafluoride during an investigation of organic fluorine compounds in glass equipment is generally understood to imply the transient formation of hydrogen fluoride; this interpretation should be applied here. An interesting point, not yet fully understood, is the appearance of nitroalkane and carbinol only in the reaction of trityldifluoramine with excess acid.

In general, the results observed are best understood as the consequences of electrophilic attack on the alkyldifluoramines. The fact that such attack did not occur when trityldifluoramine was treated with hydrochloric acid, an even stronger electrophile, tends to cloud this simple picture. It becomes necessary to invoke the simultaneous participation of an oxidative process in some way which is not yet clear.

Assuming that protonation of the alkyldifluoramine does occur, elimination of difluoramine and formation of a tertiary carbonium ion would logically follow.

$$R_3CNF_2 + H^+ \longrightarrow R_3\overset{+}{C}NF_2H \qquad (9)$$

$$R_3\overset{+}{C}NF_2H \longrightarrow R_3C^+ + HNF_2 \qquad (10)$$

The failure of difluoramine to appear among the final products is not particularly surprising. In the presence of nitric acid and/or nitrogen oxides, it might easily be oxidized and may well constitute the source of the silicon tetrafluoride. The formation of a carbonium ion from trityldifluoramine would be favored by resonance stabilization. In the t-butyl case, on the other hand, this driving force is not present and formation of the ion would be expected to occur less readily. In addition, both the t-butyl carbonium ion and the difluorammonium ion from which it is derived would be more subject to a variety of side reactions than the corresponding trityl species.

Reaction of the carbonium ion with water or with nitrate ion would produce the carbinol and the ester, respectively. Alternatively, the carbinol might be

$$R_3C^+ + H_2O \longrightarrow R_3COH + H^+ \qquad (11)$$

$$R_3C^+ + NO_3^- \longrightarrow R_3CONO_2 \qquad (12)$$

$$R_3COH + HNO_3 \longrightarrow R_3CONO_2 + H_2O \qquad (13)$$

esterified by nitric acid. For the reasons cited above these reactions contributed substantially to the overall result only in the trityldifluoramine reactions.

Experimental

Materials - The phenyllithium and n-butyllithium used in this work were commercial products supplied by Foote Mineral Company in ether-benzene and hexane solutions, respectively. Trityldifluoramine was obtained from Pennisular Chem Research and purified by recrystallization from methanol, m.p. 80-81.5° (uncorr.). t-Butyldifluoramine was prepared by the method of Smith and Castellano[4d] and stored under prepurified nitrogen. The quantity desired for each experiment was distilled from the storage bulb under vacuum and was measured by volume as a gas, assuming ideality. It was condensed directly into the reaction flask from the vacuum line.

Reaction of t-Butyldifluoramine with Phenyllithium

t-Butyldifluoramine (0.55 g., 0.005 mole) was dissolved in 10 ml. of sodium-dried ether and the solution was cooled to 0-5°. In a dropping funnel under nitrogen, 2.5 ml. (0.005 mole) of phenyllithium solution in benzene-ether (Lithium Corporation of America) was diluted with dry ether to 10 ml. This solution was added to the stirred difluoramine solution during one hour. A red-brown color appeared and deepened gradually during the addition. A gentle stream of nitrogen was passed through the reaction flask and then bubbled into a standardized solution containing 5.27 meq. of acid, while 20 ml. of distilled water was added dropwise to the reaction mixture (20 min.). Stirring was continued for one hour. The acid solution was titrated with base and 5.19 meq. was found. The decrease (1.5%) was not considered to be significant. The aqueous and organic phases of the reaction mixture were separated. The water layer was washed with 15 ml. of ether. The wash and the organic layer were combined and washed with three 10 ml. portions of distilled water. These washes were combined with the aqueous solution, which was subjected to analyses as discussed above.

The ether-benzene solution was dried first over Drierite and then over anhydrous sodium sulfate and distilled at atmospheric pressure. The flask was heated in a bath at 55-60° throughout distillation of the bulk of the solvents and raised to 95-100° for 20 min. at the end. A brown tarry residue weighing 1.10 g. remained. The distillate was collected at Dry Ice temperature to avoid the loss of unreacted t-butyldifluoramine or low-boiling products. The mass spectrum of the "non-volatile" fraction contained peaks at 33(NF), 41 (C_3H_5), 45 (CNF), and 57 (C_4H_9) mass units. The trace of ether observed (m/e = 59) was not sufficient to account for the intensity of the peak at 57, to be attributed to t-butyldifluoramine. The most probable source of these fragments is the substitutes hydrazine (V).

The several components of the less volatile fraction were separated by vapor phase chromatography, using a Perkin-Elmer Model 154 C instrument. The six-foot column was packed with di-n-decyl phthalate on firebrick and was maintained at 90° with a helium flow rate of 53 ml/min. Since fractions were expected to be too small to be collected individually, the effluent stream was fed directly into the inlet of a Bendix time-of-flight mass spectrometer. In one fraction mass peaks at 57 (C_4H_9), 71 (C_4H_9N), and 85 ($C_4H_9N_2$) units were observed, in relative intensities identical to those found in azoisobutane IV. Reaction of t-Butyldifluoramine with n-Butyllithium.

A solution of 1.1 g. (0.01 mole) t-butyldifluoramine in 10 ml. hexane was treated with 26.0 ml. (0.04 mole) of n-butyllithium solution, by adding the

organometallic reagent dropwise over a one hour period at 5-10°. The dark brown mixture was stirred for 2.5 hrs at 10-25° and then treated with water. The organic solution was separated and dried over anhydrous Na_2SO_4 while the aqueous solution was analyzed and found to contain 0.197 g. (0.0104 mole, 52.0%) of fluoride ion. The solvent was evaporated from the organic solution and the residual brown oil was distilled to yield 0.32 g. of a liquid, b.p. 79-82°/0.3 min. On the basis of infrared and spectral data, the liquid product was identified as N, N, di-n-butyl-t-butylamine.

Reaction of Trityldifluoramine with n-Butyllithium

A solution of 5.9 g. (0.02 mole) of trityldifluoramine, m.p. 80-81°C, in 40 ml. of hexane was cooled to 0° in a 200 ml. three-neck flask while 25.8 ml. (0.04 mole) of n-butyllithium solution was added dropwise with stirring over a 1.5 hr. period. A deep red color developed as the butyllithium came into contact with the hexane solution, but the color changed to a bright yellow on continued stirring at 5-10°. At the completion of the addition, the solution was allowed to come to room temperature and it was stirred at 25° for 2 hr. Water was then added to the mixture, the organic phase was separated, washed with water and dried over anhydrous Na_2SO_4. The solvent was evaporated, leaving 5.72 g. of brown semi-solid. The material was kept under 0.5 mm pressure for 1 hr., a liquid nitrogen trap being employed to collect any liquid distillate. A liquid (0.3 g.) was obtained and submitted for infrared analysis. It showed very strong absorptions indicative of O-H, aliphatic C-H, C-CH_3, C-OH and -$(CH_2)_n$>4. In addition, a medium strength band at 1710 cm^{-1} (C=O) was also present.

The residue was recrystallized from MeOH to yield 2.15 g. (42%) of yellow crystals, m.p. 112-113°, which were identified by infrared and elemental analysis as N-phenylimidobenzophenone (benzophenone anil).

Anal. Calcd. for $C_{19}H_{15}N$: C, 88.68; H, 5.88; N, 5.44.

Found : C, 88.85; H, 5.86; N, 5.61.

The physical constants are in excellent agreement with the literature (m.p. 113-114° [11]).

The methanol solution from the recrystallization was evaporated to dryness to yield 3.3 g. of a mixture of trityldifluoramine and N-phenylimidobenzophenone. In addition, the infrared spectrum of this material showed weak absorptions due to aliphatic C-H, C=O and C-N or C=C.

A solution of 1.48 g. (0.005 mole) of trityldifluoramine in 30 ml. hexane was treated with 6.5 ml. (0.01 mole) of n-butyllithium solution as in Section 1. Water was added to the reaction mixture and the organic phase was separated and washed with four 100-ml portions of distilled water. The combined aqueous washings were transferred to a 500 ml. volumetric flask and adjusted to volume with distilled water. This solution was found to contain 146 mg. F^- (0.0077 mole, 77%) and 0.0028 mole OH^-.

11. Weston and Michaels, J. Am. Chem. Soc., 73, 1381 (1951).

The hexane solution was dried over Na_2SO_4 and the solvent evaporated. The residue was taken up in CH_2Cl_2 and chromatographed on alumina. The chromatogram was followed by the yellow band which moved down the column. This yellow CH_2Cl_2 eluate was evaporated to dryness and the residue was recrystallized from ether to yield 0.92 g. (0.0036 mole, 72%) benzophenone anil, m.p. 112-113°. The column was eluted with MeOH and the solvent was evaporated to give 0.13 g. of brown solid. The infrared spectrum of this material showed strong absorptions indicative of aliphatic C-H, aromatic C-H, C=N or C=O (1660 cm^{-1}), a trace of N-F, and substituted aromatic.

t-Butyldifluoramine and Nitric Acid

1. t-Butyldifluoramine (1.02 g., 9.3 mmoles) was condensed under vacuum into a flask containing 10 ml. (150 mmoles) of concentrated HNO_3. The mixture was warmed to room temperature and stirred. The pressure rose to 210-220 mm. and remained constant for 16 hr. After this period, the pressure rose within 1-1/2 hr. to 730 mm., with the evolution of brown gas. On cooling the reaction flask to -70°, the pressure dropped to 340 mm. A sample of this gas was subjected to infrared analysis and found to contain C-H (3.33/6.75μ), $C-CH_3$ (7.27μ), N_2O (4.5μ), N_2O_4 (5.72/6.15μ), N-F(attributed to starting material, 10.30/11.35μ), NO_3F (10.85/12.65/13.90μ), CO_2 (4.35/15.96μ), SiF_4 (9.75μ), and NOCl (presumably from attack on NaCl window, 5.53/5.58μ). Mass spectrometric analysis confirmed the presence of starting difluoramine, CO_2 and/or N_2O, SiF_4, and NO_3F, and established the absence of H_2 and O_2. A second gas sample taken at 0° was found to contain some of these components, but no additional products. The acid solution was extracted with pentane to remove organic products. Infrared analysis of this extract revealed the presence of alkyl nitrite and nitrate (C-H at 3.51/6.90μ, possible $C-CH_3$ at 7.28μ, C-ONO at 6.41μ, and $C-ONO_2$ at 6.10μ).

2. Concentrated nitric acid (0.67 ml., 10.0 mmoles) was delivered by pipet into a 50 ml. round-bottomed flask, which was fitted with a magnetic stirring bar and a suitable adapter, and attached to a vacuum line. The acid was frozen in a liquid N_2 bath and the flask was evacuated. The acid was melted and refrozen twice, with evacuation to effect degassification. t-Butyldifluoramine (1.09 g., 10.0 mmoles) was evaporated into an evacuated calibrated storage bulb to the calculated pressure and then condensed into the flask with liquid N_2. The reactor portion of the line (with manometer) was closed off, and the flask was allowed to warm to room temperature. The mixture was stirred at 26-29° for 24 hr., during which the pressure remained essentially constant (186-198 mm. Hg). The liquid mixture became yellow, but no brown fumes appeared in the vapor space.

Gas samples for infrared and mass spectral analyses were taken, with the reaction flask at 25° and -78°. Both samples contained an alkyl nitrate, N_2O, t-butyldifluoramine and some additional N-F material, and a trace of NO_3F.

The liquid reaction mixture was extracted with CCl_4. Infrared analysis of the extract did not indicate any additional products. The aqueous residue was evaporated to dryness at room temperature and a few needle crystals were recovered. The infrared spectrum of this solid showed only absorptions due to water. Attempts to dehydrate the small amount of product which remained were unsuccessful.

Trityldifluoramine and Nitric Acid

1. Recrystallized trityldifluoramine (1.0 g., 3.4 mmoles, m.p. 80-81.5°) and a small magnetic stirring bar were placed in the bottom of a reaction tube having a small side chamber. Concentrated (70%) nitric acid (2.5 ml., 38 mmoles) was placed in the side chamber and the tube was connected to a vacuum line by means of standard taper joints. The nitric acid was frozen by immersion in a liquid nitrogen bath and the system was evacuated. The cold bath was removed. Then the tube was rotated so that the nitric acid, as it melted, flowed onto the trityldifluoramine.

The resulting slurry was stirred at 22-25° for 24 hr. The reaction mixture bubbled and became progressively darker and brown fumes were observed in the vapor space. The pressure rose exponentially to reach a maximum of approximately 400 mm. in 2.5 hr. (system volume - 180 ml.) and then remained constant.

After 24 hr., the reaction mixture was cooled to -78°, and a gas sample was taken for analysis, Infrared and mass spectrometric examination revealed the presence of NO_2, N_2O, SiF_4, and either NOCl or NO_2F.

The reaction tube was then warmed to room temperature, flushed with nitrogen, and opened. The reaction mixture was diluted with distilled water (color changed from dark brown to bright orange) and the solid product was removed by filtration. The filtrate was neutralized with Na_2CO_3 (color changed from pale amber to brown) and extracted with benzene. No residue was obtained upon evaporation of an aliquot of the benzene extract. Reacidification of the aqueous layer lightened the color, but not to the original shade. The remaining color was too intense to permit the determination of fluoride ion.

The orange solid product was washed with water, dried in vacuum over P_2O_5, and chromatographed on an alkaline alumina column. The first fraction, 420 mg., yellow to pale orange crystals eluted with pentane-benzene, proved to be the principal constituent of the mixture. It was recrystallized from pentane-benzene to give a nearly colorless compound, m.p. 162.5-163°. Its infrared spectrum was identical with that of triphenylcarbinol (lit.[12] m.p. 162.5°).

Anal. Calcd. for $C_{19}H_{16}O$: C, 87.66; H, 6.20.

Found : C, 87.06/87.21; H, 6.29/6.41.

2. Trityldifluoramine (2.95 g., 10 mmoles) was placed, along with a small magnetic stirring bar, in a test tube having a standard taper glass joint. The tube was flushed with dry nitrogen and placed in a liquid nitrogen bath. Concentrated HNO_3 (0.67 ml., 10 mmoles) was introduced slowly and allowed to freeze on the side of the tube without contacting the trityldifluoramine. The reaction tube was then connected via a suitable adapter to a vacuum system, evacuated, and allowed to warm to room temperature. After the mixture was stirred for 18 hr. at 25-28°, a sample of the gaseous products (p = 55 mm. in 180 ml.) was taken in an evacuated cell. The system was then filled with nitrogen to atmospheric pressure. The reaction mixture was diluted with distilled water and the yellow insoluble product was removed by filtration. The yellow aqueous filtrate was extracted three times with methylene chloride, the third extract contained very little color, although the

12. N. A. Lange, Handbook of Chemistry

aqueous solution remained a strong yellow. On standing, the combined extracts became orange in color, as did the solid product on the filter.

Infrared analyses of the gas sample and the methylene chloride extract (differential vs. solvent) showed no significant absorptions. The aqueous solution was found to contain 7.41 meq. of free acid and 25 mg. (1.3 meq.) of fluoride ion. The infrared absorption spectrum of the bright yellow-orange solid (m.p. 79-81°) was superimposable upon that of trityldifluoramine.

Acknowledgement - The authors wish to thank Dr. Murray S. Cohen of these laboratories for his interest and encouragement during the course of this work. Analytical assistance by Alan Fremmer, John Creatura, Raymond Storey and Donald Y. Yee is gratefully acknowledged.

The Formation of N-Isopropylidene-N-fluoro-N-methylammonium Ion from t-Butyldifluoramine

K. Baum

Chemical Products Division
Aerojet-General Corporation
Von Karman Center
Azusa, California

The reaction of triphenylmethyldifluoramine with concentrated sulfuric acid has been reported by Graham and Parker[1] to give difluoramine and triphenylmethyl cation.

$$(C_6H_5)_3CNF_2 \xrightarrow{H_2SO_4} (C_6H_5)_3C^{\oplus} + HNF_2$$

Thus, the difluoramino entity functions as a leaving group under the driving force of the formation of the highly stable trityl cation. It was of interest to determine whether this type of cleavage would occur in the reaction of acids with another difluoramine derivative that is not capable of producing such a highly stabilized carbonium ion. The compound might be inert or it might undergo an alternative mode of degradation.

Reactions of t-butyldifluoramine with acids were studied in the present work. The synthesis of this compound has been reported by Petry and Freeman[2] by the reaction of azoisobutane with tetrafluorohydrazine:

$$(CH_3)_3C\text{-}N{=}N\text{-}C(CH_3)_3 \xrightarrow{N_2F_4} (CH_3)_3CNF_2 + N_2$$

The reaction of t-butyldifluoramine with concentrated sulfuric acid was first examined by introducing a sample of this N-F compound into an evacuated glass bulb containing sulfuric acid. The pressure in the bulb began to decrease immediately, and was reduced to 8% of the molar theoretical value in four hours and to 5% in two days. The infrared spectrum of the remaining gas showed that it was mainly silicon tetrafluoride, and that no difluoramine was present. Thus, this reaction is not analogous to that of trityldifluoramine with sulfuric acid. A product soluble in sulfuric acid was formed.

The nature of this product was examined by nuclear magnetic resonance spectroscopy. A fresh solution was prepared by shaking a mixture of t-butyldifluoramine and sulfuric acid in a stoppered test tube. A clear solution was formed in about ten minutes. The proton NMR spectrum[3] at 60 m.c. consisted of a doublet at 4.09 p.p.m. with a coupling constant of 18.7 c.p.s., a complex multiplet at 156 c.p.s. and a small singlet at 2.90 p.p.m. which increased with time. The position of the singlet was identical with that of a solution of acetone in sulfuric acid, indicating that acetone was a decomposition product of the initial product.

The 56.4 m.c. F^{19} NMR spectrum of the sulfuric acid solution was recorded using trifluoroacetic acid as an external standard. The spectrum consisted of a partially resolved quartet at -141.57 p.p.m. with splitting of approximately 15 c.p.s., and a singlet at -116.8 p.p.m. The latter resonance was assigned to HF; its position was identical to that of a solution of HF in sulfuric acid.

The observed NMR peaks are those which would be expected for the N-fluoro-N-methyl-isopropylidenimmonium ion, a species having carbonium and immonium resonance contributions.

Thus, the F^{19} spectrum indicates coupling of a fluorine to three protons. The proton doublet at 4.09 p.p.m. is assigned to the N-methyl group and the 156 c.p.s. peak, to the C-methyls.

The formation of the N-fluoro-N-methylisopropylidenimmonium ion can be rationized as a nucleophilic methyl migration with fluoride leaving:

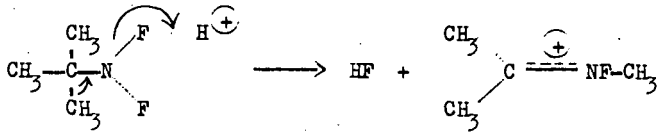

This rearrangement was also affected by a Lewis acid. When a mixture of boron trifluoride and nitrogen was bubbled through a solution of t-butyldifluoramine in pentane at -78°, a white solid precipitated. This solid was filtered under nitrogen and was dried under vacuum to give a 60% yield of N-fluoro-N-methylisopropylidenimmonium fluoborate.

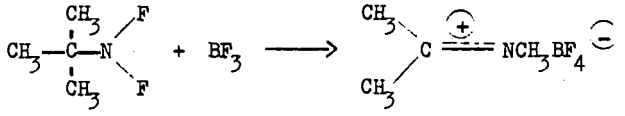

This salt was extremely hygroscopic, but a satisfactory elemental analysis was obtained on a sample that was handled in a dry box.

Anal. Calc'd for $C_4H_9NF_5B$: C, 27.1; H, 5.08; N, 7.91; F, 53.6.

Found: C, 26.9; H, 5.22; N, 7.80; F, 51.9.

The reaction of t-butyldifluoramine with boron trifluoride also took place in the absence of solvent at -78°, and in liquid sulfur dioxide at its boiling point.

The proton NMR spectrum of the fluoborate was obtained using concentrated sulfuric acid as the solvent. The resulting spectrum was identical to that of the solution that was prepared by treating t-butyldifluoramine with concentrated sulfuric acid. The F^{19} NMR spectrum of this solution consisted of a quartet at -141.5 p.p.m., with a coupling constant of 18.5 c.p.s., and singlets at -116.9 p.p.m. and +67.5 p.p.m. The position of the quartet is within experimental error of that of the sulfuric acid catalyzed rearrangement product of t-butyldifluoramine. The latter two peaks were also found in the F^{19} spectrum of a solution prepared by adding commercial aqueous fluoboric acid to concentrated sulfuric acid. The -116.9 p.p.m. band corresponds to HF but the +67.5 p.p.m. band is shifted somewhat from that of a solution of BF_3 in sulfuric acid (+65.82 p.p.m.). The equilibrium of HBF_4 with HF and BF_3 is well known in aqueous solutions.[4]

Although the fluoborate was very hygroscopic and decomposed rapidly when it was exposed to the atmosphere, it did not change under prolonged storage under dry nitrogen at room temperature. The addition of the salt to water gave acetone, which was isolated as its 2,4-dinitrophenylhydrazone.

$$(CH_3)_2C \overset{\oplus}{=\!=} NFCH_3\ BF_4^{\ominus} \xrightarrow{H_2O} (CH_3)_2CO$$

The different paths followed by the reactions of trityldifluoramine and t-butyldifluoramine with acids, C-N cleavage for the former and N-F cleavage with rearrangement for the latter, are paralleled by the reactions of the corresponding azides with sulfuric acid. Thus, trityl azide in concentrated sulfuric acid exists in equilibrium with the trityl cation and hydrazoic acid.[5]

$$(C_6H_5)_3CN_3 \underset{}{\overset{H_2SO_4}{\rightleftharpoons}} (C_6H_5)_3C^{\oplus} + HN_3$$

Tertiary alkyl azides, on the other hand, rearrange to the corresponding Schiff bases.[6]

$$R_3CN_3 \xrightarrow{H_2SO_4} \left[R_2C{=}N{-}H\right] \xrightarrow{H_2O} R_2CO + RNH_2$$

The N-fluoro-N-methylisopropylidenimmonium salts are the first members of a new class of compounds potentially useful in organic synthesis. The generality of the rearrangement of alkyldifluoramines catalyzed by Lewis or protonic acids is being investigated.

Acknowledgement

This work was financed by the Advanced Research Projects Agency and monitored by the Office of Naval Research. The author is indebted to Dr. H. N. Nelson for the N.M.R. analysis, to Mr. K. Inouye for the elemental analysis and to Mr. F. J. Gerhart for assistance in the synthesis work.

References

1. W. H. Graham and C. O. Parker, J. Org. Chem., 28, 850 (1963).

2. R. C. Petry and J. P. Freeman, J. Am. Chem. Soc., 83, 3912 (1961).

3. Tetramethylammonium chloride was used as an internal reference. The signal positions are given in p.p.m. or c.p.s. downfield from tetramethylsilane based on a difference of 3.10 p.p.m. between tetramethylammonium ion and tetramethylsilane in 96% H_3PO_4. (N. C. Deno, H. G. Richey, Jr., N. Friedman, J. D. Hodge, J. J. Houser, and C. U. Pittman, Jr., J. Am. Chem. Soc., 85, 2991 (1963).

4. A. V. Topchiev, S. V. Savgorodnii and Y. M. Panshkin, "Boron Fluoride and its Compounds as Catalysts in Organic Chemistry," Pergamon Press, 1959 p. 56.

5. M. M. Coombs, J. Chem. Soc., 1958, 4200.

6. C. Schuerch and E. H. Huntress, J. Am. Chem. Soc., 71, 2238 (1949); German Patent 583,565 (1935).

HYDROLYSIS OF THE NITROGEN FLUORIDES

Gerald L Hurst and S. I. Khayat

THE HARSHAW CHEMICAL COMPANY
1945 East 97th Street
Cleveland 6, Ohio

BASIC HYDROLYSIS OF NF_3

Nitrogen trifluoride is extremely resistant to chemical attack by water and aqueous acid; the compound can be recovered quantitatively after one week in contact with excess dilute acid (HNO_3, H_2SO_4, $HClO_4$) or pure water at 133°C. In the presence of aqueous base, however, slow hydrolysis occurs at 100°C yielding nitrite and fluoride.

$$NF_3 + 4\ OH^- \xrightarrow{100°C} NO_2^- + 3F^- + 2H_2O \qquad \text{I}$$

This behavior differs sharply from that of nitrogen trichloride, which is known to give ammonia and hypochlorite under similar conditions. The latter products are readily explained in terms of nucleophilic attack directed at the chlorine atoms, a mechanism which appears reasonable in view of the fact that the electronegativities of N and Cl are very nearly the same and that the halogen may easily expand its valence shell. Obviously, these considerations cannot be applied to the nitrogen trifluoride molecule since fluorine is considerably more electronegative than nitrogen and it has no available d orbitals. Although the nitrogen atom also has no free orbitals, the relatively low electron density would at least offer less resistance to the approach of a nucleophile

$$HO:^- \rightarrow N(F)(F)(F) \xrightarrow[H_2O]{\text{Slow}} HONF_2 + F^- \xrightarrow[\text{Fast}]{-HF} NOF \xrightarrow[\text{Fast}]{OH^-} NO_2^- \qquad \text{II}$$

The proposed intermediate $HONF_2$ would be expected to be unstable with respect to the loss of HF, as is apparently the case with the unknown perfluoro alcohols.[1]

Two other reaction modes worth considering include the formation of an intermediate activated complex with water

$$NF_3(aq.) \xrightarrow{\text{Slow}} NF_3^{\ddagger}(aq.) \xrightarrow[\text{Fast}]{OH^-} \text{Products} \qquad \text{III}$$

and the intriguing but unlikely reversible ionization of NF_3.

$$NF_3(aq.) \underset{}{\overset{\text{Slow}}{\rightleftharpoons}} NF_2^+(aq.) + F^-(aq.) \xrightarrow[\text{Fast}]{OH^-} \text{Products} \qquad \text{IV}$$

or

$$NF_3(aq.) \underset{\text{Fast}}{\rightleftharpoons} NF_2^+(aq.) + F^-(aq.) \xrightarrow[\text{Slow}]{OH^-} \text{Products} \qquad \text{V}$$

Preliminary experiments indicated that the rate of reaction of gaseous NF_3 with caustic soda solution in a static system was first order with respect to NF_3 with little dependence on the initial concentration of the base. Although these observations are apparently consistent with the first order equations III and IV more detailed studies show that these results are misleading.

If the reactions were first order in NF_3 only, the rate of decrease of the partial pressure (P) of NF_3 with time (T) in a closed system should be given by the following equations

$$\frac{dP}{dT} = \frac{KV_c}{V_o} P$$

$$\frac{V_o}{V_c} \log \frac{P_o}{P} = K T$$

where V_o is the volume available to gaseous NF_3, V_c is the volume of the caustic soda solution and P_o is the initial pressure of NF_3. The assumption is made that a Henry's law equilibrium is established between gaseous and dissolved NF_3.

In Fig. 1 the results of a number of experiments are shown plotted according to the integrated form of the rate equation. The points of line "B" and group "A" were calculated from data furnished by H. J. Bronaugh. The line "B" was obtained from a series of experiments in which samples of NF_3 (4.83-7.16 mmole) at a constant initial pressure of one atmosphere were allowed to react with 20 ml of 0.5 N NaOH for varying lengths of time. The curvature of the line clearly suggested that the steadily decreasing hydroxyl ion concentration (up to 90% neutralization) does indeed tend to decrease the reaction rate, but the effect is much less than would be expected for the 2nd order equation

$$NF_3 + OH^- \rightarrow \text{Products} \qquad \text{VI}$$

The group of points "A" was derived from reactions involving samples of NF_3 at initial pressures ranging from 0.25 to 2 atmospheres (1.7-8.7 mmole) and 30 ml of 0.5 NaOH. The positions of the top four points of this group, which were obtained from simultaneous runs, again indicate that the extent of conversion of NF_3 depends on the concentration of OH^-. Thus the height of the individual points decreases inversely with the corresponding degree of neutralization of the caustic soda. More important, however, is the fact that group "A" lies well below "B" showing that the reactions involving 20 ml of base were more than 2/3 as fast as those with 30 ml. Since the

REACTION OF NF_3 WITH NaOH SOLUTION AT 100° C.

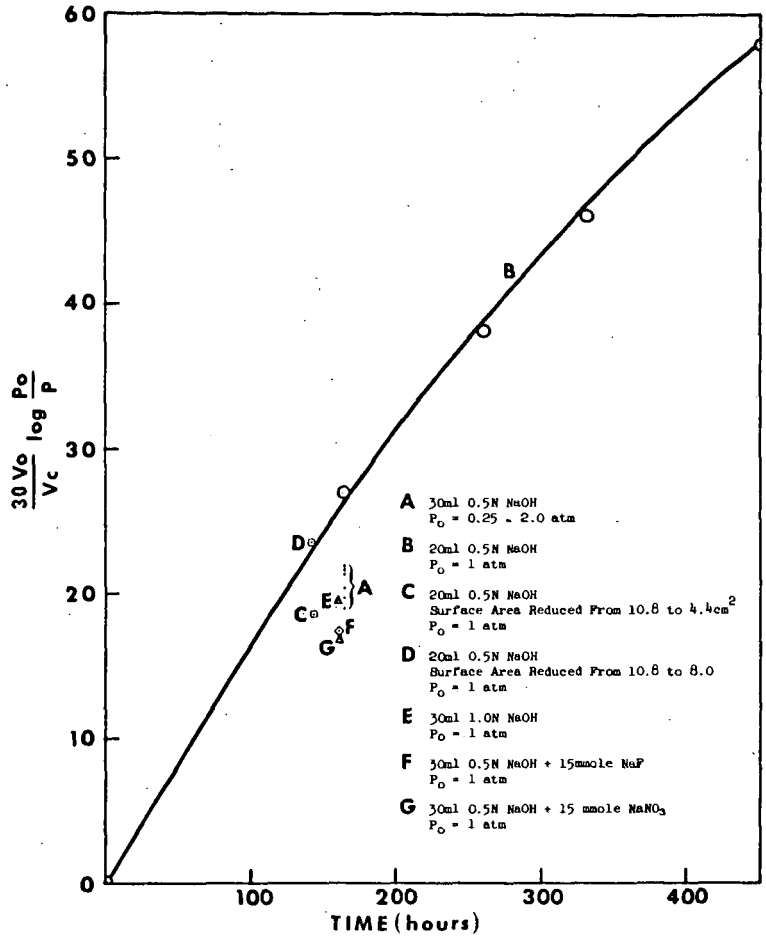

FIG. 1

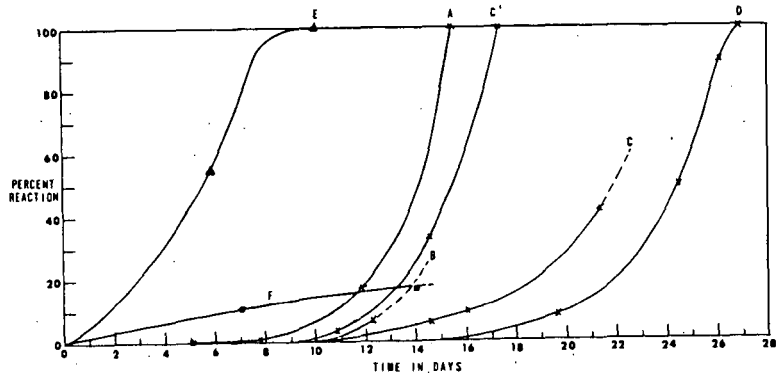

A) N_2F_4 (9.01 mmole/100ml) + H_2O (5ml)
B) N_2F_4 (6.82 mmole/100ml) + H_2O (5ml)
C, C') N_2F_4 (4.58 mmole/100ml) + H_2O (5ml)
D) N_2F_4 (2.27 mmole/100ml) + H_2O (5ml)
E) N_2F_4 (4.56 mmole/100ml) + 10% NO + H_2O (5ml)
F) N_2F_4 (2.27 mmole/100ml) + NaOH (2N) (5ml)

FIGURE 2 - HYDROLYSIS OF N_2F_4 AT 60°C

solutions were contained in upright "Teflon" cups of identical diameter in each case, the data indicate that the rate of conversion of NF_3 was significantly influenced by the available surface area. Presumably, the NF_3 failed to reach an equilibrium concentration in solution in spite of the long reaction times. The dependence of the reaction rate on the area of the gas-liquid interface was confirmed in the experiment represented by points "D" and "C" in which the surface areas of the solutions (20 ml 0.5 N NaOH) were reduced from 10.8 cm^2 to 8.0 and 4.4 cm^2 respectively.

The apparently small effect of the initial OH^- concentration on the rate of hydrolysis of NF_3 is probably due not only to the surface area phenomenon described above, but also to a reduction in the solubility of the gas resulting from increased ionic strength. The proposed "salting-out" effect is demonstrated in the experiments represented by points "E", "F" and "G". In "E", 1.0 N NaOH (30 cc) was used in place of the 0.5 N caustic soda employed by H. J. Bronaugh for group "A", yet the extent of reaction was approximately the same. Half normal NaOH was also used in "F" and "G" but the total ionic strength of the solutions was increased to the equivalent of 1.0 N NaOH by the addition of NaF and $NaNO_3$ respectively. In each of the latter experiments the reaction rate was significantly lowered, indicating that inhibition due to rising ionic strength tends to partly offset the acceleration associated with increasing OH^- concentration. In this connection it should be noted that concentrated NaOH (12 N) reacts extremely slowly with NF_3.

It is of interest that the rate of basic hydrolysis is decreased to exactly the same extent (within the experimental accuracy) by equivalent amounts of NaF or $NaNO_3$. If the reaction involved mechanism V, NaF would be expected to act as an inhibitor by shifting the equilibrium to the left. Thus it appears that the reaction proceeds via the nucleophilic mechanism given in equation II.

REACTION OF NF_3 WITH AQUEOUS HCl

Additional support for the proposed nucleophilic mechanism of the basic hydrolysis has been provided by a study of other aqueous systems such as hydrochloric acid. Although NF_3 is unaffected by prolonged contact with either pure HCl or pure water at 133°C, the compound reacts slowly with aqueous HCl at this temperature, yielding products which vary with the concentration of the acid. Nitric oxide and nitric acid are formed by the dilute solution (0.5 N)

$$3NF_3 + 6H_2O \xrightarrow[133°C]{\text{Dil. HCl}} 3HNO_2 + 9HF \xrightarrow{H^+} 2NO + NO_3 + H_2O \qquad \text{VII}$$

while the more highly concentrated reagent (4 N) yields elementary nitrogen and chlorine.

$$2NF_3 + 6HCl \xrightarrow[133°C]{H_2O} N_2 + 3Cl_2 + 6HF \qquad \text{VIII}$$

As in the case of the basic hydrolysis the rate of conversion of NF_3 was found to vary only slightly with the strength of the solution. The fact that NF_3 reacts with aqueous HCl but not with the pure compound clearly suggests that ionic attack is involved. The active species in the reaction is almost undoubtedly Cl^- since it has been shown that while NF_3 is inert to many acids, it reacts readily with hot, neutral sodium chloride solution (4 N).

$$NF_3 \xrightarrow[H_2O]{NaCl} N_2,\ NO_3^-,\ F^-,\ Cl_2 \qquad \text{IX}$$

REACTION OF NF_3 WITH AQUEOUS NUCLEOPHILES

Further indirect evidence for the postulated nucleophilic behavior of Cl^- and OH^- has been obtained from a series of experiments in which NF_3 was allowed to react with solutions containing anions of varying nucleophilic strength. It was found that for those species tested the extent of reaction within a given time and temperature range increased monotonically with the accepted value[2] of the nucleophilicity of the anion. Furthermore, although NF_3 did not react with acid solutions of weak nucleophiles, the reaction rate with halides was increased by the presence of hydronium ion, as would be expected for an S_n2 mechanism involving the loss of fluoride

$$F_2N\text{-}F + H_3O^+ \rightleftharpoons F_2N\text{-}FH^+ + H_2O \qquad \text{X}$$

$$X:^- + F_2N\text{-}FH^+ \rightarrow XNF_2 + HF \rightarrow \cdots$$

The results of a number of experiments involving nucleophilic reagents are listed in Table I. In the strictest sense it is not possible to compare the relative degrees of reaction solely on the basis of the nucleophilicity of the starting material because reactive intermediates may influence the overall conversion rate. The varying stoichiometries also impose restrictions for those experiments which involve small quantities of aqueous reagent and are thus subject to unequal changes in concentration for a given amount of NF_3 reacted. In spite of these limitations the data clearly indicate that the reaction rates increase with nucleophilic strength in the order

$$NO_3^-,\ ClO_4^-,\ SO_4^= << Cl^- < Br^- < OH^- < I^- < S_2O_3^=$$

REACTIONS OF NF_3 WITH ELECTROPHILES

In his early work on NF_3 Ruff[3] reported that the compound was stable to $AlCl_3$ at red heat. Investigations in this laboratory show that NF_3 does react with $AlCl_3$ under mild conditions (80°C, 4 days) to produce nitrogen and chlorine. Chlorine is liberated rapidly at 135°C. The reaction presumably involves coordination of a fluorine atom of NF_3 to the vacant orbital of the aluminum atom, as is believed to be the case with the chlorination of fluorocarbons by $AlCl_3$. Reactions conducted in a Teflon IR cell gave no evidence for the formation of gaseous intermediates such as NF_2Cl.

TABLE I - REACTIONS OF NF_3 WITH NUCLEOPHILES IN AQUEOUS SOLUTION

Reagent	Molarity Volume (ml)	Temp. (°C)	Reaction Time (hrs)	Initial NF_3 (mmole)	P_o NF_3 At Reaction Temp.(atm)	NF_3 Reacted (%)	Product (mmoles)
$HClO_4$	0.5-20	133	159	2.14	0.585	1.0	-
HNO_3	0.5-20	133	159	2.10	0.574	1.0	-
H_2SO_4	0.5-20	133	159	3.34	0.99	1.0	-
H_2SO_4	4 -20	133	159	3.52	1.02	1.0	-
HCl	0.5-20	133	235	3.00	1.00	54.4	NO 0.73; NO_2^- 0.12; NO_3^- 0.81; F^- 4.74
HCl	4 -20	133	235	3.16	1.02	63.6	N_2 1.06; Cl_2 2.75; F^- 5.38
HCl	0.5-20	133	159	2.14	0.636	13.5	Cl_2 0.12
NaCl	4 -20	133	306	4.37	1.047	24.7	N_2 0.33; NO_3^- 0.42
HBr	0.5-20	133	159	1.98	0.633	67.7	N_2 0.31; N_2O .06; Br_2 2.44; F^- 3.84
NaCl	0.5-30	100	160	2.97	0.936	1.0	-
HCl	0.5-30	100	160	2.98	0.939	1.0	N_2; Cl_2
NaBr	0.5-30	100	160	3.07	0.957	14.0	NH_4^+ 0.44; F^- 1.37
HBr	0.5-30	100	160	3.01	0.938	22.6	N_2 0.1; NH_4^+ 0.33; F^- 1.74, Br_2 0.94
NaOH ✱	0.5-30	100	160	3.01	0.939	38.2	NO_2^- 1.15; F^- 3.35
NaI	0.5-30	100	160	2.97	0.91	50.8	N_2 0.50; N_2O 0.05; NH_4^+ 0.72; F^- 4.84
HI	0.5-30	100	160	3.15	0.952	71.8	NH_4^+ 2.11; I_2 5.05
$Na_2S_2O_3$	0.5-30	100	160	2.79	0.837	61.3	S 5.1; F^- 3.75; NH_4^+ 1.50

✱ NaOH reaction data were calculated.

Nitrogen trifluoride is readily converted to ammonium ion by acidic or neutral ferrous sulfate solution at 60°C.

$$4H^+ + 6Fe^{+2} + NF_3 \rightarrow NH_4^+ + 3F^- + 6Fe^{+3} \qquad \text{XI}$$

In a typical experiment NF_3 (3.18 mmole, P_o = 0.69 atm) was maintaind in contact with the aqueous salt (20 ml, 0.5 N) for 12 days, resulting in the destruction of about 44 per cent of the NF_3.

Ferric chloride solutions react very slowly with NF_3 at 100°C; the $FeCl_3$ acts as a hydrolysis catalyst, yielding nitric oxide and nitrate. This catalysis is not a general property of the transition metal ions as shown by the total inertness of NF_3 to solutions of $CoCl_2$, $MnSO_4$, $CuSO_4$ and $NiSO_4$ at 100°C over periods up to seven days.

HYDROLYSIS OF N_2F_4

Dinitrogen tetrafluoride reacts more readily than NF_3 with aqueous solutions; at 133°C it is rapidly destroyed by contact with acidic, basic and neutral solutions. The reaction with caustic soda produces mainly nitrous oxide and nitrite along with a trace of nitrogen.

$$N_2F_4 + 4OH^- \xrightarrow{133°C} 2NO + 4F^- + 2H_2O$$

$$4NO + 2OH^- \xrightarrow{133°C} N_2O + 2NO_2^- + H_2O \qquad \text{XII}$$

With water and aqueous HCl significant quantities of nitrogen and nitrate are formed in addition to nitric oxide. Surprisingly, the amount of nitrogen produced was found to be greater with water than with 4 N HCl, and in neither instance was as much N_2 formed as in the corresponding reaction of NF_3 with 4 N HCl. At lower temperatures (60-100°C) N_2F_4 is nearly quantitatively converted to NO by water and dilute HCl (0.5 N).

The results of a number of experiments on the kinetics of the N_2F_4-H_2O system are summarized in Figure 2. The hydrolytic mechanism is obviously complex as indicated by the long induction periods and the subsequent exponential increase in the reaction rates. The total time required to completely destroy the N_2F_4 shows a difficultly reproducible inverse dependence on the initial pressure of this compound. The effect of N_2F_4 pressure on the overall reaction rate has been confirmed in other experiments. In a typical series, N_2F_4 samples at concentrations of 0.65, 1.27, 2.53, 3.85 and 5.22 mmole/100 ml were heated with water for 5 days at 35°C, 6 days at 50°C and 6 days at 60°C. The first three samples (low pressures) were recovered quantitatively while the fourth and fifth samples reacted to the extent of 6% and 100% respectively.

The marked acceleration of the hydrolysis with time is apparently a result of secondary reactions initiated by the product nitric oxide. The fastest and slowest reaction ["E" and "D"] illustrated in Fig. 2 were conducted under identical conditions except for the addition of

10 mole % of nitric oxide to the N_2F_4 in "E". The hydrofluoric acid formed also exerts a positive influence on the rate, but to a lesser degree than nitric oxide.

Both hydrochloric acid (0.5 N) and sodium hydroxide (2 N) profoundly alter the reaction. The halide causes the complete destrubtion of N_2F_4 at low pressures in less than 10 days while the hydroxide produces a slow, steady reaction with no indication of an induction period or increasing rate with time (line "F").

Experimental results on the N_2F_4-H_2O reaction were very difficult to duplicate; the lines C and C', which are vastly different, were obtained from supposedly identical runs, using N_2F_4 and water from the same sources. The large variations in reaction rate are believed to be due to minute amounts of oxygen remaining in the starting materials even after careful purification including boiling and vacuum degassing of the water. In control experiments, oxygen was found to be at least 10 times as effective as nitric oxide in promoting the reaction; the addition of about one mole per cent of the gas (based on N_2F_4) to the mixture reduced the total conversion time by a very conservatively estimated factor of four.

The above observations are consistent with the following reaction scheme:

$$N_2F_4 + 2H_2O \xrightarrow{\text{Slow}} 2NO + 4HF \qquad \text{XIII}$$

$$NO \xrightarrow[N_2F_4,\ H_2O]{\text{Slow}} NO_2 \qquad \text{XIV}$$

$$NO + NO_2 + H_2O \rightleftharpoons 2HNO_2 \overset{+2/3H_2O}{\rightleftharpoons} 4/3HNO_3 + 2/3NO \qquad \text{XV}$$

$$2NO_2 + N_2F_4 \xrightarrow{\text{Fast}} 4NOF \qquad \text{XVI}$$

$$2NOF + H_2O \xrightarrow{\text{Fast}} NO_2 + NO + 2HF \qquad \text{XVII}$$

The formation of some nitrogen dioxide (eq. XIV) at 60°C appears likely in view of the fact that large quantities of this gas were observed in the products of similar reactions at higher temperatures (133°C). Experiments in this laboratory have confirmed that N_2F_4 is readily attacked by NO_2 (eq. XVI) giving NOF, which would in turn rapidly hydrolyze and thus regenerate the NO_2 (eq. XVII). Increasing acidity would favor higher concentrations of free NO_2 by shifting the equilibrium (XV) to the left. By analogy to the chemistry of NF_3 caustic soda might be expected to be more efficient than water in the direct (nucleophilic) attack on N_2F_4, but secondary reaction would be inhibited by the removal of NO_2. Obviously oxygen would immediately convert any NO present to NO_2.

HYDROLYSIS OF cis- AND trans-N_2F_2

Few authors who have worked with difluorodiazine have failed to

comment on the "vast" difference in the reactivities of the two isomers. It is therefore surprising that trans-N_2F_2 is only moderately more resistant than cis-N_2F_2 to attack by water. Both materials are unaffected by excess water at 60°C over a period of 15 hours. The cis-isomer hydrolyzes slowly at 74°C (30% in 17 hours) while the trans- compound reacts at a similar rate at 89°C. In each case the major products are nitrogen, oxygen and hydrogen fluoride.

$$2N_2F_2 + 2H_2O \rightarrow 2N_2 + O_2 + 4HF \qquad \text{XVIII}$$

Nitrous oxide is also formed, but only in minor quantities (< 3%).

The results of a number of hydrolytic experiments with the cis- and trans-N_2F_2 are summarized in Figures 3 and 4.

The data in Figure 3 were obtained by allowing samples of trans-N_2F_2 at 89°C to react with 5 ml portions of water, aqueous NaOH (2 N) or aqueous HCl (0.5 N) in Pyrex ampoules. The line "A", drawn through the circled points, shows the logarithmic rate of change in the number of millimoles of trans-N_2F_2 in contact with water. Line "B" was derived by plotting the function log (N_o-2/3 n) where N_o is the initial concentration of trans-N_2F_2 and n is the total amount of non-condensible gas produced at any given time. The lines "C" and "D" were obtained from experiments involving aqueous NaOH (2 N) and aqueous HCl (0.5 N) respectively and were plotted on the same basis as line "A".

If the reaction proceeded quantitatively according to equation XVIII, lines "A" and "B" should be superimposed. The difference between these lines is at least partly due to the formation of nitrous oxide. Also, infrared spectroscopic studies on the original and partially reacted trans-N_2F_2 suggest that the material may have contained a small amount of undetectable impurity which would have caused a slight but proportionally consistent overestimation of the amount of N_2F_2 present.

A similar set of experiments involving a mixture of cis- and trans-N_2F_2 (67% cis) at 74°C is recorded in Fig. 4. The reaction rates of trans- and cis-N_2F_2 are given by lines "E" and "F" respectively. The points enclosed by squares express the rate of formation of non-condensible gases (N_2 and O_2) from cis-N_2F_2 in terms of the function log[N_o-2/3n -Δ)] where N_o is the initial amount of the cis isomer, n is the total amount of non-condensible gas produced in the given time and Δ is the amount of trans-isomer reacted as calculated from line "E". The excellent agreement between the non-condensible function and line "F" is probably somewhat fortuitous since detectable quantities of N_2O were also formed.

After the completion of the preceding experiment, the remaining isomeric mixture was allowed to react with 2 N NaOH under similar conditions of temperature and pressure. No change in the reaction rate occurred as is indicated by the points in parentheses in Fig. 4.

The above data suggest two important conclusions:

1. The reactions of cis- and trans-N_2F_2 with water are each first order with respect to the nitrogen fluoride.

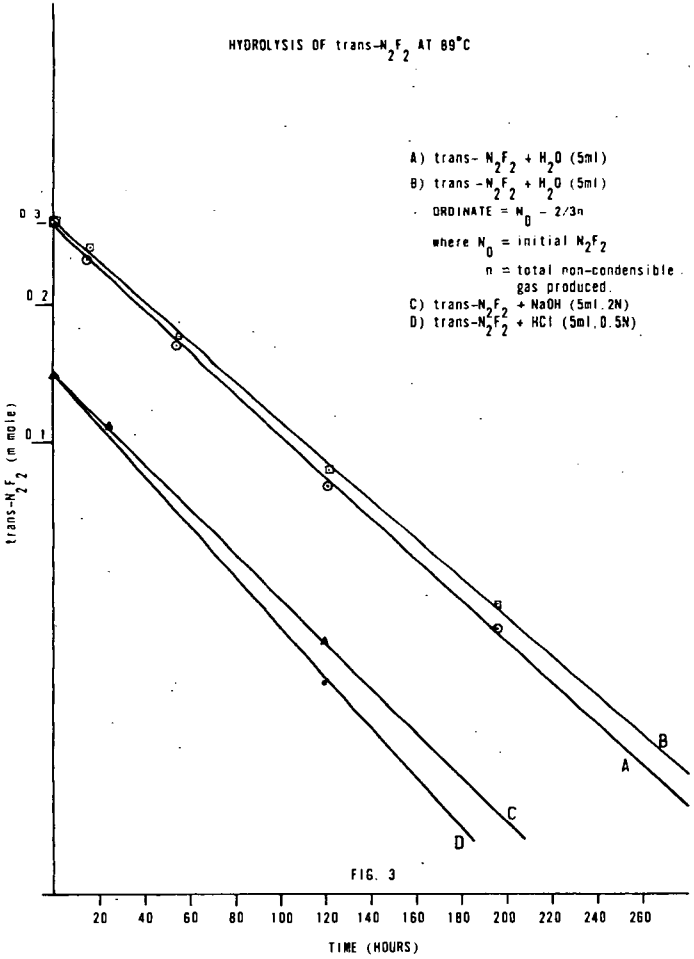
HYDROLYSIS OF trans-N_2F_2 AT 89°C
A) trans- N_2F_2 + H_2O (5ml)
B) trans- N_2F_2 + H_2O (5ml)
ORDINATE = N_0 - 2/3n
where N_0 = initial N_2F_2
n = total non-condensible gas produced.
C) trans-N_2F_2 + NaOH (5ml, 2N)
D) trans-N_2F_2 + HCl (5ml, 0.5N)
trans-N_2F_2 (m mole)
0.3
0.2
0.1
20 40 60 80 100 120 140 160 180 200 220 240 260
TIME (HOURS)
A
B
C
D

FIG. 3

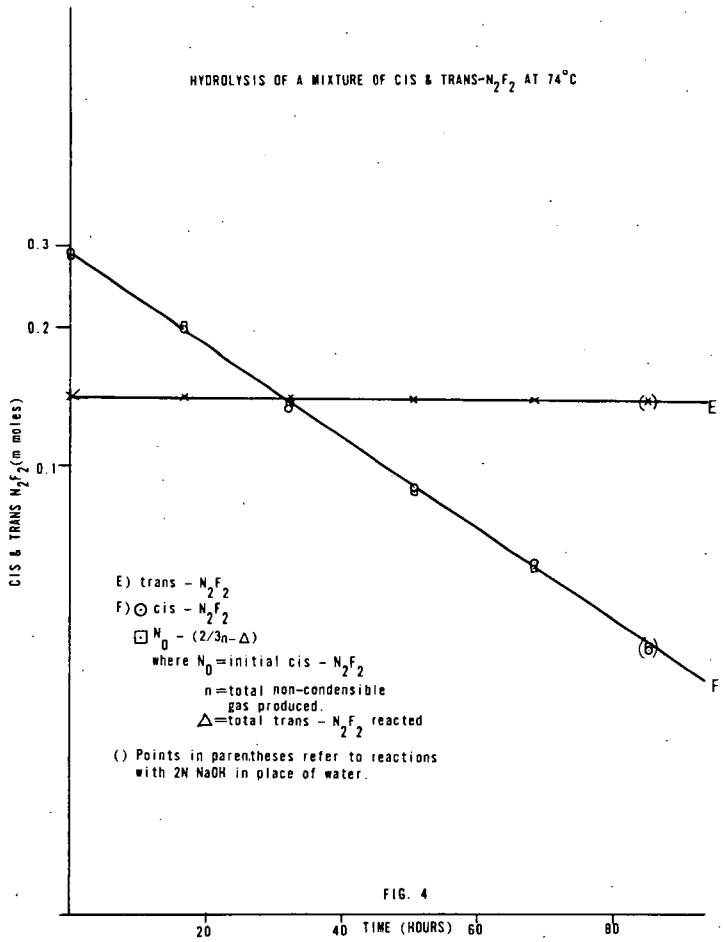
HYDROLYSIS OF A MIXTURE OF CIS & TRANS-N_2F_2 AT 74°C
CIS & TRANS N_2F_2 (m moles)
0.3
0.2
0.1
E) trans - N_2F_2
F) ⊙ cis - N_2F_2
⊡ N_0 - (2/3n-Δ)
where N_0 = initial cis - N_2F_2
n = total non-condensible gas produced.
Δ = total trans - N_2F_2 reacted
() Points in parentheses refer to reactions with 2N NaOH in place of water.
20 40 TIME (HOURS) 60 80
E
F

FIG. 4

2. The hydrolyses do not proceed via nucleophilic attack on N_2F_2.

The second conclusion is based on the observations that the strong nucleophile OH^- does not significantly accelerate the reactions, and on the fact that very little nitrous oxide is produced.

Because N_2F_2 is a strongly endothermic[4] compound, it is necessary to consider not only direct chemical attack by water

$$FN_2 \overset{F\cdots H}{\diagdown\!\diagup} + \overset{H}{\diagup\!\diagdown} OH \rightarrow F_2N\cdot + \cdot OH + HF \xrightarrow{H_2O} \text{Products} \qquad \text{XIX}$$

but also the thermal decomposition of the nitrogen fluoride to the elements. The reported reactivity[5] of cis-N_2F_2 toward glass poses an additional question of possible competing reactions with the container walls.

In an effort to resolve these problems a study was made of the decomposition of N_2F_2 in glass, both alone and in the presence of elementary nitrogen. The experimental results given in Table II indicate that both isomers decompose slowly at the previously established hydrolysis temperatures and that the reaction rates increase with the total pressure of the system. Variations in the available glass surface area apparently do not significantly alter the rates. These observations suggest that the hydrolytic reactions may proceed, at least in part, via a simple decomposition mechanism of the type

$$N_2F_2 + M \rightarrow N_2 + F_2 + M \xrightarrow{H_2O} \text{Products} + M \qquad \text{XX}$$

where M is any molecule. Hydrolytic attack is not completely precluded by the above evidence since water vapor (in equilibrium with the liquid) was found to be approximately twice as efficient as an equal pressure of nitrogen in destroying the isomers. In this connection it may be noted that nitric oxide was considerably more active than water under similar conditions.

The sensitivity of the decomposition rate to pressure offers a reasonable explanation for the reported high degree of reactivity of cis-N_2F_2 (under high pressures) toward glass[5] at ambient temperatures as compared with the relative inertness (at low pressures) of this system observed in this laboratory.

Obviously, all of the above experimental results may be equally well interpreted in terms of the reversible formation of an activated intermediate

$$N_2F_2 + M \rightleftharpoons N_2F_2^{\ddagger} + M \xrightarrow[H_2O,\ \text{etc.}]{SiO_2} \text{Products} + M \qquad \text{XXI}$$

at least in the case of the trans isomer, mechanism XXI is supported by the work of Schaap, Nevitt and Zletz[6] which indicates that the compound is stable in steel at 82°C under pressures as high as 3,400 atm. The cis isomer was reported to detonate under similar conditions.

TABLE II

DECOMPOSITION OF cis- AND trans-N_2F_2 IN GLASS

Initial N_2F_2 (mmole)	Initial Partial Pressure Of N_2F_2 At Reaction Temp. (mm Hg)	Partial Pressure Of N_2 (mm Hg)	Surface Area / Volume (cm^{-1})	Reaction Temp. (°C)	Time (hrs)	Decomposition (%)
trans (0.240)	40	500	1.8	89	18	9
trans (0.246)	40	500	1.8	89	16	11
trans (0.229)	40	nil	1.8	89	16	5
trans (0.217)	36	nil	1.9	89	18	5
trans (0.412)	69	nil	1.8	89	16	5
trans (0.412)	69	500	1.9	89	16	10
trans (0.040)	67	500	6.7	89	16.5	11
cis (.028) trans (0.137)	cis (6) trans (29)	300	1.9	75	18	cis (15) trans (nil)
cis (0.024) trans (0.437)	cis (5.1) trans (29)	nil	1.9	75	18	cis (8) trans (nil)
cis (0.104) trans (0.063)	cis (18) trans (10)	nil	6.7	75	18	cis (9) trans (nil)
✱trans(0.246)	-	500	1.8	-	-	nil

✱ Control run to establish efficiency of recovery technique.

In a study of the isomerization of trans-N_2F_2 in copper, Colburn et al [5] noted that extensive decomposition to the elements occurred at temperatures above 300°C. Similar experiments in this laboratory have shown that this reaction also occurs at much lower temperatures (175-200°C) and that the rate is strongly pressure-dependent. The results of a typical series of runs, as given in Table III, demonstrate that the extent of decomposition increases greatly with the pressure. The relatively low ratio of cis- to trans-N_2F_2 recovered in Experiment 1 suggests that the cis isomer is more rapidly destroyed than the trans compound.

TABLE III

ISOMERIZATION OF trans-N_2F_2

Expt.	Pressure (mm)	Reaction Time (sec)	Reaction Temp. (°C)	Total N_2F_2 Recovered (%)	cis-N_2F_2 In Recovered N_2F_2 (%)
1	370	30	175-200	16	29
2-7	14-20	90	175-200	70	67

EXPERIMENTAL

Sealed pyrex ampoules (ca. 135 ml) equipped with one or more break seals were used for all hydrolytic reactions. In the experiments involving NF_3 and caustic soda, the base was contained in loose-fitting Teflon cups within the ampoules to prevent attack on the glass. Infrared spectroscopy was generally used for the analysis of gaseous products.

Nitrogen trifluoride and dinitrogen tetrafluoride were obtained from Peninsular ChemResearch Inc. and Air Products Inc. respectively. Difluorodiazine was prepared by the reaction of N_2F_4 with $AlCl_3$ at -78°C. [7]

REFERENCES

1. A. M. Lovelace, D. A Rausch and W. Postelnek. Aliphatic Fluorine Compds., Reinhold, N. Y. 1958 (p. 137).

2. J. Hine. Physical Organic Chemistry, McGraw-Hill, N. Y. 1956 (p. 140).

3. O. Ruff. Z. Anorg. Chem. 197, 283 (1931).

4. A. V. Pankratov, A. N. Zerchaninon, O. G. Talakin, O. M. Sokolov and N. A. Knyazeva. Z. Fiz. Khim 37, 1399 (1963), C. A. 59, 8191C (1963).

5. C. B. Colburn, F. A. Johnson, A. Kennedy, K. McCallum, L. C. Metzger and C. O. Parker. JACS 81, 6397 (1959).

6. L. A. Schaaf, I. D. Nevitt, and A. Zletz. ARPA Propellant Contractors Synthesis Conference, April 13-15 1964, Chicago. pp. 293-305.

7. G. L. Hurst and S. I. Khayat. Unpublished work.

G. L. Hurst
S. I. Khayat

C/

December 8, 1964

PRELIMINARY DATA FROM A SURVEY STUDY OF THE EFFECTS OF IONIZING RADIATION ON VOLATILE INORGANIC COMPOUNDS OF FLUORINE, OXYGEN, AND NITROGEN

R. P. Nielsen, C. D. Wagner, V. A. Campanile and J. N. Wilson

Shell Development Company, Emeryville, California

Introduction

Very little has appeared in the literature concerning the radiation chemistry of covalent inorganic compounds in condensed phase. In the search for new high energy oxidizers, it sounds plausible that ion fragmentation, electron capture, ion-molecule reactions and free radical combination reactions at low temperatures may be utilized.

Conversion of several per cent of low molecular weight materials by non-chain reactions requires radiation doses of the order of 100 megarads. A 3 Mev Van de Graaff with a gold target supplies this dose to a small sample in one hour. The sample can be held at any desired temperature in a Dewar flask. Detection of products, many of them highly reactive, is accomplished by direct distillation at low temperature and very low pressure into a time-of-flight mass spectrometer. With this basically simple technique, a survey of radiolysis of many systems, both pure and binary, is under way. This report describes results obtained thus far.

Experimental[a)]

Horizontal X-ray source. Large doses of 2-3 Mev bremsstrahlung (up to 100 megarad/hr) are generated by directing the 3 Mev electron beam from a Van de Graaff accelerator onto a water-cooled gold target (Figure 1). The vertical electron beam is deflected 90°, producing a horizontal beam, so that sample placement may be facilitated (Figure 2).

Reaction vessel. Samples to be irradiated are condensed into the cooled tip of a 4 mm o.d. thin-walled stainless steel tube. A brass slug, silver-soldered over the end of the tube, acts as a heat sink. A metering valve (Nupro No. SS-4M) connected to the tube with Swagelok fittings and equipped with a Kel-F O-ring seal and a micrometer handle complete the vessel.

Sample size. A standardized sample size of 0.075 mmole of reactant was chosen. In a binary reaction system the total sample comprises 0.15 mmole. These amounts provide a convenient sample for analysis and are considered to be safe in the event of an explosion in the 2 ml reaction vessel.

---

a) Further experimental details may be found in Papers Presented, ARPA Propellant Contractors Synthesis Conference, IIT Research Institute, Chicago, April 13-15, 1964.

Cooling provisions. The irradiations are carried out at 77°K by immersing the reaction vessel in liquid nitrogen within a specially constructed vacuum flask (Figure 3) which contains a cooled side arm that is also convenient for accurate placing of the sample tube. A thermocouple and demand system replenishes the liquid nitrogen as necessary.

Dosimetry. Liquid dosimeters are of too large a volume to allow accurate determination of the dose delivered to the small (~50 µl) samples used in this study. A new cadmium dosimeter based on photoactivation has been developed by one of us[a] and is useful in this study. When cadmium nuclei are irradiated with >1.25 Mev photons, metastable Cd^{111m} nuclei are produced which decay with a 49 minute half life and emit 149 and 247 kev photons. A 50 µl volume (430 mg) of cadmium metal which has been irradiated for 5 minutes provides a sufficient activity count for accurate dosimetry.

Analysis. The samples under study are maintained at 77°K before, during and after irradiation. No warming is allowed until the sample tube has been connected to the mass spectrometer and analysis for non-condensable gases is complete. At 77°K the gases observed may include F_2, N_2 and O_2. When analysis for the non-condensable gases is complete these gases are pumped off through another valve until the pressure reaches ~0.05 mm, at which point analysis for gases which are condensable at 77°K, but which exert a significant vapor pressure at this temperature, is accomplished. Both NF_3 and OF_2 are among the compounds which may be seen at this point. The liquid nitrogen bath is removed when these data have been collected and in its place is substituted a 77-350°K variable cryostat. That sample is now slowly warmed and sequential fractions are distilled into the Bendix time-of-flight mass spectrometer. A rough separation is thus accomplished and the identification of products is made somewhat easier. Excess amounts of all components observed in the product mixture are pumped off at the temperature at which they are observed before the temperature is raised and the next fraction examined. The data thus obtained provide a qualitative indication of the compounds produced in the radiolysis and will serve as a guide for future, larger scale work.

Results

Irradiations of pure substrates. Irradiation of one-component systems is a desirable prerequisite for the study of multi-component systems. The irradiation of a pure compound provides data which may indicate the identity of active intermediates which may then be considered for use as reactants in mixed systems. In addition, the possibility exists that products will result from such treatment that will be interesting in their own right. Also, it is necessary to obtain as much product identification data as possible in single-component systems in order to simplify the analytical problems encountered when mixtures are irradiated.

The data in Table 1 are presented in the following manner: the second column lists the temperature of the sample tube from which the products are distilled into the mass spectrometer at ~ 8×10^{-6} mm; the third

a) C. D. Wagner, to be reported elsewhere.

column lists the products as identified by the mass spectra obtained at the respective temperatures, and the fourth column lists ions observed but for which no identification could be made.

Irradiations of Binary Mixtures. The low temperature irradiation of binary mixtures is being studied as a unique synthetic method which may produce compounds which have not been previously observed because of their low thermal stabilities. Their synthesis by purely chemical means may be very difficult or perhaps impossible, thus the collection of data describing such structures is a primary aspect of this study. The data below are presented in the same manner as those above (Table 2).

DISCUSSION

The basic processes which are responsible for reaction on irradiation of these covalent inorganic systems are due almost entirely to excitation and ionization of the molecules by the secondary electrons generated in the sample by Compton scattering. The primary species produced are excited molecule ions, and excited molecules; these species decompose to fragment ions and radicals and react with the bulk substrate and with one another to give the observed products. At present little is known of the reactions of such species at 77°K, and in this study, which is intended merely to indicate areas for promising further research, little emphasis has been placed on the elucidation of possible mechanisms of reactions. Such information can only be gained by considering the yields of the various products in a quantitative manner.

Without quantitative yield data one can say little concerning proposed sources of the observed products. It is even difficult without such data to state with certainty which products appear in predominant quantities and whether or not a chain reaction has been found. At this point it appears that the yields are modest and are those which one would expect of non-chain processes with G values of the order of 5-10.

Some of the problems facing the investigator in a study such as this should be mentioned before one proceeds into a discussion of the irradiated systems. Many of the experimental difficulties have been successfully solved: application of a high dose rate of photons to a small sample, adequate cooling of the samples during irradiation, accurate dosimetry on the geometry of small samples, micro separation of the irradiation products, and analysis of micromolar amounts of highly reactive species via time-of-flight mass spectrometry. Aspects which can be improved include a method for mixing reactants in micro quantities at 77°K to be sure that an intimate mixture is obtained and perhaps a mass spectrometric method which would be capable of better identification through higher resolution. The mass spectrometric identification of compounds which are present in the mass spectrometer for a few fleeting seconds in some instances is tenuous. The ambiguity in the identification of ions from their m/q values alone is also a constant source of difficulty, as in the case of polyoxygen fluorides, where the $O_4F_2^+$ ion and the $HOSiF_3^+$ ion both possess a m/q value of 102, and the difference between these masses amounts to only 0.0015 amu.--an unresolvable difference with a TOF mass

spectrometer. Fortunately, most systems lend themselves to TOF mass spectrometry without too much ambiguity. Differences in the volatility of the compounds encountered help to make rational decisions about the identify of the species observed (Table 3).

As the data demonstrate, a large variety of products may be expected in the irradiations of compounds containing the -NF and -OF groups. In most of the irradiations of these fluorine-containing compounds, elemental fluorine, F_2, is observed as a product. In those cases where no F_2 is found, one may wish to examine the system in order to see if either the starting material(s) or one of the products is likely to be attacked by F_2 at 77°K . Thus, in the case of SF_6, where one might expect one or both of the following reactions on irradiation,

$$2SF_6 = F_5S\text{-}SF_5 + F_2$$

$$SF_6 = SF_4 + F_2,$$

no product is observed. One hypothesis that might be suggested for this result is that these reactions may proceed in the reverse direction spontaneously at 77°K, the temperature at which the irradiation is performed. A test for this hypothesis would be the successful trapping of the intermediates before the reverse reaction occurs. Using NF_3, no reaction occurs with SF_6 on irradiation:

$$SF_6 + NF_3 = \text{no products observed.}$$

In the presence of OF_2, however, it is found that products are generated in the irradiation,

$$SF_6 + OF_2 = O{=}SF_4 + 2F_2,$$

thus, it appears that either an irradiation product of OF_2 attacks SF_6 successfully, or some sulfur-containing intermediate has been trapped. In any case, the sulfur-oxygen bond formed resists attack by fluorine and a product is observed.

Similar behavior is exhibited in the case of SO_2. Alone, SO_2 gives no products on irradiation. In the presence of either NF_3 or OF_2, however, reaction occurs and all the fluorine which one would normally see from NF_3 or OF_2 alone appears in the products, SO_2F_2, SF_4O, and (possibly) SF_4. In the case of SiF_4, no reactionhhas yet been effected, either alone or with possible trapping agents (NF_3 and OF_2).

The nitrogen oxides seem to be fairly regularly interconverted on irradiation. An exception to this is that nitric oxide never appears among the products at 77°K, where we know from experience that it can be observed in a product mixture and quantitatively pumped off. In systems which generate both NO and O_2, it is probable that the NO is lost in the reaction,

$$NO + 1/2\ O_2 = NO_2,$$

which requires little activation energy. In order for us not to see NO in these systems, the above reaction must occur before analysis.

The interesting phenomenon of oxygen hold-up occurs in the irradiation of dinitrogen tetroxide. Whereas no O_2 is observed at 77°K on analysis of a sample of irradiated N_2O_4, when the temperature is raised to about 175°K, O_2 and NO are evolved. Since we have not observed the trapping of oxygen in the solid N_2O_4 lattice previously, it appears that at 175° a decomposition is occurring; no additional data are yet available concerning the compound(s) which may be the source of this decomposition.

The irradiation of CF_3Cl in the presence of Xe appears to give a higher product yield than does CF_3Cl alone. Also, more products are observed, as might be expected from a higher conversion. Xe thus exerts a synergistic effect and may act as an efficient energy transfer agent. Carbon dioxide seems to display a similar effect in the irradiation of NF_3.

The products from nitrosyl fluoride and nitrosyl chloride show that a great many processes must occur when these systems are irradiated. Although no oxygen is observed among the products, in the case of O=NF all of the O_xF_2 species normally seen from OF_2 are produced, though OF_2 itself is not seen. If oxygen or OF_2 are products, they must be quantitatively used in secondary reactions. The great variety of N-F compounds and nitrogen oxides produced in these systems add to the confusion, but most striking is the production of apparent dimers (and possibly trimers) of the nitrosyl halides, $(O=NF)_2$ and $(O=NCl)_2$, for which no structure is yet suggested. Many such structures can be written.

The two systems which have been most thoroughly studied in this work are the NF_3 and the OF_2 systems. These materials were both irradiated early in the program and then frequently again both alone and admixed with other reactants. The products of these irradiations, by virtue of the fact that they involve only two elements each, are confined to a small number:

NF_3	N_2, F_2, <u>cis</u>-N_2F_2, <u>trans</u>-N_2F_2, and N_2F_4
OF_2	O_2, F_2, O_2F_2, O_3F_2, and O_4F_2(?) .

The chemistry involved, however, is complicated. We see in the first case that by some means that all of the fluorine atoms have been stripped from NF_3, producing N_2.

The mass spectrum of NF_3 shows NF_3^+, NF_2^+ and NF^+ as predominant ions with significant yields of N^+ and even F^+ as well;(4) the formation of

(4) C. H. Colburn and A. J. Kennedy, J. Am. Chem. Soc. <u>80</u>, 5004 (1958).

the fragment ions is presumably accompanied by formation of F_2 and F. Similar products may arise from the initial excitation of NF_3 during radiolysis in the condensed phase, but here the detailed course of events may be modified by collisions between excited species and surrounding molecules.

Recombination of ions and electrons should lead to the formation of $\cdot NF_2$ and :NF radicals. Formation of $\cdot NF_2$ radicals and F^- ions may occur also by the exothermic process

$$NF_3 + e^- \rightarrow \cdot NF_2 + F^- .$$

Formation of N_2F_4 can clearly occur by recombination of $\cdot NF_2$ radicals; N_2F_2 may form similarly from :NF radicals though the energy release will favor decomposition of the product. The exothermic cross-coupling radical reaction

$$:NF + \cdot NF_2 \rightarrow \cdot N_2F_3^* \rightarrow N_2F_2 + \cdot F$$

is also a possibility. A possible route to N_2 and F_2 is provided by the related reaction

$$:NF + :NF \rightarrow N_2F_2^* \rightarrow N_2 + F_2$$

in which the first step makes available about 4 ev of excitation energy. Still other possibilities are provided by ion-molecule reactions such as

$$\cdot NF^+ + NF_3 = NF_2^+ + \cdot NF_2$$

which may be slightly exothermic, and by reactions of F^- with any of the positive ions mentioned above.

Similar reasoning can be made to account qualitatively for the products obtained from OF_2. The task ahead will be to gain more data concerning these systems, to obtain more concrete evidence for the mechanism of the reactions and to attempt to devise experiments in which some of the intermediate species postulated may be trapped and identified.

Conclusion

The technique described and the results obtained serve to indicate that low temperature radiation synthesis is indeed a tool which may prove to be of value in the study of endothermic oxidizing agents of low thermal stability. Although no quantitative product distribution has been measured, and some of the products are still not identified, the guidelines established by a survey study such as this will be of great value in choosing systems worthy of further study. The mass spectrometric analysis scheme for the product mixtures will provide a monitoring system in guiding the separation of larger amounts of the irradiation products. Other techniques, such as gas-liquid chromatography, infrared and U.V. spectroscopy, as well as NMR, will, of course, have to be applied in the characterization of those compounds which we have until now deemed "uncharacterized".

Acknowledgment

This work was supported by the Advanced Research Projects Agency, Department of Defense, under contract No. DA-31-124-ARO(D)-54, monitored by the Chemistry Division, U. S. Army Research Office, Durham, North Carolina.

Table 1

Compound Irradiated	Temp, °K	Products Identified (In Approximate Order of Abundance)	Ions Observed-Source Unidentified
NF_3	77	N_2, F_2 (see Fig. 4)	
	100	cis-N_2F_2, trans-N_2F_2	
	134	N_2F_4	
N_2F_4	77	N_2, F_2, NF_3	
	105	cis-N_2F_2, trans-N_2F_2	
FNO	77	N_2, NO	
	123	N_2O, cis-N_2F_2, trans-N_2F_2	
	161	O_2F_2, O_3F_2, O_4F_2 (?) N_2F_4	
	223	N_2O_4, NO_2F (?)	N_3F^+, O_2^+,(2) N_2O^+,(2) N_2F^+,(2) NOF^+, $N_2O_2F^+$, $N_2OF_2^+$
	293		$N_3O_2F^+$, plus those observed at 223
ClNO	77	N_2, NO	
	195	N_2O_4, N_2O, Cl_2	
	292		N_2OCl^+, $N_2O_2Cl^+$
N_2O	77	N_2, O_2	
	244	N_2O_4	
NO	77	N_2	
	124	N_2O	
	243	N_2O_4	
N_2O_4	77	N_2 (no O_2)	
	176	NO, O_2, trace N_2O	

2) This species evolved from a decomposition at this temperature.

(Continued)

Table 1 (Contd)

Compound Irradiated	Temp, °K	Products Identified (In Approximate Order of Abundance)	Ions Observed-Source Unidentified
OF_2	77	F_2, O_2	
	107	COF_2,(3) O_2,(2) F_2(2) OF_2(2)	
	128	O_2,(2) F_2,(2) CO_2(3)	
	176	O_3F_2, O_2F_2, O_2,(2) Cl_2,(3) O_4F_2 (?)	
	219	O_2F_2, O_3F_2 (trace), O_2,(2) $CClF_3$ (trace)(3)	
SO_2		No products observed to 350°.	
SO_2F_2	83	O_2, OF_2	
	143	CO_2 (trace)(3)	
	253	SOF_4, SF_6	SO_4F^+, $SO_2F_3^+$
SF_6		No products observed to 350°.	
SiF_4		No products observed to 350°.	
CF_3Cl	77	CF_4	
	293	C_2F_6, CF_2Cl_2, Cl_2, and $C_2Cl_2F_4$ or C_2ClF_5.	
CCl_4	208	Cl_2	
	293	C_2Cl_6, plus a C_3 species, probably C_3Cl_8.	

2) This species evolved from a decomposition at this temperature.
3) From the action of the sample on the Kel-F grease on the O-ring seal.

Table 2

Compound Irradiated	Temp, °K	Products Identified (In Approximate Order of Abundance)	Ions Observed-Source Unidentified
NF_3 & O_2	77	N_2	
	100	F_2(2)	NO^+, N_2O^+, NO_2^+, N_2F^+, OF^+
	143	F_2,(2) O_2,(2) FNO N_2O, cis-N_2F_2, trans-N_2F_2, NO_2F (?)	
	211	Cl_2,(3) OF_2,(2) O_3F_2 OF_2,(2) O_2(2)	
	253	N_2O_4	
NF_3 & OF_2	77	N_2, O_2, F_2,	
	108	cis-N_2F_2, trans-N_2F_2, COF_2(3)	NO^+
	116	CO_2,(3) N_2O	
	211	O_2F_2	
	253	N_2O_4	
NF_3 & N_2O	77	N_2, O_2, F_2	
	110	cis-N_2F_2, trans-N_2F_2,	
	179	FNO, Cl_2,(3) NO_2F (?)	
	253	N_2O_4	
NF_3 & NO	77	N_2	
	83		N_2^+, NF^+
	98	cis-N_2F_2, trans-N_2F_2 (large amounts)	
	113	N_2F_4 (large amounts) N_2O	
	193	N_2O_4, FNO	
NF_3 & N_2O_4	77	N_2, F_2, trace O_2	
	111	cis-N_2F_2, trans-N_2F_2	
	148	N_2F_4, N_2O, FNO NFO_2 (?)	O_2^+, N_2^+, NF_2^+
	204	N_2O_4	

2) This species evolved from a decomposition at this temperature.

3) From the action of the sample on the Kel-F grease on the O-ring seal.

(Continued)

Table 2 (Cont'd)

Mixture Irradiated	Temp, °K	Products Identified (In Approximate Order of Abundance)	Ions Observed-Source Unidentified
$NF_3 + SO_2$	77	N_2, F_2	
	99	cis-N_2F_2, trans-N_2F_2	
	123	N_2F_4, SO_2F_2, SF_4 (trace), CO_2(3)	
	169	SOF_4 (?)	
$NF_3 + SF_6$		No products other than observed up to 350°.	those of NF_3 alone
$NF_3 + SiF_4$		(Same as above)	
$NF_3 + CCl_4$	77	N_2, CF_4	
	128	N_2F_4, cis-N_2F_2, trans-N_2F_2, CCl_2F_2	
	173	Cl_2, NF_2CCl_3 (?)	NCl^+, NF_2CCl^+, $NFCCl_2^+$,
	195	CCl_3F	
	293	C_2Cl_6	
$NF_3 + C_2H_2$	77	N_2	
	89	cis-N_2F_2, trans-N_2F_2	
	156	CHF=CHF	
	186	C_6H_6, NF_2CH=CHF (?)	NF_2^+, CHF^+, $CHNF^+$, $C_2NF_2^+$, $C_2NF_2H^+$, $C_2NF_2H_2^+$
$NF_3 + CO_2$		Increased yields of normal NF_3 irradiation products as well as some COF_2	
NF_3+F_2C=CH_2	77	N_2, CF_4	
	130	N_2F_4, cis-N_2F_2, (traces) trans-N_2F_2 (traces)	
	293	CF_3CH_2F, $F_2NCH_2CF_3$ (?)	NF_2^+, CF_3^+, $C_2NF_2^+$, $C_2NF_2H^+$, (weak intensities)

3) From the action of the sample on the Kel-F grease on the O-ring seal.

(Continued)

Table 2 (Cont'd)

Mixture Irradiated	Temp, °K	Products Identified (In Approximate Order of Abundance)	Ions Observed-Source Unidentified
$OF_2 + N_2$	77	O_2, F_2, NF_3	
	107	cis-N_2F_2, trans-N_2F_2	
		N_2,(2) O_2,(2)	
		OF_2(2)	
	128	N_2O, CO_2, N_2,(2)	
		O_2,(2) OF_2,(2)	
		NO_2F (?)	
	191	N_2O_4	N_2F^+
$OF_2 + O_2$	77	(No F_2 observed)	
	93	O_3	
	133	SiF_4,(4)	
	173	CO_2,(3) COF_2,(3)	
		O_2,(2) F_2(2)	
	192	O_3F_2, O_2F_2,	
		O_2,(2) F_2(2)	
$OF_2 + N_2O$	77	F_2, N_2, O_2	
	132	COF_2,(3) FNO,	
		NO_2F (?)	
	199	N_2O_4	
OF_2 + NO(5)	77	O_2, N_2, F_2, OF_2, NF_3	
	158	N_2O, COF_2,(3)	
		SiF_4,(4) FNO,	
		NO_2F (?)	
	193	N_2O_4	N_2F^+
$OF_2 + N_2O_4$	77	O_2, F_2	
	131	O_2,(2) CO_2,(3)	
		COF_2,(3) NO_2F(?)	
	193	O_2F_2, FNO, O_2(2)	

2) This species evolved from a decomposition at this temperature.
3) From the action of the sample on the Kel-F grease on the O-ring seal.
4) Impurity.
5) Mixture exploded before irradiation. Products were analyzed in the usual manner.

(Continued)

Table 2 (Cont'd)

Mixture Irradiated	Temp, °K	Products Identified (In Approximate Order of Abundance)	Ions Observed-Source Unidentified
$OF_2 + SO_2$	77	O_2F, F_2, SF_2 (?)	SF_2^+, SF^+, S^+ (weak intensities)
	110	SO_2F_2, SF_4, SOF_4, SF_6	
	143	CO_2(3) (trace)	
$OF_2 + SF_6$	77	O_2, F_2	
	137	O_2F_2, CO_2,(3) O_2,(2) F_2,(2) OF_2(2)	
	161	SOF_4	
$OF_2 + SiF_4$		No products other than those of OF_2 alone observed up to 350°.	
$OF_2 + CCl_4$		Poor data - ambiguity exists in distinguishing OF from ^{35}Cl.	
$OF_2 + CO_2$	77	F_2, trace O_2	
	103	O_2(2) (large amount)	
	120	COF_2(3)	
	133	O_2,(2) OF_2(2)	
	181	O_2F_2, C_3F_2	
	220	O_2,(2) OF_2,(2) CO_2(2)	$CO_4F_4^+$, $CO_4F_3^+$, $CO_2F_3^+$, $C_2OF_3^+$, $C_2O_2F_2^+$, COF_3^+, $CO_2F_2^+$, $C_2O_3^+$, CO_2F^+
$CF_3Cl + Xe$	77	CF_4	
	112	Cl_2, C_2F_6, CF_2Cl_2	
	183	$C_2Cl_3F_3$, $C_2Cl_2F_4$, CCl_3F, XeF_2 (?)	Xe (?) ~132; XeF (?) ~151; XeF_2 (?) ~170
$Cl_2 + Xe$		No products observed up to 350°.	

2) This species evolved from a decomposition at this temperature.
3) From the action of the sample on the Kel-F grease on the O-ring seal.

Table 3
Emergence order of compounds observed in mass spectrometer ($P=8\times10^{-6}$mm) and their respective approximate distillation temperatures.

Compound	Temp, °K	Compound	Temp, °K
N_2	77	N_2F_4	130
O_2	77	FN=O	150
F_2	77	SO_2	150
NF_3	77	SF_6	160
NO	77	Cl-N=O	200
OF_2	77	N_2O_4	200
CF_4	77	CCl_4	210
C_2H_4	90		
N_2F_2	100		
Xe	100		
CH_2CF_2	100		
SO_2F_2	105		
SiF_4	110		
CF_3Cl	110		
COF_2	120		
N_2O	125		
C_2H_2	125		
CO_2	125		
SiF_4	125		

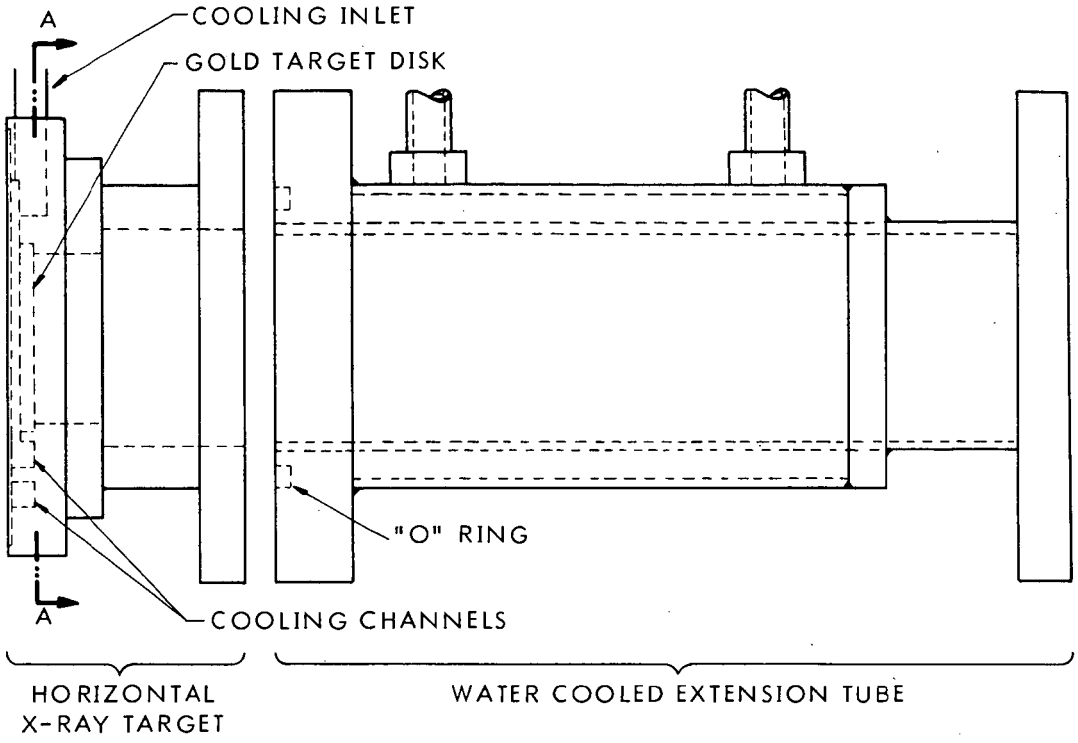

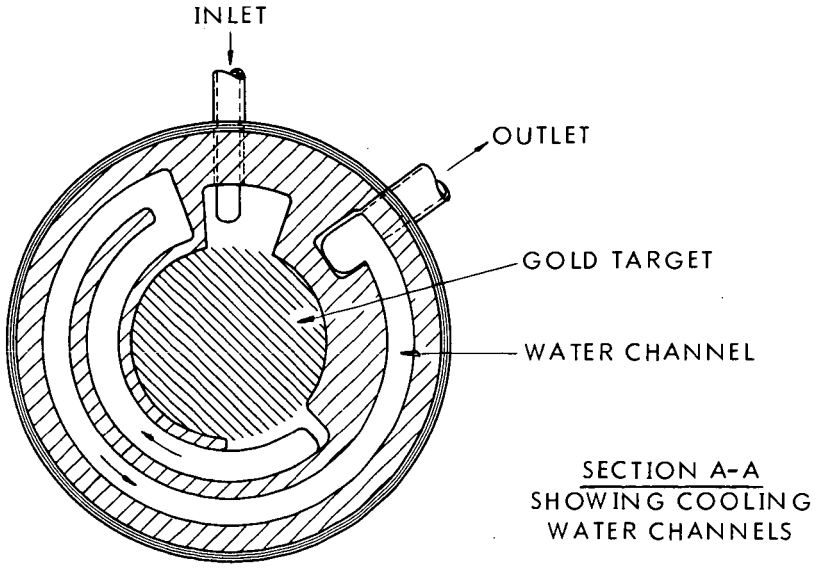

Figure 1. HORIZONTAL X-RAY TARGET WITH WATER COOLED EXTENSION TUBE

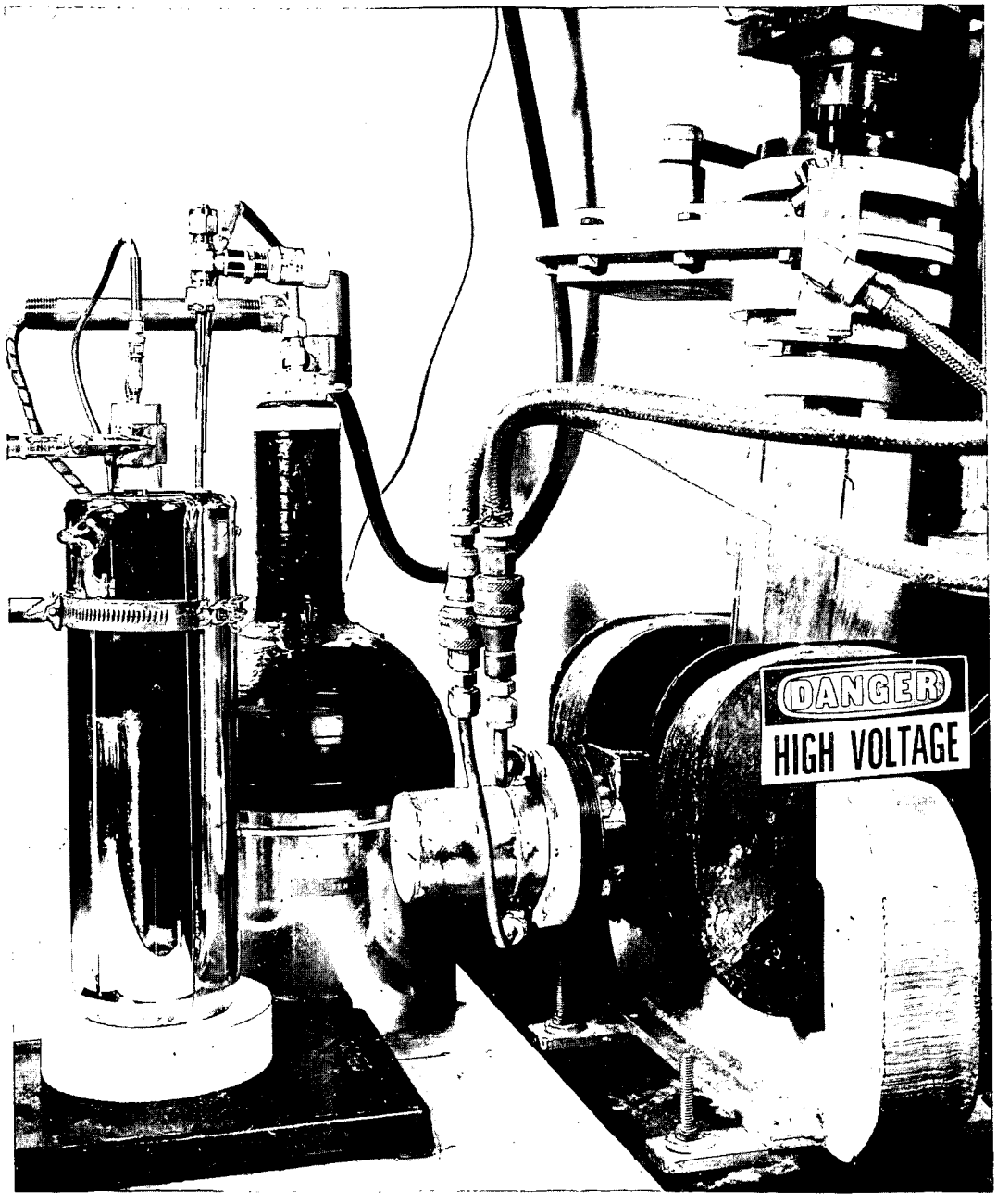

Figure 2. APPARATUS FOR IRRADIATION WITH HIGH ENERGY PHOTONS

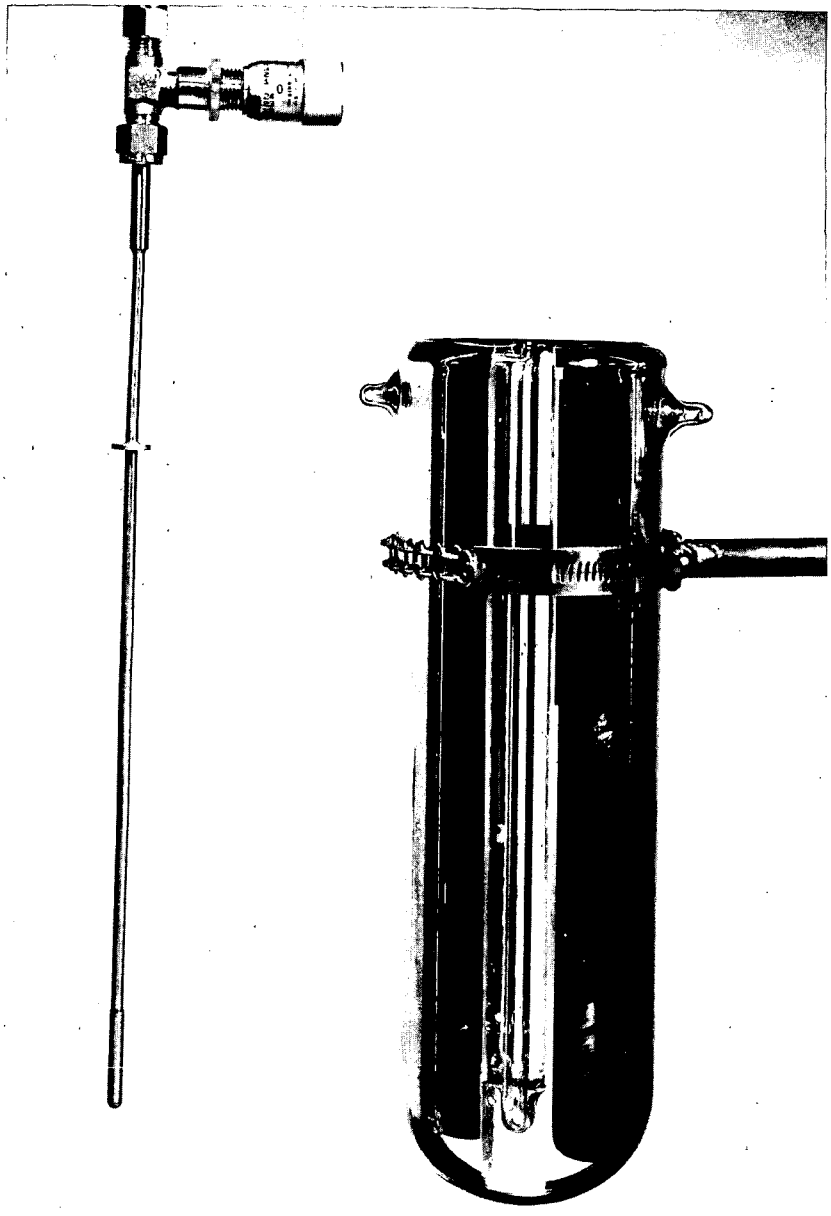

Figure 3. SPECIAL DEWAR FOR HOLDING SAMPLE DURING IRRADIATION AT -196°

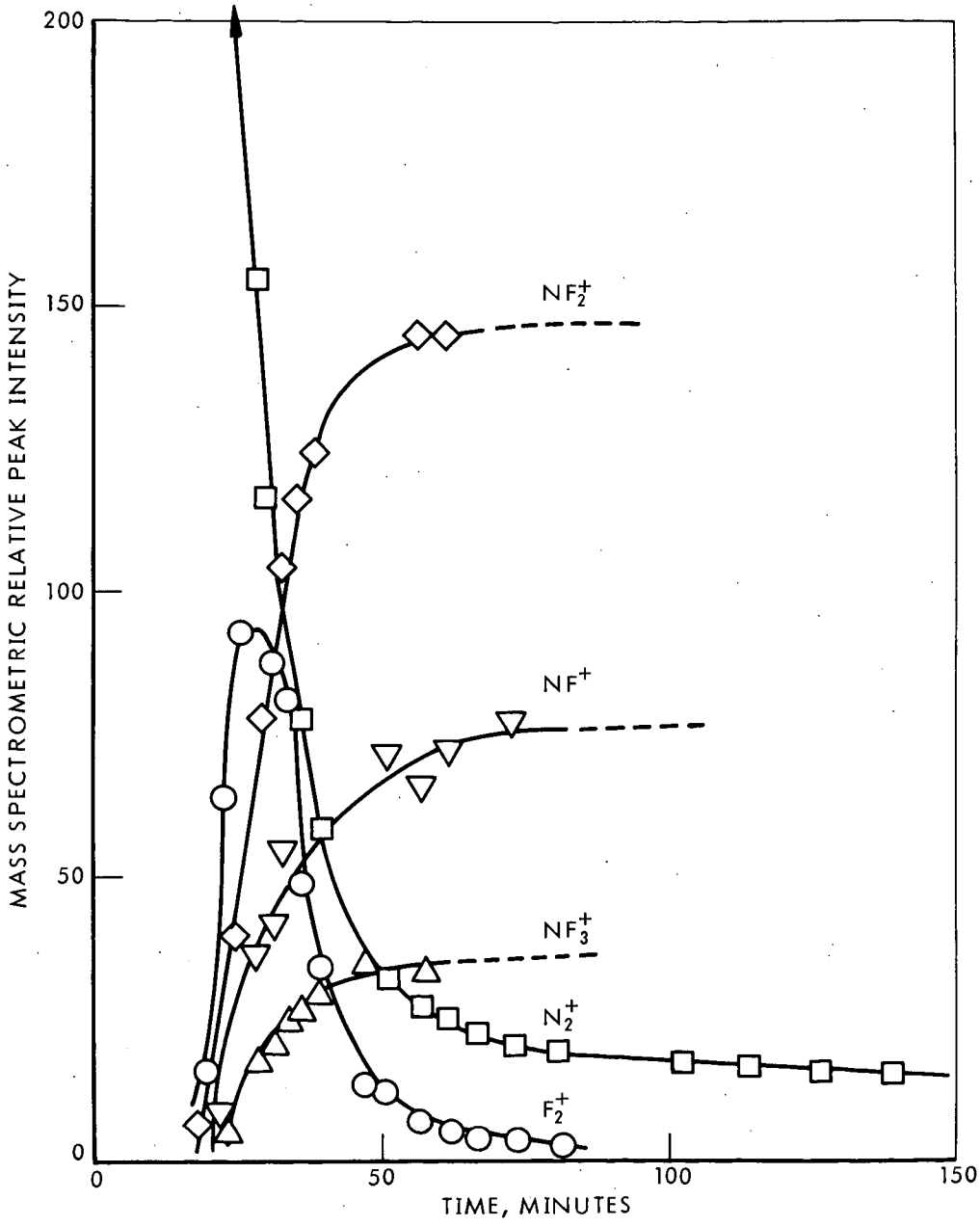

Figure 4. NF_3 IRRADIATION PRODUCT ANALYSIS: TIME vs PEAK INTENSITY AT -196°

OF_2 FORMATION BY ELECTROLYSIS OF WET HF*

J. A. Donohue, T. D. Nevitt, and Alex Zletz

Research and Development Department, American Oil Company, Whiting, Indiana

INTRODUCTION

The best oxidizers for hydrocarbon fuels are: 1) a mixture of O_2 and F_2 (Flox), and 2) oxygen difluoride (OF_2) (1). Although F_2 is difficult to handle, much effort is being devoted to obtaining the benefits of Flox. On the other hand, OF_2 represents the optimum O/F ratio for hydrocarbon oxidation, and its use would reduce handling problems and lead to better performance because of higher density. However, because OF_2 is expensive and has a high flame temperature, interest in it has been limited.

The generally cited method for the preparation of OF_2 from F_2 and base (2) utilizes F_2 inefficiently. Although the presence of OF_2 in the electrolysis of HF has been known since 1927 (3), this process was not suggested as the preferred method for OF_2 production until 1955 (4). Yields of 60% OF_2 have been claimed for electrolysis of HF containing 1-20% water (5), but our results are quite different.

Our work to determine the mechanism of OF bond formation has provided data that not only are useful in evaluating the electrolytic process, but also establish operating conditions that ensure consistent yields of OF_2. In studying how the electrolysis variables affect the product distribution, we found that the concentration of H_2O in the HF is a significant variable, and that periodic interruption of the electrolysis will stabilize the otherwise erratic production of OF_2.

EXPERIMENTAL

Our initial experiments involved a basic procedure in which the electrolyte was 250 ml of HF containing about 1 mole % KF, and electrolysis was carried out with nickel anodes at 7.0-7.6 volts and 0-3°C in a static system. Our main purpose was to determine how the H_2O concentration in the electrolyte affected the product distribution. Thus, we added a known amount of water to the electrolyte, allowed the electrolysis to proceed through an induction period, and then collected and analyzed the gaseous products--H_2 at the cathode, and OF_2, F_2, O_2, and O_3 at the anode.

As our work progressed, we developed other electrolysis cells, a convenient method for monitoring and maintaining the H_2O concentration in the HF, and accurate methods for analyzing most of the products. Consequently our later experiments were more closely controlled.

Electrolysis Apparatus

Development of the electrolysis cell involved several designs. Generally, smaller anodes were used as the analyses were improved (presently 10 cm^2), but the electrolyte volume was held constant at 250 ml to simplify monitoring of the H_2O concentration.

The present design is shown in Figure 1. The cell itself is a 300-ml Kel-F cup equipped with a stainless steel cap and a Teflon gasket. (The liquid level can be observed through the translucent Kel-F.) The cap includes a thermocouple well and electrode leads; separate ports for introducing electrolyte, adding H_2O, replacing anode, and flushing with helium; and separate lines for circulating the electrolyte to an infrared cell and for passing the gaseous products through a

* Research reported in this publication was supported by the Advanced Research Projects Agency through the U.S. Army Research Office-Durham under contract DA-31-124-ARO(D)-78. This report also discloses proprietary information owned by the American Oil Company, and its use by others is prohibited, except as may be provided by the contract.

dry ice (-78°C) condenser. A NaF scrubber is located after the condenser to remove the last traces of HF from the gases. During the electrolysis, the cell is immersed in an ice bath. However, circulation through the infrared cell and electrolysis cause the electrolyte to stay at 12-15°C.

The power supply is an Electro Products Model D-612T. For automatic interrupted operation, it is connected to the electrolysis cell through a mercury relay that is operated by a flexopulse timer (Eagle Signal Corp.).

For study of surface deposits and weight changes, the anode is removed and rinsed with HF to remove KF. The HF is removed at reduced pressure.

Gas Analysis

In our early experiments, the gaseous products were allowed to react with KI solutions, which were then analyzed for I_2 and fluoride ion. In a later improvement, O_3 was trapped out on silica gel (6) and analyzed separately. Then, a dual-column gas chromatograph, one column to remove O_3 followed by one to separate other components, was added to increase the speed of analysis and include H_2 and O_2.

Further improvements in speed and sensitivity were obtained with the temperature-programmed, single-column setup shown in Figure 2. Because the products are oxidizers, the materials of construction are limited to dry and degreased metals and fluorocarbon plastics. Passivation with OF_2 and O_3 is also necessary. The 6-in. columns of silica gel used in the setup are a compromise in length--to minimize O_3 decomposition and still permit separation of H_2 and O_2 at a readily obtainable temperature.

For a typical analysis, the columns are cooled to about -75°C by dry air which has been passed through a coil in liquid N_2. Then the gases to be analyzed are injected into one column by a Perkin-Elmer sampling valve, and the reference carrier gas is treated in the same way on the second column. After sampling is complete, the liquid N_2 is removed and the air flow is continued for about 5 minutes, or long enough to warm the columns to about -10°C and remove the O_3. Yields, as percent of current, are calculated from the gas chromatographic data and amperage, sample volume, and total gas flow measurements.

This analysis still has limitations with respect to H_2, F_2, and O_3. The thermal conductivity detector has a low sensitivity for H_2, and high concentrations cannot be allowed because response is not linear. Consequently, the flow of helium through the electrolysis cell must be adjusted to keep the H_2 concentration in the sensitive range. Also, even after prolonged passivation, the components of the system still react with F_2, so that only qualitative trace peaks are obtained for F_2. Because O_3 decomposes readily and is difficult to detect and determine reliably (7), the true O_3 yields may be higher than reported; O_2 yields would be correspondingly lower.

Analysis and Control of H_2O Concentration in Electrolyte

Because HF has a marked affinity for water, we could not analyze by ordinary Karl Fisher (8) or infrared (9) techniques. The difficulties were resolved by the closed system for continuous analysis shown in Figure 3. A diaphragm pump (with all parts that contact the electrolyte made of Teflon, except the Hasteloy C balls in the check valves) circulates the electrolyte to an Infracord through FEP or Kel-F tubing. The cells, shown in Figure 4, are made of tubing compressed to a thickness of about 2 mm between CaF_2 plates. The H_2O absorption is measured at 1.95μ, and to increase the sensitivity, a metal screen is placed at the widest aperture of the reference beam to balance the instrument to near full-scale reading when the cell containing the dry electrolyte is in the sample beam. However, because a gradual fogging of the tubing and the CaF_2 plates causes all cells to show a slow shift in base line, the usual absorbance vs. concentration calibration cannot be used. Instead, a "compensated" transmittance (Tc) vs. concentration was calculated from the absorption at 1.12μ, where H_2O does not absorb:

$$Tc = \frac{\%T \text{ 1.95}\mu \text{ of electrolyte vs. screen}}{\%T \text{ 1.12}\mu \text{ of electrolyte vs. air}}$$

The motor-driven syringe (Figure 3) is used to add H_2O to the electrolyte and thus to maintain a constant H_2O concentration during electrolysis.

Hydrogen peroxide is a possible component of the electrolyte, but, if present, its maximum concentration did not exceed 0.005 mole %. Our tests showed that added concentrations of 0.05 mole % had a negligible effect on the 1.95μ absorption.

Although KF does absorb at 1.95μ, its concentration was held constant and therefore was not a problem.

RESULTS

One of our early experiments to determine the effect of H_2O concentration on the product distribution is shown in Figure 5. Here, electrolysis was continuous and H_2O was added incrementally. The OF_2 yield dropped very rapidly as H_2O increased beyond about 0.5% and then leveled out at 7-10% OF_2. Ozone increased as OF_2 decreased and appeared to pass through a broad maximum. Oxygen apparently is largely independent of the other products, since it remained constant at 45-50%. Current efficiency for H_2 and total anode gas decreased as H_2O increased, possibly because the cathode was depolarized by dissolved anode products.

Figure 6 shows three sets of data for OF_2 yields. Curve A is the same run shown in Figure 5. Curve B is also a continuous run, except that the H_2O concentration of the electrolyte was high initially and then decreased as H_2O was consumed. Curve C is a run in which electrolysis was stopped after each sample had been taken for gas analysis, and H_2O was added before electrolysis was continued. Among these runs the yield of OF_2 was not the same at a given H_2O concentration and appeared to depend on the manner of operation. All three curves show maximum OF_2 yields over a narrow range of H_2O concentration centering below 1.0%. At higher H_2O levels, the interrupted electrolysis gave better OF_2 yields than the continuous. Continuous electrolysis at high H_2O concentration does not permanently affect the anode, because high OF_2 yields were restored as the electrolyte dried (Curve B).

Figure 7 (Run 1) shows the effect of time on OF_2 yield during continuous electrolysis at 0.56 mole % H_2O. A fairly constant (35-36%) yield was obtained for about 3 hours, and then a sharp unexplained drop occurred. There was no break in the current density that might indicate an anode surface change. Even the 3-hour plateau was not reproducible, because the next run (Run 2) showed OF_2 yields that fell rapidly from the start. Nevertheless, the interrupted operation gave higher OF_2 yields, in that Run 2 started off at the same OF_2 yields as did Run 1. Thus the system showed no permanent effect from a run that lasted many hours and ended with a low OF_2 yield. The O_2 and O_3 showed slight increases with time, while H_2 was reasonably constant at 85-90% at this low water level. As anode total is less than H_2, some unidentified anode products are possible.

The consistent pattern in which off-on operation gives higher OF_2 yields suggested operating with planned interruption. The result was not only a higher OF_2 yield but a more constant yield with time (Figure 8). Moreover, only the OF_2 yields were higher; O_2, O_3, H_2, and current density were lower. The small effect of H_2O on OF_2 yields in this concentration range was consistent with the earlier results (Figure 5).

DISCUSSION

The high (45+%) OF_2 yields that we have observed for long periods (3-4 hours) show that we are approaching the consistent operation necessary for synthesis or detailed mechanism studies. Achieving maximum yields will require study of variables other than water.

In addition to yields, current density and anode life are also important in the evaluation of an electrochemical synthesis. Although the current density should depend on electrolyte concentration and should drop as water (a strong electrolyte in HF) is consumed in the electrolysis, it does not always. Instead for the first 15-30 minutes of electrolysis, whether or not water concentration is maintained, the current density increases in both continuous and interrupted electrolysis. This may be due to a breakdown in a resistive anode coating. Once

a maximum current is reached, the current density remains constant; however, it drops as the last few tenths percent water is consumed. Also, high water levels (> 3%) cause low current densities. The maximum current densities were noted at 0.5 to 1.0 mole % water.

We have observed that nickel anodes lose weight at low water concentration during continuous electrolysis:

Mole % H_2O	Volts	Faradays cm^2	OF_2 Yield % of Current	Weight Loss % of Current
		Mostly Continuous Operation		
0.2	5.0 - 8.2	.0132	6.0	5.0
0.2 - 0.5	7.6	.0324	20 - 47	1.0
0.5 - 1.5	7.6	.0670	25 - 10	.01
		Automatic Interrupted Operation		
0.32	7.0	.0398	35 - 46	none
0.62	7.0	.1084	30 - 45	none

The surface of the nickel anode is quite different when electrolyzed at below 0.2% water, where F_2 is generated, and at higher water, where little or no F_2 is made. At low water a flaky deposit is formed, while at higher water a thin, uniform, adherent deposit is formed. At low water NiF_2 and $KNiF_3$ were detected by x-ray and electron diffraction, while only NiF_2 was found at higher water. Electron microscopy indicates a soft, porous, microcrystalline NiF_2 film when compared to that produced by action of F_2 on nickel at high temperature (10). With interrupted operation no weight losses were found at comparable water levels and faradays. However, the lower voltages and improved H_2O control may have also contributed to anode stability. While the times here (10-30 hours) are short, the data indicate that anode life should be long.

The anode is a key component in the electrolysis. The surface influences product formation and at the same time is influenced by electrolysis reactions. The restoration of high OF_2 yields as excess H_2O is electrolyzed away (Figure 6, Curve B) indicates that the surface is formed reversibly. The nickel-nickel fluoride anode is unique and essential to OF_2 formation. We have found other metals (Cu, Al) either passivate completely and require very high voltages, or disintegrate (Pt) rapidly (11). Only O_2, no O_3 or OF_2, was found with these metals. The nature of changes in the nickel-nickel fluoride anode surface, such as occur during start-up, is still uncertain. Several possibilities exist, i.e., mechanical break-up of the film, different forms of NiF_2 (α, β, γ) (12), or mixed oxide-fluoride films.

Speculation (13) on electrochemical fluorination considers free F_2 as a possible intermediate in product formation. Our data appear to eliminate this route for OF_2. In cases where F_2 is found in the products, adding H_2O does not increase OF_2 yields until the current is interrupted. Another route to OF_2 is fluorination of water by K_2NiF_6 or K_3NiF_6 in the film. However, this path is unlikely because K_2NiF_6 and K_3NiF_6 react with water to give only O_2 (14).

The formation of O_3 along with OF_2 and the absence of O_3 as well as OF_2 with anodes other than nickel suggest that the oxygen atom is a reaction intermediate. Increase in O_3 yield when OF_2 yield drops suggests that oxygen atoms are being diverted from OF_2 to O_3 formation. Further study may reveal the precise nature of the intermediate species.

The overall current yield of OF_2 and conversion of HF to OF_2 are higher with the one-step electrolysis than the two-step process of reacting F_2 with base:

	Current Efficiency for OF_2	Conversion of HF to OF_2
$HF \xrightarrow[\text{elect.}]{98\%(15)} F_2 + OH^-$; $OH^- \xrightarrow{60\%(1b)} OF_2 + 2F^- + H_2O$; $OH^- \xrightarrow{40\%} O_2 + 2F^- + H_2O$	< 30%	30%
$HF + H_2O \xrightarrow[\text{elect.}]{} OF_2 + O_3 + O_2$	45%	100%

Therefore in our opinion, much lower cost OF_2 would result from a development of this electrolysis. Our present study has provided the necessary analysis, control techniques, and yield data and has indicated areas for further possible improvements.

ACKNOWLEDGMENT

We thank W. A. Wilson for suggesting the study of wet HF electrolysis, and J. Markovich, F. S. Jones and R. R. Hopkins for help in various parts of the program.

REFERENCES

1. a) E. G. Haberman, Chem. Eng. Prog. 60, No. 7, 72 (July 1964).
   b) A. G. Streng, Chem. Rev. 63, 607 (1963).
2. D. M. Yost and G. H. Cady, Inorganic Synthesis, Vol. I, 109 (1939).
3. a) P. Le Beau and A. Damiens, Comp. Rend. 185, 652 (1927).
   b) H. Emeleus, J. Chem. Soc. 441 (1942).
   c) R. C. Downing, et al, Ind. Eng. Chem. 39, 259 (1947).
   d) J. H. Simons, et al, J. Electrochem. Soc. 95, 47 (1959).
4. a) W. T. Grubb, U.S. Patent No. 2,716,632 (1955).
   b) H. Schmidt and H. D. Schmidt, Z. Anorg. Chem. 279, 289-299 (1955).
5. A. Engelbrecht and E. Nachbaur, Monatsh, Chem. 90, 367-370 (1959).
6. a) G. A. Cook, et al, Ozone Chemistry and Technology, Advances in Chemistry Series, Vol. 21, p. 44, ACS Publications, Washington, D. C. (1959).
   b) J. A. Donohue and W. A. Wilson, U.S. Patent 3,134,656 (1964).
7. C. E. Thorp, Bibliography of Ozone Technology, Vol. 1, Armour Research Foundation, Chicago, Illinois (1954).
8. J. Mitchell and D. M. Smith, Aquametry, Interscience Publishers, Inc., New York (1948) p. 243.
9. a) H. H. Hyman, M. Kilpatrick, and J. J. Katz, J. Am. Chem. Soc. 79, 3668 (1957).
   b) R. H. Maybury, J. J. Katz, and S. Gordon, Rev. Sci. Inst. 25, 1133 (1954).
10. a) R. L. Jarry, et al, J. Electrochem. Soc. 110, 346 (1963).
    b) C. F. Hale, et al, AEC Report No. K-1459, Union Carbide Nuclear Co. (1960).
11. The FO Radical and High Pressure Reactions of N_2F_2-Quarterly Reports. Contract No. DA-31-124-ARO(D)-78, American Oil Company (1963) ARPA Order 402, Task 3
12. A. F. Clifford and A. C. Tulumello, J. Chem. Eng. Data 8, 425 (1963).
13. J. Burdon and J. C. Tatlow, Advances in Fluorine Chemistry, Vol. 1, p. 160, Butterworth Scientific Publications, London (1960).
14. Progress in Inorganic Chemistry F. A. Cotton, Vol. II, p. 200, Interscience Publishers, Inc., New York (1960).
15. A. P. Huber, J. Dykstra and B. H. Thompson, Proc. of 2nd U. N. International Conference on Peaceful Uses of Atomic Energy, Vol. 4, pp. 172-80 (1958).

FIGURE 1

HF ELECTROLYSIS CELL

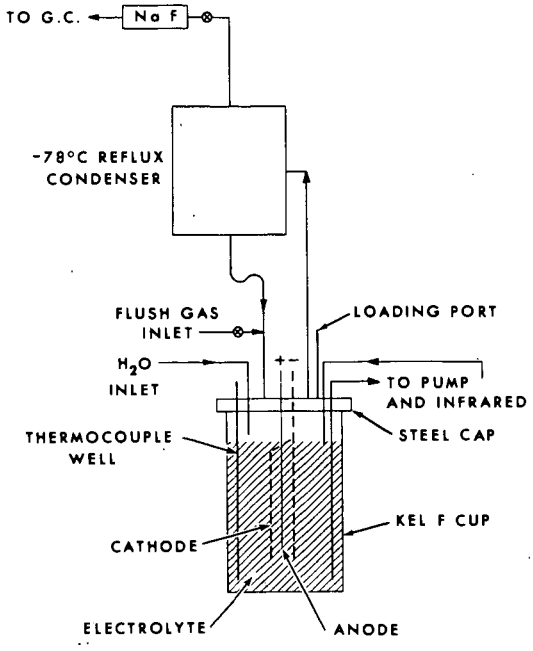

FIGURE 2

LOW TEMPERATURE PROGRAMED GAS CHROMATOGRAPH

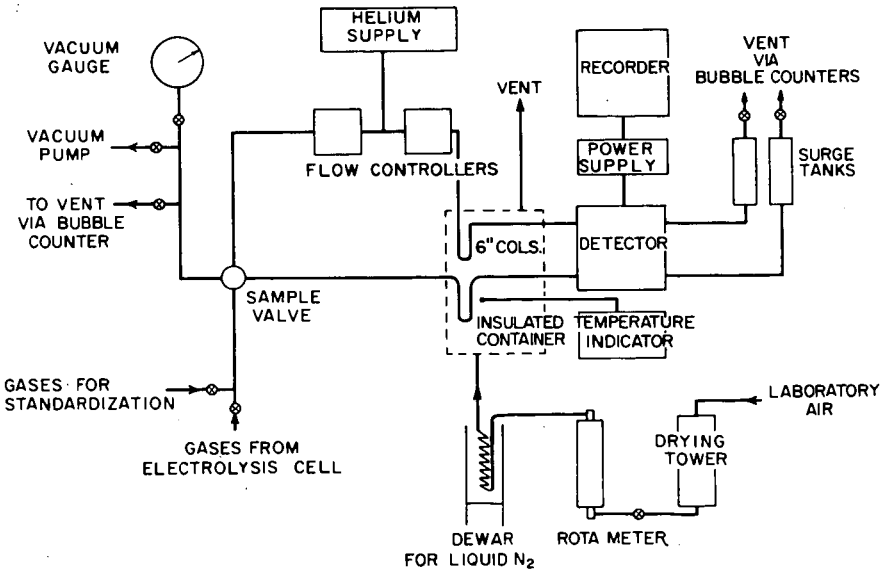

FIGURE 3

ARRANGEMENT FOR CONTINUOUS WATER CONTROL AND ANALYSIS BY INFRARED

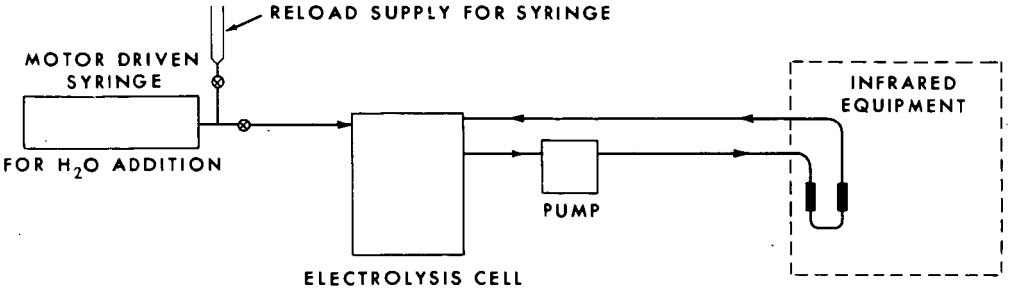

FIGURE 4

INFRARED CELL

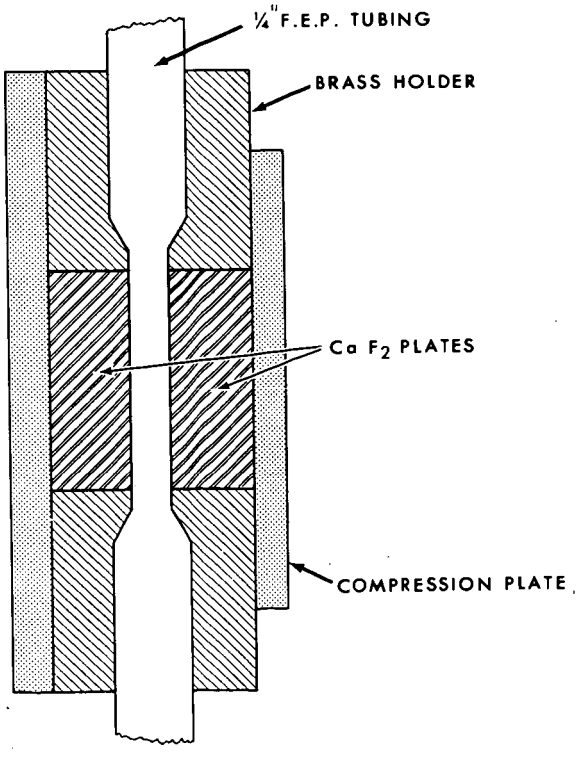

FIGURE 5

YIELDS AT CHANGING WATER CONCENTRATION

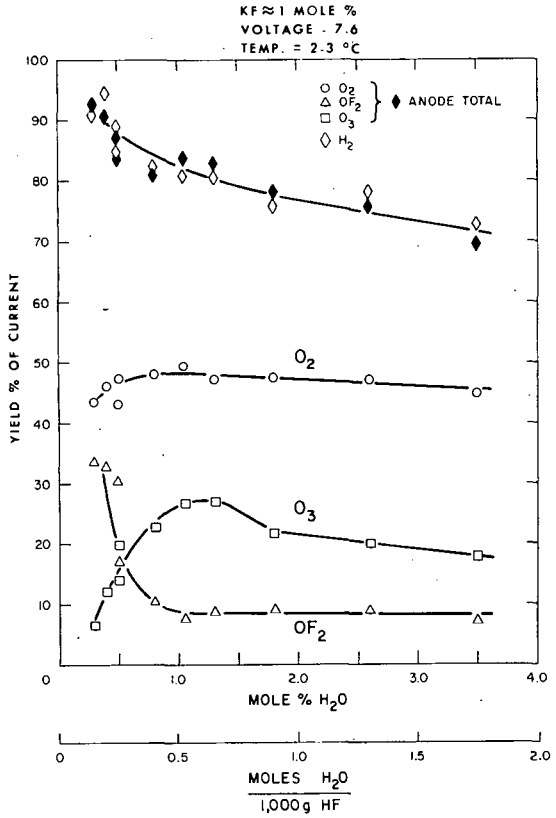

FIGURE 6

OF_2 YIELDS AT CHANGING WATER CONCENTRATION

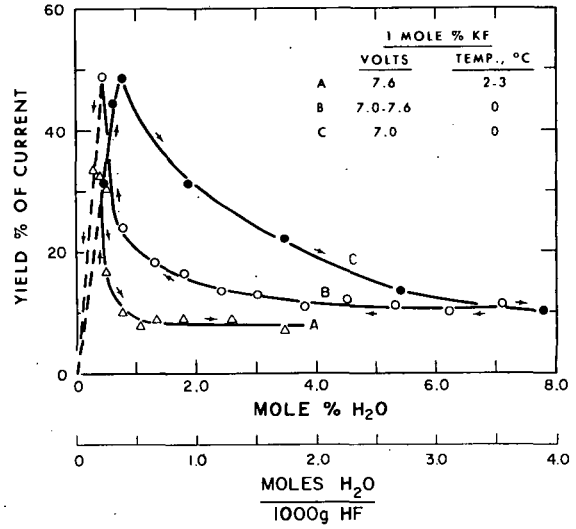

FIGURE 7

CONTINUOUS ELECTROLYSIS

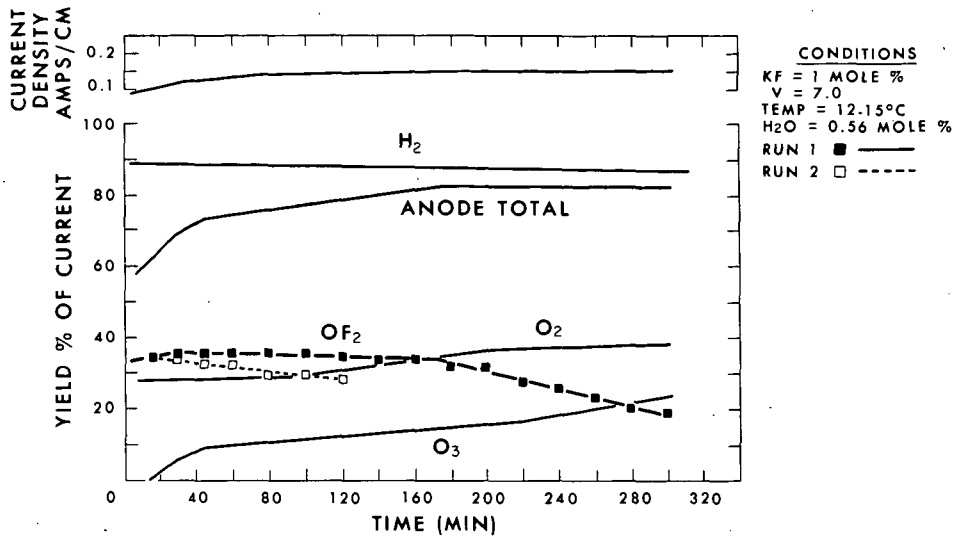

FIGURE 8

INTERRUPTED ELECTROLYSIS

RUN NO.	KEY	MOLE % H_2O	INTERRUPTION RATE
1	■ ——	0.62	1/60
2	— — — —	0.56	NONE CONTINUOUS
3	□----------	0.31	1/60

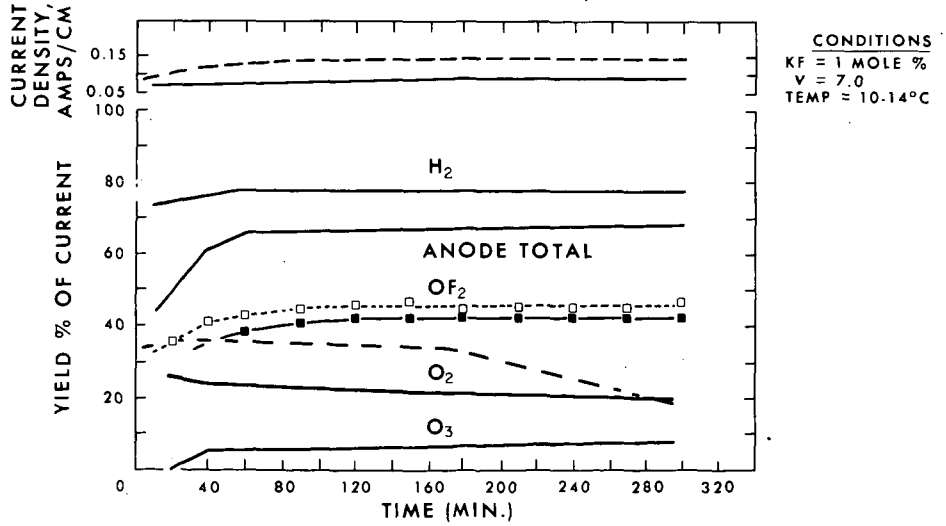

ELECTRON PARAMAGNETIC RESONANCE SPECTRUM OF LIQUID OXYGEN DIFLUORIDE(1)

F. I. Metz, F. E. Welsh, W. B. Rose

Midwest Research Institute
425 Volker Boulevard
Kansas City, Missouri 64110

INTRODUCTION

The electron paramagnetic resonance spectrum of liquid oxygen difluoride has been determined in conjunction with a study of the structure of liquid inorganic oxidizers. Pure liquid OF_2 exhibited no EPR signal when condensed in the absence of light. Upon photolysis, a strong doublet with a hyperfine splitting of 13.5 gauss and a g-value of 2.0036 was obtained. Concentrations were on the order of 10^{16} unpaired electrons per sample. Oxygen difluoride is a colorless gas at room temperature, and a pale yellow liquid below 128°K, its normal boiling point. It is relatively stable, with thermal decomposition beginning at about 200 - 250°C. OF_2 is nonlinear, with two equivalent O-F bonds having an FOF angle of angle of 104°.

EXPERIMENTAL

Electron Paramagnetic Resonance

EPR measurements were made using a Varian V-4502 X-band spectrometer equipped with a 6 in magnet and using 100 kc field modulation. Frequencies used were of the order of 9.1 Gc. The sample tube was a 3.0 mm I.D. quartz tube connected to a stopcock and a male ground glass joint by means of a graded seal. Sample volumes were of the order of 0.05 ml. For measurements at 77°K, the sample tube was placed in a small quartz dewar which was inserted into the cavity. Measurements in the range from 88°K to 138°K were made using a V-4557 variable temperature accessory. Peroxylamine disulfonate in a capillary affixed to the outside of the dewar was used for the scan calibration and as a standard for the g-value determination. The total width of the peroxylamine disulfonate spectrum was taken to be 26.0 gauss and the g-value used was 2.0055 (2). The frequency was determined with a Hewlett-Packard Model X-532B wavemeter. The g-value of polycrystalline DPPH was determined as a check on the procedure. Concentration measurements were made relative to a Varian 0.1 per cent pitch sample in KCl, with the number of spins taken to be $3 \times 10^{+15}$ spins/cm length of sample. The accuracy of this value is estimated to be ±25% (3). However, we are more interested in relative values of the intensities of the OF_2 spectra at various temperatures (compared with the same pitch standard) than we are in absolute values of the spin concentrations.

Photolysis studies were performed using a PEK-110 100 watt high pressure mercury arc lamp. The 3660 angstrom line was selected by means of a Bausch and Lomb second order interference filter.

Purification

The OF_2 was bled slowly from the storage tank through an HF trap and condensed on the cold vertical column. The HF trap removed hydrogen fluoride and silicon tetrafluoride (4), while the cold column separated any carbon dioxide present. This vertical column was at 77°K and jacketed with a dewar. The OF_2 condensed and drained below the cold region of the tube where it refluxed and slowly distilled into the first liquid nitrogen trap. Following Schoenfelder's procedure for N_2F_4 (5), the OF_2 was chromatographed. Table I shows the relative elution times of the impurities found to be present. Prior to the introduction of the helium carrier gas, it was passed through reduced copper oxide wire at 500°C (6) to remove oxygen and Linde molecular sieve to remove H_2O.

TABLE I

RELATIVE ELUTION TIMES ON ½" x 10' SILICA GEL COLUMN, FLOW RATE, 150 ml/min

Substance	Elution Time of Maximum (min)
O_2	4.7
N_2	5.1
OF_2	10.8
F_2	13.0
CF_4	16.5
CO_2	120.0
SiF_4	>120.0

Chemicals

The copper oxide wire was Mallinckrodt reagent grade. The molecular sieve was Linde 5A 1/16-in pellets. The OF_2 was obtained from Allied Chemical Corporation and was approximately 93 per cent pure. The silica gel (60/80 mesh) was purchased from Matheson Company.

RESULTS

No EPR signal was obtained on samples of liquid OF_2 prepared in the absence of light. Liquid OF_2 taken directly from the tank in the presence of room light showed a fairly strong, complex signal with a total linewidth of about 100 gauss. Similar results were obtained from OF_2 which had been swept through an HF trap and subsequently distilled.

A sample of chromatographed liquid OF_2, prepared in the absence of light, showed a strong doublet (Fig. 1) with a splitting of 13.5 gauss when photolyzed. The linewidth is temperature dependent with values in the range of 1.6 - 3.6 gauss. The line center of the doublet has a g-value of 2.0036 ± 0.0003. The line shape

closely approximated a Lorentzian curve. The spectra were examined at various modulation amplitudes and microwave power levels in order to ensure that no distortion due to overmodulation or power saturation occurred. The intensity of the doublet increased with time during photolysis. The concentration of paramagnetic species was calculated to be on the order of 10^{16} unpaired electrons per sample, corresponding to a concentration of about 0.001 mole per cent. An EPR spectrum of chromatographed liquid OF_2 prepared in normal room light was the same as that obtained from the photolyzed samples.

The change of the signal intensity with photolysis is shown in Fig. 2 for a number of temperatures. The rate of formation of the radical species increased with temperature. The signal intensity behavior after photolysis was strongly temperature dependent. At 77°K the signal strength increased rapidly after the lamp was turned off, then more slowly. At intermediate temperatures, 87°K, 100°K, and 105°K; the intensity leveled off after photolysis. The curves fall off more rapidly at 121°K in the absence of light. The decay at 77°K did not proceed to zero intensity, but usually reached a value which persisted even after several days storage of the sample in the dark. The signal may be caused to vanish, or at least reach a very low level by vaporization and recondensation of the sample in the absence of light.

Figure 3 shows the signal strength as a function of continued photolysis at 77°K. A peak concentration was reached at about 10 min photolysis, after which time additional photolysis produced a diminution of the signal. At $24\frac{1}{2}$ min, the signal strength corresponded to approximately 10^{12} unpaired electrons. After the lamp was extinguished, the concentration immediately increased to a value on the order of 5×10^{13} unpaired electrons. The concentration continued to increase in the absence of light. If the sample was irradiated again, the signal level rapidly dropped to the previous low value.

In general, the intensity of the EPR resonance increased with continued photolysis, reached a maximum, and dropped to a very low level. The intensity at the maximum was temperature dependent. In a series of experiments, spectra of OF_2 were taken during $7\frac{1}{2}$ min of photolysis and afterwards in the absence of light for sufficient time to observe trends in the signal intensity. The rate of formation increased with temperature. After the photolysis lamp was turned off, the intensity increased, leveled off gradually, or decreased more rapidly, depending on the temperature.

The effect of the presence of oxygen on the results of these experiments is difficult to assess at this time. However, since it is possible that oxygen may alter the mechanism of the photolytic reactions, or may broaden the EPR signal, rigorous measures described above were undertaken to affect its removal.

DISCUSSION

The lack of an EPR signal in the spectra of samples chromatographed in the absence of light is strong evidence that liquid OF_2 is not paramagnetic. In addition, one would expect a hyperfine triplet from a paramagnetic species such as $OF_2\cdot$,

rather than the observed doublet. Considering the system involved, a doublet could arise from $O_xF\cdot$ or $F\cdot$ radicals, due to hyperfine interaction with a fluorine nucleus which has a spin of $\frac{1}{2}$. However, it is to be expected that the fluorine atom would react (to form F_2) much more rapidly than would the $O_xF\cdot$ radical. The fluorine radical has not been observed in the condensed phase, but has ben observed in the gas phase as six well-spaced resonances with a g-value of 4/3. At a frequency of 9.249 Gc, 4,159 gauss was the lowest value of the magnetic field at which a resonance occurred (7).

We have studied the EPR of liquid F_2 at 77°K. Tank fluorine and fluorine run through an HF trap and distilled have exhibited a weak signal with a linewidth of about 75 gauss and a g-value near 2.0. The signal strength increased with photolysis and seemed to broaden. It is probable that the observed resonance in liquid fluorine was due to impurities. Present efforts to chromatograph liquid fluorine are being made more difficult by the high vapor pressure (280 mm Hg) of F_2 at 77°K.

The small value of the coupling constant in OF_2 (13.5 gauss) is not what one would expect from hyperfine interaction of an electron with a fluorine radical. As a comparison, the hyperfine splitting due to two equivalent fluorine nuclei in liquid $NF_2\cdot$ is 64 $\pm$2 gauss (8). The hyperfine interaction due to a fluorine radical should be large, since the value calculated by assuming that the unpaired electron was wholly in the 2s orbital of the fluorine atom is 17,050 gauss (9). From a consideration of the above arguments, it is quite probable that the unpaired electron species observed in the present study is $O_xF\cdot$, and not $F\cdot$.

The EPR spectra of the higher oxygen fluorides (O_2F_2, O_3F_2, and O_4F_2) have been studied by Kirshenbaum and Grosse (10). They have observed two EPR signals from samples of O_2F_2 at 77°K. The resonances were assigned to the presence of intermediates in the decomposition $O_2F_2 \longrightarrow O_2 + F_2$ rather than to O_2, F_2, or O_2F_2 itself. The stronger of the two signals has been interpreted in terms of the presence of a radical with one unpaired electron, having a hyperfine interaction with only one fluorine nucleus. $O_2F\cdot$ was considered to be a likely possibility. The weaker resonance is associated with the presence of a radical in the triplet state.

The EPR spectrum of O_3F_2 showed (10) the same resonances as were obtained from O_2F_2, except that the intensity of the stronger signal in the case of O_3F_2 was 50 - 100 times greater than the intensity of the corresponding resonance in O_2F_2, while the triplet resonance in O_3F_2 is only twice as intense as the triplet resonance in O_2F_2. The strong signal in O_3F_2 was also assigned to the $O_2F\cdot$ radical. Contamination of the O_2F_2 with O_3F_2 was ruled out by the observation of the resonances after the O_2F_2 sample had been heated above the decomposition temperature of O_3F_2.

O_4F_2 was found to be paramagnetic (10). The EPR spectrum at 77°K consisted of a strong doublet with an average g-value of 2.009 and a doublet separation on the order of 13 gauss. In view of the dissimilarity between the spectrum of O_4F_2 and the spectra of O_2F_2 and O_3F_2, it was unlikely that the paramagnetic species in O_4F_2 was the $O_2F\cdot$ radical.

The EPR spectrum of O_3F_2 at 90°K has also been investigated by Maguire (11). A doublet with a splitting of 13.6 gauss and a g-value of 1.975 was obtained. These results have been interpreted in terms of diradical O_3F_2 being the paramagnetic species involved. One unpaired electron is thought to be localized near each of the fluorine nuclei. The coupling between the two fluorine nuclei is considered to be weak, or zero.

Considering the results of the above investigations (10,11), it is highly probable that the radical species present in photolyzed OF_2 is OF·, via the dissociation $OF_2 \xrightarrow{h\upsilon} OF\cdot + F\cdot$. However, we cannot uniquely identify the number of oxygens on the radical at this time. $^{17}OF_2$ is being prepared to make possible a more unambiguous identification of the paramagnetic species in photolyzed liquid OF_2.

The kinetics of the photolysis suggested the following as possible reactions:

(1) $OF_2 \xrightarrow[\text{chain}]{h\upsilon} OF\cdot + F\cdot$

(2) $2\,F\cdot \longrightarrow F_2$

(3) $OF\cdot + M \xrightarrow{h\upsilon} R$

(4) $OF\cdot \xrightarrow{h\upsilon} R'$

(5) $OF\cdot + N \longrightarrow R''$

As the temperature is increased, the photolysis proceeds more rapidly. More energy is available to increase the rate of reaction (1). In addition, dependent upon the temperature, reaction (1) will also proceed (via a chain mechanism) in the absence of light. Hence, a continued increase in the rate of formation at 77°K after the lamp is extinguished is observed. Reaction (3) and/or reaction (4) are the photolytic decay schemes which compete with reaction (1) when the lamp is on. With the lamp off at 77°K, the rate of formation increases rapidly for a short while, then drops back to a lower rate. This behavior can be explained by the fact that reactions (3) and (4) are not operating in the absence of light. Other, slower, temperature dependent decay schemes may be operation, i.e., reaction (5).

At higher temperatures (87°K, 100°K, 105°K), the decay of the signal is slow in the absence of light. Finally, at 120°K, the signal decays more rapidly after photolysis. The rate of the decay reactions was both temperature and photolytically dependent.

Figure 3 shows that continued photolysis caused the signal to reach a very low level. Thus, there must be a critical concentration which allowed the decay processes to predominate over the formation reactions.

SUMMARY

This study has established that oxygen difluoride dissociates photolytically into a paramagnetic species in which there is a hyperfine interaction between the unpaired electron and one fluorine nucleus. The photolytic rate of formation of the radical species increased with temperature. The behavior of the signal intensity in the absence of light after photolysis was also temperature dependent. The kinetics have been interpreted in terms of photolytic formation and decay schemes. The radical has been characterized by means of the EPR spectrum, but not identified. However, the characteristics of the spectrum indicated that the radical was OF·, rather than a higher oxygenated species or F·.

REFERENCES

1. This research was sponsored by the Advanced Research Projects Agency, Washington, 25, D.C., and was monitored by Rocket Propulsion Laboratories, Edwards, California, under Contracts Nos. AF 04(611)-9372 and AF 04(611)-10215.

2. Varian Associates, EPR at work No. 28.

3. Instruction Manual for V-4502 EPR Spectrometer Systems, p. 5-11, Varian Associates, Palo Alto, California.

4. A. G. Streng, Chem. Rev., 63, 607-624 (1963).

5. C. W. Schoenfelder, J. of Chromatography, 7, 281 (1962).

6. K. A. C. Elliott, Can. J. of Research, 27F, 299 (1949).

7. N. Vanderkooi, Jr., and J. S. MacKenzie, Adv. Chem. Series, 36, 98 (1962).

8. H. E. Doorenbos and B. R. Loy, J. Chem. Phys., 39, 2393 (1963).

9. J. R. Morton, Chem. Revs., 64, 453 (1964).

10. A. D. Kirshenbaum and A. V. Grosse, Temple Research Institute, "Production, Isolation, and Identification of the OF·, O_2F·, and O_3F· Radicals," Contract No. AF 04(611)-9555, First, Second, and Third Quarterly Progress Reports; Dec. 31, 1963; March 31, 1964; and June 30, 1964.

11. R. G. Maguire, Armour Research Foundation, "Determination of the Structure of O_3F_2," ARL Technical Report 60-287, Contract No. AF 33(616)-6433, August 1960.

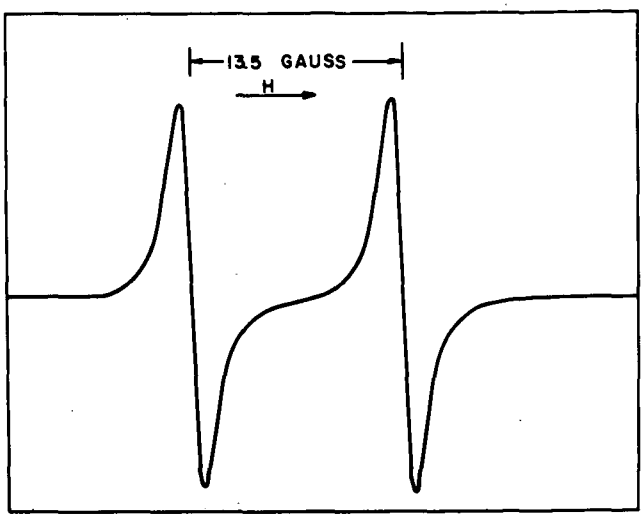

FIG.-1 EPR SPECTRUM OF LIQUID OF_2 AT 77°K

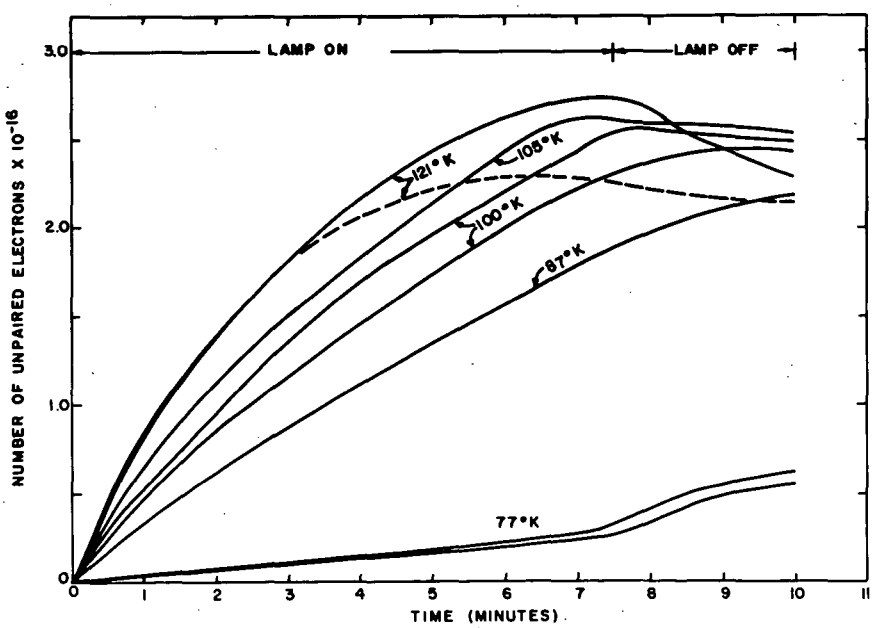

FIG.-2 PHOTOLYSIS OF LIQUID OF_2 AS A FUNCTION OF TEMPERATURE

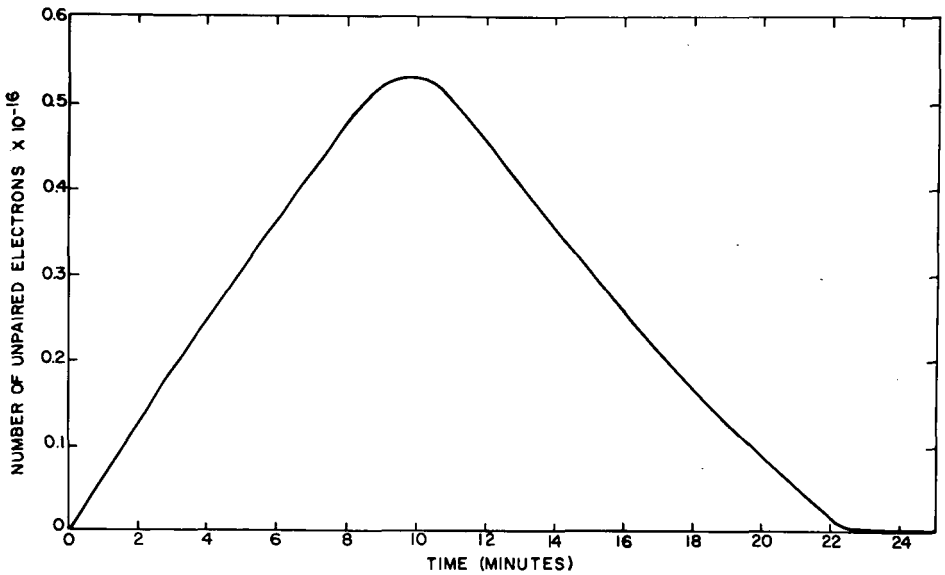

FIG-3 CONTINUED PHOTOLYSIS OF LIQUID OF_2 AT 77°K

THE HEAT OF FORMATION OF OXYGEN DIFLUORIDE

Warren R. Bisbee
Janet V. Hamilton
Ronald Rushworth
Thomas J. Houser
John M. Gerhauser

Rocketdyne
A Division of North American Aviation, Inc.
Canoga Park, California

INTRODUCTION

The currently accepted value of the O-F bond energy (-45 kcal/mole) is calculated from the standard heat of formation of OF_2 (+7.6 kcal/mole) which was based on an average of three values obtained in 1930, (5,6) the precision of which was quite poor. To determine a more reliable heat of formation of OF_2 and thus a better O-F bond energy, the heat of reaction of the following system was measured:

$$OF_2 + 2H_2 \longrightarrow H_2O + 2HF \text{ (infinite dilution)}$$

EXPERIMENTAL

MATERIALS

The OF_2 was obtained from the Allied Chemical Company. An assay found it to be greater than 99 percent pure. Active fluoride was analyzed by an iodometric method. By an infrared analysis 0.22 percent CO_2 and 0.02 percent CF_4 were found; SiF_4 was not detectable.

The hydrogen was a prepurified grade obtained from the Matheson Company.

APPARATUS AND PROCEDURE

The thermochemical measurements were made using a Parr fluorine combustion bomb and a Bureau of Standards calorimeter. The bomb cylinder and all internal parts of the bomb were monel. A monel ampoule was fitted into the top of the bomb to retain the OF_2 sample. The ampoule apparatus reduced the internal volume of the bomb to 315 cc. A diagram of the ampoule is given in Fig. 1 and 2.

The internal volume of the ampoule was found to be 8.7 cc. The top of the cylinder body and the cylinder head were designed with a 30-degree angular seat to accommodate a 1/2-inch monel burst diaphragm. A mechanism, which fits inside the bomb, was designed to rupture the burst diaphragm in the ampoule. This consisted of a piston with a knifelike wedge head (Fig. 3) and a small spring made from spring-tempered monel wire. The piston and spring were held in a compressed position by nickel-chromium alloy fuse wire of known calorific value, which was strung between the two internal electrodes in the bomb. A pinpoint breaker was also tried, however, because it merely punctured a small hole in the diaphragm, it increased the chance of obtaining incomplete combustion and was unsatisfactory.

The OF_2 sample was condensed in the ampoule which was then attached to the bomb head. Fifty ml of water were placed in the bomb to absorb the HF formed during reaction and thus reduce corrosion. The reaction bomb was assembled, pressurized with hydrogen (75.0 psig) and sealed. To start the reaction the sample was released into the hydrogen by electrically fusing the nickel-chromium alloy wire. This released the piston which ruptured the diaphragm and allowed the reactant gases to mix. Combustion occurred rapidly and completely; the temperature rise of the calorimeter

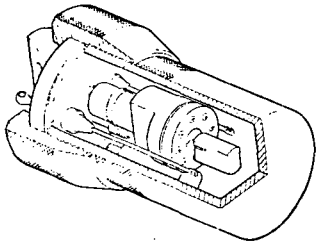

FIGURE 1

Nickel Parr Combustion Bomb with Sample Ampoule

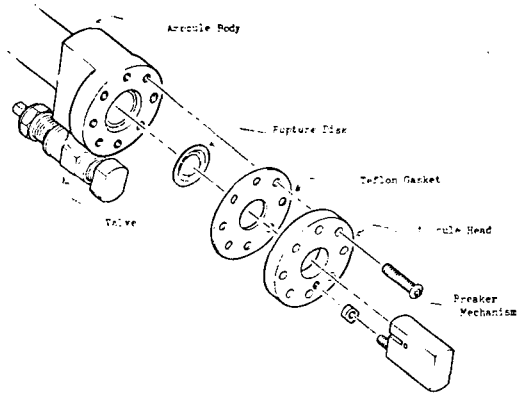

FIGURE 2

Ampoule, Exploded View

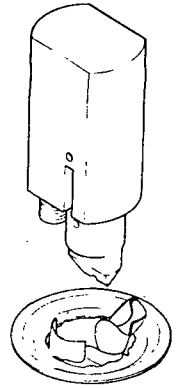

FIGURE 3

Effect of Wedge Breaking Mechanism on Rupture Disk

was measured by means of a platinum resistance thermometer constructed and calibrated by the Leeds and Northrup Company. The thermometer, of the four-lead cable type, was used in conjunction with a Leeds and Northrup G-2 Mueller Bridge and a high sensitivity galvanometer.

Dickinson's method was employed in order to obtain the corrected resistance change (1).

To check the mass balance of the reaction, the reaction products were analyzed after each run by a thorium nitrate method for fluoride and by a sodium hydroxide titration for hydrogen ions.

The analyses were within experimental error, but were always lower than stoichiometric for each OF_2-H_2 run. It was believed the approximate 5% of HF unaccounted for was consumed in the slight corrosion of the stainless-steel screw heads in the ampoule. Qualitative analysis of the screw heads did show the corroded film on the screws was the metal fluorides. The necessary thermal corrections were made on the data for this side reaction, which amounted to the formation of roughly 0.0015 mole of iron and chromium fluorides. As an additional check, a OF_2-H_2 run was made with the stainless-steel screws replaced by nickel-plated steel screws. No corrosion was found with the new screws and the heat of reaction agreed, within experimental error, with the results which had been corrected for the small amount of corrosion.

CALIBRATION

The energy equivalent of the calorimeter was determined by burning National Bureau of Standards Sample 39h benzoic acid. Its heat of combustion per gram under standard conditions at 25° was reported as 26,434 abs. j/g mass (weight in vacuo) with an estimated uncertainty of ±3j/g. This value was converted (3) to the bomb conditions used throughout this investigation and found to be 26,432.8 abs. j/g.

In a series of five calibration determinations, the mean energy equivalent for the system was 48,533.4 ±6.5 calories/ohm.

RESULTS AND CALCULATIONS

The data are referred to a standard temperature of 25°. The energy unit used is the calorie which is defined as equal to 4.1840 absolute joules.

The quantity of heat observed during the reaction, Q, was calculated from equation (1):

$$Q = (E_s + \Delta e_2)\,\Delta R_c \qquad (1)$$

where E_s is the energy equivalent of the calorimeter; Δe_2 is a correction for deviations from the standard calorimeter system and was computed from the heat capacities of OF_2, H_2, and H_2O; and ΔR_c is the corrected temperature rise. The value of the heat capacity of OF_2 was taken as 10.35 cal/deg-mole (2).

The heat of reaction per mole in the thermodynamic standard bomb process, ΔE°_R, was calculated for each experiment from equation (2):

$$-\Delta E^\circ_R = (Q - q_1 - q_2)/n \qquad (2)$$

where q_1 includes corrections for nonideality of the reactant gases, condensation of water in the vapor phase, and heat of dilution of the HF solution to infinite dilution; q_2 is the energy supplied by the corrosion of the screw heads; and n is the number of moles of OF_2. This value was reduced to the standard heat of reaction at 25°C. The calculation of ΔH°_R from ΔE°_R was done in two steps:

a) Heats of reaction at 28°C were calculated from the energy of reaction

using the thermodynamic equation $\Delta H_R^o = \Delta E_R^o + \Delta nRT$ where Δn is the change in the number of moles of gaseous substances during reaction.

b) Heats of reaction at 25°C were calculated from the equation ΔH_R^o (298.16°K) = ΔH_R^o (301.16°K) + ΔC_p (298.16-301.16) where ΔC_p is the difference in the heat capacity at constant pressure of the products and reactants.

The results of the experiments with OF_2-H_2 are given in Table I.

The average value of ΔH_R^o for OF_2-H_2 is 222.93 ±0.76 kcal/mole.

DISCUSSION

Based on the measured value of the standard heat evolved from the reaction:

$$OF_2\ (g) + 2H_2\ (g) \longrightarrow H_2O\ (l) + 2HF\ (\text{infinite dilution})$$

and combined with existing thermodynamic data (4) the calculated standard heat of formation, ΔH_F^o, of OF_2 (g) is -4.40 ±0.82 kcal/mole.

The uncertainty in the heat of formation was calculated by taking the square root of sum of the squares of the precision error, the accuracy error, and the calibration error. The precision error reflects the reproducibility of the experiments and was taken as twice the standard deviation. The accuracy error was obtained by estimating the effect of the various factors on the reaction (such as purity of reactants and limits of error involved in the analyses).

The heat of formation value, combined with the most recent bond dissociation energies for fluorine and oxygen as listed in the JANAF thermochemical tables (2), yields a value of -50.8 kcal for the O-F bond energy in OF_2.

ACKNOWLEDGMENT

We wish to acknowledge the assistance of Dr. Neal N. Ogimachi who synthesized the OF_2 used in preliminary runs and helped in loading the ampoule. The support of the research by the Air Force under contracts AF33(616)-6768 and AFO4(611)-7023 is gratefully acknowledged also.

TABLE I

DATA ON OF_2 - H_2 HEAT OF REACTION

Run No.	n (moles OF_2)	Δe_2 cal/ohm	ΔR_c ohm	Q cal	q_1 cal	q_2 cal	$-\Delta E^o_R$ kcal/mole	q_3 kcal/mole	q_4 kcal/mole	$-\Delta H^o_R$(298.10°K) kcal/mole
1	0.023042	505.0	0.10417	5108.3	-75.7	79.2	221.54	-1.80	+0.51	222.83
2	0.023474	505.0	0.10580	5188.3	-84.1	63.4	221.91	-1.79	+0.50	223.20
3	0.025011	505.2	0.11325	5553.6	-80.9	87.1	221.80	-1.80	+0.48	223.12
4	0.024748	505.2	0.11174	5479.6	-80.4	95.0	220.83	-1.79	+0.48	222.14
5	0.023437	505.0	0.10637	5216.2	-76.9	97.9	221.67	-1.80	+0.50	222.97
6	0.014507	504.1	0.06469	3172.2	-51.5	0	222.22	-1.79	+0.70	223.31

mean $-\Delta H^o_R$ = 222.93 ±0.76 kcal/mole*

n is the number of moles of OF_2; Δe_2 is the correction for deviations from the standard calorimeter system; ΔR_c is the corrected temperature rise in the calorimeter; Q is the quantity of heat observed during the reaction; q_1 includes corrections for nonideality of the reactant gases, condensation of water in the vapor phase and heat of dilution of HF solution to infinite dilution; q_2 is the energy supplied by corrosion of the screw heads; $-\Delta E^o_R$ is the heat of reaction per mole in the thermodynamic standard bomb process; q_3 is the ΔnRT term to convert energy of reaction to heat of reaction; q_4 is the difference in the heat capacity at constant pressure of the products and reactants; and $-\Delta H^o_R$ is the standard heat of reaction at 25°C.

*uncertainty indicated is twice the standard deviation.

REFERENCES

1. H. C. Dickinson, Bulletin of National Bureau of Standards, 11, 189 (1914).

2. JANAF Interim Thermochemical Tables, Joint-Army-Navy-Air Force Thermochemical Panel and Dow Chemical Company, Midland, Michigan.

3. National Bureau of Standards Certificates for Standard Sample 39h Benzoic Acid.

4. F. Rossini, "Selected Values of Chemical Thermodynamic Properties," U. S. National Bureau of Standards Circular No. 500, Washington, D. C. (1954).

5. O. Ruff, W. Menzel, Z. Anorg U. Allgem, Chem., 198, 375 (1931).

6. H. Von Wartenberg, F. Klinkhott, Z. Anorg. U Allgem. Chem. 193, 409 (1930).

CHEMICAL ANALYSIS OF CORROSIVE OXIDIZERS

B. C. Neale et al.

Rocketdyne, A Division of NAA, Inc.
Research Department, Chemistry Section
Canoga Park, California

ABSTRACT

Instrumental techniques have been developed for the analysis of nitrogen tetroxide and chlorine trifluoride. Commercial NTO consists of N_2O_4, NO_2, N_2O_3, NO and H_2O (as HNO_3 and HNO_2). The applications of NMR spectrometry for the proton content and gas-solid chromatography for the nitrogen oxides content are described.

Quantitative analysis of chlorine trifluoride has been carried out by gas chromatography using a custom-built gas chromatograph with a specially prepared column containing Halocarbon oil on Kel-F. Special sampling techniques, sample handling, and sample introduction techniques are described. Retention times for F_2, CF_4, ClF , $FClO_3$, Cl_2, ClO_2, and ClF_3 have been determined. A near-infrared method is presented for the determination of HF in ClF_3.

THE ELECTRICAL CONDUCTIVITY OF SOLID CHLORINE AND BROMINE TRIFLUORIDES

Madeline S. Toy and William A. Cannon

Astropower Laboratory of Douglas Aircraft Co., Inc.
Newport Beach, California

Introduction

The interest in conductivity measurements on fluorinated inorganic compounds at cryogenic temperatures lies in the ability of these compounds to form ions for possible synthesis of potential solid oxidizers. In the present study we are concerned with the conductivity measurements on solid chlorine and bromine trifluorides to determine their electrical conductivities and their bearing on structural problems. Specific conductivities of $< 10^{-6}$ at 0°C(1) and 10^{-9} ohm^{-1}cm^{-1}(2) have been reported for chlorine trifluoride and 8.0×10^{-3} ohm^{-1}cm^{-1} at 25°C(1) for bromine trifluoride. In this work a conductivity cell has been developed for measurement of fluorine-containing oxidizers at cryogenic temperatures. The variations of conductivity with temperature of chlorine trifluoride have been measured from -11.3°C (b.p.) to -130°C (well below m.p., -83°C) and of bromine trifluoride from +80°C to -196°C (m.p., 8.8°C). Possible mechanisms are discussed.

Experimental

Materials. - Chlorine and bromine trifluorides were obtained from the Matheson Co. Chlorine trifluoride was purified by passing the vapor through a sodium fluoride scrubber to remove possible hydrogen fluoride impurity and then fractionally distilled. Bromine trifluoride was used without additional purification.

Conductivity Measurements. - Cell resistance measurements were made with a General type 1650-A Impedance Bridge. It is equipped with an internal, 1000-cycle signal source and tuned null detector. For more sensitive balance at high resistances, a Hewlett Packard 400L vacuum tube voltmeter is used as an external null detector.

The conductivity cell is modified from a conventional type. It is made of borosilicate glass, which resists the attack of anhydrous chlorine and bromine trifluorides, and is equipped with two smooth platinum electrodes to minimize electrode corrosive effects. These electrodes are approximately 12 x 25 mm in size held 1.5 mm apart with borosilicate glass spacers. The arrangement of electrodes and leads is shown in Figure 1. An internal thermocouple well leads from the top of the cell to a point near the electrodes and contains a copper-constatan thermocouple. The cell constant is determined by measuring the cell resistance while the cell is filled with 0.001 N KCl solution at 25°C (cell constant = specific conductivity x observed resistance, where specific conductivity of 0.001 N KCl at 25°C = 0.00014695 ohm^{-1}cm^{-1}). The change in cell constant due to changes in cell and electrode dimensions has been calculated to be insignificant to as low as -195°C and is therefore ignored in this work.

The possibility of imperfect contact of the solid with the electrode does not seem to be a problem in view of the uniformity of the curves and reproducibility as indicated below.

Results and Discussion

Conductivity Versus Temperature of Chlorine Trifluoride. - The conductivity of chlorine trifluoride has been measured over the temperature range from near the boiling point (+11.3°C) to -130°C. Figures 2 and 3 are plots of the conductivity as a function of temperature as the sample of chlorine trifluoride is cooled from the boiling point at a rate of approximately 2 to 3°C per minute. The conductivity increases slightly as the sample is cooled and displays a small maximum before the freezing point (m.p. -83°C) is reached. Below the freezing point the conductivity increases rapidly to a sharp maximum. The temperature versus conductivity plot (Figure 2) for a sample purified by low temperature fractionation[3] no longer has the small maximum occurring just above the freezing point and the maximum peak has been broadened and displaced to a lower temperature. It was thought that the broadening of the peak may reflect the presence of trace carbon halides or chlorine impurities which might have been introduced through reaction of chlorine trifluoride with Kel-F grease used on the stopcocks in the distillation apparatus. Therefore, the distillation manifold was rebuilt using stainless steel needle valves in place of stopcocks. No grease was used in any part of the distillation equipment or manifold (Figure 4). When the experiment was repeated the same general trend was noted, i.e., the disappearance of the small discontinuity above the freezing point, and the displacement to lower temperature and broadening of the conductivity maximum. The results are plotted in Figure 3. It is likely that the necessarily long residence time in glass (ca. 24 hr.) required for the distillation results in pickup of ionic impurities. This could account for the enhanved conductivity in both the solid and liquid after low temperature fractionation.

Solid chlorine trifluoride has a negative temperature coefficient for the conductivity within a narrow temperature range below the freezing point. This negative temperature effect is likely due to a decrease in stability of one or both of the postulated ionic species (ClF_2^+ and ClF_4^-) with increasing temperature rather than electronic conduction. Indirect evidence of the existence of ClF_2^+ cation is supported by the isolation of the compounds ClF_2AsF_6 and ClF_2SbF_6 by Seel and Detmer[4] and ClF_2BrF_4 by Selig and Shamir.[5] An alternative possibility is that the solid is polycrystalline and that conduction depends on grain boundary surface. Such a solid would be molecular and conduction would occur in surface and grain boundary films where ClF_3 is slightly ionized. The portion of ions in such absorbed films is greater than in the bulk liquid since ionization would favor absorption on the possibly dipolar solid. The decrease in conductivity with increasing temperature is then due to a decrease in inner surface.

Conductivity Versus Temperature of Bromine Trifluoride. - The conductivity of bromine trifluoride has been measured over a range of 80 to -196°C (Figure 5). There is little variation of conductivity with temperature in the liquid state; the liquid has a tendency to supercool. The value of specific conductivity at 25°C is 5.03×10^{-3} ohm^{-1} cm^{-1}; literature value is 8×10^{-3} ohm^{-1} cm^{-1}.[1] The ions accounting for the conductivity are probably BrF_2^+ and BrF_4^-. Woolf and Emeleus[6] reported the existence of the ionic equilibrium

$$2\ BrF_3 \rightleftharpoons BrF_2^+ + BrF_4^-$$

in liquid bromine trifluoride by the isolation of compounds BrF_2SbF_6 and $(BrF_2)_2SnF_6$ for BrF_2^+ cation and $KBrF_4$, $AgBrF_4$ and $Ba(BrF_2)_2$ for BrF_4^- anion.

Conductivity of solid bromine trifluoride decreased rapidly with temperature leading to a marked discontinuity around the melting point (+8.8°C). Another discontinuity is observed at ca. -20°C (Figure 5). There are two curves with different slopes, a higher temperature portion and a lower temperature portion. This is similar to the behavior of AgCl, AgBr, TlCl and TlBr as described by Lehfeldt.[7]

This suggests that solid bromine trifluoride may have an ionic lattice of BrF_2^+ and BrF_4^- ions and exhibit electrolytic conduction as these salts. Phosphorous pentachloride, which conducts to a small extent in the solid, has been shown to possess a lattice of PCl_4^+ and PCl_6^- ions. Electrolytic conduction is expressed as the exponential

$$\sigma = \sigma_o e^{-Q/kT} \tag{1}$$

where σ_o is a constant that can be expressed in terms of mobilities, and Q is the activitation energy.[9] For the solid BrF_3 curve shown in Figure 5, it is to be expected that

$$\sigma = \sigma_o e^{-Q_1/kT} + \sigma'_o e^{-Q_2/kT} \tag{2}$$

since two processes are operating. The activation energy Q_1 for the lower temperature process (between -20 and -196°C) is of the order of 3.81 Kcal/g mole, or one-eighth the value of Q_2, 29.8 Kcal/g mole (between +8.8° to -20°C), whereas σ_o (2.13×10^{-11} ohm^{-1}cm^{-1}) is many orders of magnitude greater than σ'_o (1.73×10^{-29} ohm^{-1}cm^{-1}).

Acknowledgment

We wish to thank the Advanced Research Projects Agency for its support through Contract No. DA-31-124-ARO(D)-115. The authors are indebted to Drs. N. A. Tiner, W. D. English and M. J. Plizga for helpful discussions and Mr. S. Miranda for assistance.

References

1. A. A. Banks, H. J. Emeleus and A. A. Woolf, J. Chem. Soc., 2861 (1949).
2. A. A. Woolf and N. N. Greenwood, J. Chem. Soc., 2200 (1950).
3. M. S. Toy, W. A. Cannon and W. D. English, "Solution and Conductivity Studies in Fluorine-Containing Liquid Oxidizers," Astropower Laboratory, Douglas Aircraft Co., Inc., Quarterly Report 144-Q4, Contract No. Da-31-124-ARO(D)-115, 10 March to 15 June, 1964.
4. F. Seel and O. Detmer, Angew. Chem., 70, 163 (1958) and Z. Anorg. Chem., 301, 113 (1959).
5. H. Selig and J. Shamir, Inorg. Chem., 3, 294 (1964).
6. A. A. Woolf and H. J. Emeleus, J. Chem. Soc., 2865 (1949).
7. W. Lehfeldt, Z. Physik, 85, 717 (1933).
8. D. Clark and H. M. Powell and A. F. Well, J. Chem. Soc., 642 (1942).
9. M. J. Sinnott, The Solid State for Engineers, John Wiley, p. 356 (1958).

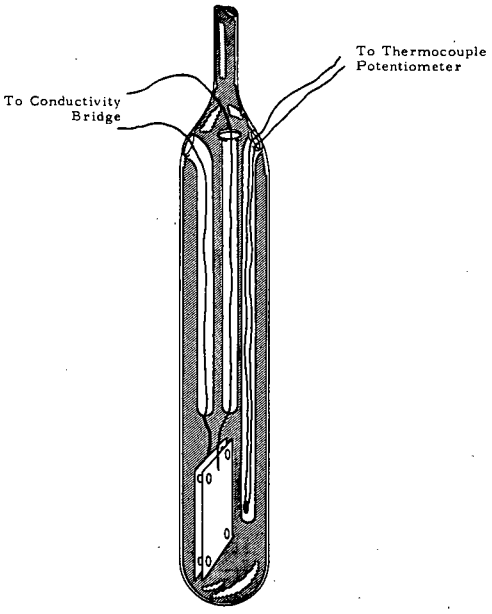

Figure 1. Conductivity Cell

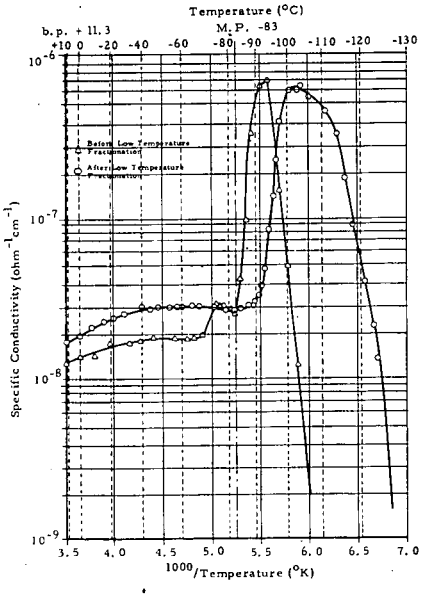

Figure 2. Conductivity of Chlorine Trifluoride as a Function of Temperature (1)

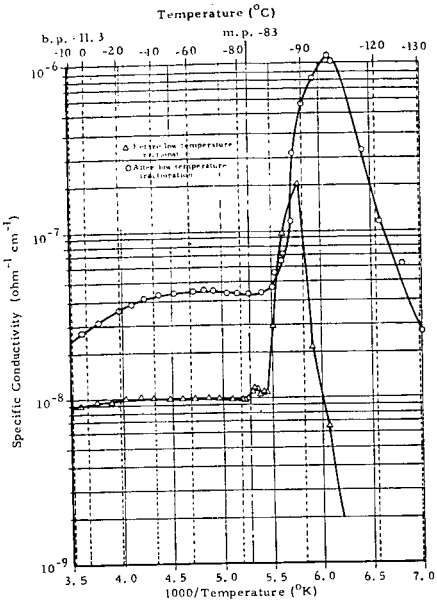

Figure 3. Conductivity of Chlorine Trifluoride as a Function of Temperature (11)

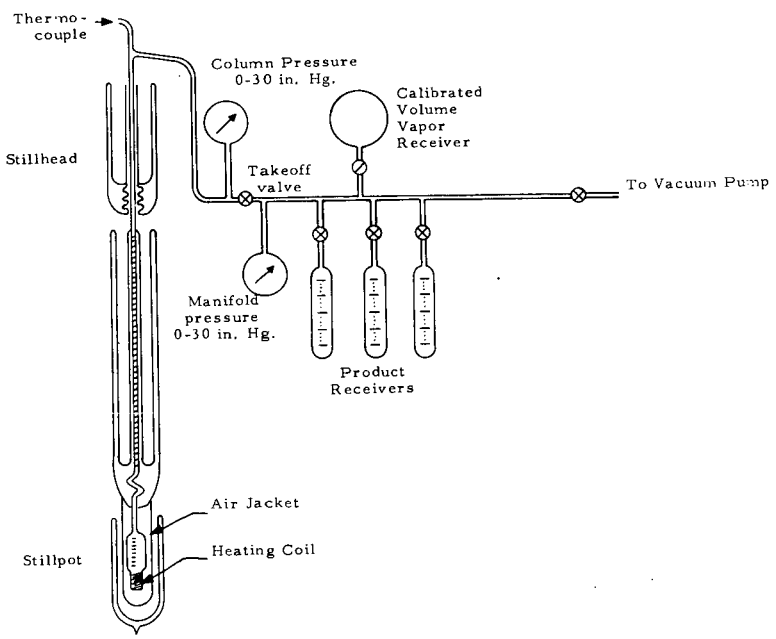

Figure 4. Schematic Diagram of Low Temperature Fractionation Apparatus and Vacuum Manifold

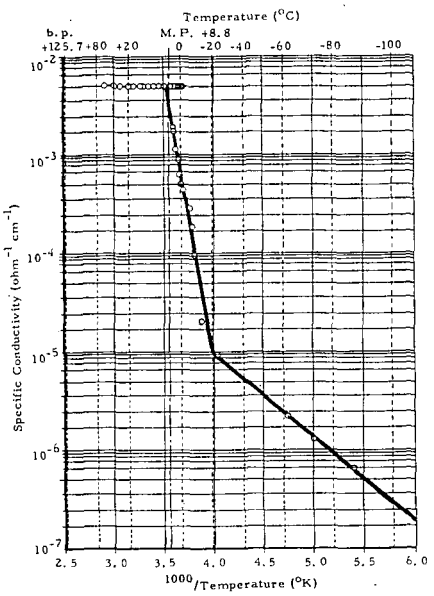

Figure 5. Conductivity of Bromine Trifluoride as Function of Temperature